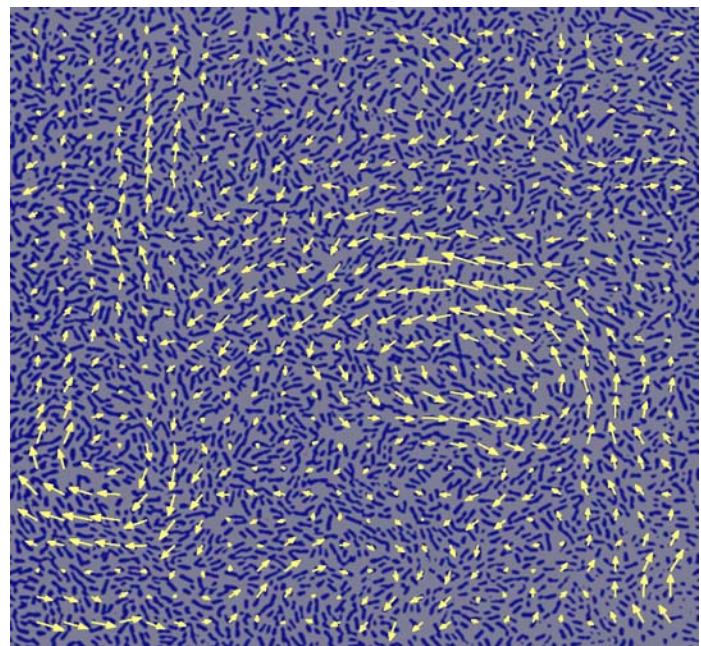
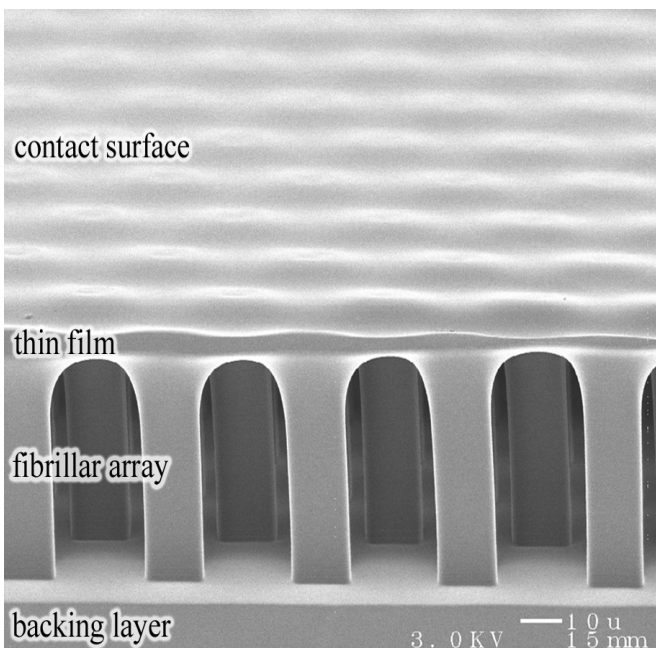
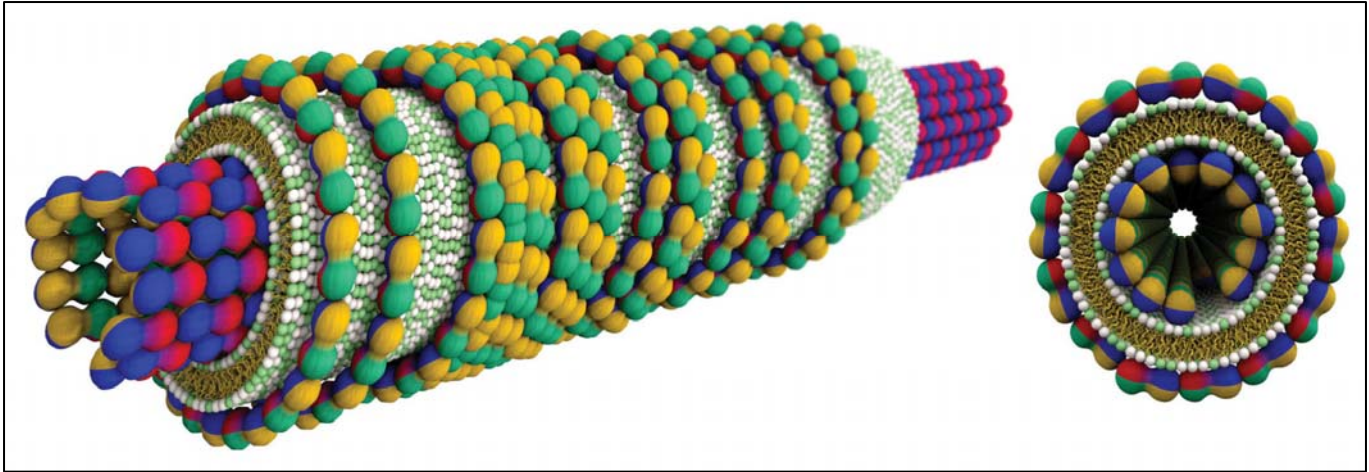


# Biomolecular Materials Contractors' Meeting – 2007

*November 4 – 7, 2007*

*Airlie Conference Center, Warrenton, VA*



**Office of Basic Energy Sciences**

**Division of Materials Sciences and Engineering**

**Office of  
Science**  
U.S. DEPARTMENT OF ENERGY

## On the Cover

- Top: Two views of lipid-protein nanotubes made of microtubule protein and lipid bilayer membranes, which in turn are coated by tubulin protein rings or spirals. Microtubule proto-filament number (which sets the inner diameter of the tubule) is modulated in a step-wise fashion by the charge density of the enveloping lipid bilayer.  
U. Raviv et al. *Biophys. J.*, **2007**, 92, 278.  
*Courtesy: Cyrus Safinya, University of California-Santa Barbara*
- Bottom Left: Synthetic bio-inspired structure with enhanced adhesion and contact compliance, consisting of a film-terminated fibrillar array. While inspired by the sorts of structures seen in lizards, its architecture is most similar to the one found in the grasshopper, *Tettigonia Viridissima*.  
N.J. Glassmaker et al. *Proc. Nat. Acad. Sci. USA*, **2007**, 104 [26] 10786.  
*Courtesy: Anand Jagota, Lehigh University*
- Bottom Right: Self-organized collective flows in the colony of swimming bacteria *Bacillus Subtilis* confined in thin free-standing liquid film. Bacteria are shown as short blue stripes, yellow arrows indicate the flow velocity.  
A. Sokolov et al. *Phys. Rev. Lett.* **2007**, 98, 158102.  
*Courtesy: Andrey Sokolov and Igor Aranson, Argonne National Laboratory*

## Foreword

This volume comprises the scientific content of the 2007 Biomolecular Materials Contractors' Meeting sponsored by the Division of Materials Sciences and Engineering (DMS&E) in the Office of Basic Energy Sciences (BES) of the U. S. Department of Energy (DOE). The meeting, held on November 4-7, 2007 at Airlie Conference Center, Warrenton, VA, is the second Contractors' Meeting on this topic and is one among a series of research theme-based Contractors' Meetings being held by DMS&E. The meeting's focus is on research at the intersection of materials sciences and biology, and it also features research that cuts across several other DMS&E core research program areas where appropriate and relevant.

Biomolecular Materials is a relatively new but growing Core Research Activity (CRA) in DMS&E. This program formally came into existence following the recommendations of a workshop sponsored by the Basic Energy Sciences Advisory Committee (BESAC) in 2002 to explore the potential impact of biology on the physical sciences, in particular the materials and chemical sciences. The major programmatic emphasis is on exploring the molecules, molecular assemblies, processes and concepts of the biological world that could be utilized or mimicked in designing novel materials, processes and devices with potential energy significance in support of DOE's mission.

The purpose of the Biomolecular Materials Contractors' Meetings is to bring together researchers funded by DMS&E in this burgeoning area on a periodic basis (currently once every two years), in order to facilitate the exchange of new results and research highlights, to nucleate new ideas and collaborations among the participants, and to identify needs of the research community. The meeting will also help DMS&E in assessing the state of the program, identifying new research directions and recognizing programmatic needs. The agenda at this year's meeting exemplifies some of the major research themes covered within the broad, expanding field of biomolecular materials.

Many of the BES Contractors' Meetings are passing the quarter-century mark in longevity and are very highly regarded by their participants. I earnestly hope that the Biomolecular Materials Contractors' Meetings will continue to be just as successful and uphold this long-standing BES tradition.

It is my great pleasure to express sincere thanks to all of the meeting attendees, especially the invited speakers, for their active participation and sharing their ideas and new research results. The dedicated efforts and invaluable advice of the Meeting Chairs, Cyrus Safinya and Millie Firestone, towards organizing this meeting are deeply appreciated. My heartfelt thanks also go to Christie Ashton in DMS&E and Sophia Kitts in the Oak Ridge Institute of Science and Education (ORISE) for their outstanding work in taking care of all the logistical aspects of the meeting.

Arvind Kini  
Program Manager, Biomolecular Materials  
Division of Materials Sciences and Engineering  
Office of Basic Energy Sciences  
U.S. Department of Energy

**U. S. Department of Energy**  
**Office of Basic Energy Sciences**  
*Biomolecular Materials Contractors' Meeting*  
Airlie Conference Center, Warrenton, VA  
November 4 – 7, 2007  
Cyrus Safinya and Millie Firestone, *Meeting Chairs*

**SUNDAY, NOVEMBER 4**

3:00 – 6:00 pm	Arrival and Registration
5:00 – 6:00 pm	Reception (No Host)
6:00 – 7:00 pm	***** Dinner *****
7:00 pm	<b>Introductory Remarks</b> Harriet Kung, <i>Director, Division of Materials Sciences and Engineering</i> Arvind Kini <i>Program Manager, Biomolecular Materials</i>
<b>Session I</b>	<b>Topic: Biomolecular Assemblies – Membranes, Liposomes and Adaptive Structures</b> <u>Chairs:</u> Cyrus Safinya and Millie Firestone
7:30 – 8:00 pm	Jay Groves, Lawrence Berkeley National Laboratory <i>Bending Mechanics and Molecular Organization in Lipid Membranes</i>
8:00 – 8:30 pm	Steve Granick, University of Illinois-Urbana Champaign <i>Structured, Stabilized Phospholipid Vesicles</i>
8:30 – 9:00 pm	Darryl Sasaki, Sandia National Laboratory <i>Adaptive and Reconfigurable Nanocomposites</i>
9:00 – 9:30 pm	Mike Therien, University of Pennsylvania <i>Design, Synthesis &amp; Characterization of Novel Electronic &amp; Photonic BioMolecular Materials</i>
9:30 – 10:00 pm	Frank Robb, Center for Marine Biotechnology, University of Maryland ( <i>Invited Plenary Lecture</i> ) <i>Biomolecular Stability and Life in Extreme Conditions</i>

## MONDAY, NOVEMBER 5

7:00 – 8:00 am	Breakfast
<b>Session II</b>	<b>Topic: Self- and Directed-Assembly – I</b> <b>Chair:</b> Sam Stupp
8:00 – 8:30 am	Cyrus Safinya, University of California-Santa Barbara <i>Miniaturized Hybrid Materials Inspired by Nature</i>
8:30 – 9:00 am	Ben Ocko, Brookhaven National Laboratory <i>Directed Self-Assembly of Soft-Matter and Biomolecular Materials</i>
9:00 – 9:30 am	Uwe Bunz, Georgia Institute of Technology <i>Water-Soluble Poly(Paraphenyleneethynylene)s: Bioinspired Fluorescent Building Blocks for Controlled Assembly of Hybrid Materials</i>
9:30 – 10:00 am	Igor Aronson, Argonne National Laboratory, and Ray Goldstein, Cambridge University and University of Arizona <i>Collective Dynamics, Self-Assembly, and Mixing in Active Microparticle Ensembles</i>
10:00 – 10:30 am	**** Break ****
<b>Session III</b>	<b>Topic: Self- and Directed-Assembly – II</b> <b>Chair:</b> Jeff Brinker
10:30 – 11:00 am	Oleg Gang, Brookhaven National Laboratory <i>Biology-Inspired Programmable Assembly of Functional Nano-Structures</i>
11:00 – 11:30 am	Phil Geissler and Paul Alivisatos, Lawrence Berkeley National Laboratory <i>Statistical Mechanics of Biomolecular Materials: Theory and Modeling of DNA and Viral Capsids as Building Blocks for Large-Scale Structures</i>
11:30 – 12:00 Noon	Ned Seeman, New York University ( <i>Invited Plenary Lecture</i> ) <i>DNA: Not Merely the Secret of Life</i>
12:00 Noon – 1:00 pm	**** Lunch ****
1:00 – 4:00 pm	<b>Time for Interactions &amp; Discussions</b>
4:00 – 6:00 pm	<b>Poster Session I</b>

6:00 – 7:00 pm

\*\*\*\*\* Dinner \*\*\*\*\*

**Session IV**

**Topic: Novel Tools and Techniques for Probing Biomolecular Materials and Processes**

Chair: Sunil Sinha

7:00 – 7:30 pm

Klaus Schmidt-Rohr, Ames Laboratory  
*Solid-State NMR of Polymers and Nanocomposites*

7:30 – 8:00 pm

Paul Gourley, Sandia National Laboratory  
*Optical Techniques for Studying Novel Biomaterials*

8:00 – 8:30 pm

Geri Richmond, University of Oregon  
*Wet Interfaces: Developing a Molecular Framework for Understanding the Behavior of Materials in Aqueous Solutions*

8:30 – 9:00 pm

Pulak Dutta, Northwestern University  
*In Situ Studies of Nucleation and Assembly of Soft-Hard Interfaces*

9:00 – 9:30 pm

P. Thiyagarajan, Argonne National Laboratory (***Invited Plenary Lecture***)  
*Advance Photon Source (APS) Capabilities for the Study of Soft and Biomolecular Materials*

9:30 – 11:00 pm

***Continuation of Poster Session I***

**TUESDAY, NOVEMBER 6**

7:00 – 8:00 am

Breakfast

**Session V**

**Topic: Biotemplated Synthesis of Large-Scale Structures**

Chair: Matt Francis

8:00 – 8:30 am

James De Yoreo, Lawrence Livermore National Laboratory  
*Assembly at Nanoscale Chemical Templates*

8:30 – 9:00 am

Jim Culver, University of Maryland, and  
Mike Harris, Purdue University  
*Virus Assemblies as Templates for Nanocircuits*

9:00 – 9:30 am

Balaji Narasimhan and Marit Nilsen-Hamilton, Ames Laboratory  
*Bioinspired Hybrid Elastic Nanomagnets*

9:30 – 10:00 am	John Evans, New York University <i>Material Lessons of Biology: Structure-Function Studies of Protein Sequences Involved in Inorganic-Organic Composite Material Formation.</i>
10:00 – 10:30 am	***** Break *****
<b>Session VI</b>	<b>Topic: 3-D Structures and Hierarchical Assembly</b> <b>Chair:</b> Jennifer Lewis
10:30 – 11:00 am	Anna Balazs, University of Pittsburgh <i>Designing Smart Surfaces and Responsive Microcapsules for Creating Micro-reactor Arrays</i>
11:00 – 11:30 am	Erik Luijten, University of Illinois-Urbana Champaign <i>Prototypical Patchy Particles: Self-assembly and Dynamics of Janus Colloids</i>
11:30 – 12:00 Noon	Huajian Gao, Brown University ( <b><i>Invited Plenary Lecture</i></b> ) <i>What Can We Learn From Nature About the Principles of Hierarchical Materials?</i>
12:00 Noon – 1:00 pm	***** Lunch *****
1:00 – 4:00 pm	<b>Time for Interactions and Discussions</b>
4:00 – 6:00 pm	<b><i>Poster Session II</i></b>
6:00 – 7:00 pm	***** Dinner *****
<b>Session VII</b>	<b>Title: Biomimetic/Bioinspired Materials and Concepts in Lubrication, Friction and Adhesion</b> <b>Chair:</b> Dan Morse
7:00 – 7:30 pm	Carolyn Bertozzi, Lawrence Berkeley National Laboratory <i>Biomimetic Coatings for Bio/Material Interfaces</i>
7:30 – 8:00 pm	Lynden Archer, Cornell University <i>Interfacial Friction of Multi-Tiered Thin Films</i>
8:00 – 8:30 pm	Tonya Kuhl, University of California-Davis <i>Structure-Property Relationships of Polymer Brushes in Restricted Geometries and their Utilization as Ultra-Low Friction Lubricants</i>

- 8:30 – 9:00 pm Sanat Kumar, Columbia University, and  
Georges Belfort, Rensselaer Polytechnic Institute  
*Influence of Surface Chemistry and Folding Free Energy on  
Protein Adsorption*
- 9:00 – 9:30 pm Anand Jagota, Lehigh University, and  
Herbert Hui, Cornell University  
*Designing Two-Level Biomimetic Fibrillar Interfaces*
- 9:30 – 11:00 pm ***Continuation of Poster Session II***

## WEDNESDAY, NOVEMBER 7

- 7:00 – 8:00 am Breakfast
- Session VIII** **Topic: Biomolecular Assemblies and Approaches for  
Hydrogen Production**  
Chair: Andy Shreve
- 8:00 – 8:30 am Les Dutton, University of Pennsylvania  
*Modular Designed Protein Constructions for Solar Generated H<sub>2</sub>  
from Water*
- 8:30 – 9:00 am John Golbeck, Pennsylvania State University  
*A Hybrid Biological-Organic Photochemical Half-Cell for  
Generating Dihydrogen*
- 9:00 – 9:30 am Annabella Selloni and Roberto Car, Princeton University  
*Theoretical Research Program on Bio-inspired Inorganic  
Hydrogen Generating Catalysts and Electrodes*
- 9:30 – 10:00 am Bruce Eaton and Dan Feldheim, University of Colorado  
*RNA Mediated Assembly of Inorganic Metal and Metal Oxide  
Nanoparticles*
- 10:00 – 10:30 am \*\*\*\*\* Break \*\*\*\*\*
- Session IX** **Topic: Solar Hydrogen Production and Catalysis**  
Chair: Hiroshi Matsui
- 10:30 – 11:00 am Trevor Douglas, Montana State University  
*Protein Architectures for Photo-Catalytic Hydrogen Production*
- 11:00 – 11:30 am Blake Simmons, Sandia National Laboratory-California (***Invited  
Talk***)



*Basic Research Needs Workshop on Catalysis for Energy Applications*

11:30 – 12:00 Noon

Closing Remarks

Cyrus Safinya and Millie Firestone, *Meeting Chairs*

Arvind Kini, *Program Manager, Biomolecular Materials*

12:00 Noon

\*\*\*\*\* Lunch and Adjourn \*\*\*\*\*

(Optional Box Lunches Available)

## Poster Session I – Jefferson Room

Monday, November 5, 2007, 4:00-6:00 PM and 9:30-11:00 PM

P-I-1 - Bioinspired Polymers: Self-Assembled Polymer - Hydroxyapatite Nanocomposites,  
*Alex Travesset and Surya Mallapragada, Ames Laboratory*

P-I-2 - Nanostructured Biocomposites: Designing and Tailoring The Abiotic-Biotic Interface,  
*Millicent A. Firestone, Brian D. Reiss, Sashishakara P. Adiga, Peter Zapoll, Orlando Auciello, Leonidas Ocola, Deborah K. Hanson, Philip D. Laible, Argonne National Laboratory*

P-I-3 - Development of Biocompatible Polymeric Electrodes for Protein Based Devices,  
*Chris Burns, Millie Firestone, Argonne National Laboratory*

P-I-4- Wetting Morphologies on Chemically Nanopatterned Surfaces,  
*A. Checco and B.M. Ocko, Brookhaven National Laboratory*

P-I-5 - Self-Assembly of 2D TMV Arrays on Lipid Monolayers at Substrate-Buffer and Buffer-Air Interfaces, *S.T. Wang, A. Checco, Z. Niu, Q. Wang, M. Fukuto, and L. Yang, Brookhaven National Laboratory*

P-I-6 - Development of Integrated Photocatalytic Systems Using the Tobacco Mosaic Virus,  
*Matt Francis, Lawrence Berkeley National Laboratory*

P-I-7 - Bioinspired Polymers as Synthetic Enzyme Mimics,  
*Jean Frechet, Lawrence Berkeley National Laboratory*

P-I-8 - Observation of In-Situ Biological Processes in the Dynamic TEM,  
*J. B. Pesavento, J. Lee, J. De Yoreo, and N. D. Browning (Presenter: Wayne King), Lawrence Livermore National Laboratory*

P-I-9 - Biological Assisted Templating of Fluorescent Nanoclusters,  
*Jennifer S. Martinez, Yuping Bao, Chang Zhong, Jennifer Belyea, Dung M. Vu, and R. Brian Dyer, Los Alamos National Laboratory*

P-I-10 - Carbon Nanotube Fluorescence and Sensing in Silica Composite Materials,  
*Satishkumar B. Chikkannanavar, Steven K. Doorn and Andrew M. Dattelbaum, Los Alamos National Laboratory*

P-I-11 - Artificial Microtubule Organizing Centers: Reconstructing Natural Architectures, *Erik D. Spoerke, Andrew K. Boal, George D. Bachand, Ann Bouchard, Gordon Osbourn, and Bruce C. Bunker, Sandia National Laboratory*

P-I-12 - Cell Directed Assembly of Novel Biotic/Abiotic Materials and Interfaces,  
*C. Jeff Brinker, Eric Carnes, Seema Singh, DeAnna Lopez, Sandia National Laboratory*

P-I-13 - Silicatein: Semiconductor-Synthesizing Protein Discovered in Glass,  
*Michi Izumi and Daniel E. Morse, University of California, Santa Barbara*

P-I-14 - Electrets: Applications and Mechanistic Insight,  
*Samuel Thomas and George M. Whitesides, Harvard University*

P-I-15 - Biomolecular Sacs, Strings, and Membranes: From Nanometers to Centimeters with Self-Assembly, *Samuel I. Stupp, Helena Azevedo, Ramille Capito, Megan A. Greenfield, Liang-shi Li, Alvaro Mata, Liam C. Palmer, Yuri S. Velichko, and Shuming Zhang, Northwestern University*

P-I-16 - Water-Immersed Polymer Interfaces and the Roles of Their Materials Properties on Biolubrication, *Yingxi Elaine Zhu, University of Notre Dame*

P-I-17- Biopolymers Containing Unnatural Amino Acids,  
*Roshan Perera and Peter G. Schultz, The Scripps Research Institute*

## Poster Session II – Jefferson Room

Tuesday, November 6, 2007, 4:00-6:00 PM and 9:30-11:00 PM

P-II-1 - DeBUGging the Verwey Transition: Learning from Nature,  
Tanya Prozorov and Surya Mallapragada, Ames Laboratory

P-II-2- Effect of Biotin Density on Lipid Monolayer-Assisted 2D Crystallization of Streptavidin at the Liquid-Vapor Interface, *M. A. Lohr, S. T. Wang, L. Yang, and M. Fukuto, Brookhaven National Laboratory*

P-II-3- Manipulating Nature's Molecular Machines, *Dirk Trauner, Lawrence Berkeley National Laboratory*

P-II-4- Water-soluble PPV with Tunable Optical and Electronic Properties: Untangling the Role of Aggregates, *Chun-Chih Wang, Yuan Gao, Chang Zhong, Jennifer Martinez, Andrew P. Shreve, Mircea Cotlet, Leeyih Wang and Hsing-Lin Wang, Los Alamos National Laboratory*

P-II-5- Optical Detection of Ion-Channel-Induced Proton Transport in Supported Phospholipid Bilayers, *Eric L. Kendall, Seema Singh, Calvin Yang, Chanel K. Yee, Andrew M. Dattelbaum, C. Jeffrey Brinker, Andrew P. Shreve, and Atul N. Parikh, Los Alamos, National Laboratory, Sandia National Laboratory, University of California-Davis*

P-II-6- Hydrothermal Processing of Carbohydrates: Reaction Pathways to Tailored Interfaces, *Gregory J. Exarhos and Yongsoon Shin, Pacific Northwest National Laboratory*

P-II-7 - Bio-Integration: Active Assembly of Dynamic and Adaptable Materials, *George Bachand, Bruce Bunker, Erik Spoerke, Sandia National Laboratories*

P-II-8 - Metal-Lipid Nanocomposites from Reconfigurable Bicellar Structures, *John A. Shelnut, Yujiang Song; Darryl Y. Sasaki; Frank van Swol; Sivakumar Challa; Rachel Dorin; Robert Garcia, Sandia National Laboratories*

P-II-9 - Molecular Dynamics Simulations of Non-grafted and Grafted Polystyrene Melts in Confined Geometries, *Petra Traskelin, Roland Faller and Tonya Kuhl, University of California-Davis*

P-II-10 - Dynamic Self-Assembly: Functional Reorganizations in Biomembranes, *Babak Sanii, Atul N. Parikh and Sunil K. Sinha, University of California-Davis and University of California-San Diego*

P-II-11 - Bio-inspired Growth of Low-Dimensional Metal Oxide Structures, *Andrea Tao, Richard Brutchey and Daniel E. Morse, University of California-Santa Barbara*

P-II-12 - Probing the Mechanism of RNA-mediated Particle Growth Using Fluorescence Polarization Anisotropy, *Jessica Rouge, Bruce Eaton and Daniel Feldheim, University of Colorado*

P-II-13 - Poly(paraphenyleneethynylene)s: Probing the Biological Interface with Biomolecular Materials, *Ronnie Phillips, Ik-Bum Kim, and Uwe Bunz, Georgia Institute of Technology*

P-II-14- Oscillatory Behavior of Arrays of Flamelets, *Ryan Chiechi and George M. Whitesides, Harvard University*

P-II-15 - Adhesion and Frictional Properties of a Biomimetic Film-Terminated Fibrillar Interface, *Lulin Shin, Shilpi Vajapayee, Herbert Hui and Anand Jagota, Cornell University and Lehigh University*

P-II-16 - Self-Assembly of Virus-Structured High Surface Area Nano-Materials, *Elizabeth Roysten, Jim Culver and Mike Harris, University of Maryland and Purdue University*

P-II-17 - Self-Assembling Biological Springs: Force Transducers on the Micron and Nanoscales, *B. Khaykovich, N. Kozlova, C. Hossain, A. Lomakin, D. E. Moncton, and G. B. Benedek, Massachusetts Institute of Technology*

P-II-18 - Room-Temperature Synthesis of Semiconductor Nanowires by Templating Collagen Triple Helices and Their Precise Assembly into Electrical Circuits by Biomolecular Recognition, *Hiroshi Matsui, City University of New York, Hunter College*

***TABLE OF  
CONTENTS***

## Table of Contents

<b>Foreword</b> .....	i
<b>Agenda</b> .....	ii
<b>Poster Session I</b> .....	viii
<b>Poster Session II</b> .....	x
<b>Table of Contents</b> .....	xii

### Laboratory Projects

#### *Bioinspired Nanoscale Hybrid Materials*

<b>Alex Traveset, M. Akinc, K. Schmidt-Rohr, and S. Mallapragada</b> .....	1
--	---

#### *Bioinspired Hybrid Elastic Nanomagnets*

<b>Balaji Narasimhan, Marit Nilsen-Hamilton, D. Bazylinski, P. Canfield, M. Lamm, S. Mallapragada, P. Palo, R. Prozorov, T. Prozorov, J. Schmalian, R. Sknepnek, A. Traveset, and L. Wang</b> .....	5
---	---

#### *Solid-State NMR of Polymers and Nanocomposites*

<b>Klaus Schmidt-Rohr, Surya K. Mallapragada, Mufit A. Akinc, A. Rawal, and E. Levin</b> .....	9
--	---

#### *Collective Dynamics, Self-Assembly, and Mixing in Active Microparticle Ensembles*

<b>Igor Aronson and Raymond E. Goldstein</b> .....	13
--	----

#### *Nanostructured Biocomposites: Designing and Tailoring the Abiotic-Biotic Interface*

<b>Millicent A. Firestone, Brian D. Reiss, Sashishakara P. Adiga, Peter Zapol, Orlando Auciello, Leonidas Ocola, Deborah K. Hanson, and Philip D. Laible</b> .....	17
--	----

#### *Biology-Inspired Programmable Assembly of Functional Nano-Structures*

<b>Oleg Gang, Daniel van der Lelie, Dmytro Nykypanchuk, Mathew Maye, Yian-Biao Zhang</b> .....	21
--	----

#### *Directed Self-Assembly of Soft-Matter and Biomolecular Materials*

<b>Benjamin Ocko, Antonio Checco, Masa Fukuto, and Lin Yang</b> .....	25
---	----

#### *DNA Directed Assembly of Nanocrystal Molecules*

<b>A. Paul Alivisatos</b> .....	29
---------------------------------	----

<i>Engineering Bio-Material Interfaces Using Biomimetic Materials</i> <b>Carolyn R. Bertozzi</b> .....	31
<i>Development of Integrated Photocatalytic Systems Using the Tobacco Mosaic Virus</i> <b>Matthew B. Francis</b> .....	35
<i>Bioinspired Polymers as Synthetic Enzyme Mimics</i> <b>Jean Fréchet</b> .....	39
<i>Statistical mechanics of Biomolecular Materials: Theory and Modeling of DNA and Viral Capsids as Building Blocks for Large-Scale Structures</i> <b>Phillip L. Geissler</b> .....	42
<i>Biomolecular Materials Program</i> <b>Jay T. Groves, Mark Alper, Paul Alivisatos, Carolyn Bertozzi, Matt Francis, Jean Fréchet, Phillip Geissler, and Dirk Trauner</b> .....	46
<i>Assembly at Nanoscale Chemical Templates</i> <b>Jim De Yoreo, Alex Noy, and George Gilmer</b> .....	50
<i>Observation of In-Situ Biological Processes in the Dynamic TEM</i> <b>J. B. Pesavento, J. Lee, J. De Yoreo, and N. D. Browning</b> .....	54
<i>Molecularly Engineered Biomimetic Nanoassemblies</i> <b>Andrew P. Shreve, Hsing-Lin Wang, Jennifer Martinez, Srinivas Iyer, Reginaldo Rocha, James Brozik, Darryl Sasaki, and Atul N. Parikh</b> .....	56
<i>Molecularly Organized Nanostructural Materials</i> <b>Gregory J. Exarhos, Yongsoon Shin, Li Qiong Wang, and William D. Samuels</b> .....	60
<i>Bio-Integration: Active Assembly of Dynamic and Adaptable Materials</i> <b>George Bachand, Bruce Bunker, and Erik Spoerke</b> .....	64
<i>Cell Directed Assembly of Novel Biotic/Abiotic Materials and Interfaces</i> <b>C. J. Brinker, Eric Carnes, Seema Singh, and DeAnna Lopez</b> .....	68
<i>Optical Techniques for Studying Novel Biomaterials</i> <b>P. L. Gourley, D. Y. Sasaki, and M. B. Sinclair</b> .....	72
<i>Adaptive and Reconfigurable Nanocomposites</i> <b>Bruce C. Bunker, David R. Wheeler, Chris Orendorff, Darryl Y. Sasaki, Todd M. Alam, Dale L. Huber, and Mark J. Stevens</b> .....	76



<i>Metal-Lipid Nanocomposites from Reconfigurable Bicellar Structures</i> <b>John A. Shelnutt, Yujiang Song, Darryl Y. Sasaki, Frank van Swol, Sivakumar Challa, Rachel Dorin, and Robert Garcia</b> .....	80
<i>Artificial Microtubule Organizing Centers: Reconstructing Natural Architectures</i> <b>Erik D. Spoecke, Andrew K. Boal, George D. Bachand, Ann Bouchard, Gordon Osbourn, and Bruce C. Bunker</b> .....	84
<b>University Grant Projects</b>	
<i>Structure-Property Relationships of Polymer Brushes in Restricted Geometries and their Utilization as Ultra-Low Friction Lubricants</i> <b>Tonya Kuhl</b> .....	88
<i>Dynamic Self-Assembly: Functional Reorganizations in Biomembranes</i> <b>Atul N. Parikh and Sunil K. Sinha</b> .....	92
<i>Biological and Biomimetic Low-Temperature Routes to Materials for Energy Applications</i> <b>Daniel E. Morse</b> .....	96
<i>Miniaturized Hybrid Materials Inspired by Nature</i> <b>C. R. Safinya, Y. Li, and K. Ewert</b> .....	100
<i>RNA Mediated Assembly of Inorganic Metal and Metal Oxide Nanoparticles</i> <b>Dan Feldheim, Lina Gugliotti, Magda Dolska, J'aime Manion, Jessica Rouge, and Bruce Eaton</b> .....	104
<i>Influence of Surface Chemistry and Folding Free Energy on Protein Absorption</i> <b>Sanat Kumar and Georges Belfort</b> .....	108
<i>Interfacial Friction of Multi-tiered Thin Films</i> <b>Lynden A. Archer</b> .....	110
<i>Hyperbranched Conjugated Polymers and Their Nanodot Composites as Universal Bioinspired Architectures; Sugar-Substituted Poly(paraphenyleneethynylene)s: "Molecular Ropes" for Sensing of Bioterrorist and Disease Related Toxins</i> <b>Uwe H. F. Bunz, Mohan Srinivasarao, and Vincent M. Rotello</b> .....	114
<i>Structured, Stabilized Phospholipid Vesicles</i> <b>Steve Granick and Erik Luijten</b> .....	118
<i>Programming Function via Soft Materials</i> <b>Jeff Moore, Erik Luijten, and Steve Granick</b> .....	122

<i>Designing Two-Level Biomimetic Fibrillar Interfaces</i> <b>Anand Jagota and Chung-Yuen Hui</b> .....	126
<i>Virus Assemblies as Templates for Nanocircuits</i> <b>Michael T. Harris and James N. Culver</b> .....	130
<i>Self-Assembling Biological Springs: Force Transducers on the Micron and Nanoscales</i> <b>B. Khaykovich, N. Kozlova, C. Hossain, A. Lomakin, D. E. Moncton, and G. B. Benedek</b> .....	134
<i>Protein Architectures for Photo-Catalytic Hydrogen Production</i> <b>Trevor Douglas, John Peters, and Mark Young</b> .....	138
<i>Biomolecular Sacs, Strings, and Membranes: From Nanometers to Centimeters with Self-Assembly</i> <b>Samuel I. Stupp, Helena Azevedo, Ramille Capito, Megan A. Greenfield, Liang-shi Li, Alvaro Mata, Liam C. Palmer, Yuri S. Velichko, and Shuming Zhang</b> .....	141
<i>In Situ Studies of Nucleation and Assembly at Soft-Hard Interfaces</i> <b>Pulak Dutta</b> .....	145
<i>Water-Immersed Polymer Interfaces and the Roles of Their Materials Properties on Biolubrication</i> <b>Yingxi E. Zhu</b> .....	149
<i>Room-Temperature Synthesis of Semiconductor Nanowires by Templating Collagen Triple Helices and Their Precise Assembly into Electrical Circuits by Biomolecular Recognition</i> <b>Hiroshi Matsui</b> .....	152
<i>Material Lessons of Biology: Structure-Function Studies of Protein Sequences Involved in Inorganic-Organic Composite Material Formation</i> <b>John S. Evans</b> .....	156
<i>Wet Interfaces: Developing a Molecular Framework for Understanding the Behavior of Materials in Aqueous Solutions</i> <b>Geraldine L. Richmond</b> .....	160
<i>Design, Synthesis &amp; Characterization of Novel Electronic and Photonic Biomolecular Materials</i> <b>J. K. Blasie, W. F. DeGrado, J. G. Saven and M. J. Therien</b> .....	164
<i>Modular Designed Protein Constructions for Solar Generated H<sub>2</sub> from Water</i> <b>P. Leslie Dutton</b> .....	168

<i>A Hybrid Biological-Organic Photochemical Half-Cell for Generating Dihydrogen</i> <b>John. H. Golbeck and Donald A. Bryant</b> .....	172
<i>Designing Smart Surfaces and Responsive Microcapsules for Creating Micro-Reactor Arrays</i> <b>Anna C. Balazs</b> .....	176
<i>Theoretical Research Program on Bio-Inspired Inorganic Hydrogen Generating Catalysts and Electrodes</i> <b>Annabella Selloni and Roberto Car</b> .....	180
<i>Biopolymers Containing Unnatural Amino Acids</i> <b>Peter G. Schultz</b> .....	183
 <b>Invited Talks</b>	
<i>Biomolecular Stability and Life in Extreme Conditions</i> <b>Frank Robb</b> .....	187
<i>DNA: Not Merely the Secret of Life</i> <b>Nadrian C. Seeman</b> .....	188
<i>What Can We Learn from Nature about the Principles of Hierarchical Materials?</i> <b>Huajian Gao</b> .....	189
 <b>Author Index</b> .....	190
 <b>Participant List</b> .....	191

***LABORATORY  
PROJECTS***

## Bioinspired Nanoscale Hybrid Materials

Alex Travesset, M. Akinc, K. Schmidt-Rohr and S. Mallapragada  
Ames Laboratory, Ames IA 50011, [trvsst@ameslab.gov](mailto:trvsst@ameslab.gov)

**Program scope:** This subtask deals with the bioinspired synthesis and characterization of hierarchical multiscale self-assembled polymer-inorganic nanocomposites. Nature has constructed increasingly complex systems from a relatively small set of building blocks. The organic component of the biomaterial imparts toughness to the otherwise brittle inorganic phase and serves as a substrate for nucleation and growth of inorganic phase. Controlling the structure at the molecular level as well as impressing hierarchical order over multiple length scales as seen commonly in Nature is a formidable challenge that has not been achieved yet, but significant progress is being made. Therefore, the ability to tailor synthetic nanocomposite materials to exhibit such hierarchical structures at multiple length scales opens up possibilities for bottom-up approaches for designing materials with unique properties that are relevant to DOE's mission (e.g. lightweight, high-strength materials, and materials with unique photoresponsive and transport properties).

Our recent work has shown that synthetic block copolymers that undergo self-assembly at multiple length scales can serve as effective templates for precipitation of calcium phosphates on nanoscale micelles, which can self-assemble further into macroscale gels and solids.<sup>1</sup> This is one of the first approaches for bottom-up design of macroscale composites with hierarchical order down to the nanoscale completely by self-assembly.. We have synthesized a family of multiblock copolymers with zwitterionic and anionic blocks as hierarchically assembling copolymer templates. Along with other characterization methods, we present neutron and x-ray scattering experiments that support the structural picture of the polymer-inorganic nanocomposite superstructure. An integration of experimental and theoretical approaches are being used to obtain insights into the mechanisms of templating and the role of the inorganic phase on the self-assembly of the polymer templates. The theoretical component is focused on predicting the phases of block copolymer aqueous solutions, with and without inorganic components, and understanding their static and dynamical properties.

**Recent progress:** Bioinspired nanocomposite synthesis: Ionic thermoreversibly gelling hierarchically assembling pentablock copolymers were synthesized by atom transfer radical polymerization and used as templates for biomineralization. Initial studies with triblock Pluronic copolymers of poly(ethylene oxide)-b-poly(propylene oxide)-b-poly(ethylene oxide) and cationic pentablock copolymers as templates for inorganic nanocrystal synthesis showed good templating ability, but low fraction of the inorganic phase.<sup>1</sup> Studies of monolayers have shown that ionic blocks such as carboxylic groups or phosphobetaines are ideal for calcium phosphate precipitation. The Pluronic copolymers were used as macroinitiators and pentablock copolymers based on either zwitterionic (PentaPZ) blocks containing polysulfobetaine side chains, or poly(acrylic acid) blocks (PentaPAA) were synthesized. The polymers were dissolved in aqueous solutions containing calcium and phosphate ions and the calcium phosphate phase was allowed to precipitate on the nanoscale micelles before raising the temperature to 37<sup>0</sup>C and allowing the inorganic-coated micelles to self-assemble further into *organized macroscale gel and solid nanocomposites completely by self-assembly*. Polymer-inorganic hybrids such as PentaPAA36-5 were formed, the last two digits representing the weight percent of the polymer in solution and the pH of the gel respectively.

Proof of Nanocomposite Formation by NMR: Thermogravimetric analysis showed significant inorganic fractions, around 33% inorganic for PentaPAA27-5 and PentaPAA36-5 and around 27% for PentaPZ46-5 nanocomposites. The X-ray pattern of PentaPAA27-5 revealed the typical reflections for crystalline synthetic brushite (CaHPO<sub>4</sub>·2H<sub>2</sub>O). XRD results for Penta-PAA36-5 showed only broad reflections indicating that the calcium phosphate phase might be either nanocrystalline or a minor volume fraction compared to the polymer. In order to prove nanocomposite formation and templating of the inorganic phase by the polymer micelles, <sup>1</sup>H-<sup>31</sup>P NMR with spin diffusion NMR and scattering measurements of polymer-inorganic gel composites were conducted. To reveal the presence of a nanocomposite, two-dimensional <sup>1</sup>H-<sup>31</sup>P heteronuclear correlation NMR experiments with <sup>1</sup>H spin diffusion were conducted, where cross peaks between polymer protons and inorganic phosphate prove the intimate contact between the organic and inorganic phases that is the

characteristic of nanocomposites. The  $^{31}\text{P}$  NMR spectra of the three nanocomposites showed a considerable variety of bands, and the HetCor spectra confirmed that each sample contains at least two different types of phosphates. Application of NMR techniques to Penta PZ46-5 in Fig. 1 shows slow spin diffusion from the polymer, but the low broad component centered at  $-1.8$  ppm, which in spite of its low peak height accounts for 66% of the phosphate according to the quantitative spectrum, exhibits close contact with the polymer, indicating the presence of a nanocomposite. Domain thicknesses of a few nm for the different samples were obtained from  $^{31}\text{P}\{^1\text{H}\}$  HARDHIP NMR.

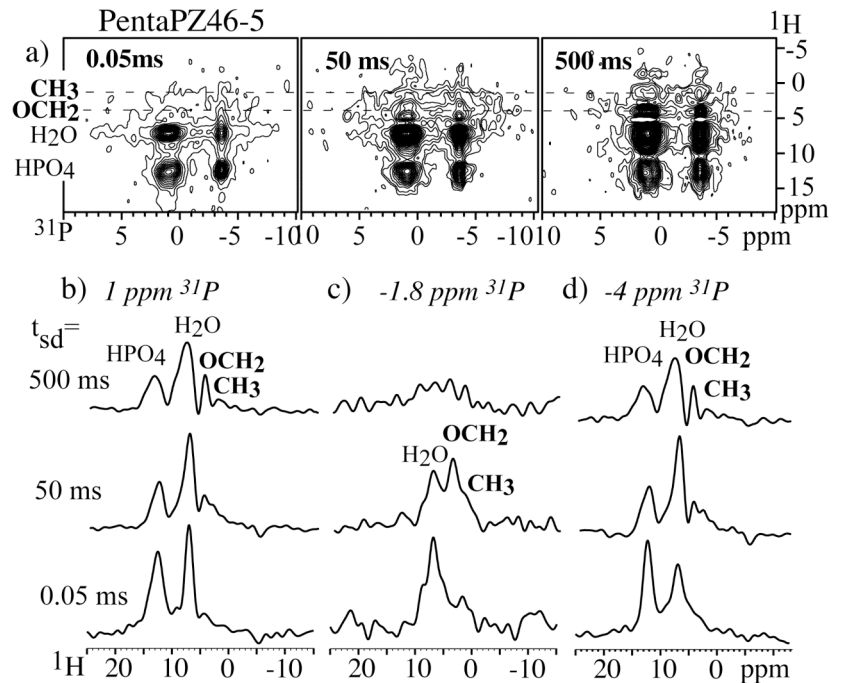


Fig. 1 a) 2D  $^1\text{H}$ - $^{31}\text{P}$  HETCOR spectra of PentaPZ46-5 with spin diffusion mixing times of 0.05 ms, 50 ms, and 500 ms. b), c) and d) are cross sections of the 2D spectra at 1.0,  $-1.8$  and  $-4.0$  ppm  $^{31}\text{P}$ .

**Proof of Templating by Small Angle Scattering:** Proof of templating of the inorganic phase by the polymer was obtained by small angle X-ray (SAXS) and neutron scattering (SANS) studies at Argonne. SAXS and SANS analyses were performed to

investigate the ordered superstructure of the polymer-based nanocomposites. The self-assembled PentaPZ46-5 copolymer gel both with and without the calcium phosphate phase showed distinct diffraction peaks in SANS (Fig 2). These peaks are contributions from several peaks, and the system exhibits fcc ordering of the micelles

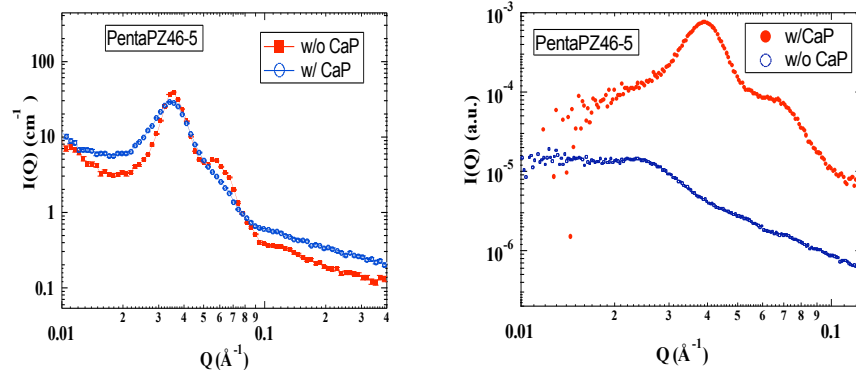


Fig. 2a) SANS and b) SAXS of PentaPZ46-5 polymer inorganic nanocomposites a featureless scattering curve, this proves conclusively that the polymer templates the CaP structure to a significant extent. The d-spacings of the gel structures of PentaPAA27-5 and PentaPAA36-5 were around 18 nm, and there was a reduction in the inter-particle distance with CaP.

TEM analysis of the diluted gel samples showed some of the polymer micelles surrounded with the calcium phosphate in the polymer gels and HRTEM experiments illustrated the crystalline phase in the amorphous polymer structures. TEM micrographs of 5 wt% PentaPAA and PentaPZ prepared in deionized water revealed approximately 15 nm spherical micelles (Fig. 3)

similar to that of Pluronic calcium phosphate nanocomposites gels observed by us previously.<sup>1</sup> With the addition of CaP, the peaks become more distinct, indicating a more ordered and compact superstructure in the presence of inorganic particles. The SAXS curves in Fig.2b show the same peak pattern for the nanocomposite. Given that the polymer by itself produces

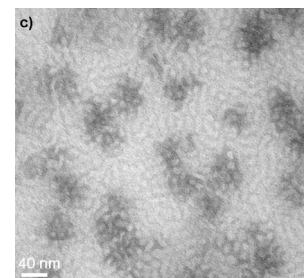


Fig. 3. TEM of PentaPAA36-5 diluted to 5 wt% polymer solution

which are in agreement with the SAXS and SANS results and our previous studies. In addition, atomic Ca/P ratio of 1.9 was also observed for PentaPAA36-5, indicating the presence of a second calcium phosphate phase other than brushite, which supports the solid state NMR findings. NMR identification of calcium phosphates for PentaPAA27-5 showed two relatively sharp bands that agree with the chemical shifts of brushite and hydroxyapatite. This is fully consistent with the XRD analysis of this sample. The spectra of PentaPAA36-5 and PentaPZ46-5 showed multiple peaks or shoulders, which might arise from different phases or from different sites in the unit cell of one phase. In order to distinguish these two situations, we performed  $^{31}\text{P}$  2D exchange experiments. The PentaPAA36-5 was found to contain crystalline brushite and a partially disordered phosphate component at a molar ratio of 12:88. The latter has particle thicknesses  $< 2$  nm, while the brushite crystallites are larger. This shows the power of NMR and other complementary techniques to completely characterize the size and composition of the bioinspired nanocomposite. The experimental studies of nanocomposite formation and characterization using a bottom-up approach were complemented by theoretical investigations using coarse grained MD simulations to theoretically predict the pure phases of the polymers, and the self-assembly of the polymers in the presence of the inorganic phase.

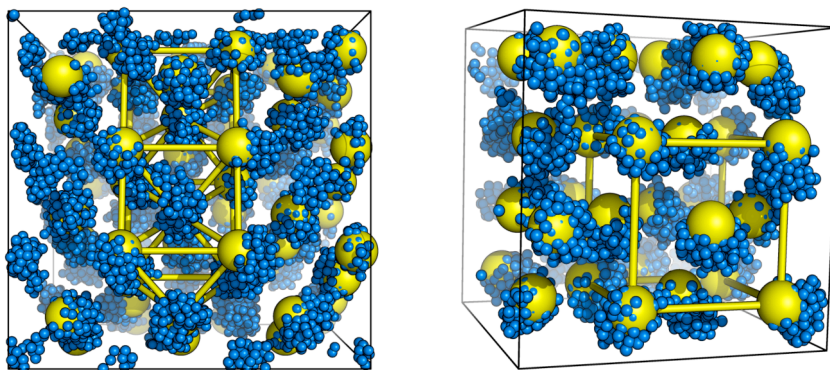


Fig. 4: (Left) Example of a snapshot of a bcc phase at 15% volume of the coarse grained F127. (Right) Example of a 20% simulation showing a fcc phase. Only hydrophobic blocks are shown. The yellow spheres are the positions of the center of mass micelles in real space

#### Prediction of phase diagrams of pure and functionalized Pluronic systems:

We have developed coarse-grained models both considering the solvent explicitly<sup>5</sup>, suitable to investigate properties of single micelles, and implicitly<sup>6</sup>, thus allowing the investigation of entire phase diagrams. The key assumption in our models is that the hydrophobic effect is entirely responsible for the strong temperature sensitivity of Pluronic, and that the kinetic temperature is a fixed parameter. The different interactions are modeled as Lennard-Jones type potentials. Examples of bcc and fcc phases of Pluronic are shown in Fig. 4. In all cases, the analysis of the structure factor displayed at least the first 40 Bragg peaks for each structure, thus providing a very stringent phase identification.

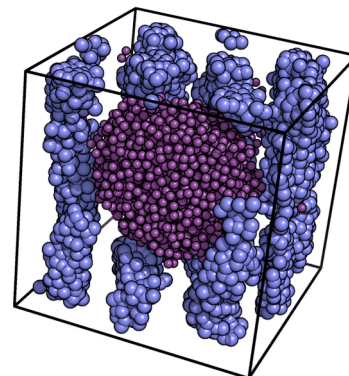
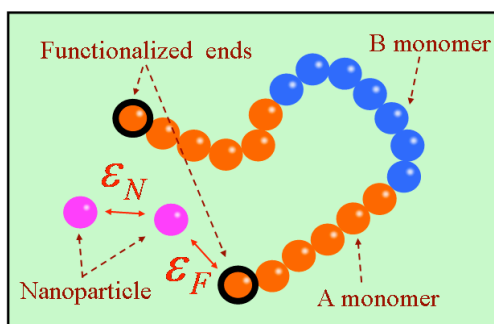


Fig. 5: (Left) Functionalized triblock interacting with inorganic nanoparticles. The model has two parameters  $\epsilon_N$ , the nanoparticle-nanoparticle attractive energy, and  $\epsilon_F$ , the attractive energy of each functionalized end with the nanoparticles. (Right) nanoparticles aggregating, showing the inability of non-functionalized copolymers to template inorganic phases

Block copolymer gels as templates for nanocrystalline self-assembly: The goal is to establish general conditions for an inorganic phase to crystallize following the mesoscopic order imposed by a polymeric matrix, which serves as a template. Our simulations have considered Pluronic as template and calcium phosphates as

the inorganic phases. We model the inorganic phase as single beads, referred to as nanoparticles, which attract each other with a characteristic energy  $\epsilon_N$ , as schematically shown in Fig. 5. Nanoparticle attraction models the tendency of the inorganic phase to aggregate. In the absence of any particular affinity with the triblock, nanoparticles aggregate into a single crystal, that is, the polymeric matrix is not rigid enough to template the

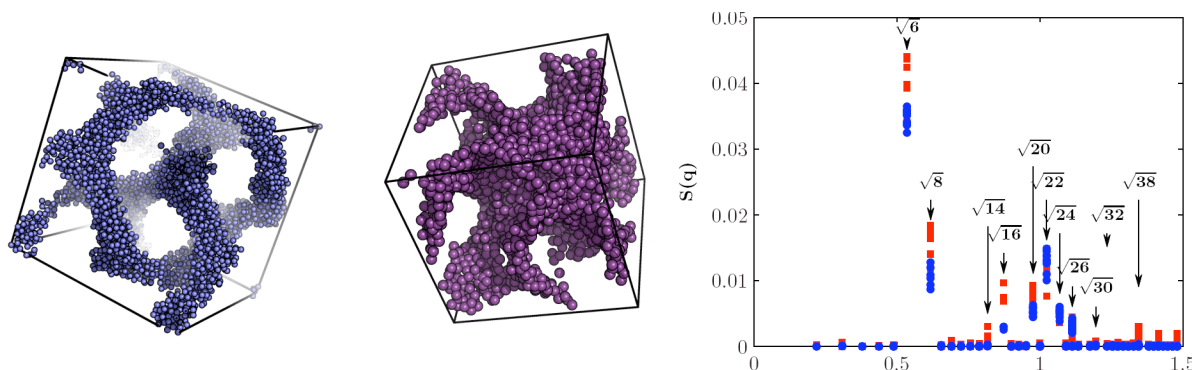


Fig. 6: (Left) Snapshot of a Gyroid phase of a functionalized triblock, where only the hydrophobic blocks are shown. (Center) Snapshot where only the nanoparticles are shown. (Right) The analysis of the structure factor shows the gyroid Bragg peaks (space group  $Ia\bar{3}d$ ), both for the hydrophobic blocks (•) and the nanoparticles (■).

inorganic phase, as shown in Fig. 5. Successful templating, however, follows for triblocks functionalized at their ends, modeled as an attractive interaction between nanoparticles and end-polymer beads, (Fig. 5). This is consistent with the experimental studies where the anionic and zwitterionic block polymers exhibited higher inorganic fractions and better templating compared to polar block copolymers. As  $\epsilon_F$  becomes of the order of  $k_B T$  each end polymer provides a nucleation center for nanoparticle crystal growth, and the system self-assembles into different lamellar and gyroid phases, with the crystalline inorganic phase displaying the mesoscopic order of the polymeric matrix. In Fig. 6, snapshots of a gyroid ( $Ia\bar{3}d$  space group) are shown, but the full phase diagram is extremely rich, and includes, for eg, gyroids with  $I4_132$  space group symmetry<sup>7</sup>.

In summary, a bottom-up approach to nanocomposite design was developed based on templating of calcium phosphates by hierarchically self-assembling polymer micelles. A combination of solid-state NMR, SAXS, SANS, and TEM provided valuable insights into the nanocomposite formation and templating processes. The complementary MD simulations mapped the phase diagram of the polymers with and without the inorganic.

**Future plans:** We plan to generalize this bottom-up approach for nanocomposite synthesis to other inorganic components such as titania and zirconia, that are of energy relevance, using selectively binding peptides attached to the ends of the polymer chains. In addition, block copolypeptides will be used as templates for the formation of nanocomposites. Motivated by the theoretical results, an exciting direction will be the investigation of functionalized Pluronic systems whose pure phases are hexagonally ordered, as our theoretical results clearly show that this provides an optimal scenario for successful templating of inorganic phases. Motivated by experiments, the models will investigate the robustness of the predicted new phases against more general functionalization protocols. This work was supported by the DOE-BES under Contract No. DE-AC02-07CH11358.

#### REFERENCES (DOE-BES sponsored publications – not a comprehensive list, due to space limitations)

1. D. Enlow, A. Rawal, M. Kanapathipillai, K. Schmidt-Rohr, S. Mallapragada, C. T. Lo, P. Thiyagarajan and M. Akinc, *J. Mat. Chem.* **17** (16), 1570-1578 (2007). Highlighted as a "hot" article.
2. M. D. Determan, J. P. Cox, S. Seifert, P. Thiyagarajan and S. K. Mallapragada, *Polymer* **46** (18), 6933-6946 (2005).
3. M. D. Determan, L. Guo, P. Thiyagarajan and S. K. Mallapragada, *Langmuir* **22** (4), 1469-1473 (2006).
4. S. Peleshanko, K. D. Anderson, M. Goodman, M. D. Determan, S. K. Mallapragada and V. V. Tsukruk, *Langmuir* **23** (1), 25-30 (2007).
5. Y. Chushak and A. Travesset, *The Journal of Chemical Physics* **123** (23), 234905-234907 (2005).
6. J. A. Anderson and A. Travesset, *Macromolecules* **39** (15), 5143-5151 (2006).
7. C.D. Knorowski, J.A. Anderson and A. Travesset, *Physical Review Letters* (submitted)



## Bioinspired Hybrid Elastic Nanomagnets

PIs: [Balaji Narasimhan](#), [Marit Nilsen-Hamilton](#), Ames Laboratory, Ames, IA 50011. Email addresses: [nbalaji@iastate.edu](mailto:nbalaji@iastate.edu), [marit@iastate.edu](mailto:marit@iastate.edu)

Research Team: D. Bazylinski, P. Canfield, M. Lamm, B. Narasimhan, M. Nilsen-Hamilton, S. Mallapragada, P. Palo, R. Prozorov, T. Prozorov, J. Schmalian, R. Sknepnek, A. Travesset, L. Wang

**Program Scope:** The world of biology offers a deep, mainly unexplored source of molecules, architectures and inspiration for the development of new materials and processes. Nature has numerous examples of hybrid self-assembly; for example, many migratory birds and animals and magnetotactic bacteria have been found to contain magnetoreceptors, which are aggregates of magnetite ( $\text{Fe}_3\text{O}_4$ ) nanocrystals. Magnetotactic bacteria have magnetosomes, which are unique intracellular magnetite nanoparticles surrounded by lipid bilayers and aligned in chains that are fixed within the cell and act as a tiny 'magnetic compass' (1). The nanostructure of the hybrid system is crucial for its function (e.g., homing) and is facilitated by mineralization proteins (2). The ability to tailor hybrid materials to exhibit bioinspired behavior such as hierarchical self-assembly *independent of living organisms* opens up possibilities for the design of robust materials with unique properties relevant to DOE's mission such as quantum computing, magnetic actuators, spintronics etc. To mimic these living systems, we have designed hierarchically self-assembling multiblock polymeric materials that serve as templates for the directed growth of nanocrystals in a process mediated by mineralization proteins. This facilitates a bottom-up approach to form novel macroscale functional elastic materials with ordered and controlled placement of magnetic nanocrystals.

The use of bacterial mineralization proteins to create magnetic nanoparticles *in vitro* offers the potential for facile synthesis of uniform magnetic nanocrystals with desirable morphologies and magnetic properties. We have shown that Mms6, a magnetosome membrane-associated protein from *M. magneticum* strain AMB-1, possesses the ability to template the formation of magnetite ( $\text{Fe}_3\text{O}_4$ ) nanocrystals (3) *in vitro* and we have extended this bioinspired approach to make it more general for the synthesis of complex magnetic nanoparticles such as cobalt ferrite nanocrystals (4), which are not normally found in living organisms.

**Recent Progress:** We have cloned and expressed Mms6 protein from magnetotactic bacteria in *E. coli* and used a self-assembling polymer template to control the ordered placement of magnetic nanocrystals in an elastic matrix, while minimizing aggregation of the magnetic nanoparticles. A key hypothesis was that the viscosity of the reaction media is an important factor in the formation of

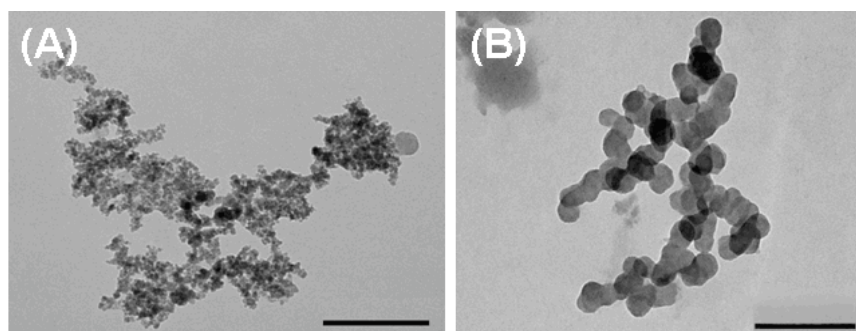


Figure 1. TEM images of magnetite nanoparticles obtained by co-precipitation of  $\text{FeCl}_2$  and  $\text{FeCl}_3$ : (A) without protein, (B) with Mms6. Scale bar: 200 nm (from Ref. 3).

uniform magnetite nanocrystals. Our multi-scale assembling triblock copolymer is a Pluronic<sup>®</sup> F127 copolymer that undergoes thermoreversible gelation to mimic the synthetic environment and diffusion limitations within a living organism. We have used these copolymers together with Mms6 to chemically synthesize magnetic nanocomposites containing magnetite nanoparticles (3). We have demonstrated that, in the presence of recombinant

histidine tagged Mms6 (his-Mms6), magnetite nanoparticles with similar size and shape to the bacterial magnetite can be synthesized *in vitro*.

The protein-free magnetite nanoparticles (Fig. 1A) showed significant size and shape dispersity. In contrast, Mms6 appears to facilitate the formation of uniform magnetite nanoparticles in solution with defined morphology, with a mean crystallite size of ca. 30 nm, as seen in Fig. 1B. None of several other control proteins studied (ferritin, BSA, Lcn2) were found to promote nanocrystal formation with the same size and shape as the Mms6-mediated particles.

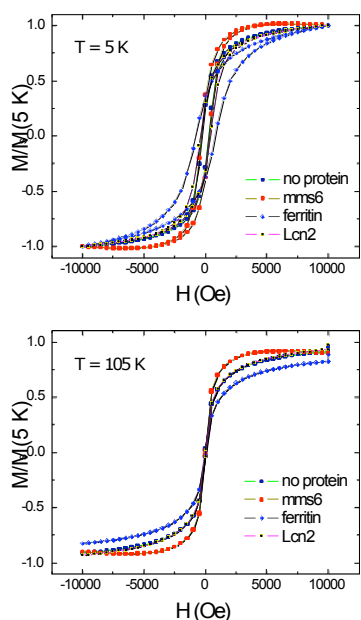


Figure 2. Normalized  $M(H)$  loops for different samples as described in the text. Upper frame: at  $T=5$  K (below  $T_B$  temperature); lower frame: at  $T=105$  K (above  $T_B$ ) (from Ref. 3)

In addition, magnetic property measurements show that the Mms6-derived magnetite nanoparticles show large magnetization values above the blocking temperature ( $T_B$ ) as well as large magnetic susceptibility. The superparamagnetic nature of the nanoparticles was established by comparing zero-field cooling (ZFC) and field-cooling (FC) curves. The characteristic  $T_B$  determined from the maximum of the ZFC curve in 500 Oe applied field was between 30 and 50 K for all samples studied. Fig. 2 shows magnetization loops for different samples, normalized to the saturation value obtained at  $H=5$  Tesla. The width of the hysteresis loops is indicative of the collective barrier strength in the blocked state; the steepness of the  $M(H)$  curve at low fields is related to the effective magnetic moment of individual nanoparticles. From Fig. 2, the largest hysteresis below  $T_B$  was observed for the ferritin-derived sample, which is consistent with a strongly interacting assembly of small particles. However, the magnetization curve in the material obtained with Mms6 climbed to saturation in smaller fields, which is indicative of a higher magnetic moment per particle. Its hysteretic behavior is similar to that of the protein-free and the His-Lcn2-derived samples. At temperatures well above the  $T_B$  (lower frame in Fig. 2), hysteresis is negligible in all the samples.

When the magnetic field was turned off at 5 K after completing the FC-C measurements, there is remanent (trapped) non-equilibrium magnetization determined by both collective barrier and individual coercivities of nanoparticles. Below  $T_B$ , remanent magnetization is mostly determined by the collective barrier; above  $T_B$ , only individual coercivities contribute. The individual particle coercivity is significantly enhanced in crystalline and well-shaped particles. The magnetite particles formed in the presence of Mms6 showed large remanence lasting well above  $T_B$ . Such behavior is

indicative of a larger magnetic moment per particle and consistent with presence of magnetite with a well-defined crystalline structure (1).

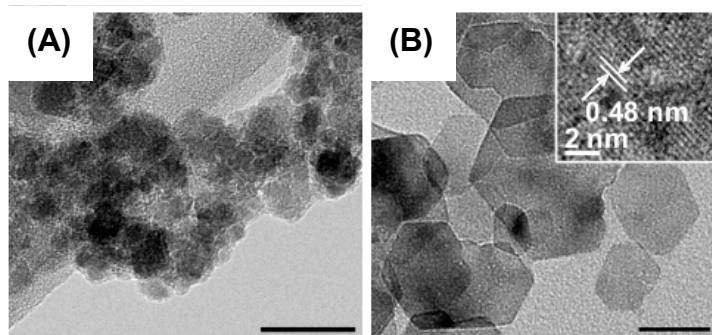


Figure 3. TEM of  $\text{CoFe}_2\text{O}_4$  nanocrystals obtained (A) in the presence of unbound *c25-mms6*; (B) in the presence of Pluronic<sup>®</sup> conjugated *c25-mms6*. Inset: high-resolution TEM image of a fragment of the central particle with a lattice spacing of 0.48 nm between the (111) planes. The scale bar in all images is 50 nm (from Ref. 4).

This bioinspired pathway can be used to synthesize complex and highly magnetic nanocrystals such as cobalt ferrite, which are *not* known to occur in living organisms. Two forms of Mms6 were used: a recombinant polyhistidine-tagged full-length Mms6 (His-Mms6), and a synthetic C-terminal domain of this protein containing 25 amino acids (*c25mms6*). To control placement of the nanocrystals and to minimize nanoparticle aggregation, the proteins were covalently attached to the

Pluronic<sup>®</sup> using N-hydroxysuccinimide chemistry. These were used to template hierarchical CoFe<sub>2</sub>O<sub>4</sub> nanostructures from aqueous solution via the oxidative co-precipitation of Fe<sup>2+</sup> and Co<sup>2+</sup>. This new biosynthetic pathway enables facile room-temperature shape-specific synthesis of complex magnetic crystalline nanoparticles in the range of 40-100 nm (Fig. 3) that are difficult to produce using conventional techniques. The c25mms6 forms nanoparticles *in vitro* that are smaller in size (15-20 nm; Fig. 3A). Larger particles of 50-80nm diameter are produced when c25mms6 is covalently linked to Pluronic<sup>®</sup> (Fig. 3B).

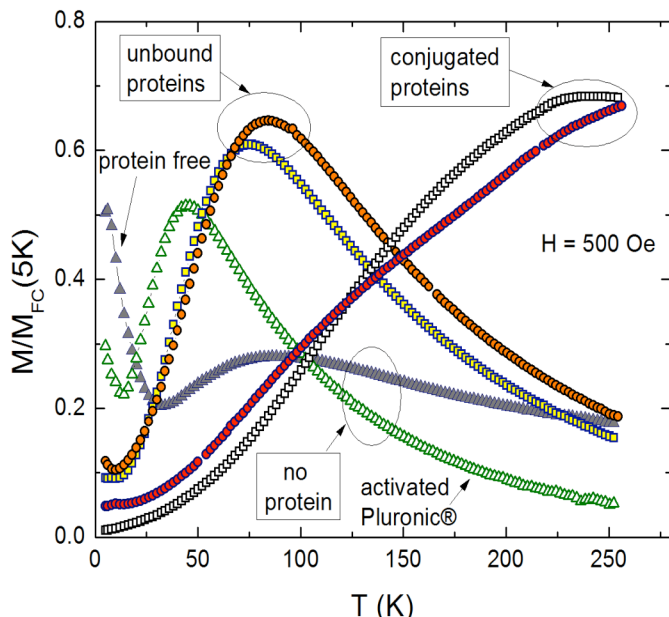


Figure 4. Zero-field cooled measurements for the CoFe<sub>2</sub>O<sub>4</sub> samples. There is significant difference in the  $T_B$  between the samples without the biomineralization proteins, with unbound *his*-mms6 and c25mms6 (two middle curves) and conjugated *his*-mms6 and c25mms6, which have the largest  $T_B$  (from Ref. 4).

In terms of magnetic properties, nanoparticles grown in the activated Pluronic<sup>®</sup> without proteins exhibit the lowest  $T_B$  (Fig. 4). Nanoparticles grown in Pluronic<sup>®</sup> gels with either unbound c25mms6 or unbound *his*-mms6 show an elevated  $T_B$ . Finally, nanocrystals grown in the presence of protein-conjugated Pluronic<sup>®</sup> show the largest  $T_B$  values. These results are consistent with the TEM images (Fig. 3), indicating large well-formed particles grown in the presence of Pluronic<sup>®</sup> conjugated *his*-mms6 and c25mms6.

Although the mechanism by which Mms6 promotes nanoparticle formation is yet unknown, the protein is hypothesized to act as a template by multimerizing and forming a surface of negative charges that align the metal ions and initiate crystal formation. To gain a better understanding of how Mms6 interacts with the Pluronic<sup>®</sup> to promote or initiate magnetite crystallization, we have devised a simple coarse-grained bead-spring model (5) shown in Fig. 5. We found a rich phase diagram with a number of distinct phases (Fig. 6a), including two

uncommon phases: a novel square-columnar phase (Fig. 6b) and the gyroid phase. The square columnar phase likely results from the optimal packing of cylinders of different diameters. Models of the interaction between protein and Pluronic<sup>®</sup> show that the spatial organization of protein multimers can be driven by the polymer environment.

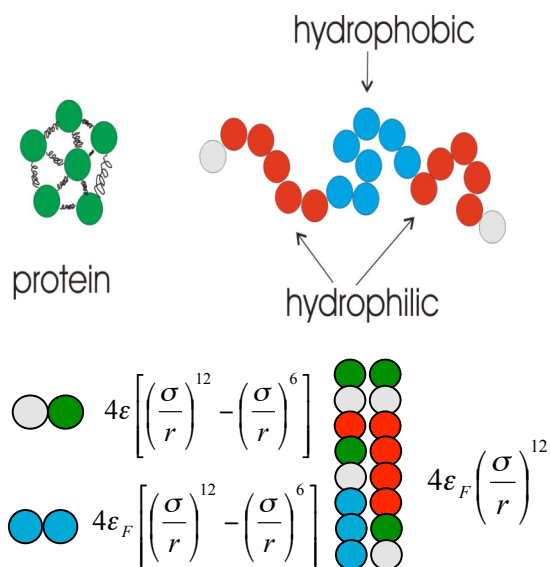
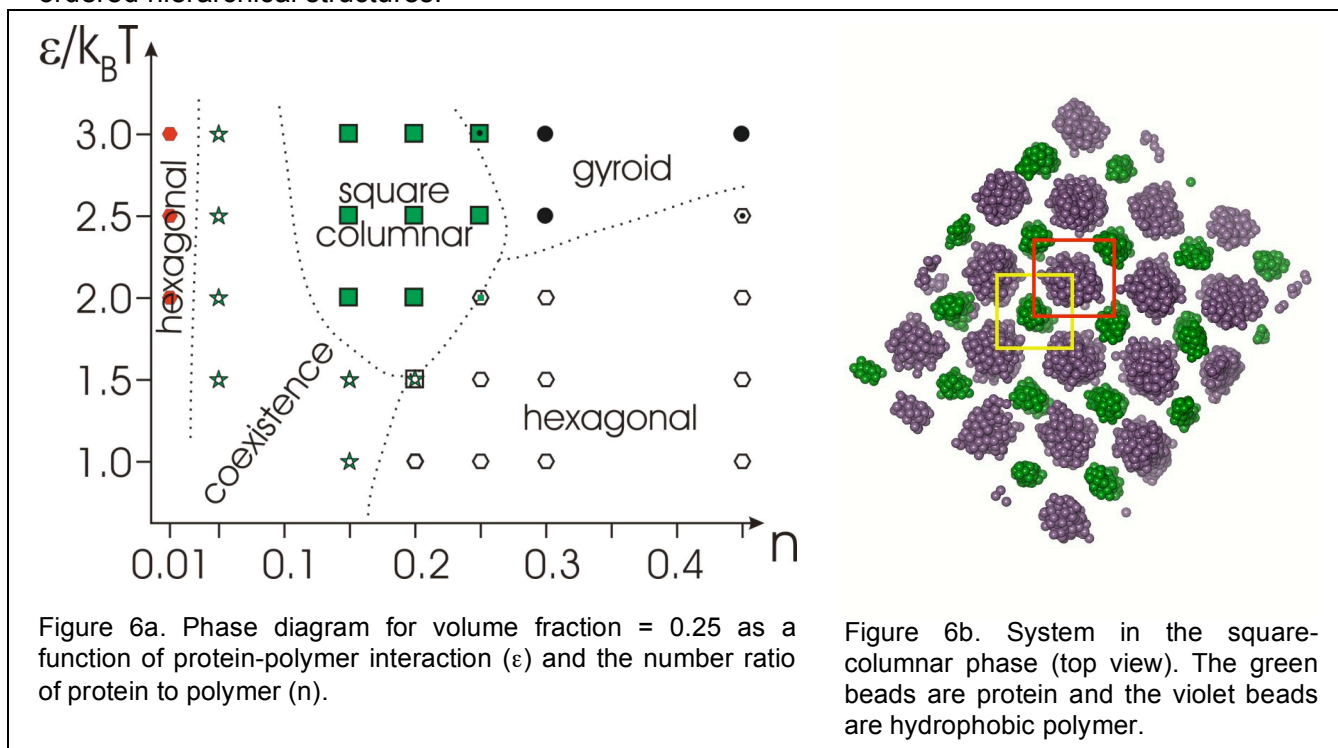


Figure 5. Top: Coarse-grained bead spring model for protein in Pluronic<sup>®</sup>. Bottom: Interactions between different beads.  $\epsilon_F = \sigma = 1$ ,  $\epsilon$  is the only tuning parameter.

**Future Work:** Our ongoing work is focused on multiple avenues. We are currently investigating the molecular mechanisms of nanocrystal formation due to protein templating using a combination of small angle scattering, electron microscopy, and solid state NMR. The mechanism by which Mms6 promotes magnetite crystallization will be investigated biochemically by examining the role of specific amino acid residues in the C-terminal domain. In parallel, we are investigating the development of aptamers for non-covalent and reversible attachment of the proteins to the self-assembling polymers. Simulations are currently underway to investigate how varying the

relative sizes of protein to polymer affects template formation. We plan to include the actual magnetic nanoparticles into our model. Finally, we are pursuing the creation of arrays of nanoparticles by exploiting the ability of the conjugated Mms6 conjugated with the Pluronic<sup>®</sup> to form ordered hierarchical structures.



**Acknowledgments:** This work was supported by the DOE-BES under Contract No. DE-AC02-07CH11358.

#### References (DOE-BES supported work indicated by an asterisk)

- \*1. Prozorov, R., T. Prozorov, S.K. Mallapragada, B. Narasimhan, T.J. Williams, and D.A. Bazylinski, Magnetic irreversibility and the Verwey transition in nanocrystalline bacterial magnetite. *Phys. Rev. B*. **76**: 055476, 2007
2. Arakaki, A., J. Webb, and T. Matsunaga, A novel protein tightly bound to bacterial magnetic particles in *Magnetospirillum magneticum* strain AMB-1. *Journal of Biological Chemistry*. **278**(10): 8745-8750, 2003
- \*3. Prozorov, T., S.K. Mallapragada, B. Narasimhan, L. Wang, P. Palo, M. Nilsen-Hamilton, T.J. Williams, D.A. Bazylinski, R. Prozorov, and P.C. Canfield, Protein-mediated synthesis of uniform superparamagnetic magnetite nanocrystals. *Adv. Funct. Mater.* **17**: 951-957, 2007
- \*4. Prozorov, T., L. Wang, P. Palo, M. Nilsen-Hamilton, D. Jones, S.K. Mallapragada, B. Narasimhan, P.C. Canfield, and R. Prozorov, Cobalt ferrite nanocrystals: Outperforming magnetotactic bacteria. *ACS Nano* (Submitted)
- \*5. Anderson, J.A. and Travasset, A., Coarse-grained simulations of gels of nonionic multiblock copolymers with hydrophobic groups. *Macromolecules*. **39** (15): 5143-5151, 2006
- \*6. Peleshanko, S., K.D. Anderson, M. Goodman, M.D. Determan, S.K. Mallapragada, and V. Tsukruk, Thermoresponsive behavior of multistimuli Pluronic<sup>®</sup>-based pentablock copolymers at the air-water interface. *Langmuir*. **23**: 25-30, 2007. Invited article
- \*7. Determan, M.D., P. Thiyagarajan, and S.K. Mallapragada, Supramolecular self-assembly of multiblock copolymers in solution. *Langmuir*. **22**: 1469-1473, 2006
- \*8. Westfahl, H. and J. Schmalian, Correlated disorder in random block copolymers. *Phys. Rev. E*. **72**: 011806, 2005

## Program Title: Solid-State NMR of Polymers and Nanocomposites

**Principal Investigator:** Klaus Schmidt-Rohr, Ames Laboratory and Department of Chemistry, Iowa State University, Ames IA 50011. srohr@iastate.edu

**Contributors:** Surya K. Mallapragada, Mufit A. Akinc. **Coworkers:** A. Rawal, E. Levin

### Program Scope

We develop and apply advanced solid-state nuclear magnetic resonance (NMR) methods to elucidate the composition, supramolecular structure, and dynamics of heterogeneous polymer-based systems, with an emphasis on nanocomposites. Our studies of the bone nanocomposite were initiated by our involvement in a subtask on Bioinspired Nanoscale Hybrid Materials and now greatly benefit our work in both subtasks. In our investigations of nanostructured materials, we combine our detailed NMR characterization, for instance using the novel X{<sup>1</sup>H} HARDSHIP method, with new approaches in the quantitative analysis of scattering data.

Our program covers the development of NMR methods not only for biological nanocomposites but also for synthetic polymers such as the Nafion fuel-cell membrane. In this Abstract, we will focus on the aspects of our program with bio-relevance. This work is tightly integrated with a subtask on biomimetic nanocomposites led by Drs. Surya Mallapragada and Mufit Akinc.

### Recent Progress

#### NMR Methods for Characterizing Biological and Biomimetic Nanocomposites

**Proof of nanocomposite formation by NMR.** While it is well established that NMR can determine the composition of materials, we have shown now that it is also an excellent method for proving formation of an organic-inorganic nanocomposite. This can be achieved by two-dimensional <sup>1</sup>H-<sup>31</sup>P heteronuclear correlation NMR experiments with <sup>1</sup>H spin diffusion, where cross peaks between polymer protons and inorganic phosphate prove the intimate contact between the organic and inorganic phases that is the characteristic of nanocomposites. Such cross peaks are not observed at short spin diffusion times, where the phosphate “sees” only the nearest protons, i.e. those in the inorganic phase. In a nanocomposite, the polymer proton peaks appear within tens to hundreds of milliseconds of spin diffusion, see Figure 1a. The corresponding dramatic change in the heteronuclear correlation spectra are indeed observed in a biomimetic blockcopolymer—calcium phosphate nanocomposite prepared by the Mallapragada and Akinc groups, PentaPAA36-5, see Figure 1. Figure 1a shows contour plots of the 2D spectra for 0.05 ms, 5 ms, and 50 ms. Cross sections along the <sup>1</sup>H dimension, taken at 1.4 and 4.7 ppm in the <sup>31</sup>P dimension, are shown in Figure 1b,c. Within 50 ms, the polymer proton (OCH<sub>2</sub> and CH<sub>3</sub>) peaks have become completely dominant.

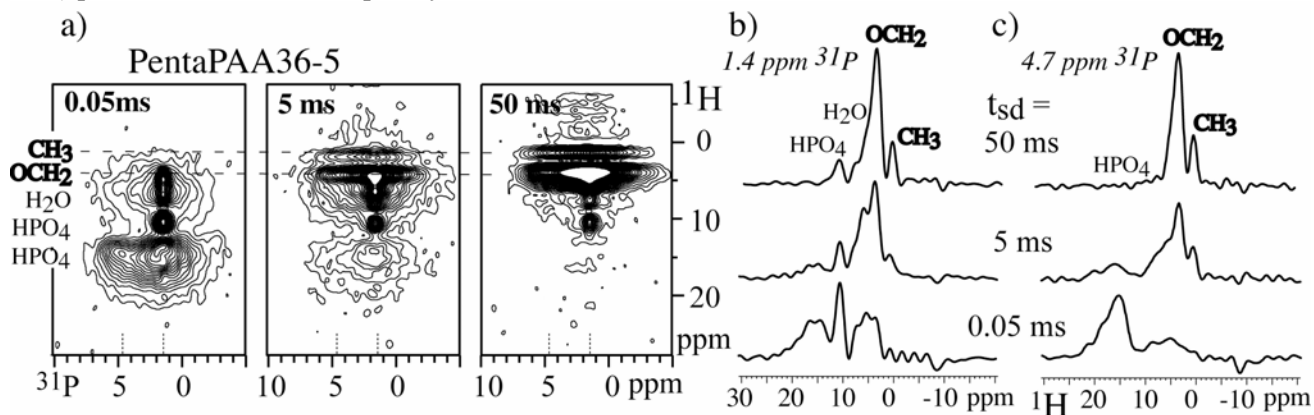


**Figure 1.** 2D <sup>1</sup>H-<sup>31</sup>P HETCOR spectra of a pentablock copolymer—calcium phosphate nanocomposite, PentaPAA36-5, with spin diffusion mixing time of a) 0.05 ms, b) 5 ms, and c) 50 ms. e) and f) are cross sections of the 2D spectra at 1.4 and 4.7 ppm <sup>31</sup>P.

**Domain thickness from  $^{31}\text{P}\{^1\text{H}\}$ HARDSHIP NMR.** The  $^1\text{H}$  spin diffusion method requires that there are protons within the inorganic phase, at a significant concentration. If that is not the case, for instance in hydroxyapatite, we can use a complementary method based on the strongly distance-dependent dipolar couplings between  $^{31}\text{P}$  in the nanoparticles and the protons in the polymer matrix, see Figure 2a. The couplings of  $^{31}\text{P}$  to dispersed protons within the inorganic phase, which would interfere with this approach if simple  $^{31}\text{P}\{^1\text{H}\}$  REDOR was used, are refocused in our recently introduced  $^{31}\text{P}\{^1\text{H}\}$  HARDSHIP method. The pulse sequence alternates heteronuclear recoupling for  $\sim 0.15$  ms with periods of homonuclear dipolar dephasing that are flanked by canceling  $90^\circ$  pulses, see Figure 2b,c. The HARDSHIP dephasing curve reflects the specific surface (surface-to-volume ratio) of the inorganic phase, with an accuracy that is significantly greater than that of  $^1\text{H}$  spin diffusion in nanocomposites.  $^{31}\text{P}\{^1\text{H}\}$  HARDSHIP dephasing in plates of 4-nm thickness or spheres of 12-nm diameter can be observed quite easily. Applications to a clay-polyvinylalcohol nanocomposite and the apatite-collagen nanocomposite in bone are shown in Figure 2d,f. This method, combined with a variant where the dephasing by the dispersed protons is switched on selectively, has proven that carbonate is incorporated into bioapatite, at an intermediate depth, not as a surface or central nucleation layer.

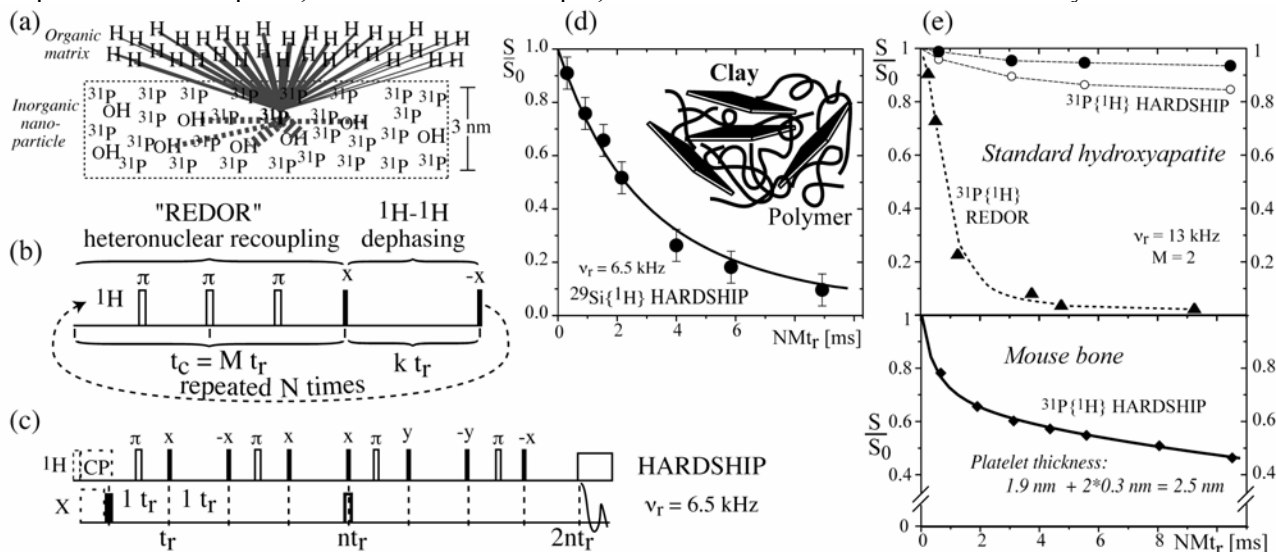


**Figure 2.** (a) Illustration of the principle of depth and thickness measurements in nanocomposites using  $^1\text{H}$ -X (X =  $^{31}\text{P}$  in the figure) dipolar couplings. (b) Basic cycle of HARDSHIP, which alternates heteronuclear recoupling with periods of transverse  $^1\text{H}$  coherence. (c) Implementation for spinning frequencies near 6.5 kHz. (d) Application to a clay-polymer nanocomposite. (e) Application to (top) standard hydroxyapatite, where REDOR produces strong dephasing due to OH protons, while this is avoided by HARDSHIP NMR. Bottom: HARDSHIP dephasing of phosphorus in apatite by collagen protons in mouse bone.

**The nanocomposite in bone.** The load-bearing material in bone is a nanocomposite of  $\sim 3$ -nm thick apatite (calcium phosphate) platelets imbedded in a collagen matrix, with a volume ratio typically near 45:45 and the remaining 10% accounted for by water. Being a target for biomimetic materials synthesis, the composition of bone apatite needs to be known more accurately. We have quantified it by multinuclear ( $^{31}\text{P}$ ,  $^1\text{H}$ ,  $^{13}\text{C}$ ,  $^{23}\text{Na}$ ) NMR spectroscopy combined with energy-dispersive analysis (EDA), and measured the depth distribution of the various ions by HARDSHIP NMR. Now we are looking at and across the apatite-collagen interface.

**Collagen residues at the interface with apatite.** The organic moieties at the organic-inorganic (collagen-apatite) interface in bone have been identified by  $^{13}\text{C}\{^{31}\text{P}\}$  rotational echo double resonance (REDOR) NMR, which provides selective spectra of carbon near phosphate, see Figure 3b. The resonances of interest were further analyzed by spectral editing and two-dimensional NMR experiments. It has been suggested that the resonances should be assigned to sugar rings. Our data disprove this, and instead support assignment to COH in hydroxyproline with unusual hydrogen bonding and to COOH in glutamate residues. Quantitative analysis of the  $^{13}\text{C}\{^{31}\text{P}\}$  REDOR data show that COO $^-$  of the glutamate and hydroxyproline C $_7$ OH are at a distance of  $\sim 0.5$  nm from the apatite surface phosphorus, consistent with an intervening water layer.

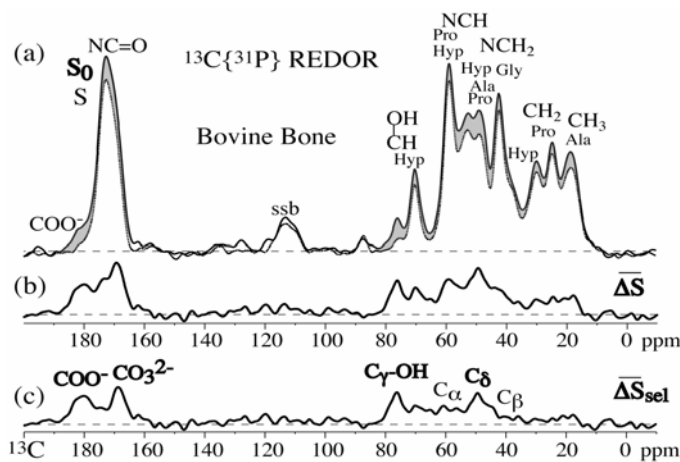


**Figure 3.**  $^{13}\text{C}\{^{31}\text{P}\}$  REDOR spectra of bovine bone. (a) Full spectrum (“ $S_0$ ”) and spectrum with recoupled dipolar dephasing (“ $S$ ”) with the shaded areas indicating the dephasing. (b) Total regular-difference spectrum ( $\Delta S$ ) of carbons near phosphorus (summed for spectra with,  $Nt_r = 3$  ms, 4.66 ms, 6 ms and 7.66 ms) and (c) total scaled-difference spectrum. The spectrum  $S$  was scaled up by 1.1 to match the 42-ppm peak of Gly in  $S_0$  and thus reduce contributions from the long-range dephasing of all collagen residues. Total measuring time: 19 days.

**Water at the apatite-collagen interface.** Two major forms of water are detected at the interface: Strongly bound molecules (Figure 4c), and a layer of more mobile but still viscous water (Figure 4a,b). The location of both types of water at or near the organic-inorganic interface is proved by fast transfer of magnetization to  $^{31}\text{P}$  in apatite and to  $^1\text{H}$  in collagen, Figure 4d,e. The rotational correlation time of the mobile water estimated from its  $T_{1\rho}$  indicates that it is  $10^6$  times more viscous than liquid water. Each of the water components accounts for 7% of the sample volume, while collagen makes up 41% and apatite 45%. This indicates that the mobile water layer is monomolecular.

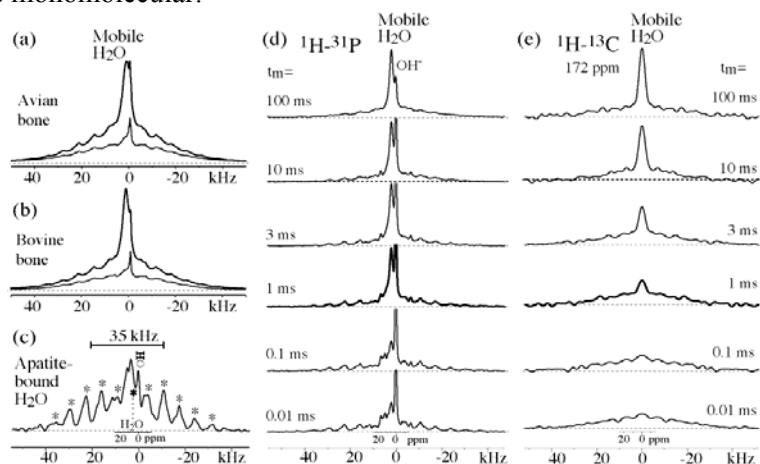


**Figure 4.** (a) Top trace:  $^1\text{H}$  spectrum of avian bone (after background suppression). Bottom trace: Same after 2.2-ms  $T_{1\rho}$  filtering. The partially narrowed signal at 5 ppm is suppressed. (b) Same as (a) for bovine bone. (c)  $^1\text{H}$  spectrum of bound water near  $^{31}\text{P}$  after  $T_2$  and  $T_{1\rho}$  filtering (avian bone), obtained in a  $^1\text{H}$ - $^{31}\text{P}$  WISE experiment. Dipolar sidebands are marked by \*. (d, e): Series of cross sections from (d)  $^1\text{H}$ - $^{31}\text{P}$  WISE and (e)  $^1\text{H}$ - $^{13}\text{C}$  WISE spectra of bovine bone with increasing duration  $t_m$  of  $^1\text{H}$  spin diffusion. The faster transfer from the mobile water to  $^1\text{H}$  near  $^{31}\text{P}$  proves that the mobile, viscous water is at the apatite surface.

Figure 5 shows a model of the collagen-bioapatite interface on the basis of these data, where the viscous mobile water acts as “glue” between collagen and the apatite nanocrystals.

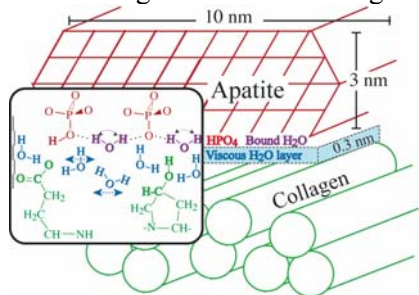


**Figure 5.** Model of the apatite-collagen interface, based on our NMR measurements, such as the  $^{13}\text{C}\{^{31}\text{P}\}$  REDOR spectra shown at the bottom. An enlarged molecular-scale view is shown in the square on the left. Blue double arrows indicate rotational and translational mobility of water molecules.

### Future plans

**Size and shape of nanocrystallites in bone.** To determine the size and shape of bioapatite crystals in bone, we will simultaneously simulate high-quality HARDSHIP data, wide-angle X-ray diffraction (using a numerical evaluation of the Debye formula), and SAXS data (using our numerical-FT algorithm) obtained on the same samples. The smooth Porod region in SAXS proves a distribution of thicknesses, which will be a primary parameter in the new simulations. The thickness of the collagen layers, which is constrained by the known volume fractions, will be analyzed by simulations of  $^{13}\text{C}\{^{31}\text{P}\}$  REDOR and  $^1\text{H}$  spin diffusion data.

**Hyp conformation and dynamics at the interface.** The apatite-bound and interior hydroxyproline (Hyp) CH-OH moieties show a significant difference in  $^{13}\text{C}$  NMR (75 vs. 70 ppm, respectively, see Figure 3). Whether the 5-ppm  $^{13}\text{C}$  chemical-shift difference is due to a different conformation or due to different H-bonding is presently unknown. In order to characterize these binding sites in more detail, we will study the relation between chemical shift and conformation or H-bonding in model peptides. The five-membered ring in Hyp and Pro is known to take differently puckered conformations, see Figure 6, which can interconvert. Slow dipolar dephasing of the 75- but not the 70-ppm Hyp signal shows that the ring of the former undergoes larger-amplitude dynamics. It has the longer  $T_{1\rho}$  relaxation time, which suggests that the motion is in the fast-motion regime. We will test this hypothesis by variable-temperature measurements of  $T_{1\rho}$ .

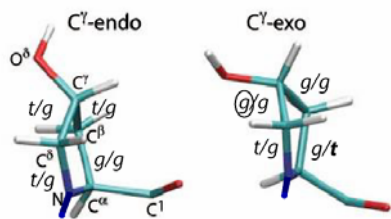


**Figure 6.** Conformations of the hydroxyproline ring. Figure adapted from Park et al., 2005. The bonds are labeled for the approximate trans (t) (anti) and gauche (g) conformations present. The gauche conformation stabilizing the exo pucker due to the gauche effect of the O-C-C-N dihedral angle is highlighted by an oval. The trans conformation that, according to the empirical  $\gamma$ -gauche effect, would produce a  $\sim 5$  ppm downfield shift of the  $\text{C}_\gamma$  resonance is highlighted in bold.

**Nanometer-scale structure of enamel from NMR.** The hardest material in mammals is the enamel covering their teeth, and it should thus serve as a good model for the bioinspired design of high-performance materials. Its inorganic component, like that of bone, consists of bioapatite. According to the literature, the organic fraction is low ( $\sim 2$  wt%, 6 vol%) and SEM pictures show crystalline rods with  $\mu\text{m}$ -diameters. This would suggest that the structural features of enamel are too large for studies by NMR. Nevertheless, in preliminary  $^{31}\text{P}\{^1\text{H}\}$  HARDSHIP experiments we have found significant dephasing for enamel from bovine teeth. We have also observed surface sites directly in  $^1\text{H}\{^{31}\text{P}\}$  and  $^{31}\text{P}$  NMR spectra. In addition, despite the reported small organic fraction, we have obtained a  $^{13}\text{C}$  NMR spectrum of enamel overnight. We plan to use  $^1\text{H}$ - $^{13}\text{C}$  WISE NMR with  $^1\text{H}$  spin diffusion to see whether the protein is within spin-diffusion range from the OH of enamel.

**Biomimetic nanocomposites.** Mallapragada, Akinc, and coworkers will prepare energy-relevant copolymer — titania and —zirconia nanocomposites using biomimetic approaches. We plan to perform  $^{47/49}\text{Ti}$ , and  $^{91}\text{Zr}$  HARDSHIP NMR on these samples, with signal enhancement being a crucial aspect.

**Biological silicates and carbonates.** Silicates in diatoms and carbonates in mollusk shells show intricate biological control of biomineralization. The single-cell diatoms produce a finely patterned cell wall consisting of amorphous silica and organic components such as silaffin cell-wall proteins and long-chain polyamines. These organic molecules exert a drastic influence on silica formation in vitro. For studies of *biocarbonate* mineralization, the abalone shell has been a prime candidate because of its highly repeating aragonite domains. The shell is a microlaminate composite material composed of 98 wt% calcium carbonate and 2 wt% organic material. The organic-inorganic composition of the nacre has a 3,000 times higher fracture resistance than pure aragonite. We will explore to what extent our  $\text{X}\{^1\text{H}\}$  HARDSHIP method, which we have successfully demonstrated on clay silicate and carbonate in bone, can provide structural information on these materials. The organic content is low and the inorganic particles are thought to be  $>$  tens of nm thick, but it is well possible that as in enamel, protonated surfaces and/or minor organic fractions still produce significant dephasing.  $^{29}\text{Si}$  and carbonate signal enhancement developed earlier in this program will be crucial for success of this project.

### Publications 2005-2007

*Related to this topic: (+ four publications not closely relevant to biomolecular systems)*

K. Schmidt-Rohr, A. Rawal, X.-W. Fang, “A new NMR method for determining the particle thickness in nanocomposites, using  $T_{2,H}$ -selective  $\text{X}\{^1\text{H}\}$  recoupling”, *J. Chem. Phys.* **126**, 054701-(1-16) (2007).

K. Schmidt-Rohr, “Simulation of Small-Angle Scattering (SAXS or SANS) Curves by Numerical Fourier Transformation”, *J. Appl. Cryst.* **40**, 16-25 (2007).

D. Enlow, A. Rawal, M. Kanapathipillai, K. Schmidt-Rohr, S. Mallapragada, C.-T. Lo, P. Thiyagarajan, M. Akinc, “Synthesis and Characterization of Self-assembled Block Copolymer Templated Calcium Phosphate Nanocomposite Gels”, *J. Mater. Chem.* **17**, 1570 – 1578 (2007).

*This work was supported by the Department of Energy-Basic Energy Sciences under Contract No. DE-AC02-07CH11358.*



## Collective Dynamics, Self-Assembly, and Mixing in Active Microparticle Ensembles

Igor Aronson

Materials Science Division, Argonne National Laboratory, 9700 S Cass Av, Argonne, IL60439,  
[aronson@msd.anl.gov](mailto:aronson@msd.anl.gov)

Raymond E. Goldstein

Department of Applied Mathematics and Theoretical Physics, Centre for Mathematical Sciences,  
University of Cambridge, Wilberforce Road, CB3 0WA, United Kingdom  
[R.E.Goldstein@damtp.cam.ac.uk](mailto:R.E.Goldstein@damtp.cam.ac.uk)

and

Department of Physics, Program in Applied Mathematics, and BIO5 Institute,  
University of Arizona, 1118 E. 4<sup>th</sup> St., Tucson, AZ 85721

### Program Scope

This project focuses on the emergent coherent dynamics found in ensembles of active microparticles at high volume fraction, where recent experiments have revealed novel, large-scale coherent structures which arise from hydrodynamic interactions between the particles. These structures are found in two complementary systems - electromagnetically-driven metallic microparticles and self-propelled micro-organisms such as bacteria and algae. They provide fundamental challenges to our understanding of collective flows, mixing, and transport in nonequilibrium systems. High-speed imaging, particle imaging velocimetry, and microrheology are used to characterize the dynamics and correlations in these systems, to provide benchmarks for the refinement of theories of such behavior, and to explore possible applications in nanoscale self-assembly, microfluidic mixing, and targeted drug delivery. Current activities include experimental and theoretical studies of the onset of collective behavior in ensembles of the swimming bacterium *Bacillus subtilis* in the confined geometry of thin film samples, rheology of bacteria-laden fluids, and fundamental studies of flagella-driven flows, mixing and transport in unicellular and multicellular volvocine green algae. Future directions encompass active control of bacterial motion by electric and magnetic fields, enhanced mixing due to bacterial stirring and its role in quorum sensing, and the physics of cytoplasmic streaming.

### Recent progress

Experiment: *Bacillus subtilis* are flagellated, rod-shaped micro-organisms, ~5 microns long and capable of swimming up to 20 microns/second. The hydrodynamic and chemical interactions between cells and with their environment result in remarkably rich collective behavior; self-concentration due to gradients of dissolved oxygen or pH, phase transitions and self-organization in confined geometries. The self-organization often takes the form of coherent structures with typical sizes that are many times larger than those of the individual bacteria. We have conducted experimental investigations of emergent collective behavior in dense bacterial populations in suspended liquid films with controlled thickness. Our studies led to a new way of controlling the density of bacteria and of separating living and dead cells by means of engineered electric fields. A key result was the experimental determination of the dependence of the scale of emergent dynamic structures on the concentration of cells. In a parallel investigation, we have continued the refinement of particle imaging velocimetry methods to characterize the

swimming correlations in thin, three-dimensional fluid drops of bacterial suspension, and studied the probability distribution of swimming velocities in the collective regime.

Theoretical Modeling: We have focused on generic biological systems of active particles exhibiting large-scale collective behavior: hydrodynamically interacting swimming bacteria. These bacteria are represented by self-propelled rods interacting via Stokesian hydrodynamic fields. Starting from a stochastic microscopic model of inelastically colliding polar rods with an anisotropic interaction kernel, we derive set of equations for the local concentration and orientation of the rods. This model shows that above a critical concentration the rods exhibit an orientational instability and thus the onset of large-scale coherence. This approach is applied to colonies of the swimming bacterium *Bacillus subtilis* confined in thin fluid films, so the model is formulated as thickness-averaged, two-dimensional equations for the local density and orientation of bacteria coupled to the Stokes equations for the fluid velocity. The collective swimming of bacteria is represented by additional source term in the fluid equations. We demonstrate that this system exhibits formation of dynamic large-scale patterns with the typical scale determined by the density of bacteria as observed in our experiments.

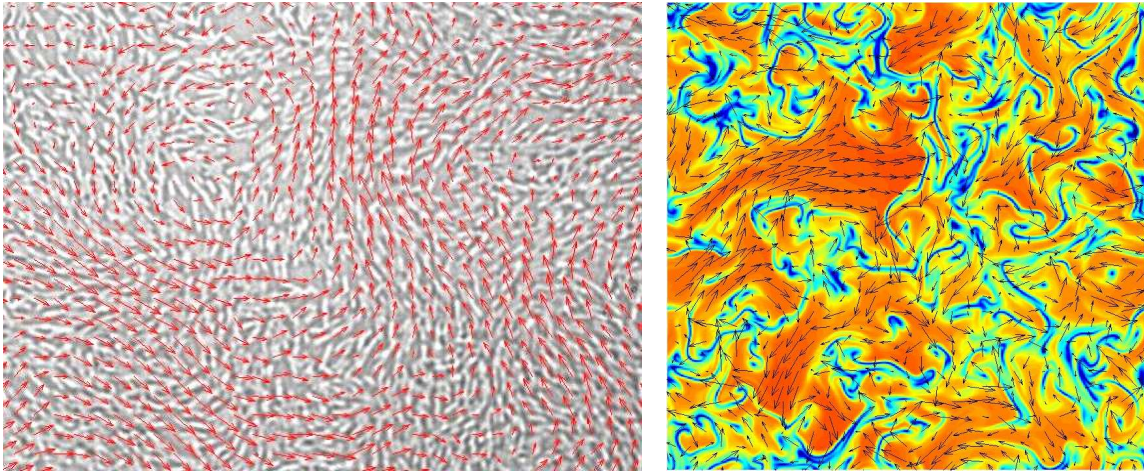


**Figure 1.** Left panel: large-scale collective flows generated by swimming bacteria (seen as short white rods, average length 5 microns) in a thin film. Arrows indicate the direction of the velocity field (maximum velocity is 80 microns/sec). Right panel: results of mathematical modeling, arrows indicate the velocity field, and colors depict the degree of local orientation (with red being the maximum).

## Future Plans

In our earlier studies, we demonstrated that bacteria can be effectively controlled, manipulated, and separated in the thin-film geometry. We propose to expand the frontiers of our research by developing an entirely new capability related to microrheological

studies. Related experiments indicate that bacteria greatly enhance diffusion of tracers in the film. This enhancement of the diffusion may in part be interpreted as a decrease of the effective viscosity of the fluid. The explanation of this phenomenon lies in the fact that bacteria convert chemical energy of the surrounding nutrient medium into mechanical energy of motion, and, thus, compensate for energy loss due to viscous dissipation. In order to probe the microrheology of the bacterial film directly, we propose conducting a series of dedicated experiments and development of new experimental techniques. In particular, we will measure directly the effective viscosity of the suspension as a function of bacterial density in the thin-film samples by creating controlled perturbations of the film by a moving microfiber. Since the suspensions of swimming bacteria are likely non-Newtonian fluids, we will explore the frequency dependence of viscosity. We expect to discover elastic properties of the bio-suspension and study the dynamics of the ensemble of bacteria in systems of different sizes (from 50 microns to 2 mm) confined within fluid films (open film geometry) and thin channels (microfluidic devices).

Later, we plan to use a non-invasive technique: attaching small magnetic tracer particles to *B. subtilis* cells or using the bacterial species *Magnetospirillum* that synthesizes internal magnetic particles termed “magnetosomes”. The hydrodynamic flows will be created directly by exposing the film to an alternating magnetic field, and rheological data will be extracted by image processing from the response of the film to time-dependent magnetic fields.

A separate line of investigation will examine the manner in which collective bacterial stirring can enhance the rates of chemical reactions. Since the Peclet number of the generated flows can greatly exceed unity, even though that of isolated, individual swimming organisms is quite small, studies of this regime can help elucidate the dynamics of quorum sensing, a key biological phenomenon in which bacteria sense the presence of others by secreting and detecting diffusible chemicals. Such sensing can trigger the formation of biofilms. We will examine mixing and reactions in these systems through flash photolysis uncaging of suspended fluorescent dye.

The experimental studies will be combined with theoretical modeling. For this purpose, we plan to generalize the approach used in previous work on the onset of collective motion in the bacterial systems. We will model elongated bacteria by dumbbell structures (two impenetrable spheres connected by a rigid rod). The effect of flagella will be modeled by a point-wise force dipole. For a dilute suspension of these self-propelled objects we expect to obtain a modification of the well-known Einstein result for the linear increase of the apparent viscosity of dilute suspensions of spheres with the increase of volume fraction of spheres. For the case of swimming bacteria we anticipate the opposite trend. The derived relations for the effective viscosity will be validated by simulations of suspensions of “active swimmers”.

Our continuing investigations of flagella-driven flows in algal systems have led us to begin studies of collective dynamics of these eukaryotic organisms. There are two fundamental issues here that bear on the larger problems. First is the manner in which large numbers of beating flagella synchronize. Second is the nature of hydrodynamic interactions between and collective swimming of colonial multicellular organisms. We

have developed preliminary protocols for these investigations, allowing us to study the onset of flagellar synchronization and the rather complex hydrodynamic interactions between pairs of Volvox.

#### **DOE Sponsored Publications in 2007.**

1. A. Sokolov, I. S. Aranson, J.O.Kessler, and R. E. Goldstein, Concentration dependence of the Collective Dynamics of Swimming Bacteria, *Phys. Rev. Lett.* **98**, 158102 (2007).
2. I. S. Aranson, A. Sokolov, J. O. Kessler, and R. E. Goldstein Model for dynamical coherence in thin films of self-propelled microorganism, *Phys. Rev. E* **75**, 040901 (2007).
3. A. Sokolov, I.S. Aranson and W.-K. Kwok, Process for dynamic concentration and separation of bacteria, ANL invention 06-012 (2007).
4. I. S. Aranson, D. Volfson, and L. S. Tsimring, Swirling motion in a system of vibrated elongated particles, *Phys. Rev. E* **75**, 051301 (2007).
5. M. Belkin, A. Snezhko, I.S. Aranson and W.-K. Kwok, Driven magnetic particles on a fluid surface: Pattern assisted surface flows, *Phys. Rev. Lett.*, in press (2007)
6. C.A. Solari, J.O. Kessler, and R.E. Goldstein, Motility, mixing, and multicellularity, *Genet. Program Evolvable Mach.* **8**, 115-129 (2007).
7. L.H. Cisneros, R. Cortez, C. Dombrowski, R.E. Goldstein, J.O. Kessler, Fluid dynamics of self-propelled microorganisms, from individuals to concentrated populations, *Exp. Fluids* **43**, in press (2007).
8. R.E. Goldstein, I. Tuval, and J.-W. van de Meent, Microfluidics of cytoplasmic streaming and its implications for intracellular transport, submitted (2007).

## Nanostructured Biocomposites: Designing and Tailoring The Abiotic-Biotic Interface

Millicent A. Firestone<sup>1</sup>, Brian D. Reiss<sup>1</sup>, Sashishakara P. Adiga<sup>1</sup>, Peter Zapol<sup>1</sup>, Orlando Auciello<sup>1,3</sup>, Leonidas Ocola<sup>3</sup>, Deborah K. Hanson<sup>2</sup>, Philip D. Laible<sup>2</sup>

<sup>1</sup>Materials Science, <sup>2</sup>Biosciences Divisions and <sup>3</sup>Center for Nanoscale Materials  
Argonne National Laboratory, Argonne, IL 60439

### Program Scope

The *Nanostructured Biocomposite Materials for Energy Transduction* research program has as its overarching goal the design, synthesis, and characterization of functional nanoscale materials that exploit the native capabilities of biological molecules to store and transduce energy. Membrane proteins, for example, facilitate many key cellular processes, including signal recognition, ion transport, and energy transduction. In effect, they possess all of the basic properties necessary for the construction of nanoscale devices appropriate for any of a variety of tasks, including optical/electronic signal amplification, switching, gating, data storage, sensing, and energy storage and conversion.[1] The use of membrane proteins as the basis for functional nanoscale devices, however, has received considerably less attention than have water-soluble proteins, a result of the lack of materials allowing their structural and functional stabilization outside of their native environment. To address this challenge, we are developing soft materials platforms to organize a variety of biomolecules whose structure and function mimic those of natural cell membranes. These synthetic/biological molecule composites will ultimately be stabilized by integrating them with selected hard (inorganic), nanostructured materials. Integration of the soft and hard components enables connection of the nanoscopically-organized biomolecule arrays to the macroscopic world, an important requirement if the resultant composites are to find application. *The current challenge addressed is the “tuning” of the interface between the hard (inorganic) and the soft materials so as to provide both a non-denaturing environment for the biomolecules and optimum “communication” across the interface.*

### Recent Progress

The integration of dissimilar materials such as biomolecules and inorganic substances to create functional materials/composites is an important area of research, and represents a critical step in the development of next-generation materials for energy capture, conversion and storage. The role of the interface is complex but ideally, should ensure maintenance of biological structure and function, precise positioning and patterning of active components, and effective communication between the biological and non-biological components of the system. In addition, the interface should be tailorable using inexpensive, high-throughput fabrication strategies (i.e. self-assembly). Our recent work has focused on the development of two bio-based composites. In the first, an array of membrane proteins, bacterial photosynthetic reaction centers (RCs), have been asymmetrically surface-coupled and “hardwired” to metal electrodes, demonstrating that they can function as components to create a photobioelectronic device.[4] In the second system, we have used viruses (phage display) to identify peptides that selectively bind to an inorganic (perovskite) ferroelectric and have obtained preliminary data suggesting that the electric field polarizability of the surface-tethered peptides can provide the basis of a biomolecular switch.[7,9,11]

In the first area of investigation, a conventional metal (Au) electrode – RC interface was designed to asymmetrically orient the photosynthetic proteins so as to

achieve directional electronic transport. The RC is a multi-subunit, transmembrane protein complex whose native function is to convert light into electrochemical energy through generation of a stabilized, transmembrane charge separation (of ca. 30 Å). The electron transfer properties of the RC equate to current moving through the protein; thus, the RC could be used as the basis for fabrication of a nanoscale, bioinorganic optoelectronic or photovoltaic device. To adapt RCs as the basis for such a device, however, three general materials challenges must be addressed: stabilization of the protein outside its native biomembrane, unidirectional orientation of the protein, and efficient coupling of the internal electron transfer cycle to an external electrode system. To address these challenges, we have interfaced RCs to gold electrodes by two unique protein attachment sites – a genetically introduced polyhistidine tag (located on the M-subunit) and a native cysteine residue (on the H-subunit). Electrochemical measurements demonstrate that both attachment strategies serve to orient electrochemically-active protein unidirectionally on gold electrodes. Single-protein electronic transport studies using C-AFM show that RCs wired using polyhistidine coordination to Ni-NTA-functionalized gold display diode-like *I-V* curves, a result consistent with the known directional electron transport characteristics of the protein. This work also has determined that the native cysteine located on the H-subunit is not suitable for wiring  $Q_B$ -depleted RCs to an external circuit, and that further study is needed to evaluate this coupling in  $Q_B$ -reconstituted RCs and/or to identify an attachment site suitable for coupling the external circuit to  $Q_A$  and the A-branch cofactors.

In the second area of investigation, we have studied aptamer selection (peptide phage display) as a means to identify an interfacial coupling layer that selectively binds inorganic ferroelectrics. These investigations lay the groundwork for our future efforts in exploring the use of inorganic ferroelectrics to create electric-field polarizable/actuated biocomposites. That is, we envision taking advantage of the ability to rapidly gate surface charge on the ferroelectric to both guide the electrostatic assembly of biomolecules and control their position or conformational state(s) once adsorbed to the surface. To date, we have used peptide phage display as a means to identify a peptide sequence that both strongly and selectively adheres to a perovskite ferroelectric, PZT. We have shown by immunofluorescence microscopy that the ISLLHST heptapeptide sequence selectively forms an adlayer on complex (multicomponent) lithographically patterned PZT after simply flooding the construct with a solution of the peptide. The peptide sequence was found to only attach to the PZT, demonstrating the complementary of binding between the sequence and ferroelectric surface. Neither the aqueous chemistry required for the peptide-PZT binding nor the peptide itself was found to significantly alter the ferroelectric properties of the PZT, although the remnant polarization ( $P_R$ ) was found to be reduced after brief (~ 1 h) exposure to buffered aqueous solution. This reduction most likely arises from the association of ions (derived from the buffered aqueous solution) that act to compensate charges on the PZT surface.

### **Future Plans**

Our work in the area of bio-optoelectronic materials will next focus on achieving improved electronic transport properties. As a first step, a site on the RC will be engineered so that it is closer to the acceptor cofactors. In addition, further studies will be directed at optimizing current flow in the RC-electrode composites by tuning the metal-organic interface, including adjustment of protein orientation, shortening the linker (wire), and changing the chemical composition of the linker. Once this work is completed, the challenge is to devise an approach to close the external circuit in a way amenable to the RCs. For example, one of the currently used Au electrodes will be

replaced with a conductive, flexible polymeric electrode, permitting the fabrication of a “sandwich”-type cell. Replacement of one of the solid Au electrodes with the polymer will serve to reduce the load and stress on the RCs when placed between the electrodes.

The next phase of our work on ferroelectric-biocomposite materials will involve combining theory, simulation, and experiment to delineate the molecular-level nature of association between the phage-selected peptide and the ferroelectric surface. This work is required because the peptide was determined by combinatorial approaches; thus, at present, only the amino acid sequence is known. The lack of a full understanding of the conformational state of the surface-adsorbed peptide and the specific points of surface attachment (i.e., the identity and nature of the amino acids participating in surface binding) limits our ability to effectively use the peptide as an interface for attachment of other biomolecules. The results of these studies will be used to guide our future synthetic efforts, with the aim of optimizing the biomolecules (size and charge) for electrostatic gating by the ferroelectric. Ultimately, however, we anticipate that these studies will serve to establish guiding principles for the selection of amino acid repeats or motifs that bind to a wider variety of inorganic materials.

Theory and simulation will be used to determine the chemical (e.g., amino acids, pl) and physical (secondary structure, folding, stability, water accessibility) nature of the interfacial interactions between the peptide and the surface. This work is important because while a considerable amount of attention has been directed at synthetic approaches for controlling the interface between organic and inorganic materials, less attention has been directed at developing a theoretical underpinning of this work. Because prior work has shown that the PZT thin-film surfaces are terminated in either TiO<sub>2</sub> or PbO, our initial studies will focus on TiO<sub>2</sub> (rutile (110)) since the interatomic potentials have been determined. Classical molecular dynamics (MD) will yield information on the adsorption mechanism and energies. The simulations will also provide information on vibrational spectra of the adsorption sites. Once these theoretical investigations have identified the important amino acids for binding to the surface, the results will be experimentally verified using vibrational spectroscopy and surface X-ray scattering and spectroscopy. Finally, since classical MD only permits an accurate description of physisorption, quantum chemical calculations (i.e., Gaussian) will also be conducted as a way to probe for chemisorption.

Concurrent with theory and simulations, experiments involving preparation of mutants of the heptapeptide by sequential replacement of each of the amino acids comprising the ISLLHST sequence with alanine will be conducted as a means to verify the surface binding mechanism. Determination of amino acids essential for surface binding will then allow for the engineering of proteins for the covalent coupling to the ferroelectric and assessment of their switching or gating behavior. We anticipate that these composites will find utility as nanoscale components that control transport on the nanometer length scale (i.e., nanofluidics) or for bio-logic devices.

## References

- [1] (a) Das, R.; Kiley, P. J.; Segal, M.; Norville, J.; Yu, A. A.; Wang, L. Y.; Trammell, S. A.; Reddick, L. E.; Kumar, R.; Stellacci, F.; Lebedev, N.; Schnur, J.; Bruce, B. D.; Zhang, S. G.; Baldo, M. *Nano. Lett.* **2004**, *4*, 1079-1083. (b) O'Neill, H. Greenbaum, E. *Chem. Mater.* **2005**, *17*, 2654-2661.

## DOE Sponsored Publications in 2005-2007

- 1) Batra, D.; Hay, D. N. T.; Firestone, M. A.; “Formation of a biomimetic, liquid-crystalline hydrogel by self-assembly and polymerization of an ionic liquid”, *Chem. Mater.* (2007)

19, 4423-4431

- 2) Batra, D.; Seifert, S.; Firestone, M. A. "The effect of cation structure on the mesophase architecture of self-assembled and polymerized imidazolium-based ionic liquids", *Macromolec. Chem. Phys.* (2007) 208, 1416-1427.
- 3) Rickert, P. G.; Antonio, M. P.; Firestone, M. A.; Kubatko, K. A.; Szreder, T.; Wishart, J. F.; Dietz *Tetraalkylphosphonium polyoxometalate ionic liquids: electroactive, thermally-stable "liquid POMS"*, *J. Phys. Chem. B* (2007) 111, 4685-4692.
- 4) Reiss, B. D.; Hanson, D. K.; Firestone, M. A., "Evaluation of the photosynthetic reaction center protein as a bioelectronic circuit element". *Biotechnol. Prog.* (2007) 23, 985-987.
- 5) Rickert, P. G. Antonio, M. P.; Firestone, M. A.; Kubatko, K. A.; Szreder, T.; Wishart, J. F.; Dietz, M. L. "Tetraalkylphosphonium polyoxometalates: Novel, electroactive, "task-specific" ionic liquids", *Dalton Transc.* (2007) 529-531.
- 6) Batra, D.; Seifert, S.; Varela, L.; Firestone, M. A. "Solvent-mediated plasmon-tuning in a gold nanoparticle-poly(ionic liquid) composite", *Adv. Func. Mat.* (2007) 17, 1279-1287.
- 7) Reiss, B.; Auciello, O.; Ocola, L. E.; Firestone, M. A. "Integration of biomolecules with inorganic ferroelectrics: A novel approach to nanoscale devices" in *Biosurfaces and Biointerfaces*, edited by M. Firestone, J. Schmidt, N. Malmstadt (Mater. Res. Soc. Symp. Proc. 950E, Warrendale, PA, 2007),
- 8) Adiga, S. P.; Zapol, P.; Firestone, M. A. "Modeling block copolymer interactions with biomimetic membranes", in *Biosurfaces and Biointerfaces*, edited by M. Firestone, J. Schmidt, N. Malmstadt (Mater. Res. Soc. Symp. Proc. 950E, Warrendale, PA, 2007), 0950-D15-25.
- 9) Reiss, B. D.; Ocola, L. Auciello, O.; Firestone, M. A. "Ferroelectric-specific peptides as building blocks for bio-inorganic devices", in *Molecular Motors, Nanomachines, and Engineered Bio-Hybrid Systems*, edited by S. Diez (Mater. Res. Soc. Symp. Proc. 944E, Warrendale, PA, 2006), 0944-AA02-08.
- 10) Iton, L. E.; Crisci, A. J.; Vajdova, V.; Laible, P. D.; Burns, C. T.; Firestone, M. A., "Synthesis and characterization of mesostructured silicas and gold frameworks as active matrices for biomolecule encapsulation". *Advances in Science and Technology.* (2006) 51, 30-37.
- 11) Reiss, B. R.; Guoran, B; Auciello, O.; Ocola, L.; Firestone, M. A., "Identification of peptides for the selective surface modification of perovskite ferroelectrics", *Appl. Phys. Lett.* (2006) 88, 083903.
- 12) Laible, P. D.; Kelly, R. F.; Wasielewski, M. R.; Firestone, M. A. "Electron transfer dynamics of photosynthetic reaction centers in thermoresponsive soft materials", *J. Phys. Chem. B* (2005) 109, 23670-23686.
- 13) Haralampus, N. M.; Johnson, L. J.; Firestone, M. A. "Photochromic and optical birefringence properties of azo-dye-doped polymer-grafted lipid-based complex fluids", *Macromolecules*, (2005) 38, 8971-8974.
- 14) Batra, D.; Vogt, S. Laible, P. D., Firestone, M. A. "Self-assembled mesoporous polymeric networks for patterned protein arrays", *Langmuir*, (2005) 21, 10301-10306.
- 15) Firestone, M. A.; Seifert, S. "Interaction of Nonionic PEO-PPO Diblock copolymers with lipid bilayers", *Biomacromolecules*, (2005) 6(5), 2678-2687.
- 16) Firestone, M. A.; Zaluzec, N. J.; Dietz, M. L.; Seifert, S.; Trasobares, S.; Miller D. J. "Ionogel-templated synthesis and organization of anisotropic gold nanoparticles", *Small* (2005) 1(7), 754-760.
- 17) Hay, N. T. D.; Rickert, P. G.; Firestone, M. A. "Synthesis and Characterization of an Amphiphilic Polyacrylic acid-lipid Conjugate" *Polymer Preprints* (American Chemical Society, Division of Polymer Chemistry) (2005) 46(2), 816-817.



# Biology-Inspired Programmable Assembly of Functional Nano-Structures

Oleg Gang and Daniel van der Lelie  
ogang@bnl.gov; vdlelied@bnl.gov  
Brookhaven National Laboratory, Upton, NY, 11973

Contributions: Dmytro Nykypanchuk, Mathew Maye, Yian-Biao Zhang  
Brookhaven National Laboratory, Upton, NY, 11973

## Program scope

A diversity of nanoscale objects with intriguing optical and electrical properties recently became available as a result of rapid the development of nano-synthetic methods. When these objects are assembled in specific architectures [1], newly emerging phenomena can occur that hold the promise for the creation of novel optical, magnetic and catalytic materials. There is a great demand for developing approaches for a large scale assembly with nanometer precision of these architectures, and which should overcome the limited precision and throughput of lithographic methods at the relevant scales of nano-objects. Our approach to tackle this problem utilizes a strategy of a bio-programmable assembly [2], in which biomolecules with highly selective interactions, like DNA and proteins, are engaged to guide an assembly of inorganic nano-components. The advantage of using biomolecules over more traditional chemically based methods is their tunability of sizes and programmable addressability of interactions that allow for the complexity of nanoscale architecting, an ability to disassemble or dynamically reconfigure systems, and a broad choice of nanomaterials that can be incorporated.

The main approaches for the realization of the bio-programmable assembly are based on (i) adopting the addressable, “key-lock” interactions of biomolecules to nano-environments; (ii) understanding and incorporation of diverse physical interactions, entropic effects, and energetic landscapes of biomolecules; (iii) and developing methods for tailoring biomolecular structures. Our research strategy combines the development of methods for the assembly of nano-architectures with exploration of their microscopic structures using electron and atomic force microscopies, x-ray and light scattering, and optical spectroscopy.

## Recent progress

### **Tunable particle assembly via tailored DNA interactions in micro- and nano- systems.**

**DNA mediated colloidal systems.** Our study of DNA functionalized micron sized particles has been focused on the development of novel approaches to regulate interaction between DNA functionalized mesoscale particles [3]. This study also tackled a number of fundamental issues related to understanding the phase behavior of systems with short range interactions. Micron sized latex particles with single stranded DNA grafted to the surface were used as a model system. A new approach for tuning the interactions between particles has been demonstrated. This approach allows a gradual change of the assembly rate for fixed physical conditions of a solution by mixing of hybridizing “linker” and non-hybridizing “neutral” DNA strands (Fig. 1). We showed that assembly is kinetically controlled for the fraction of hybridizing DNA on a surface above  $\sim 0.1$ , and that thermodynamic control over the assembly can be achieve for the lower fractions of hybridizing DNA. The particle assembly kinetics and the aggregate morphology have been investigated for a range of ionic strengths and “linker”/“neutral” DNA ratios. The conditions for tunable assembly kinetics have

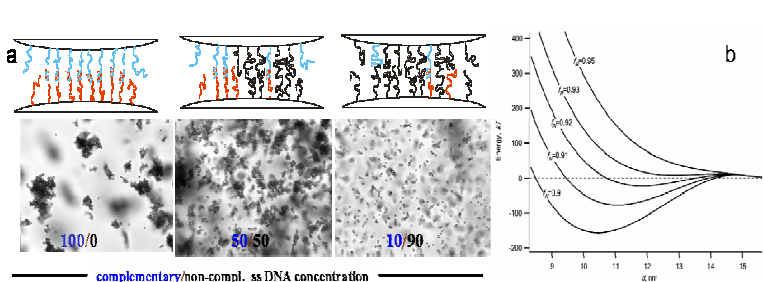


Figure 1. (a) Schematics of interaction tuning of DNA functionalized colloidal particles via increased steric repulsion. Black and colored strands represent “neutral” and complimentary DNA respectfully (top), corresponding in-situ optical images of assembled systems are at the bottom. b. Calculated interaction potential for various fraction of “neutral” DNA,  $f_N$ .

**DNA mediated nanoparticle assembly.** Similar to colloidal systems, interaction control for nanoparticle systems can be achieved by varying repulsive energy via control of fraction  $f_N$  of “neutral” DNA. Despite the conceptual similarity between colloidal and nanoparticle systems, there are many differences between the two, due to the size of DNA being comparable to the size of the nanoparticles. As a result: (i) interactions between DNA capped nanoparticles are middle- to long-ranged; (ii) fewer than 10 potential linkers can be engaged in particle hybridization, a feature that might significantly affect the aggregate structure due to the packing requirements. By changing the concentration of the neutral DNA in the particle shell, the system assembly was controlled in the broad range [4]: from the formation of aggregates with millions of particles to stabilization of individual particles (Fig. 2a), while characteristic aggregation time was correspondingly increased over several orders of magnitude. While the rapid aggregation is indicative of predominantly attractive interaction between particles, observed assembly attenuations with  $f_N$  increases asserts the presence of a rising kinetic barrier (repulsion) and/or the reduction of attraction between particles. To directly probe the effect of these interactions on the microscopic interparticle structure, we conducted in situ small-angle x-ray scattering (SAXS) measurements on the aggregates (Fig. 2b). The transition from near-constant interparticle spacing,  $d$ , of  $\sim 17.3$  nm at  $f_N < 0.5$  to an increase to 18.6 nm at  $f_N > 0.5$  suggests that kinetic effects might be responsible for the slower assembly of aggregates at lower  $f_N$ , while the influence of a stronger repulsion results in greater  $d$  at higher  $f_N$ .

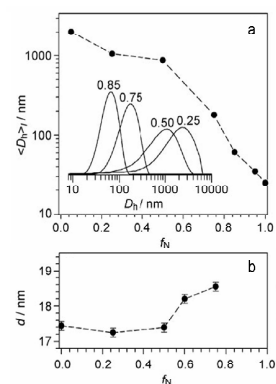


Figure 2. Aggregate hydrodynamic diameter (a) after  $\sim 2$  h assembly and interparticle spacing (b) vs.  $f_N$  as measured by dynamic light scattering and SAXS.

### 3D ordering in DNA guided assembly of nano-particles.

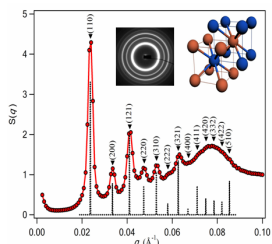


Figure 3. Structure factor, obtained from a SAXS pattern, corresponds to bcc lattice of DNA guided nanoparticles

Although numerous strategies using protein and DNA scaffolds have offered structures with designed nanoparticle placements in one- and two-dimensional systems, experimental realization in three dimensions (3D), where a rich diversity of ordered phases are expected, has remained elusive. By tailoring the design of the DNA shell the interparticle potential was modulated and the formation of 3D nanoparticle assemblies with crystalline long range ( $>0.5\mu$ ) order was discovered using synchrotron based SAXS measurements. The crystalline assemblies are thermodynamically reversible and temperature-tunable, with body centered cubic (bcc) lattices, where particles occupy only  $\sim 4\%$  of the unit cell. The DNA design and thermodynamic pathway leading to the crystallization of particles has been

explored, thus, opening the way for creation of new classes of nanoscale metamaterials.

**Kinetic control of self-assembly.** The effect of DNA structure on assembly kinetics was investigated using spectroscopic and structural methods. We demonstrated [5] that kinetic control of DNA driven nanoparticle assembly can be achieved by utilizing the DNA's conformational changes upon partial hybridization of interior DNA sequences which do not participate in assembly. An observed enhancement of assembly kinetics exhibited a twofold increase of the characteristic time, and was studied in detail using dynamic light scattering, UV-Vis, electron microscopy and SAXS. The observed effect is attributed to (i) decreased DNA interaction with gold surface due to an increased stiffness and extension of the DNA, and (ii) reduced DNA chain entropy.

### **DNA driven 2D assemblies of nano-objects**

DNA hybridization was utilized as a reversible, chemically weak and a highly selective way to assemble nanoparticles on surfaces. In this approach a steric repulsion provided by DNA, also prevents non-specific particle adsorption, and as result, preserves the 2D character of the system. We studied in-situ the assembly kinetics of the DNA-capped nanoparticles on surfaces covered with complementary DNA, as well as the structural changes with temperature in the resulting 2D DNA/nanoparticle system. Using high energy x-ray reflectivity, the microscopic structure of the 2D particle assembly was probed directly, while AFM and SEM were used to confirm the local particle's arrangement at the surface. The observed changes in the DNA/nanoparticle array, both below and above the DNA melting temperature, reveal an evolution of particle-surface distances and surface coverages, and provide insight into a mechanism of DNA-mediated particle-surface interactions.

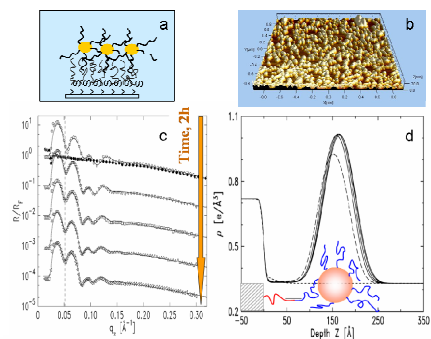


Figure 4. Schematics of surface hybridization (a), AFM image of particle monolayer (b), kinetic measurement of monolayer formation using x-ray reflectivity (c) and corresponding electron density profiles

### **Utilization of protein-protein and DNA-protein interactions**

A) We investigated the biocompatibility, specificity, and activity of a ligand-receptor protein system covalently bound to oxidized single-walled carbon nanotubes (SWNTs) as a model proof-of-concept for employing such SWNTs as biosensors [6]. SWNTs were functionalized under ambient conditions with either the Knob protein domain from adenovirus serotype 12 (Ad 12 Knob), or its human cellular receptor, the CAR protein. We confirmed the biological activity of Knob proteins immobilized on the nanotube surfaces using its labeled conjugate antibody, and evaluated the activity and specificity of bound CAR on SWNTs. In addition, current-gate voltage (I-V) measurements on a dozen nanotube devices explored the effect of protein binding on the intrinsic electronic properties of the SWNTs, and also demonstrated the devices' high sensitivity in detecting protein activity. All data showed that both Knob and CAR immobilized on SWNT surfaces fully retained their biological activities, suggesting that SWNT-CAR complexes can serve as biosensors for detecting environmental adenoviruses. This research will be further exploited

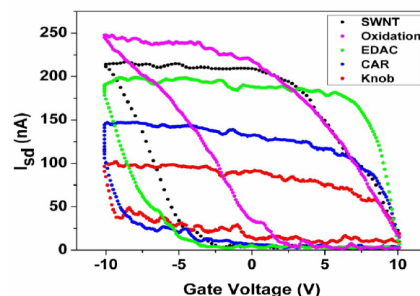


Figure 5. Measured source-drain current as a function of gate voltage for a SWNT are shown for as-grown SWNT (black), SWNTs after oxidation (purple), exposed to EDAC/NHS (green), upon CAR attachment (blue), exposed to the complementary Knob protein (red).

to design biosensors for the specific detection of heavy metal ions and radionuclides.

B) In order to design protein-functionalized DNA scaffolds we are exploring the g5p protein of filamentous bacteriophages (M13, f1, fd and cf), which binds to single-strand DNA. In the structure of the natural complex present in these bacteriophages, the dimeric g5p binds to two strands of anti-parallel ssDNA that are ordered by forming left-handed superhelical structure with outer diameter of ~8 nm and length of ~1  $\mu$ m. Engineered derivatives of the g5p protein, having affinity tags that allow their binding to nano-particles, have been used to design biological scaffolds via complex formation with DNA. These scaffolds will subsequently be used for programmable self-assembly of nanoparticles. A peptide display phage library has been introduced to select for peptides, which can specifically bind to inorganic surfaces, including Au. The selected peptides have been applied for self-assembly of inorganic nanoparticles. In this research, combination of peptide tagged g5p protein and designed DNA structures will be utilized to construct complex nano-scaffolds for ordering of Au nanoparticles.

## Future plans

**Fundamental studies on DNA mediated interactions of nano-objects.** To overcome limitation of short-range interaction character of colloid systems and to explore an influence of a wider range of the inter-particle potential on self-assembled structure, we will utilize engineered DNA constructions for particle interaction control. Our approach of using complementary and non-complementary DNA to balance attractive and repulsive interaction will be applied to this system and theoretical predictions [7] on complex phase diagram will be directly verified. We will utilize both 3D and 2D systems to explore the effects of a multiple addressability and binary composition of nano-objects on the structural and thermodynamic properties of the assembled system. In addition, optical properties of the designed nano-architectures will be farther studied [8].

**2. Functionalization of DNA-protein scaffolds.** The complex of DNA and g5p-His will be used as a template for the ordered self-assembly of Au nanoparticles. The ordered Au particles will be studied using transmission electron microscopy (TEM). The binding of g5p to ssDNA or dsDNA is dependent on salt concentrations. By playing with ssDNA and dsDNA regions scaffolds will be designed for self-assembly of peptide-tagged g5p protein, to which we will subsequently bind Au particles.

1. A. M. Kalsin et al, *Science* (2006) 312, 420; E.V. Shevchenko et al, *Nature* 439, 55 (2006)
2. E. Katz and I. Willner, *Ang. Chem.-Int. Ed.* (2004), 43, 6042 and references therein
3. D. Nykypanchuk, M. M. Maye, D. van der Lelie, and O. Gang, *Langmuir* (2007), 23 (11), 6305
4. M. M. Maye, D. Nykypanchuk, D. van der Lelie, and O. Gang, *Small* (2007), DOI:10.1002/sml.200700357
5. M. M. Maye, D. Nykypanchuk, D. van der Lelie, and O. Gang, *JACS* (2006), 128(43), 14020
6. Y. Zhang, M. Kanungo, A. J. Ho, P. Freimuth, D. van der Lelie, M. Chen, S. Khamis, S. Datta, A.T. C. Johnson, B. Panessa-Warren, J. A. Misewich, and S.S. Wong, (2007) *Nanoletters*, in press.
7. A.V. Tkachenko, *Phys. Rev. Lett.* 89, 148303 (2002)
8. H. Kang, M. M. Maye, D. Nykypanchuk, M. Clarke, P.Yim, J. Krogmeier, K. Briggman, O. Gang, and J. Hwang, *Biophysical J* (2007), 337A Suppl. S; *Proc. of SPIE* (2007), 6430, 643024

## Directed Self-Assembly of Soft-Matter and Biomolecular Materials

Benjamin Ocko (ocko@bnl.gov), Antonio Checco (checco@bnl.gov)  
Masa Fukuto (fukuto@bnl.gov), and Lin Yang (lyang@bnl.gov)  
Brookhaven National Laboratory, Upton, NY 11973

### Program Scope

A central theme of the group is to understand the effects of nanoscale confinement and the role of self-assembly in soft materials through the use of patterned templates and well-defined interfaces. We use synchrotron x-ray scattering, scanning probe and optical microscopy techniques to study fundamental properties of simple liquids, complex fluids, polymeric and biomolecular assemblies. The challenges are to understand (1) structural aspects of liquids under nano-confinement and at interfaces with solid walls, (2) how templates and confinement can be used to direct the assembly of biomolecular materials and diblock copolymer thin films, (3) to understand the fundamental interactions which give rise to similar self-assembly behavior for a wide variety of systems, (4) the relationship between the functional properties and order. Understanding structural aspects of self-assembly and thin organic films underlies many emerging organic based devices and energy technologies. Our approach uses two complementary structural probes, x-ray scattering and AFM. An important aspect of our approach is to use nanopatterned surfaces to confine liquids and complex fluids. To accomplish this, we are using AFM based local-oxidation nanolithography, e-beam lithography and polymer based self-assembly techniques. The program integrates experimentalists with a dedicated history of collaboration in liquids, wetting, biomaterials, and synchrotron-based structure characterization.

### Recent Progress

The macroscopic description of wetting and non-wetting liquid films is expected to break down at nm length scales and many theoretical predictions related to these nano-properties have not been tested due to the technical difficulties of measuring the structure of nanoliquids. Our research aims to investigate these nano-liquids by using in-situ synchrotron surface x-ray scattering (SXS) and non-contact atomic force microscopy (AFM). We have been investigating the wetting of nanopatterned substrates prepared by block copolymer films and e-beam lithography. Previously we investigated the wetting of organic liquids on parabolic shaped cavities, 20 nm wide and separated by ~40 nm. Our results show that the wetting behavior differs from the predicted  $\Delta\mu^{-1/3}$  thickness. The exact dependence, including the cross-over to the filled region, has been well described by simple models by Rascon and Perry and detailed calculations by Dietrich and coworkers, both of which are in good agreement with our results.

Another important class of nanowetting problems is on chemically patterned surfaces with two different surface chemical terminations. The liquid is chosen such that the vapor only wets one of the two regions. We have prepared these surfaces by selectively electro-oxidizing the terminal methyl groups. Recently we have reduced the patterning line width to as small as 15 nm. Controlled amounts of cyclohexane are condensed on the “chemical stripes” from the vapor and their shape is imaged in-situ versus their width ( $40 < w < 1000$  nm). At the bulk liquid/vapor coexistence, the profile shapes and the measured width ( $w$ ) dependence of the height follows a  $w^{1/2}$  behavior and agrees well with the predictions of Density Functional Theory and with previous results using ethanol.

Chemical patterns have also been used to direct the dewetting of polymer thin films into structures of complex shape in order to study the effect of the lateral confinement on the spatial orientation of diblock copolymer microdomains, so called graphoepitaxy. Under appropriate

annealing conditions, we can form ordered triangular microdomains on patterned lines and triangles. This process holds great promise for building polymer nanostructures with long-range order and this may provide a means of making ultra small self-assembled arrays.

Aerosol particles (nano- and micron-sized particles suspended in air) affect atmospheric radiation and cloud microphysics and an improved description of their behavior is crucial to accurate climate modeling. The water uptake of hygroscopic aerosols and their eventual transition to liquid state, deliquescence, has been extensively studied in aerosols but little is known how the adsorption of these particles onto surfaces modifies the behavior. Understanding these processes may improve climate models as well as elucidate the physics of nanoscale wetting. We have initiated studies of the early stages of water uptake and eventual deliquescence of sodium chloride nanoparticles deposited on silicon. The transition from a solid, faceted crystal to a liquid nanodrop is clearly observed using non-contact AFM and preliminary results suggest the possible formation of a thin liquid film prior to deliquescence.

N-alkanes longer than 6 carbons do not spread on a pure water surface. However, the spreading of a monolayer of longer n-alkanes can be induced by adding the cationic surfactant CTAB to the water. Here the CTAB monolayer effectively acts as a template for the wetting and freezing of the n-alkane monolayer. This liquid-like wetting film undergoes, upon cooling, an ordering transition into a hexagonally-packed, quasi-2D crystal. For shorter n-alkanes this surface-frozen film is a mixed monolayer of alkanes and CTAB tails. For longer n-alkanes the film is a bilayer with a crystalline, pure-alkane, upper monolayer, and a liquid-like lower layer.

In search for a platform for studying 2D self-assembly, we have conducted time-dependent, in-situ x-ray reflectivity measurements on the formation of substrate-supported lipid monolayers and bilayers at solid-liquid interfaces, buried under aqueous buffer with various concentrations of DOPC. The DOPC bilayer is formed on the hydrophilic surface of a bare Si substrate, while the DOPC monolayer is formed on a hydrophobic OTS monolayer-coated Si substrate. The evolution of the reflectivity curves from the lipid bilayers is well described by lateral growth of bilayer islands, consistent with the rupture and fusion model for the adsorption of lipid vesicles to solid-liquid interfaces. By contrast, the formation of the lipid monolayer on OTS-coated Si occurs through a relatively fast coverage of the entire interfacial area, followed by an increase in the monolayer thickness. For both monolayers and bilayers, the rate of lipid layer growth increases with increasing lipid concentration in the buffer solution.

These solid-supported lipid bilayers and monolayers subsequently were used as a mobile substrate for assembling ordered 2D structures formed by bio-nanoparticles (large protein cages and viruses). The lipid substrate on the one hand provides 2D confinement for these particles when they bind to the lipid substrate via either simple electrostatic interactions or specific ligand binding (e.g. Ni-His tag). More importantly, the intrinsic fluidity of the lipid membrane also provides the in-plane mobility for these particles. Our initial in-situ GISAXS and AFM study of assembly of Tobacco Mosaic Viruses (TMVs) on substrate-supported lipid monolayer demonstrates that this in-plane mobility is essential for developing structural order. Our study also indicates that the chemical environment (pH, ionic strength, type of ions, etc.) surrounding the particles and the geometry of the particle all affect the degree of order in the self-assembly.

In parallel to the self-assembly study at liquid-solid interface, 2D self-assembly at liquid-air interface has also been explored. The adsorption and two-dimensional crystallization of soluble protein streptavidin on a biotinylated lipid monolayer at an aqueous solution/vapor interface have been studied using in-situ x-ray and optical methods. For a given subphase and lipid condition, surface normal and in-plane structures at molecular length scales have been elucidated via synchrotron XR and GID measurements, respectively, at the solution/vapor interface. The 2D crystalline structures thus revealed were correlated with the morphologies of growing 2D crystal domains observed optically by carrying out Brewster-angle microscopy (BAM) under exactly the

same lipid, protein, and subphase conditions. The results show that at high salt concentration and moderate surface density streptavidin nearly always forms 2D crystals, but both the unit cell structures and the crystal domain shapes are different at low, intermediate and high subphase pH values

### **Future Plans**

We will extend our studies of wetting phenomena, currently focused on parabolic shaped nanocavities in silicon, to other patterned surfaces. We have carried out preliminary studies of a dry grid of 20 nm wide and 40 nm posts, with a 35-45 nm lattice spacing. These samples, prepared by Hitachi, using e-beam lithography are only 0.1 by 0.5 mm in size, yet they show remarkable GISAXS patterns due to the very low roughness. These patterns will be used as a template for nanowetting studies. Additional studies will be carried out to investigate stamps made from plastic using nanoimprint technology.

The AFM wetting studies, which have been carried out on patterned lines, will be extended to other shapes such as dots, thus allowing the role of line tension to be explored. In addition to static wetting experiments, dynamics will be also studied. More specifically, AFM will be used to image the spreading of a viscous, nonvolatile liquid, such as oil, along the patterned lines (so called “open” nanofluidic experiment).

Many chain molecules, such as nalkanes, exhibit the unusual phenomena of surface freezing whereby the top molecular layer freezes while the underlying bulk remains fluid. To date, this phenomenon has only been observed at flat interfaces. It has been predicted that the high curvature associated with nanoliquids might suppress surface freezing. To test this hypothesis, AFM studies will be carried out on chemically patterned surfaces coated with alkane nanoliquid drops.

When a fluid near a continuous phase transition is spatially confined, the competition between diverging critical fluctuations and finite system size is expected to mediate an effective force between confining surfaces, known as the critical Casimir force. However, there have been limited experimental observations of this effect. Direct measurements of this effect will be carried out using AFM.

To date, measurements of the surface of nanoliquids have been conducted in non-contact mode using a commercially available instrument. Although this instrument has provided contributed to exciting scientific results, it can only be operated at ambient pressure and the environmental chamber does not provide a perfect seal. To overcome the limitations the current instrument, we plan to build a custom, state-of-the-art, environmental Atomic Force Microscope specifically designed to work under vacuum and high pressure.

We will continue to explore creating longer-ranged order in 2D assemblies of nanoparticles on lipid membranes. The lipid membrane itself provides a means of tuning the interaction between nanoparticles. Lipid membranes that consist of multiple lipid species are 2D mixtures that can give rise to Casimir force and may be used to promote formation of ordered arrays of nanoparticles. The study of these mixtures also helps to provide insights into the origin and nature of “lipid rafts”—small functional domains found in biological membranes that have distinct lipid compositions. The density of binding sites in the lipid membrane may determine the mobility of the nanoparticle and therefore influences the kinetics of formation of ordered structures. Templates will be used to limit the orientation of ordered domains so that they may coalesce into larger domains.

## DOE Sponsored Publications (2005-2007)

1. Wetting, mixing and phase transitions in Langmuir-Gibbs films, E. Sloutskin, Z. Sapir, C.D. Bain, Q. Lei, K.M. Wilkinson, L. Tamam, M. Deutsch, and B.M. Ocko. *Phys. Rev. Lett.* (accepted).
2. Pentacene Nanostructures on Surface Hydrophobicity-controlled Polymer/SiO<sub>2</sub> Bilayer Gate-Dielectric, H. Yang, S. H. Kim, L. Yang, S. Y. Yang, and C. E. Park, *Adv Materials* (accepted).
3. In-Situ X-ray Studies of Self-Assembled Ordered Virus Arrays on a Lipid Layer, L. Yang, S. Wang, M. Fukuto, A. Checco, Z. Niu, Q. Wang, *nanoletters* (submitted).
4. Alkyl-thiol Langmuir films on the surface of liquid mercury. H. Kraack, L. Tamam, E. Sloutskin, M. Deutsch, and B. Ocko. *Langmuir* **23**, 7571-7582 (2007).
5. Freezing transition of Langmuir-Gibbs alkane films on water. E. Sloutskin, Z. Sapir, L. Tamam, B.M. Ocko, C.D. Bain, and M. Deutsch. *Thin Solid Films* **515**, 5664-5668 (2007).
6. The surface structure of concentrated aqueous salt solution. E. Sloutskin, J. Baumert, B. M. Ocko, I. Kuzmenko, A. Checco, L. Tamam, E. Ofer, T. Gog, O. Gang, and M. Deutsch. *J. Chem. Phys.* **126**, 054704 (2007).
7. High resolution non-contact AFM imaging of liquid condensed onto chemically nanopatterned surfaces. A. Checco, Y. Cai, O. Gang, and B. Ocko. *Ultramicroscopy* **106**, 703-708 (2006)
8. Capillary wave fluctuations and intrinsic widths of coupled fluid-fluid interfaces: An x-ray scattering study of a wetting film on bulk liquid, M. Fukuto, O. Gang, K. J. Alvine, and P. S. Pershan, *Phys. Rev. E* **74**, 031607 (2006)
9. Direct structural observation of a molecular junction by high-energy x-ray reflectometry. M. Lefenfeld, J. Baumert, E. Sloutskin, I. Kuzmenko, P. Pershan, M. Deutsch, C. Nuckolls, and B. M. Ocko. *PNAS* **103**(8), 2541-2545 (2006).
10. Liquid nanostripes. A. Checco, O. Gang, and B. Ocko. *Phys. Rev. Lett.* **96**, 056104 (2006).
11. Salt complexation in block copolymer thin films. S. H. Kim, M.J. Misner, L. Yang, O. Gang, B.M. Ocko, and T.P. Russell. *Macromolecules* **39**, 8473-8479 (2006).
12. Chemoresponsive monolayer transistors. X. Guo, M. Myers, S. Xiao, M. Lefenfeld, R. Steiner, G. Tulevski, J. Tang, J. Baumert, F. Leibfarth, J. Yardley, M. Steigerwald, P. Kim, and C. Nuckolls. *PNAS* **103**(31), 11452-11456 (2006).
13. Solvent mediated assembly of nanoparticles confined in mesoporous alumina. K. Alvine, D. Pontoni, O. Shpyrko, P. Pershan, D. Cookson, K. Shin, T. Russell, M. Brunnbauer, F. Stellacci, and O. Gang. *Phys. Rev. B* **73**, 125412 (2006).
14. Capillary wave fluctuations and intrinsic widths of coupled fluid/fluid interfaces: An x-ray scattering study of a wetting film on bulk liquid. M. Fukuto, O. Gang, K.J. Alvine, and P. Pershan. *Phys. Rev. E* **74**, 031607 (2006).
15. Dislocations and grain boundaries in semiconducting rubrene single-crystals, Chapman, B. D., A. Checco, R. Pindak, T. Siegrist, and C. Kloc, *J. Cryst. Growth* **290**, 479 (2006)
16. Modulated phase of phospholipids with a two-dimensional square lattice, L. Yang and M. Fukuto, *Phys. Rev. E* **72**, 010901, (2005)
17. Crystalline phases of alkyl-thiol monolayers on liquid mercury. B. Ocko, H. Kraack, P. Pershan, E. Sloutskin, L. Tamam, and M. Deutsch. *Phys. Rev. Lett.* **94**, 017802 (2005).
18. Real time GISAXS study of Micelle hydration in CTAB templated silica thin films. S. Dourdain, A. Rezaire, A. Mehdi, B. Ocko, and A. Gibaud. *Physica B: Physics of Condensed Matter* **357**(1-2), 180-184 (2005).
19. Surface layering in ionic liquids: an x-ray reflectivity study. E. Sloutskin, B. Ocko, L. Tamam, I. Kuzmenko, T. Gog, and M. Deutsch. *J. Amer. Chem. Soc.* **127**, 7796-7804 (2005).
20. Determination by x-ray reflectivity and small angle x-ray scattering of the porous properties of mesoporous silica thin films. S. Dourdain, J.-F. Bardeau, M. Colas, B. Smarsly, A. Mehdi, B. Ocko, and A. Gibaud. *Appl. Phys. Lett.* **86**, 113108 (2005).
21. Electro pen nanolithography. Y. Cai and B. Ocko. *J. Amer. Chem. Society* **127**, 16287-16291 (2005).
22. Liquids on topologically nano-patterned surfaces. O. Gang, K. Alvine, M. Fukuto, P. Pershan, C. Black, and B.M. Ocko. *Phys. Rev. Lett.* **95**, 217801 (2005).
23. Large scale fabrication of protein nanoarrays based on nanosphere lithography. Y. Cai and B.M. Ocko. *Langmuir* **21**, 9274-9279 (2005).
24. Determination by x-ray reflectivity and small angle x-ray scattering of the porous properties of mesoporous silica thin films. S. Dourdain, J.-F. Bardeau, M. Colas, B. Smarsly, A. Mehdi, B. Ocko, and A. Gibaud. *Appl. Phys. Lett.* **86**, 113108 (2005).



**Lawrence Berkeley National Laboratory – Materials Sciences Division  
Biomolecular Materials Program**

A. Paul Alivisatos  
1 Cyclotron Road, Mailstop 66  
Berkeley, CA 94720 USA  
paul.alivisatos@gmail.com

**DNA directed assembly of nanocrystal molecules**

This project is dedicated to exploring the assembly of colloidal nanocrystals with DNA. In recent years, we have established methods for preparing colloidal nanocrystals bearing a specific number of oligonucleotides, and we have shown that it is possible for the DNA to be used to direct the nanocrystals into specific groupings. For example, we have prepared groups of particles in which a central colloidal quantum dot is surrounded by Au nanocrystals varying in number from 1 to 8 (QD(Au)<sub>1-8</sub>). There are two major goals of the present activity: to determine the degree of fluctuonality of the DNAdirected assemblies, and to investigate collective behavior of the nanocrystal molecules.

Fluctuonality of the DNA assembled nanocrystal molecules: We have used Small Angle Xray Scattering to study the complete distribution of separations in an ensemble of Au nanocrystal dimers, with DNA acting as the tether. These experiments have been performed as a function of DNA length (12 to 100 bp), salt concentration, and base pair sequence (fraction AT, GC content). We find that the distribution of distances is unexpectedly broad and skewed to smaller separatiions compared to the predictions of the worm like chain model of the DNA. We are working closely with our theory colleague Phil Geissler to explain these results, possibly based on a model that includes local melting phenomena in the DNA.

Plasmon coupling in DNA directed nanocrystal molecules. The through space coupling of surface plasmons extends over a length scale proportional to the diameter of the Au nanocrystal. Thus Au nanocrystal dimers and more complex molecules have distinct plasmon scattering spectra. We have investigated the spectra of these nanocrystal molecules using single molecule dark field microscopy, and we are examining how the single molecule spectra can be used to examine the fluctuations in nanoparticle separations, as well as change in conformation induced by proteins binding to the DNA. This system is being developed into a nanoscale ruler for measuring distances.

Finally, we are investigating more complex nanocrystal molecules, such as those which may arise when nanocrystals are bound to the vertices of a DNA pyramid.

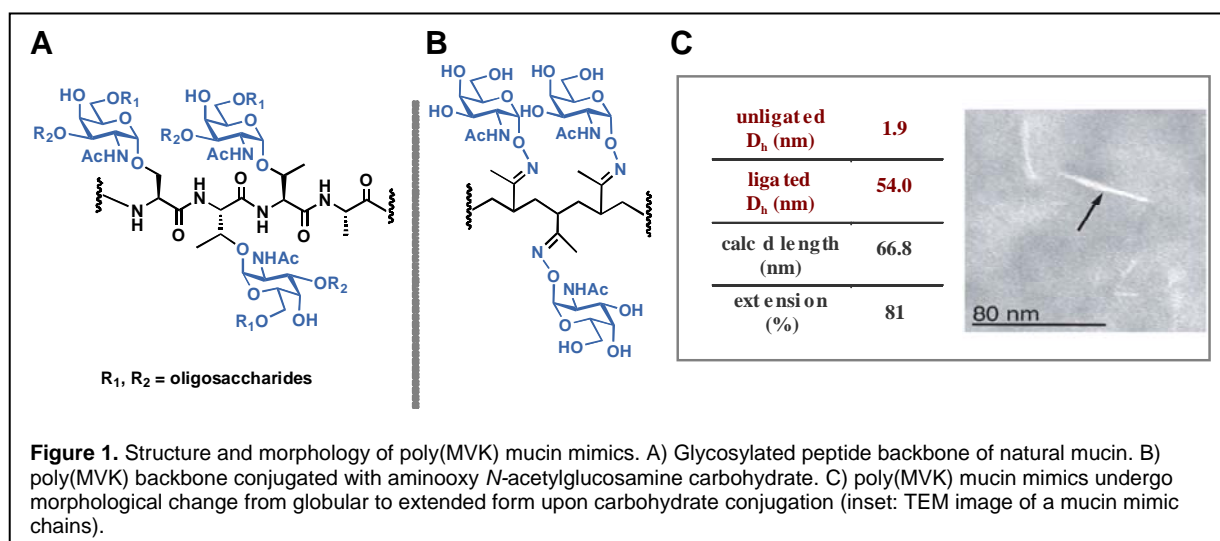
Present work is dedicated towards investigating the optical properties of the resulting nanocrystals molecules. Early efforts have focused on Au nanocrystal dimmers, which are examined using single particle dark field microscopy. We have mapped how the light scattering spectrum and intensity depends upon distance in these pairs. Future work will examine more complex nanocrystal groupings which may serve as nanoscale sensors of conformational change.

## Engineering bio/material interfaces using biomimetic materials

Professor Carolyn R. Bertozzi, The Molecular Foundry, Lawrence Berkeley National Laboratory, and Departments of Chemistry and Molecular and Cell Biology, UC Berkeley Berkeley, CA 94720-1460; Email: crb@berkeley.edu

### Program overview

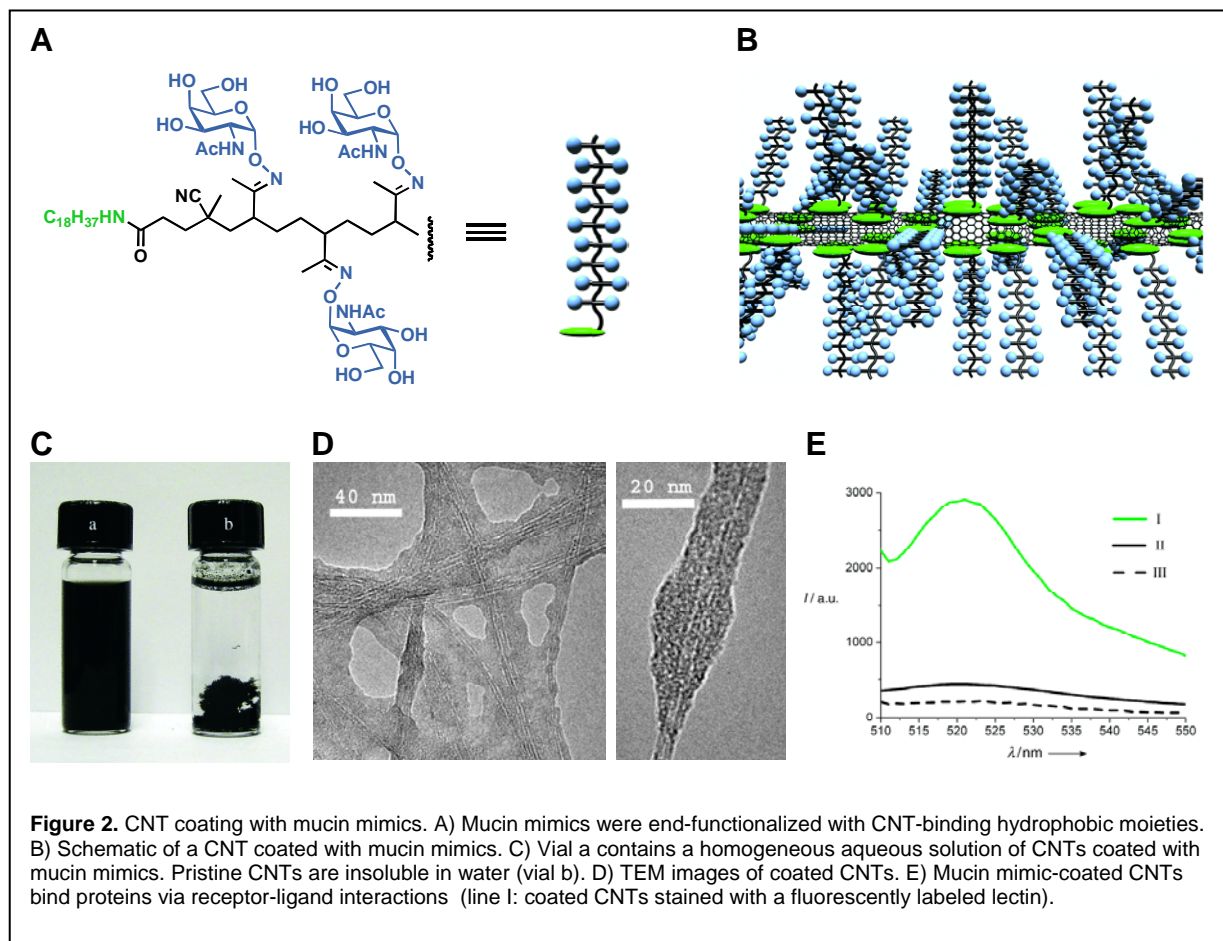
The broad objective of this program is to develop new functional materials with design elements derived from nature. A key aspect of the program involves development of technologies that interface synthetic materials with biological materials, and to generate hybrid materials with functions related to energy and biological inquiry. Nature serves as an obvious source of inspiration for the design of novel materials with well-defined structure and function. Various molecular scaffolds provide living systems with a) *structural* and b) *functional* support. Some of the most common *structural* supports in living systems are represented by, for example, collagen (a fibrous protein and the main component of the extracellular matrix and bone tissues) and chitin (a long-chain polysaccharide found throughout the natural world as a principal constituent of cell walls of fungi and exoskeletons of arthropods, such as crustaceans and insects). An example of a *functional* motif utilized by nature is the densely glycosylated cell membrane-bound protein, mucin. Mucins serve a dual purpose as a part of mechanism of cell wall protection and in mediation of cellular adhesion and intracellular communication. Both, *structural* and *functional* biomolecular systems are highly complex and specifically tailored by nature for their particular purposes. The common denominator of all these natural biomaterials is the relatively large size of their main molecular components; i.e., long polypeptides in collagen or mucins and large polysaccharide chains in chitin. While common in nature, such structures are difficult to prepare synthetically in large quantities and in an economical fashion. This project attempts to circumvent this problem by substituting the biopolymeric backbones in the naturally occurring materials with easily accessible synthetic ones in their man-made equivalents.



### Recent progress

To demonstrate this approach, we designed synthetic polymers that mimic mucin glycoproteins.<sup>i,ii</sup> The polymers comprised of a methylvinyl ketone (MVK) backbone that, upon conjugation with aminoxy sugars, adopts an extended structure similar to mucin (Figure 1).

These polymers bind, in a ligand-specific manner, naturally occurring mucin-binding proteins (lectins). In a subsequent stage of the project, we focused on conjugation of our mucin mimics with synthetic materials. Of particular interest was their conjugation with carbon nanotubes (CNTs, Figure 2). The polymers, functionalized with hydrophobic CNT-binding moieties, coated CNTs and displayed several attractive properties relevant to applications in biology. Mucin mimic-coated CNTs were soluble in water, resisted non-specific protein binding and bound specifically to proteins via receptor-ligand interactions. Most importantly, CNTs coated with the mucin mimics were non-toxic to cultured cells, opening new avenues for applications in biosensing.

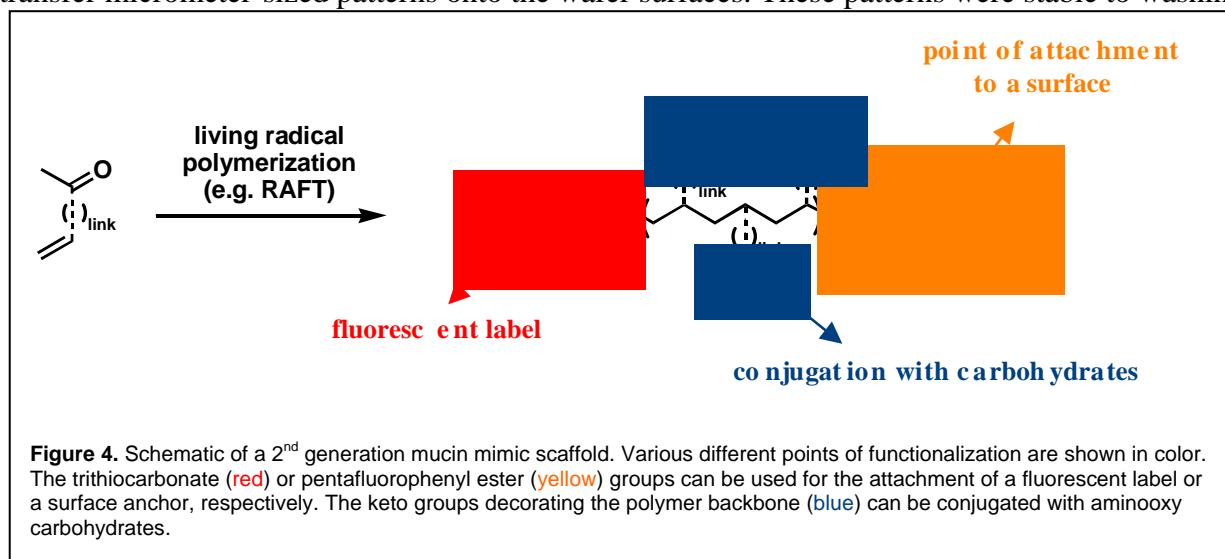


Alternatively, functionalization of mucin mimics with lipid end-groups allowed for their incorporation into supported lipid bilayers (SLBs, Figure 3).<sup>iii,iv</sup> Labeling of the gopolymers with a small amount of a fluorescent probe in conjunction with common spectroscopic techniques allowed us to establish that the polymers efficiently incorporated into SLBs and, most importantly, remained fluid – a behavior typically observed for natural membrane-bound proteins in cells. These findings present the possibility to utilize the mucin mimics to study phenomena related to the presence of natural mucins on the surfaces of living cells.

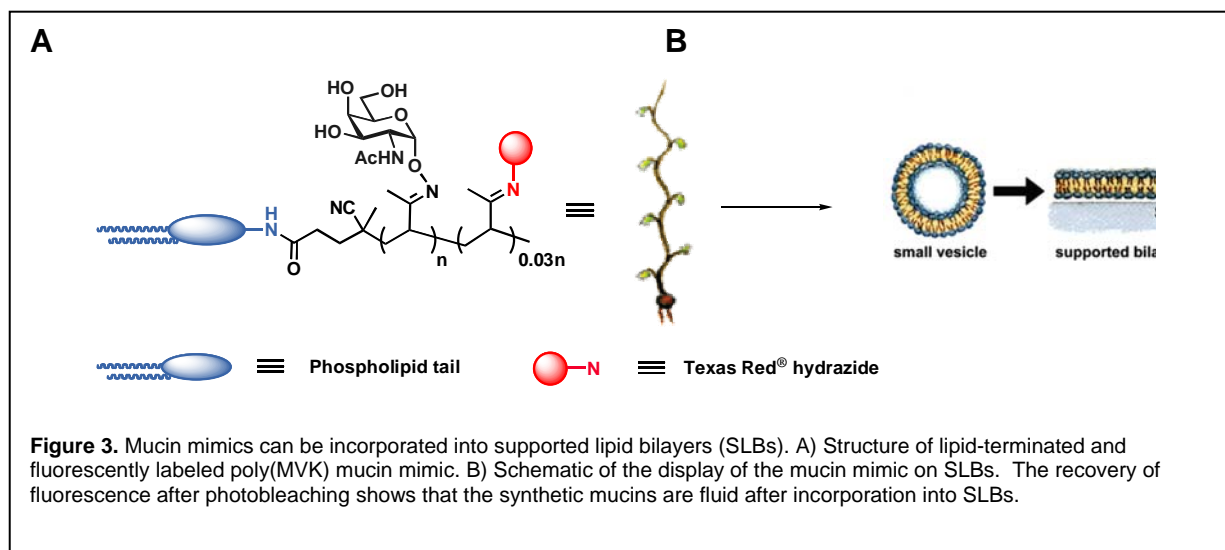
In order to better control the polydispersity and spatial control of chemical functionality, we developed a 2<sup>nd</sup> generation synthetic approach. Acrylate and MVK polymeric backbones of various sizes and narrow chain-length distributions were synthesized using living radical

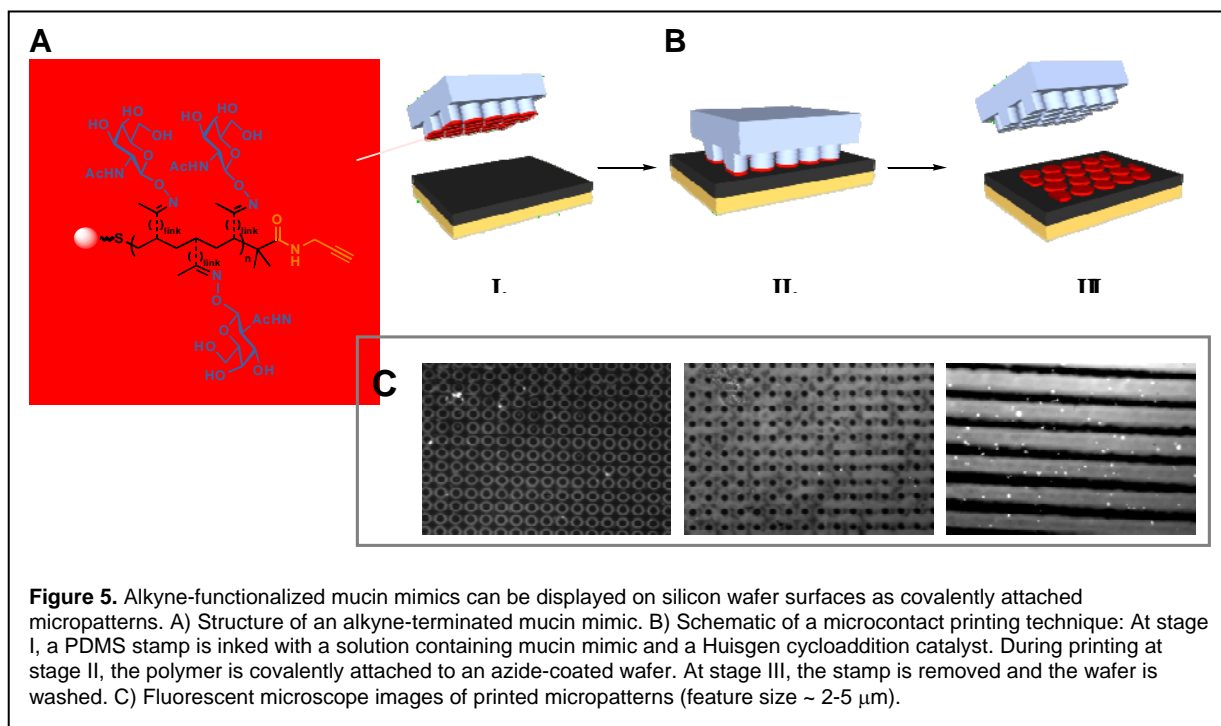
polymerization techniques.<sup>v</sup> This new approach allowed us to control various structural and morphological characteristics of these polymers. While the poly(MVK) mucin mimics adopt linear and extended morphology, the polyacrylate mimics exist in solution in a globular form. In addition, the nature of the polymerization technique employed provides a means for facile functionalization of the termini of the polymeric chains with various functional groups. For example, one terminus can carry an optical probe, while the other might serve as a point of attachment to surfaces.

We explored ways to pattern the mucin mimetic glycopolymers on silicon oxide surfaces. One terminus of the glycopolymers was functionalized with alkyne functionality, which can subsequently be reacted and covalently linked with azide-coated silicon wafers via the Huisgen 1,3-dipolar cycloaddition reaction (Figure 5).<sup>vi</sup> Micro-contact printing technology<sup>vii</sup> was used to transfer micrometer-sized patterns onto the wafer surfaces. These patterns were stable to washing



with water as well as organic solvents. Functionalization of the remaining free terminus of the polymer chain with a fluorescent probe allowed us to determine the quality of this transfer using fluorescent microscopy. This technique will enable us to explore a number of different applications including development of biosensors.





## Future Plans

In the future, the modular nature of our synthetic approach to the preparation of mucin mimics can be extended to other systems as well. We wish to explore the spatial orientation and morphology of the surface bound polymers in solution and in solid phase using scanning microscopy techniques. The ability to control the shape of the macromolecules (i.e. their extended or globular form) and modulating the type and combinations of carbohydrates displayed on the polymeric backbone could lead to development of various new materials. Linear polymers would be expected to form fibrous structures, while the globular polymers might be capable of forming three-dimensional hydrogel constructs. The combination of both morphological features using copolymerization techniques could provide even a greater number of possibilities. Furthermore, extending on our previous success in the area of CNT coating, we envision the possibility of intercalating CNTs (or other nano- and microstructures) with the 3-D scaffolds to arrive at hybrid biomaterials responsive to external stimuli such as electric current, light or magnetic field and compatible with living systems.

<sup>i</sup> X. Chen, G. S. Lee, A. Zettl, C. R. Bertozzi, Biomimetic Engineering of Carbon Nanotubes by using cell surface mimics," *Angew. Chem. Int. Ed.* **43**, 6112-6116 (2004).

<sup>ii</sup> X. Chen, U. C. Tam, J. L. Czapinsky, G.S. Lee, D. Rabuka, A. Zettl, C. R. Bertozzi, "Iterfacing carbon nanotubes with living cells," *J. Am. Chem. Soc.* **128**, 6292-6293 (2006).

<sup>iii</sup> D. Rabuka, R. Parthasarathy, G. S. Lee, X. Chen, J. T. Groves, C. R. Bertozzi, "Hierarchical assembly of model cell surfaces: Synthesis of mucin mimetic polymers and their display on supported bilayers," *J. Am. Chem. Soc.* **129**, 5462-5471 (2007)

<sup>iv</sup> R. Parthasarathy, D. Rabuka, C. R. Bertozzi, J. T. Goves, "Molecular orientation of membrane-anchored mucin glypoprotein mimics," *J. Phys. Chem. B* (in press)

<sup>v</sup> G. Moad, Y. K. Chong, A. Postma, E. Rizzardo, S. H. Thang, "Advances in RAFT polymerization : the synthesis of polymers with defined end-groups," *Polymer* **46**, 8458-8468 (2005).

<sup>vi</sup> R. Huisgen, "1,3-Dipolar cycloaddition chemistry," Wiley, New York (Ed.: A. Padwa), pp. 1-176 (1984).

<sup>vii</sup> Y. Xia, G. M. Whitesides, "Soft Lithography" *Angew. Chem. Int. Ed.* **37**, 550-575 (1998).

# Development of Integrated Photocatalytic Systems Using the Tobacco Mosaic Virus

Matthew B. Francis

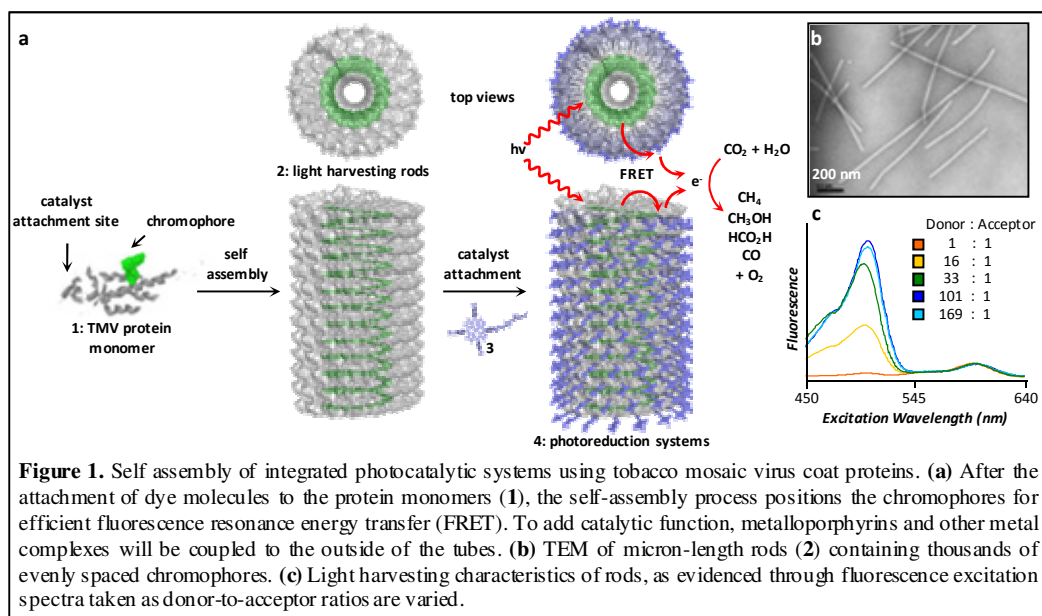
Lawrence Berkeley National Labs, Materials Sciences Division, Berkeley, CA 94720

francis@cchem.berkeley.edu

## Program Scope

Virtually all carbon-based energy sources are produced through the fixation of CO<sub>2</sub> by photosynthetic organisms. This is accomplished through a series of enzymatic transformations fueled by ATP and the reducing agent NADPH. Both of these components are generated by catalytic photosystems comprising a beautifully organized set of chromophores, electron transfer moieties, catalysts, and molecular machines. As our understanding of these systems has increased, it has inspired the design of fully synthetic systems that can achieve CO<sub>2</sub> reduction using the energy of collected sunlight.<sup>1</sup> Successful systems have been developed for this purpose using metalloporphyrins,<sup>2</sup> ruthenium complexes,<sup>3</sup> nanoparticles,<sup>4</sup> and coated carbon electrodes<sup>5</sup> as the reaction centers. In addition to offering a method for carbon dioxide sequestration, the mixtures of methane, methanol, and formate, and CO that these reactions produce can themselves be used as biofuels or feedstocks for other production processes. Although these systems have provided important leads, several factors must be addressed to increase their efficiency before they will be ready for widespread use. These include poor matching of the absorption characteristics to the solar spectrum, catalyst deactivation through aggregation pathways, and poor reactive surface area.

It is proposed that many, if not all, of these approaches would benefit from the ability of biological systems to orient the individual components with rigidly defined spatial relationships. By achieving this on small length scales, properly tuned chromophores could be directly coupled to combinations of metal catalysts and high-surface area nanoparticles for maximal light collection. To explore these possibilities, we are developing integrated systems for efficient catalytic photoreduction using the self-assembling scaffold of the tobacco mosaic virus as a material template. Through a combination of biological manipulations, chemical synthesis, optical analysis, and computational modeling, the high energy electrons produced by these systems will be explored as a means to reduce carbon dioxide (Figure 1a), generate hydrogen gas through electrolysis, and generate photocurrent to supply additional energy for biofuel processing and transport.

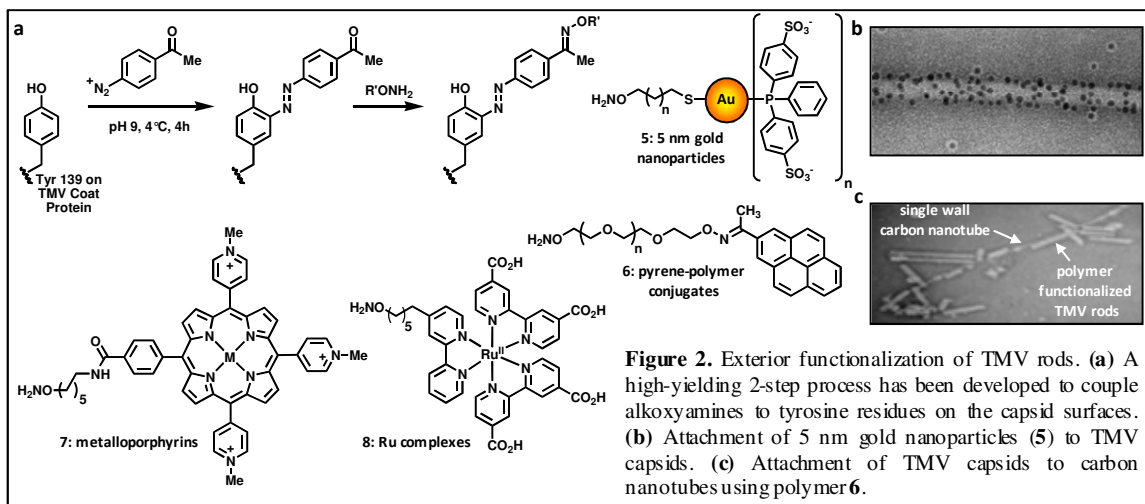


## Recent Progress and Future Plans

**(a) Self Assembly of Efficient Light Harvesting Systems.** The rod-shaped capsid of the tobacco mosaic virus (TMV) provides a practical scaffold for the construction of bulk quantities of nanostructured materials. Propagation of the virus in as few as 30 tobacco plants yields over 2 grams of the protein capsids, allowing multikilogram quantities to be produced from a single acre of tobacco farmland.<sup>6</sup> The capsid shell comprises 2100 identical protein monomers arranged in a hollow helix that is 18 nm in diameter. In recent studies,<sup>7,8,9</sup> we have developed 4 efficient chemical strategies that can be used to attach virtually any synthetic group of interest to the exterior, interior, “top end”, or “bottom end” surfaces of the tube. Taken together, these modification reactions render the TMV capsid one of the most versatile scaffolds available for the construction of nanoscale materials.

As a first step toward energy collection, modified TMV assemblies have been used to create light harvesting systems reminiscent of those found in photosynthetic bacteria.<sup>9</sup> These structures were accessed by first preparing a cysteine mutant of the capsid protein to allow the attachment of organic chromophores, Figure 1a. Following conditions elucidated by Klug and coworkers,<sup>10</sup> the protein conjugates were assembled into disk and rod structures through variation of the pH and ionic strength. In the case of rods, the individual assemblies spanned lengths in excess of 1500 nm and contained >7500 dye molecules, Figure 1b. The close spacing of the chromophores within the protein helix allowed efficient fluorescence resonance energy transfer to occur, transferring the light collected by over 30 individual donors to a single acceptor, Figure 1c. As many of these donors are located beyond Förster radius for the donor/acceptor pair, the absorbed energy is presumed to be shuttled through multiple donor-to-donor interactions (see Figure 3a). Three chromophore systems have also been prepared for broad spectrum light collection with over 93% efficiency.

**(b) Incorporation of Catalytic and Electron Transfer Groups.** The key next step in these studies is the attachment of electron transfer groups to secondary sites on the assemblies. In previous reports we have accomplished this through the reaction of exterior tyrosine residues (Tyr139) with diazonium salts, allowing 2200 new functional groups on the exterior surface of each 300 nm capsid, Figure 2a. These sites have then been used to position polymers,<sup>7,8</sup> chromophores,<sup>7</sup> gold nanoparticles (Figure 2b) and carbon nanotubes<sup>8</sup> (Figure 2c) on the exterior surfaces of the rods. More recently, asymmetrically substituted porphyrins (such as **7**, Figure 2) have been synthesized and attached to these sites to incorporate catalytic function. This strategy positions them well within the Förster radius for energy transfer from the chromophores placed inside the rods, as suggested in Figure 1a. Although porphyrins and similar metal ligand frameworks have been shown to catalyze the photoreduction of CO<sub>2</sub>,<sup>2</sup> porphyrin chemistry in





general is hampered by the facile oligomerization of these species in solution (particularly as  $\mu$ -oxo dimers). The TMV-based scaffold provides an attractive solution to this problem, as the porphyrins on its surface are held at fixed distances of 3.3 nm, and therefore cannot aggregate. In current experiments, cobalt ions capable of  $\text{CO}_2$  photoreduction are being introduced into these sites. We are also attaching (bipyridyl)ruthenium(II) complexes to these locations, as they are well-known to undergo photoinitiated electron transfer.<sup>3,11</sup> The light harvesting components within will be altered as needed to match the spectral input of the catalyst to the solar spectrum. Following electron transfer, catalyst regeneration is envisioned to occur using inexpensive sacrificial reductants (such as alkyl amines) as described in the original systems,<sup>2</sup> or through the oxidation of the electrolyte solutions themselves.

As an alternative building block, a growing number of nanoparticles have been shown to reduce  $\text{CO}_2$  to methane, methanol, and formate upon photoexcitation. Titania<sup>4a-c,4e</sup> and  $\text{ZnS}$ <sup>4d</sup> systems have demonstrated notable capabilities in this regard, but they typically require irradiation with UV light due to their large band gap. To improve the light absorption characteristics of these particles, we are coupling them to TMV-based sensitizer systems that possess carboxylate-substituted  $\text{Zn}(\text{porphyrin})$  complexes on the exterior. Once formed, these systems will again be evaluated for their ability to produce  $\text{CO}_2$  reduction products as a function of varying excitation wavelength.

**(c) Theoretical Modeling for System Optimization.** Due to the complex and sometimes unpredictable nature of biomolecular self-assembly, any device that is fabricated in this way must be able to tolerate a certain number of “defect” sites. In addition, systems that rely on organic chromophores or metal-ligand complexes must be able to resist deactivation caused by photobleaching. Because the TMV template systems represent three dimensional assemblies, it was hypothesized that they would exhibit an enhanced resistance to these effects due to the presence of redundant energy transfer pathways that can circumvent blockage arising from missing or deactivated chromophores, Figure 3a. To determine if this was the case, we have collaborated with the Geissler Group (also in the Biomolecular Materials Program) to develop several computational models that simulate the energy transfer occurring in these systems. These systems were built using the transfer rate parameters measured for our systems and the known distance relationships established by the capsid functional groups. By applying different numbers of defect sites and photobleaching rates, it was found that the three dimensional systems should indeed exhibit significantly longer device lifetime, Figure 3b. In initial experiments, this has been verified experimentally through the observation of much higher transfer efficiencies for TMV rods than for simple disks.<sup>9</sup>

As catalytic groups are incorporated, these computational methods will provide an indispensable means to optimize these systems. More advanced simulations will be conducted to determine optimal catalytic and electron transfer rates for variations in photon flux. They will also be used to guide the selection of chromophores to generate optimal systems that use of the full solar spectrum.

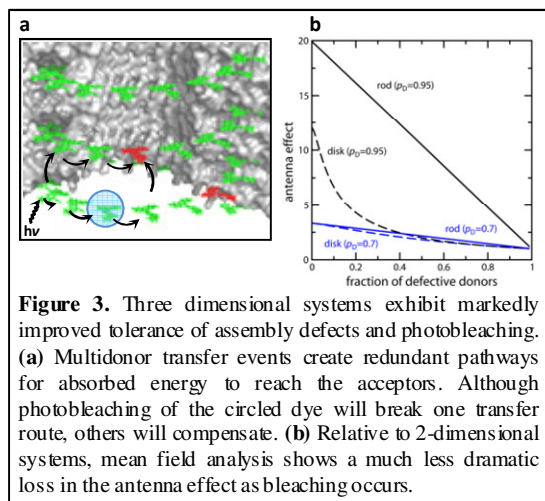


**Figure 3.** Three dimensional systems exhibit markedly improved tolerance of assembly defects and photobleaching. (a) Multidonor transfer events create redundant pathways for absorbed energy to reach the acceptors. Although photobleaching of the circled dye will break one transfer route, others will compensate. (b) Relative to 2-dimensional systems, mean field analysis shows a much less dramatic loss in the antenna effect as bleaching occurs.

## Outcome

These studies will yield a well-defined scaffold that can be used to develop a wide range of new photocatalytic systems. The robust capsids offer a uniquely high density of functionalizable sites, and thus can be used to access systems of unprecedented complexity. Another key advantage of the TMV backbone is that it is both non-toxic and fully biorenewable. As such, efforts will be undertaken to derive chromophores and ligand structures from porphyrins, corrins, chlorins, and other building blocks that are produced by plants and bacteria. Through collaborative efforts in the Helios Program, biorenewable electron transfer membranes are also being developed for incorporation into these systems.

## Research Publications Sponsored by this Program (2005-2007)

1. Schlick, T. L.; Ding, Z.; Francis, M. B. "Dual Surface Modification of the Tobacco Mosaic Virus" *J. Am. Chem. Soc.* **2005**, *127*, 3718-3723.
2. Miller, R. A.; Presley, A. D.; Francis, M. B. "Self-Assembling Light Harvesting Systems From Tobacco Mosaic Virus Capsid Proteins" *J. Am. Chem. Soc.* **2007**, *129*, 3104-3109.
3. Hooker, J. M.; Esser-Kahn, A. P.; Francis, M. B. "Modification of Aniline-Containing Proteins Using a Chemoselective Oxidative Coupling Reaction" *J. Am. Chem. Soc.* **2006**, *128*, 15558-15559.
4. Johnson, H. R.; Hooker, J. M.; Clark, D. S.; Francis, M. B. "Solubilization and Stabilization of Bacteriophage MS2 in Organic Solvents" *Biotechnology and Bioprocess Engineering* **2007**, 224-233.
5. Kovacs, E. W.; Hooker, J. M.; Romanini, D. W.; Holder, P. G.; Berry, K. E.; Francis, M. B. "Dual Surface Modified Bacteriophage MS2 as a Prototype Viral Capsid-Based Drug Delivery System" *Bioconjugate Chemistry* **2007**, *18*, 1140-1147.
6. Holder, P. G.; Francis, M. B. "Integration of a Self-Assembling Protein Scaffold with Water-Soluble Single-Walled Carbon Nanotubes" *Angewandte Chemie* **2007**, *23*, 4370-4373.
7. Hooker, J. M.; Datta, A.; Botta, M.; Raymond, K. N.; Francis, M. B. "MR Contrast Agents from Viral Capsid Shells: A Comparison of Exterior and Interior Cargo Strategies" *Nano Letters* **2007**, *7*, 2207-2210.

## References

- 1 For general reviews, see: a) Behr, A. *Carbon Dioxide Activation by Metal Complexes*; VCH: Weinheim, 1988. b) Sutin, N.; Creutz, C.; Fujita, E. *Comments Inorg. Chem.* **1997**, *19*, 67.
- 2 a) Grodkowski, J.; Neta, P. *J. Phys. Chem. A* **2000**, *104*, 1848-1853. b) Grodkowski, J.; Behar, D.; Neta, P.; Hambright, P. *J. Phys. Chem. A* **1997**, *101*, 248. c) Behar, D.; Dhanasekaran, T.; Neta, P.; Hosten, C. M.; Ejeh, D.; Hambright, P.; Fujita, E. *J. Phys. Chem. A* **1998**, *102*, 2870. d) Dhanasekaran, T.; Grodkowski, J.; Neta, P.; Hambright, P.; Fujita, E. *J. Phys. Chem. A* **1999**, *103*, 7742.
- 3 Hayashi, H.; Ogo, S.; Abura, T.; Fukuzumi, S. *J. Am. Chem. Soc.* **2003**, *125*, 14266-14267.
- 4 a) Pathak, P.; Meziani, M. J.; Li, Y.; Cureton, L. T.; Sun, Y. P. *Chem Comm* **2004**, 1234-1235. b) Pathak, P.; Meziani, M. J.; Castillo, L.; Sun, Y. P. *Green Chem* **2005**, *7*, 667-670. c) Anpo, M.; Yamashita, H.; Ichihashi, Y.; Fujii, Y.; Honda, M. *J. Phys. Chem. B* **1997**, *101*, 2632. d) Inoue, H.; Torimoto, T.; Sakata, T.; Mori, H.; Yoneyama, H. *Chem. Lett.* **1990**, 1483. e) A. Henglein, M. Gutierrez and Ch. Fischer, *Ber. Bunsenges. Phys. Chem.* **1984**, *88*, 1704.
- 5 a) Lieber, C. M.; Lewis, N. S. *J. Am. Chem. Soc.* **1984**, *106*, 5033. b) Kapusta, S.; Hackerman, N. *J. Electrochem. Soc.* **1984**, *131*, 1511.
- 6 Chapman, S. *Methods in Molecular Biology, Vol 81: Plant Virology Protocols: From Virus Isolation to Transgenic Resistance*; pp 123-129; Humana Press: Totowa, NJ.
- 7 Schlick, T. L.; Ding, Z.; Kovacs, E. W.; Francis, M. B. *J. Am. Chem. Soc.* **2005**, *127*, 3718-3723.
- 8 Holder, P. G.; Francis, M. B. *Angewandte Chemie Int. Ed.* **2007**, *23*, 4370-4373.
- 9 Miller, R. A.; Presley, A. D.; Francis, M. B. *J. Am. Chem. Soc.* **2007**, *129*, 3104-3109.
- 10 Klug, A. *Phil. Trans. R. Soc. Lond. B* **1999**, *354*, 531-535.
- 11 For a classic example, see Oregon, B.; Gratzel, M. *Nature* **1991**, *353*, 737-740.

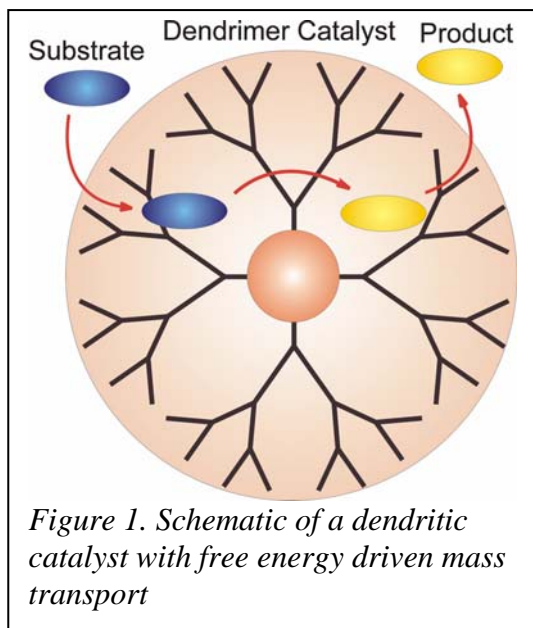
# Biomolecular Program

## *Bioinspired polymers as synthetic enzyme mimics*

Jean Fréchet,  
Division of Materials Sciences, Lawrence Berkeley National Laboratory  
Berkeley, CA, 94720  
[J.Frechet@lbl.gov](mailto:J.Frechet@lbl.gov)

### 1. Program Scope and recent work.

As part of a fundamental study of bioinspired catalysts this program explores the design and function of synthetic macromolecules that mimic the shape and function of natural enzymes.



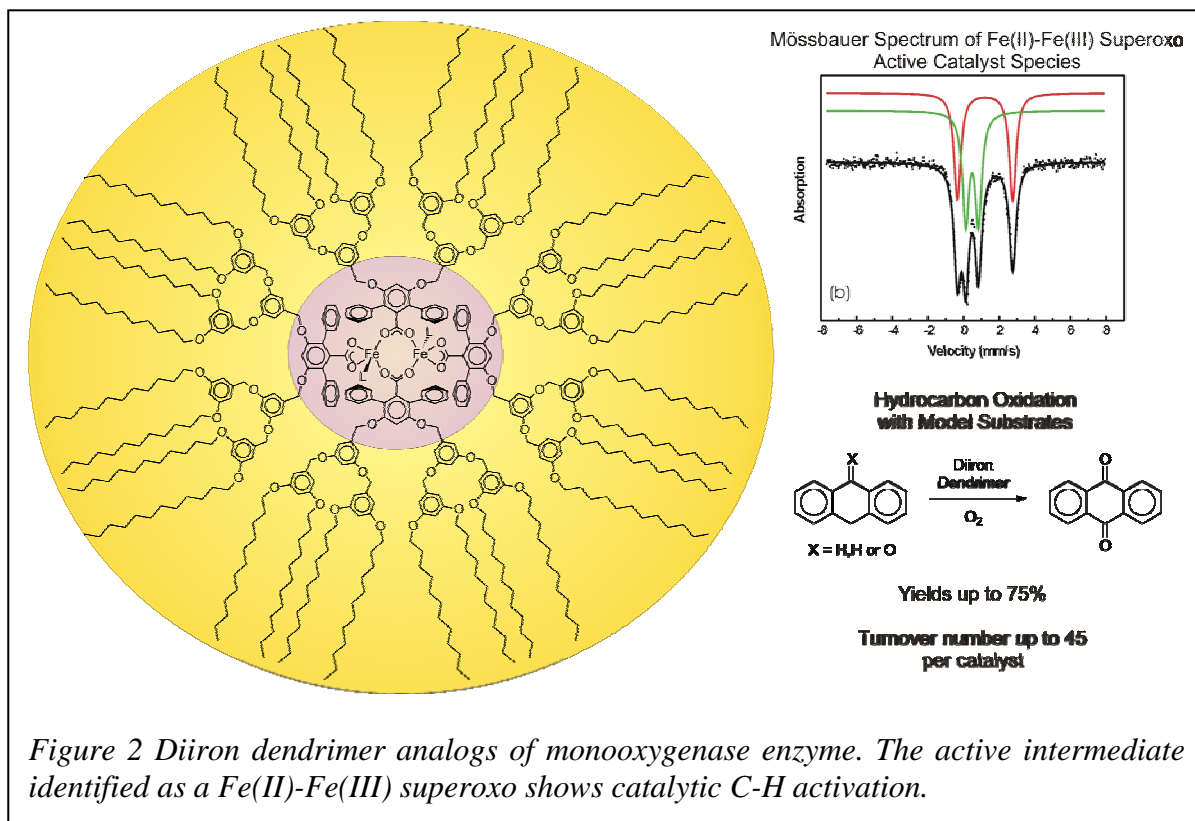
The fundamental design of the macromolecules mimics that of enzymes as it incorporates the concepts of site isolation and or free energy driven processes into synthetic macromolecules, about the same size and shape as enzymes, that act as individual nanometer sized reactors with an active catalytic center surrounded by molecular components that contribute to mass transport in and out of the active center (Figure 1). [Helms, B.; Fréchet, J. M. J. The dendrimer effect in homogeneous catalysis. *Adv. Synthesis & Catalysis* (2006), 348(10+11), 1125-1148.]

Following our early demonstration of the concept, we have explored the effect of polymer architecture and nanoenvironment on organic processes catalyzed by a variety of synthetic enzyme mimics. This work has enabled us to

demonstrate that, just as is the case with enzymes, it is the nanoenvironment that is determining in the action of the catalytic species. [Helms, B.; Liang, C.O.; Hawker, C.J.; Fréchet, J.M.J. Effects of Polymer Architecture and Nanoenvironment in Acylation Reactions Employing Dendritic Dialkylaminopyridine Catalysts. *Macromolecules* 2005, 28, 5411-5].

We have also explored the concept of site isolation in an attempt to realize a cascade of catalyzed reactions within a single reaction vessel, thus mimicking the action of a train of enzymes. This has entailed the use of two different star polymers with two normally incompatible catalytic sites located at the center of the macromolecules in such a way that they remained isolated from each other but were still accessible to small molecule substrates. These were then used to effect two consecutive reactions in one pot avoiding catalyst deactivation in a way that could not be achieved with small molecule catalysts. [Helms, B.; Guillaudeau, S. J.; Xie, Y.; McMurdo, M.; Hawker, C. J.; Fréchet, J. M. J.. One-pot reaction cascades using star polymers with core-confined catalysts. *Angewandte Chemie, International Edition* (2005), 44(39), 6384-6387]

**2. Work in progress.** Our most recent work still in progress involves the mimicry of the active sites of metalloenzymes. In the enzymes, these sites are usually deeply buried inside a hydrophobic protein sheath, which protects them from undesirable hydrolysis and polymerization reactions, allowing them to achieve their normal functions. In order to mimic the hydrophobic environment of the active sites in bacterial monooxygenases, diiron(II) compounds of the general formula  $[\text{Fe}_2([\text{G}-3]\text{COO})_4(\text{R})_2]$  were prepared, where  $[\text{G}-3]\text{COO}^-$  is a third-generation dendrimer-appended terphenyl carboxylate ligand and R is a pyridine



derivative (Figure 2). The dendrimer environment provides excellent protection for the diiron center, reducing its reactivity toward dioxygen by about 300-fold compared with analogous complexes of terphenyl carboxylate ( $[\text{G}-1]\text{COO}^-$ ) ligands. An Fe(II)Fe(III) intermediate was characterized by electronic, EPR, Mössbauer, and XAS spectroscopic analysis following oxygenation of  $[\text{Fe}_2([\text{G}-3]\text{COO})_4(4\text{-PPy})_2]$ , where 4-PPy is 4-pyrrolidinopyridine. The results are consistent with formation of a superoxo species. This intermediate can oxidize external substrates and catalysis was observed with anthrone as the substrate. We are currently formulating a catalytic oxidation mechanism describing this chemistry and this work should be ready for publication within the next few months.

### 3. Future Plans.

Having demonstrated the validity of our basic concepts we now plan to develop novel, more sophisticated enzyme mimics enabling a multiplicity of reactions to be carried out at the same time. In order to do this, we have identified three significant targets, one of which will be outlined below while the others will be outlined during the presentation:

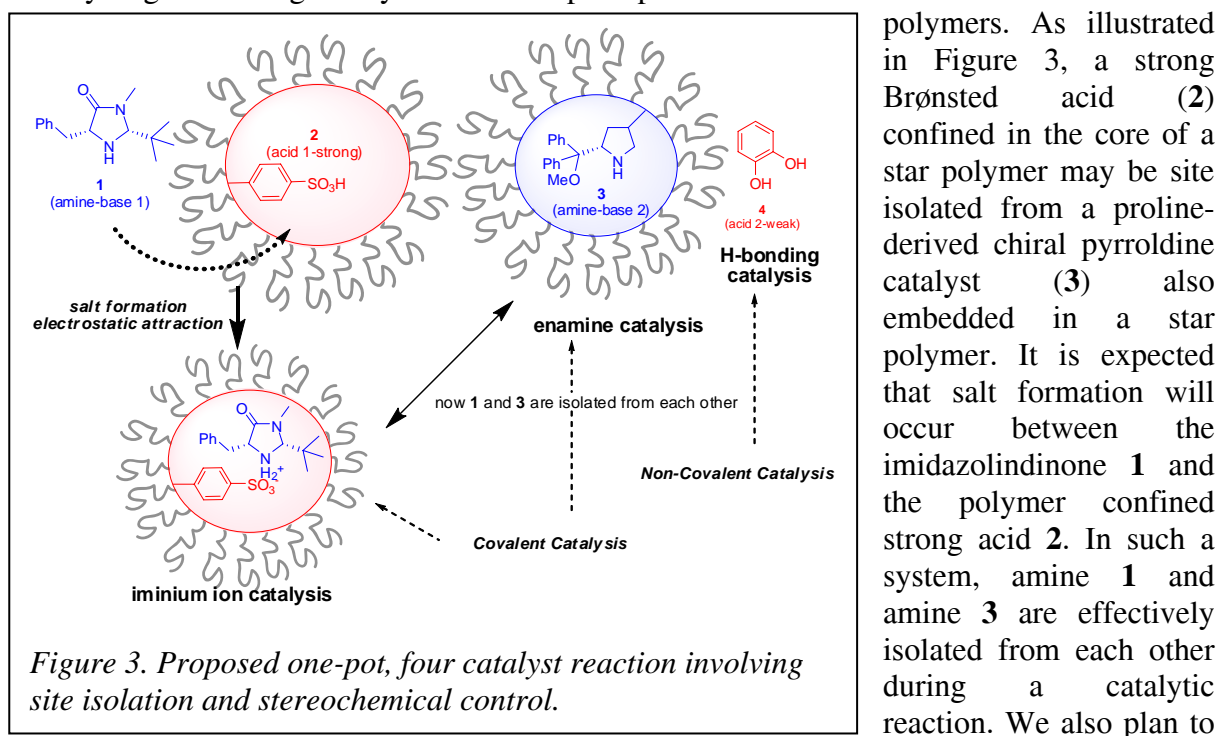
- i) Exploration of enzyme-like stereoselective, multistep, multicatalyst processes.

- ii) Development of rugged dendronized polymers frameworks providing access to tubular structures that may enable the incorporation of several site-isolated catalytic moieties *within a single molecule* acting as a nanoreactor.
- iii) Self-assembled nanospheres as enzyme mimics.

#### Stereo-incompatible catalysts.

The overall objective of this project is to apply our understanding of synthetic macromolecules (e.g. dendrimers, polymers) to mimic the site isolation properties of biomolecules for catalysis. We propose to develop site-isolated catalyst systems for cascade reactions that require three or more different catalytic entities, and simultaneously address both chemoselectivity and stereoselectivity for reactions that are much more sophisticated than any we have studied earlier. The project is expected to address fundamental challenges and enhance our knowledge in the design and synthesis of enzyme-like macromolecules, as well as to provide novel and potentially useful solutions to sophisticated cascade reactions using multiple otherwise incompatible asymmetric catalysts.

As a specific model catalytic system, we propose to combine iminium ion, enamine, and hydrogen-bonding catalysis in a one-pot operation via site isolation with soluble star polymers.



add a weak acid (e.g. catechol **4**, used as a small molecule) as hydrogen-bonding catalyst to assist in the one-pot operation. The weak acid is chosen based on the following considerations: it can activate electrophiles via hydrogen-bonding interaction, but not form salt with either of the amine catalysts (note: pKa of **4** in DMSO is around 18; while pKa of strong acid **2** is around 1; so **4** will not compete with **2** for salt formation to any significant extent). With the four catalysts, we hypothesize that iminium ion, enamine, and hydrogen-bonding catalysis can be combined in a one-pot operation for a large range of organic transformations as shown schematically in Figure 3. We are currently designing model reactions that should enable us to access unusual stereoselectivities, especially for reactions that generate multiple stereocenters.

## **Biomolecular Materials Program**

### **Statistical mechanics of biomolecular materials: Theory and modeling of DNA and viral capsids as building blocks for large-scale structures**

Principal Investigator

**Phillip L. Geissler**

Faculty Scientist, Physical Biosciences & Materials Sciences Divisions

Mailing address of PI:

Lawrence Berkeley National Laboratory

1 Cyclotron Road

Mailstop: HILDEBRAND

Berkeley, CA, 94720

Email: [geissler@cchem.berkeley.edu](mailto:geissler@cchem.berkeley.edu)

Biomolecular materials differ fundamentally from their solid state counterparts not only in the origin of their components but also in how they organize. Noncovalent forces governing intra- and inter-molecular arrangements of proteins and nucleic acids are hardly stronger than random thermal noise at room temperature. The resulting softness and fluxionality of these arrangements greatly complicate rational design of biomolecular materials, but they also enrich the possible sensitivity, adaptivity, and functional diversity that can be achieved. This project uses theoretical tools of statistical mechanics to examine how microscopic fluctuations shape structure, response, and dynamics of solutions comprising many biological molecules and other nanometer-scale components. Specific focus is on the use of DNA hybridization to template nanoparticle arrays, and on tailoring interactions among protein complexes to achieve robust and adaptive self-assembly. Research in this project is carried out in close collaboration with the laboratories of Paul Alivisatos and Matt Francis. Feedback with experiment provides both an invaluable test bed for the realism of reduced models and an opportunity to quickly implement novel design strategies that emerge from theoretical predictions.

Our work on nucleic acids to date has focused on the mechanics of individual double-stranded molecules of DNA (dsDNA), and on the optimization of nucleotide sequences for rapid and discriminating hybridization. Both areas are inspired by experiments in Paul Alivisatos's lab and directed toward providing insight necessary to overcome major practical challenges. Textbooks depict dsDNA molecules comprising fewer than 100 base pairs as rigid rods with well-defined lengths. This caricature has fueled attempts to use DNA as a kind of patterned glue for linking nanoscale objects. X-ray scattering from gold nanoparticle pairs linked by dsDNA demonstrate that this caricature leaves much to be desired. Even compared with the statistical mechanics of a fluctuating elastic rod (whose persistence length is set to that reported for dsDNA, ~50 nm), nanoparticle-linked dsDNA executes unexpectedly large fluctuations away from a straight geometry. We attempt to rationalize this behavior using reduced models which resolve individual base pairs but not atomistic detail. (Fundamental computational limitations preclude simulating in atomistic detail molecular structures of this size over

relevant time scales.) Many reduced models have been proposed and studied in other contexts. Our computer simulations show that their predictions for measured nanoparticle pair correlations vary greatly. (See Fig. 1) Only models that allow for the possibility of “melting”, i.e., fluctuations in which local base pairing is severely disrupted, can be consistent with distortions suggested by experimental data. Among these models the frequency of melts at equilibrium also varies widely, according to different notions of the factors controlling base pairing thermodynamics. Progress to date suggests that these experiments may provide a previously lacking quantitative guide for modeling nucleic acids at the nanometer scale. Most importantly, it appears that an appropriate model cannot neglect large transient fluctuations away from idealized textbook configurations.

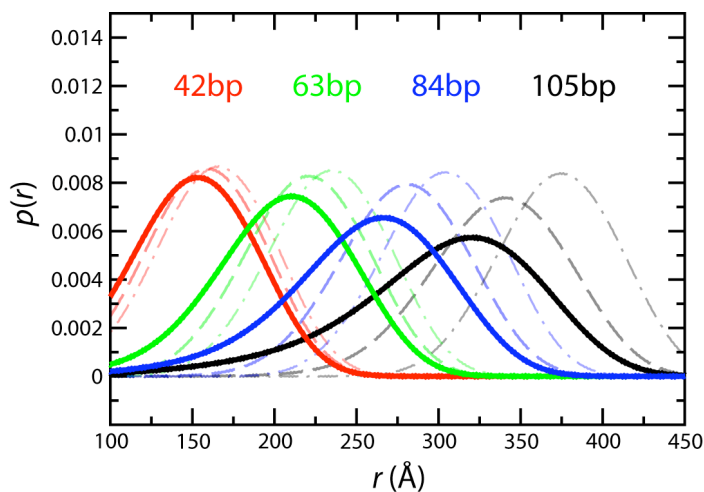


Figure 1. Predictions of three computational models for the distribution  $p(r)$  of distances  $r$  between pairs of dsDNA-linked gold nanoparticle. Nucleic acid constructs vary from 42 base pairs (bp) to 105 bp. Dot-dashed lines correspond to rigid DNA; dashed lines to a fluctuating elastic rod; and solid lines to a fluctuating elastic rod with thermally distributed disruptions of base pairing. Measured distributions possess a broad tail at small separations consistent only with the model that includes thermal melts. All

distributions have been convolved with the measured scattering function for a single nanoparticle.

The ultimate goal of understanding ensembles of dsDNA structures is to guide construction of materials patterned by its nucleotide sequences. Again, textbooks provide simple rules for base pairing of complementary sequences that appear sufficient to design complex spatial relationships of many nanoparticles, such as the schematic example depicted in Fig. 2. Such hybrid structures have not been successfully realized in the laboratory, apparently due to the failure of mixtures of many nucleic acids to hybridize as intended. We are investigating the dynamics of molecular models for hybridizing strands (slightly more detailed than those described above) in order to understand the microscopic origins of this failure, and to generate sequences better suited to imposing desired linkages. Our strategy seeks first to identify dynamical bottlenecks impeding assembly for a given nucleic acid sequence. With this capability, one could introduce random modifications to the sequence, and accept them with a probability that promotes formation of desired patterns. Eventually, a series of biased random modifications should produce optimal sequences in much the way that evolution adapts species to environmental stresses.

Even with reduced microscopic models, many of the time scales relevant for large-scale assembly remain out of reach. These slow dynamics involve collective rearrangements of multiple DNA strands, which proceed slowly in molecular dynamics simulations and hardly at all in conventional Monte Carlo simulations. We have invented new Monte Carlo methods which greatly facilitate inter-strand rearrangements. They

modify combinations of several torsional angles, effecting isolated changes in the relative conformations of paired strands. These “accordion moves” (so termed because they compress or expand internal regions of paired strands without perturbing inter-strand structure at the peripheries) dramatically improve the sampling configurations in systems comprising multiple DNA strands. Over the last year we have devised these moves, determined how they should be performed to ensure proper reproduction of equilibrium states, and developed efficient numerical algorithms for their implementation.

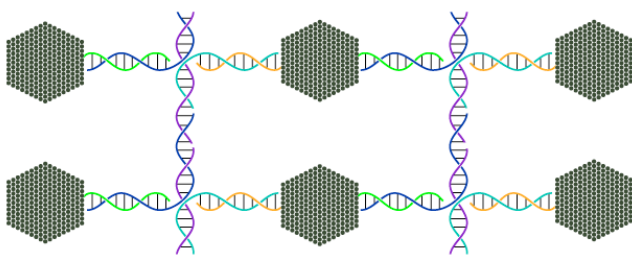


Figure 2. Schematic example of nanocrystals (depicted as dark green hexagonal lattices) arranged into regular patterns through base pairing between short strands of DNA. Orange and green strands are covalently attached to nanocrystals. The remaining strands are held in place by the strong noncovalent

forces that give hybridized DNA its double-helix structure.

Together, these techniques allow simulation of assembling DNA strands that form desired structures efficiently. But to realize sequence design, it is necessary also to gauge the efficiency of poorly designed sequences. This need calls for methods to identify the depth of kinetic traps without waiting for a system to spontaneously escape them. We have adapted standard non-Boltzmann sampling techniques for this purpose. Choosing a simple order parameter for the degree of desired hybridization, we bias configurational sampling in a way that naturally exposes the nature of certain kinetic traps. While this approach is not guaranteed to reveal all possible dynamical bottlenecks, it should be sufficient for at least the initial stages of design. With all these methods in place, we are now poised to begin systematic design of DNA sequences for nanocrystal assembly.

Our work with Matt Francis explores a different strategy for assembling nanoscale components into patterned structures. Here, the components are protein complexes that function in nature as packaging for the genetic material of viruses, chemically modified to adhere on a flat surface. Further functionalization of their exterior provides the possibility to control the strength, range, and specificity of component interactions, and therefore to prompt organization into a variety of possibly interconverting arrays.

We have developed a simple computational model for virus assembly on solid substrates and have performed exploratory simulations to characterize its range of behavior. The model represents functionalized viral capsids as hard disks in two dimensions, endowed with short-ranged, orientationally specific interactions. Kinetic Monte Carlo algorithms advance periodically replicated systems of these disks efficiently and with dynamical realism. For complete (or nearly complete) lateral functionalization, our model disks are effectively isotropic and exhibit well understood thermodynamic states: vapor (low coverage of disks on the substrate), liquid (higher coverage), and hexagonally ordered solid. Precise predictions can be made for the temperatures (or, equivalently, interaction strengths) where these phases coexist and transform, providing a useful point of comparison with experiment. More exotic phases can be generated simply by limiting the extent of chemical modification. Randomly deleting half of the disks’



interaction sites can stabilize sparse network structures that are rigid and locally compact despite their low density. Calculations are underway to establish the thermodynamics and kinetic accessibility of such phases and to locate transitions between them.

Continued theoretical modeling will focus on two-species capsid systems (see Fig. 3) whose phase separation can be induced or suppressed by adding chemical linking agents or competitive inhibitors. Of particular interest is the time scale of kinetic trapping during segregation, and the resulting long-lived spatial correlations. Using analytical as well as computational techniques, we aim to predict ranges of attraction strength, linker flexibility, and disk concentration that produce specific donor-acceptor arrangements. Because these structures are not representative of an equilibrium state, they may possess interesting chemical and physical memories that could be exploited by experimental protocols. Successive strengthening and weakening of attractions, for instance, might circumvent undesirable kinetic traps, allowing the equilibration of sub-structures which would otherwise be effectively frozen in. From a theoretical standpoint, this kind of selective relaxation offers a rich testing-ground for nonequilibrium statistical mechanics. More practically, it introduces modes of self-assembly that could not be achieved at equilibrium or in the course straightforward phase coarsening. Concerted simulation efforts and time-resolved AFM measurements promise to open new windows into these unique dynamics and their material applications.

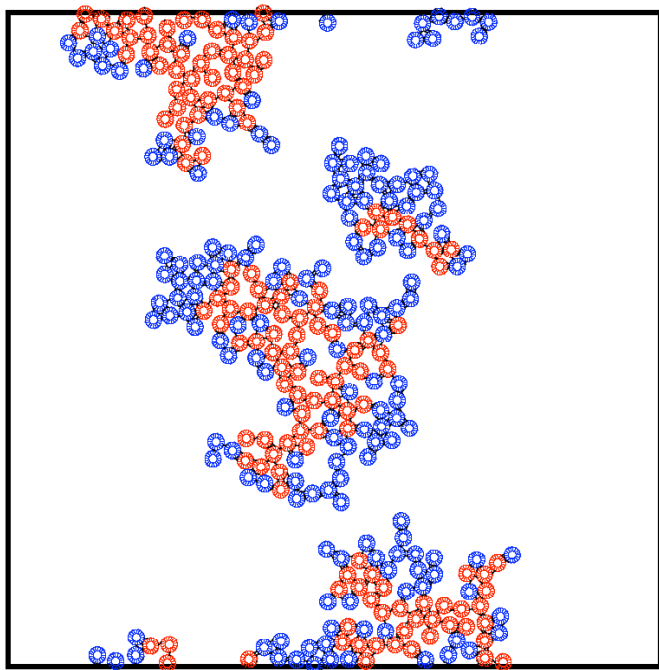


Figure 3. Self-assembly of two species of model viral capsids. Red and blue disks have been functionalized with linking sites to different degrees, and they interact with different strengths. Red disks bind strongly, providing a template onto which more weakly interacting blue disks can deposit.

# **Biomolecular Materials Program**

*Jay T. Groves (Mark Alper, Paul Alivisatos, Carolyn Bertozzi, Matt Francis, Jean Frechet, Phillip Geissler, Dirk Trauner)*

*Physical Biosciences Division  
Building 38 – Room 105 Lewis  
Lawrence Berkeley National Laboratory  
Berkeley Ca 94720-1460*

## Program Scope

Living organisms have unanimously adopted the phospholipid membrane as the material of choice for the organization and coordination of nearly all biochemical processes. Composed of a self assembling bilayer of phospholipids, cholesterol, and other amphiphilic molecules, biomembranes exhibit a collection of unusual physical properties not observed in other materials. Characteristics such as the coexistence of liquid crystalline and disordered fluid phases, thermodynamic critical points near physiological growth temperatures, and the mechanical coupling of distant biomolecular reactions (via membrane bending effects) conspire within cell membranes to enable and regulate life processes. Phospholipid membranes can be assembled on solid substrates such that both the structure and fluid nature of the membrane is preserved<sup>1</sup>. A critical and unique feature of the supported membrane interface is that the membrane fluidity permits macroscopic rearrangements of the surface<sup>2</sup>. Fluid rearrangements of the cell membrane are emerging as a broadly significant theme among cell surface interactions, and may be a definitive strategy of information exchange within multicellular organisms, including humans<sup>3</sup>. The unique interface between a solid material and a fluid membrane offered by supported membranes provides an ideal mechanism to functionalize inanimate substrates with life-like properties.

A number of past studies have demonstrated that patterning chemical and physical characteristics of a surface can significantly influence cellular behavior<sup>4-6</sup>. Despite the successes of this substantive body of work, only a handful of specific biological interactions have been functionally deployed between living cells and solid surfaces<sup>7</sup>. It is our hypothesis that development of fluid membrane surface coatings will vastly expand the functional biochemical repertoire that can be exploited to mediate interactions between material substrates and living cells.

The overarching theme of this project is to develop design rules and synthetic strategies to construct biomembrane derivitized surfaces that interact with living cells in functional and prescribed manners. Such capabilities, once achieved, will constitute a major step towards the domestication of life at the cellular level. The ability to tell cells precisely what to do and where to do it will have substantial impact in areas of chemical and material synthesis, energy transduction, and molecular detection. A hypothetical example

of such a hybrid device is illustrated in Figure 1. Key technical challenges that must be overcome to achieve these ends include: i) construction of membranes on surfaces with controlled orientation of signal-bearing proteins; ii) control of phase separated membrane structures (membrane rafts); iii) engineering of signal-bearing proteins for maximum activity and mobility in supported membranes (membrane-linked vs. full transmembrane).

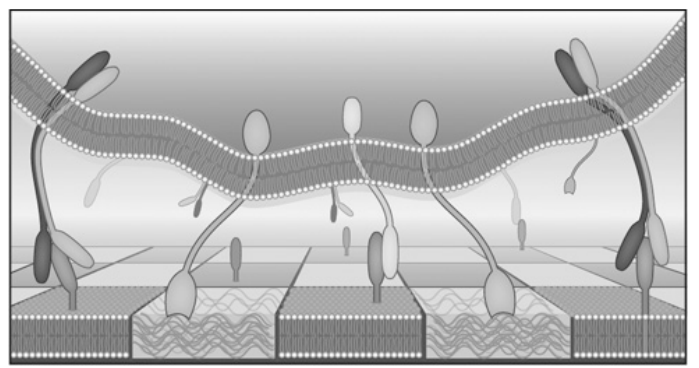


**Figure 1:** Schematic of a hybrid interface between a living cell and an inorganic substrate. Some linkages between cell and surface serve the purpose of directing the cell's position while others conduct electrons. Adapted from: J.T. Groves *Sci. STKE* 2005, pe45.

### Recent Progress

We have previously demonstrated that supported membranes can be used to modulate the adhesion and growth of mammalian cells in culture. This initial work employed an adhesion promoting lipid, PS, to direct the cellular behavior<sup>8</sup>. We established that supported membranes function under general cell culture conditions and are suitable mediators of interactions between living cells and inanimate materials. In the next phase of this work, we are emphasizing the use of specific signaling proteins to elicit more specialized cellular responses. Initial work along these lines, employing a GPI-linked form of the neuronal synapse protein neuroligin, yielded promising results and led to two new collaborative publications between the Groves and Isacoff labs in 2005<sup>9-10</sup>. We have also recently employed the same technology in a study of the mechanisms of signaling between cells and surfaces, emphasizing the T cell<sup>11</sup>. Images of synapses between live T cells and surfaces are illustrated in Figure 2, and are demonstrative of the type of functional interfaces we are developing within this program

This effort is directed towards the discovery of universal themes of signal transduction at cell surfaces with an eye to how these may be implemented within a synthetic materials context.

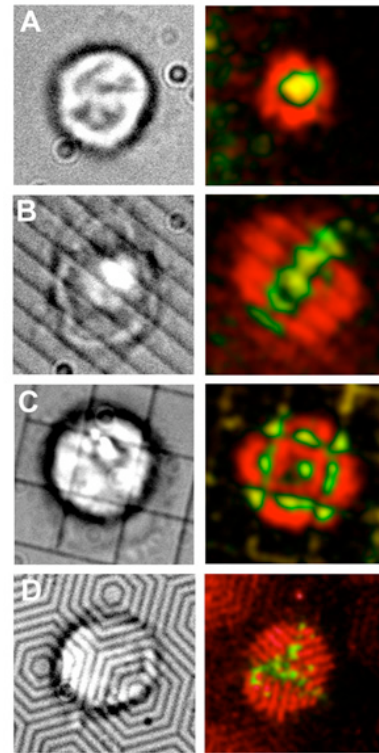


**Figure 2:** Brightfield (right) and fluorescence (left) images of live T cell synapses with patterned supported membranes. The supported membrane contains MHC (green) and ICAM (red), which engage their cognate ligands on the T cell. Patterns of proteins are induced by the T cell and guided by the substrate. From Mossman, Campi, Groves\*, and Dustin. *Science* 2005, **310**: p. 1191.

As of the present time, we have now validated this strategy with several cell signaling systems by genetically engineering proteins with the naturally occurring GPI linkage motif in order to facilitate their association with membranes.

### Future Plans

In future work, we will extend these principles beyond the GPI-linkage system by developing a variety of other linkage strategies. This advance is key to the growth of this technological platform, since production of GPI-linked proteins requires cumbersome mammalian cell culture and difficult membrane purification. In collaboration with C. Bertozzi and M. Francis, we are examining synthetic strategies for placing membrane anchors on proteins after their *in vivo* production. A precursor of some of this work was published this year as a joint paper between J. Groves and C. Bertozzi<sup>12</sup>. We are also developing a series of cell surface signaling proteins as fusion proteins with variously colored versions of the green fluorescent protein; this enables facile monitoring by fluorescence microscopy. For the membrane linkage, these proteins include a 10-histidine tail, which can bind tightly to Ni, which is chelated within specialized Ni-chelating lipids. This strategy is very attractive in that the soluble proteins can be associated with supported membranes after formation. A tremendous amount of progress was made with this histidine-Ni linkage strategy in 2006, and we are currently preparing a detailed publication and public release of these materials.

Ultimately, we will integrate specific biological functionality into larger structures, as depicted in Figure 1. This will involve combining membrane surface patterning and signal protein incorporation with other types of three - dimensional construction techniques. Good initial progress on this front was made in 2006 in studies in which we fabricated substrates with patterns of controlled curvature, which were used to direct the self-assembly of structures within the liquid supported membrane phase<sup>14</sup>. It will be important to explore combinations of other materials such as hydrogels (C. Bertozzi) or protein nanostructures (M. Francis) with the supported membrane technology to achieve maximum degrees of control over the living cellular components. As a potential target project, which will be highly synergistic with the Helios program, we are considering ways to apply the chemical technologies developed herein to the formation of electrical associations between photosynthetic cyanobacterium (*Synechocystis*) with conducting electrodes. These bacteria are already known to perform extracellular electron transport via protein nanowires<sup>13</sup>, and we would like to design surfaces that facilitate formation of stable electrical contacts.

References and DOE sponsored publications from 2005-2007 (bold)

1. M. Tanaka, E. Sackmann, *Nature* **437**, 656-663 (2005).
2. J. T. Groves, N. Ulman, S. G. Boxer, *Science* **275**, 651-653 (1997).
3. **J. T. Groves, *Angew. Chem. Int. Ed.* **44**, 3524-3538 (2005).**
4. R. Singhvi *et al.*, *Science* **264**, 696-698 (1994).
5. C. S. Chen, M. Mrksich, S. Huang, G. M. Whitesides, D. E. Ingber, *Science* **276**, 1425-1428 (1997).
6. J. T. Groves, M. L. Dustin, *J. Immunol. Methods* **278**, 19-32 (2003).
7. **J. T. Groves, *Sci. STKE* **2005**, pe45 (2005).**
8. J. T. Groves, L. K. Mahal, C. R. Bertozzi, *Langmuir* **17**, 5129-5133 (2001).
9. **S. Pautot, H. Lee, E. Y. Isacoff, J. T. Groves, *Nat. Chem. Biol.* **1**, 283-289 (2005).**
10. **M. M. Baksh *et al.*, *Langmuir* **21**, 10693-10698 (2005).**
11. **K. D. Mossman, G. Campi, J. T. Groves, M. L. Dustin, *Science* **310**, 1191-1193 (2005).**
12. **M. J. Grogan, Y. Kaizuka, r. M. Conrad, J. T. Groves, C. R. Bertozzi, *J. Am. Chem. Soc.* **127**, 14383-14387 (2005).**
13. G. Reguera *et al.*, *Nature* **435**, 1098-1101 (2005).
14. **R. Parthasarathy, C.-H. Yu, and J. T. Groves, *Langmuir* **22**, 5095-5099 (2006).**
15. **J.-M. Nam, P. M. Nair, R. M. Neve, J. W. Gray, and J. T. Groves, *ChemBioChem* **7**, 436-440 (2006).**
16. **B. L. Jackson and J. T. Groves, *Langmuir* **23**, 2052-2057 (2007).**
17. **D. Rabuka, R. Parthasarathy, G.-S. Lee, X. Chen, J. T. Groves, C. R. Bertozzi, *J. Am. Chem. Soc.* **129**, 5462-5471 (2007).**
18. **M. G. Paulick, A. R. Wise, M. B. Forstner, J. T. Groves, C. R. Bertozzi, *J. Am. Chem. Soc.* *in press*.**
19. **R. Parthasarathy, D. Rabuka, C. R. Bertozzi, J. T. Groves, *J. Phys. Chem. B* *in press*.**

## Assembly at nanoscale chemical templates

Jim De Yoreo, Alex Noy and George Gilmer

L-003, Lawrence Livermore National Laboratory, P.O. Box 808, Livermore, CA 94551

[devoreo1@llnl.gov](mailto:devoreo1@llnl.gov), [nox1@llnl.gov](mailto:nox1@llnl.gov), [gilmer1@llnl.gov](mailto:gilmer1@llnl.gov)

### Program Scope

One of the common strategies used by biological systems in organizing both macromolecular complexes and inorganic materials is to create biochemical templates that direct organization. In the case of inorganic materials, these templates modify the interfacial energies and kinetic barriers that determine the pathways of nucleation, providing a high degree of control over location, orientation, and even mineral phase [1,2]. Through this approach, organisms produce nanophase materials [3], topologically complex single-crystals [4,5], and multi-layer composites [6] with properties unexpected from single crystals of the stable bulk phase.

Using a similar approach, organisms are able to create networks of protein complexes with exceptional levels of function. This is due, in part, to the high degree of spatial density that organisms achieve, but more importantly, function stems from hierarchical organization: Multiple kinds of macromolecular complexes that are 10's of nm's in size, exhibit important structural elements at sub-nm length scales, but are organized into micron-scale structures. Moreover, each type of macromolecular complex occupies specific sites in this larger-scale structure.

In recent years, observations of control over materials and molecular assembly in biological systems has led to numerous attempts to mimic their approach with the result that a wide variety of complex structures reminiscent of those observed in nature have been created in the absence of cellular control. But much less effort has been directed towards understanding the physical principles that control assembly in these systems. The relative importance of thermodynamic versus kinetic factors is virtually unknown, as is the degree to which our understanding of assembly in small molecule epitaxial systems can be transferred to these more complicated structures. Here we describe research aimed at developing generic platforms and *in situ* methods for elucidating the principles that govern templated assembly of materials and macromolecular complexes.

### **Recent Progress I: Organization of viruses at nanoscale chemical templates**

The utility of viruses as macromolecular building blocks has recently gained attention amongst materials scientists because they can be engineered or evolved to present catalytic, electronic, optical, or materials-binding moieties. Thus they offer possibilities for fabricating hierarchical structures with near-molecular density of functionality, provided their assembly can be directed. Growth of three-dimensional crystals or deposition of uniform virus films can readily be achieved, but controlling organization into predefined 1D and 2D structures, particularly when multiple components are required, remains a major challenge. We have used scanned probe nanolithography (SPN) to direct organization into 1D and 2D patterns of three classes of viruses: icosahedral Cowpea Mosaic Virus (CPMV), wire-like M13 bacteriophage, and disk-shaped sub-segments of Tobacco Mosaic Virus (TMV) [7-10]. Chemical patterns were formed from self-assembled monolayers (SAMs) deposited by SPN and consisting of monomers designed to bind to specific sites on the viral capsids. *In situ* AFM imaging was used to investigate virus organization as pattern geometry, inter-viral potential, virus flux and virus-pattern interaction were varied. Direct measurements of interactions between virus and substrate, template and other virions were obtained using chemical force microscopy with viral capsids attached to AFM tips. Kinetic Monte Carlo (KMC) simulations were used to investigate the range of morphologies obtainable by varying these interactions.

Cowpea Mosaic Virus (CPMV) was genetically engineered to present either histidine (His) tags or cysteine (Cys) residues on the viral capsids (**Fig. 1a**). Atomically-flat gold substrates are prepared by first coating them with self assembled monolayers (SAMs) of polyethylene glycol (PEG) terminated alkane thiols (**Fig. 1b**). Nanometric patterns of alkane thiol-based chemical linkers are then made by

SPN, such that attachment to the Cys-residues and His-tags was through covalent bonding with maleimides groups or metal coordination complex linkage with nickel-chelating nitrilotriacetic acid (Ni-NTA) groups, respectively. To investigate the role of virus flux and inter-viral interactions, we varied the virus and PEG concentration of the virus solution, respectively. (Addition of PEG introduces an osmotic force that increases virus-virus attraction.)

We found that the degree of ordering depended on all parameters chosen: surface chemistry, virus flux, PEG concentration, and pattern feature size. For example, as the PEG concentration was increased, 2D arrays of viruses evolved from poorly-ordered to well-ordered rhombic to hexagonally close packed assemblies. For the 1D patterns and the His-tag:Ni-NTA linkage, as virus flux increased, the width of the virus arrays increased from one virus to multiple rows of viruses (**Fig. 1c,d**). Disordered clusters formed on the PEG terminated regions, but did not grow appreciably in size with increasing time. As the virus concentration or PEG concentration was increased, the density and size of the clusters increased. KMC simulations showed similar patterns of virus organization (**Fig. 2**). Chemical force microscopy results show how the introduction of PEG modifies the inter-viral potential to drive the observed changes in assembly morphology.

Analysis of the results suggests that the thermodynamic driver behind growth of the arrays is similar to that found in colloidal systems where solvent exclusion is a major factor. While 2D films form at sufficiently high volume fractions, the templates cause 1D condensates to form and the addition of polymer (PEG) drives those 1D structures to spread laterally. The growth rate of the arrays, however, is limited by diffusion of viruses to the surface.

Similar studies were carried out on TMV disks, assembled out of capsid monomers in a purely synthetic approach. Two sets of residues —lysine and cysteine — on opposite faces of the disk were tried as binding sites for assembly at templates. We found, however, that the methoxy-terminated PEG resist layer needed to be changed to an OH-terminated PEG layer in order to eliminate off-template binding. Moreover, numerous attempts to design SAM monomers to bind the lysine residues failed to provide high binding fractions. In contrast, maleimide-terminated SAMs gave excellent binding affinities to the cysteine residues (Data not shown). Simulations suggest that controlling the number of residues around the rim of the disks provides a means for tuning the affinity for binding to neighboring capsids and the resultant degree of order. As with the CPMV, measurements of TMV adsorption rates indicate that bulk diffusion is the limiting factor.

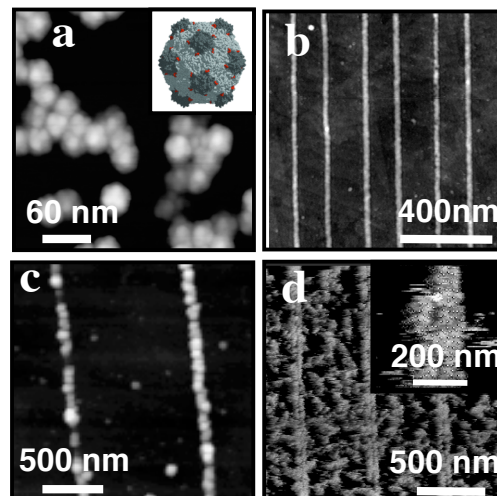


**Fig. 1** – AFM images collected in height mode showing: (a) CPMV viruses. Inset shows model of molecular structure. (b) Pattern of 30nm wide lines formed by nanografting maleimide terminated alkane thiols into a PEG terminated SAM. (c) Deposition of His-tag modified viruses onto Ni-NTA lines from solution with low virus concentration and no PEG in solution. Resulting arrays are one virus wide. (d) Same as (c) but with high concentration virus solution and moderate concentration of PEG. Inset is close-up of (d) showing rows are multiple viruses in width [7-10].

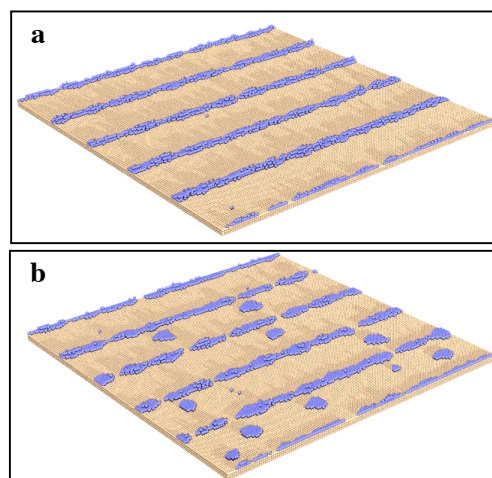


**Fig. 2** – KMC simulations for equal deposition at (a) low flux and strong binding to lines vs. (b) high flux and weak binding to lines.

## Recent Progress II: Structural development of organic film and mineral phase during templating

While organisms use organic matrices as templates that direct the nucleation of inorganic components, numerous investigations have concluded that many organisms use an amorphous precursor phase that is first deposited and then transforms into a fully crystalline material, allowing biominerals to be ‘shaped’ into complex morphologies [11,12]. The template is generally assumed to control mineral orientation and possibly stabilize and/or initiate phase transformation. The nature of that transformation and the mechanism by which it occurs are poorly understood. Because alkyl thiol self-assembled monolayers (SAMs) on gold and silver have been shown to provide a high degree of control over the plane of calcite nucleation, they have been used as a model system to mimic and investigate templating. While the high degree of order obtained on these films is attributed to distinct geometrical relationships between film structure and crystal structure, little is known about those relations or about the evolution of film and crystal structure during template-directed growth. We used near edge X-ray absorption fine structure (NEXAFS) and photoemission spectroscopies (PES) to examine the evolution of structure and bonding in SAMs prepared on Au(111) during nucleation of  $\text{CaCO}_3$  [13]. We then used SEM and optical microscopy to examine the evolution of the mineral phase, morphology and orientational order.

SAMs of 2-, 3- and 4-mercaptophenol (MP) were prepared on Au(111) substrates. The MP has an OH termination that has been shown to stabilize amorphous calcium carbonate (ACC). The precipitation of ACC and subsequent growth of crystalline  $\text{CaCO}_3$  on the MP SAMs was conducted using a  $\text{CO}_2$  diffusion method with the substrates immersed in a  $\text{CaCl}_2$  solution. Carbon K-edge NEXAFS data were recorded over a spectral range of 280-330 eV on at the Stanford Synchrotron Radiation Laboratory. The orientation of MP monomers within the SAM and the degree of SAM order was determined by analyzing the dependence of carbon K-edge peak intensity on the angle between the beam polarization and the sample normal with methods described elsewhere [14]. To correlate NEXAFS results with the uniformity of calcite orientation, X-ray diffraction spectra were collected from samples supporting prepared with identical procedures.

The NEXAFS measurements showed that, prior to exposure to Ca-bearing solutions, the 2-MP, 3-MP, and 4-MP films all exhibited a high degree of order with the phenol ring, in all cases, tilted at approximately  $60^\circ$  with respect to the surface normal, as illustrated in Fig. 3a. However, upon exposure to the  $\text{CaCO}_3$  solutions, this well defined monomer orientation was lost. Parallel experiments showed that, on a time scale longer than that required to eliminate this orientational order, a layer of precipitated  $\sim 50\text{nm}$  particles formed on the MP films and were determined by Raman spectroscopy to be ACC. When left in solution or placed in a humid chamber, the ACC films transformed into well-separated micron-scale crystals, with an 80:20 ratio of calcite to vaterite. SEM and optical observations showed that this transformation occurred through a

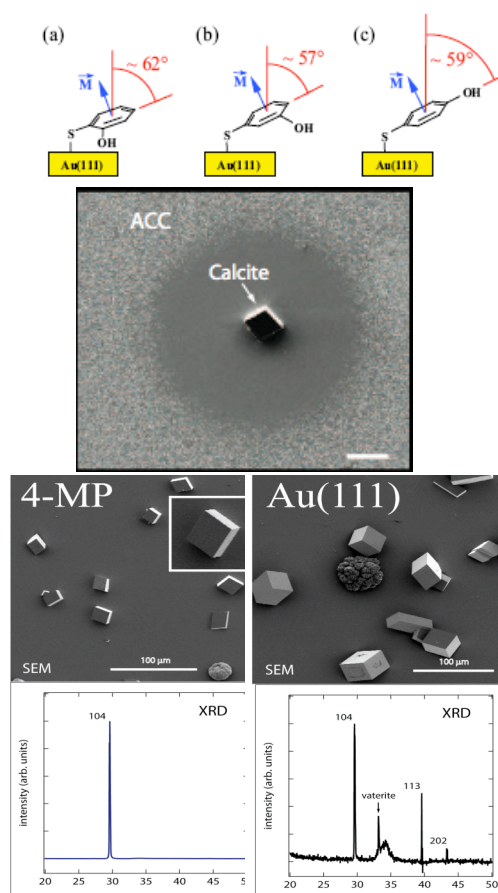


**Fig. 3** - (a) Orientations of MP monomers in well-ordered SAMs as determined by NEXAFS measurements. (b) SEM image showing transient state with calcite crystal growing at expense of ACC. (c) Resulting film of calcite crystals on 4-MP SAM exhibits a high degree of orientational control with a (104) nucleation plane. For comparison, in (d) the same process on (111) gold without the MP SAM gives randomly oriented nucleation planes [13].



dissolution re-precipitation reaction (**Fig. 3b**). Surprisingly, despite the loss of orientational order in the MP films, the resulting film of calcite crystals on 4-MP and 3-MP films was still highly oriented with >70% nucleation on (104) faces (**Fig. 3c**). Control experiments on bare gold and on OH<sup>-</sup> terminated SiO<sub>2</sub> surfaces showed no control over crystal orientation, nor did experiments on 2-MP.

These results show, that while the presence of the OH-terminated SAM is critical to obtaining the orientation control, the stereochemistry of the SAM is also a crucial factor. But the NEXAFS data clearly show that the MP SAMS, which all initially exhibit a high degree of orientational order, become disordered upon exposure to calcium carbonate solution, implying that they become similar to the OH<sup>-</sup> terminated SiO<sub>2</sub> surfaces. Consequently, the final configuration of highly-oriented calcite crystals can not easily be explained in terms of the traditional view of templating in which there is an epitaxial or stereochemical match of film to crystal. There are three alternative explanations. The first is that the interfacial energy of SAM-crystal interface is minimized for the (104) calcite plane, irrespective of lattice matching or stereochemical recognition. Because this interfacial energy enters into the nucleation rate equation as a cubic term in an exponential, even a slight depression can result in a strong bias. The second is that there are small regions (<10nm) of the SAM that remain ordered and serve as the nucleation sites. The final possibility, and the one that is most consistent with the negative control experiments, is that during the transformation to calcite the SAM monomers re-orient to provide a low-energy interface with calcite (104). That is, crystal and film template one another.

### Future Plans

For the work on virus templating, future work will focus on: 1) overcoming diffusion-limited growth by driving assembly through application of electric fields to create electrophoretic flow and 2) incorporating the chemical force data into the kMC simulations and comparing predictions of morphology with experiment. For the research into materials templating, we are: 1) synthesizing monomers with carboxyl terminations that can be used in the NEXAFS experiments and 2) commissioning an *in situ* TEM fluid cell to directly image templated nucleation at sub-nm resolution and video-rates.

### References

- 1 Addadi L. and Weiner S. *Proc. Nat. Acad. Sci.* **82**, 4110-4114 (1985).
- 2 Mann S. *Nature* **332**, 119-124 (1988).
- 3 Calvert P. *MRS Bulletin* **XVII**, (1992) 37-40.
- 4 Young J. R., Didymus J. M., Brown P. R., Prins B. and Mann S. *Nature* **356**, 516-518 (1992).
- 5 Young and Henriksen, (2003) In *Biomaterialization* **54** (eds. P. M. Dove, J. J. De Yoreo and S. Weiner). Mineralogical Society of America, pp. 1-29.
- 6 Vincent J. *Structural Biomaterials*. (Princeton University Press, 1990).
- 7 Cheung, C.L., Chung, S-W, Lin, T., Johnson, J.E., and De Yoreo, J.J., *J. Am. Chem. Soc.* **128**, 10801-10807 (2006).
- 8 Cheung, C.L., Camarero, J.A., Woods, B.W., Lin, T., Johnson, J.E., and De Yoreo, J.J., *J. Am. Chem. Soc. Comm.* **125**, 6848 (2003).
- 9 B.W. Weeks, C.L. Cheung, and J.J. De Yoreo, in X. Y. Liu and J.J. De Yoreo, *From Solid-Fluid Interfaces to Nanostructural Engineering, Vol. II: Assembly in Hybrid and Biological Systems*, (Kluwer Academic Publishers, New York, 2004) pp. 281-302.
- 10 Chung, S-W., Elhadj, S., Eaton, B.E., Feldheim, D.L., A.A. Chernov, and J.J. De Yoreo, *Scanning* (**Invited submission in prep**).
- 11 Politi, Y., Arad, T., Klein, E., Weiner, S., and Addadi, L., *Science* **306**, 1161-1164 (2004).
- 12 Addadi, L., Joester, D., Nudelman, F., and Weiner, S., *Chem. Eur. J.*, **12**, 980-987 (2006).
- 13 Lee, J. R. I., Han, Y., Willey, T. M., Wang, D., Muelenberg, R. W., Nilsson, J., Dove, P. M., Terminello, L. J., van Buuren, T., and De Yoreo, J. J. (2007) *J. Am. Chem. Soc.* (In press).
- 14 Lee, J. R. I., Willey, T. M., Nilsson, J., Terminello, L. J., De Yoreo, J. J., and van Buuren, T. *Langmuir*, **22**, 11134-11141 (2006).

## Observation of In-Situ Biological Processes in the Dynamic TEM

J. B. Pesavento, J. Lee, J. De Yoreo, and N. D. Browning

Materials Science and Technology Division, Chemistry, Materials, Earth, and Life Sciences  
Directorate, Lawrence Livermore National Laboratory, Livermore, CA 94550

In typical transmission electron microscopes (TEM), imaging of biological samples at high spatial resolution is conducted using either conventional TEM of chemically fixed and dried samples, or of frozen hydrated samples (cryo-EM). In both cases, images are taken of an arrested state of the biological process, and samples have strong structural artifacts resulting from the fixation process. What is needed to make progress in understanding biological systems is the ability to clearly image the actively functional molecular process—whether enzymatic, or cellular, and be able to understand and interpret the resultant images. With the ability to image biochemical processes in situ and in solution, the drawbacks to visualizing samples by negative stained TEM or cryo-EM are removed.

At Lawrence Livermore National Laboratory (LLNL), we have developed the Dynamic Transmission Electron Microscope (DTEM) which currently is capable of better than 10 nm spatial resolution using 15 ns pulses (**Figure 1**). The DTEM works by using a laser to illuminate the electron source and create a pulse of electrons with essentially the same time duration as the laser pulse [1-5]. The advantage of using this pulse of electrons (the 15ns packet of electrons typically contains  $\sim 10^8$  electrons), is that a full TEM image (or diffraction pattern) can be obtained with the time resolution of the pulse. Furthermore, although the number of electrons in the pulse is high, when these electrons are spread over an area of the sample and used to form a TEM image, the total electron dose is very small (typically  $\sim 0.05$  e/A<sup>2</sup>). As such the microscope is ideal for imaging biological samples. Developments currently underway will increase the applicability even further by improving contrast and spatial resolution.

A further advantage of the DTEM is that the samples being imaged do not have to be chemically fixed and can exist in a fluid environment (all motion is on a much slower timescale than the nanosecond resolution of the microscope). Therefore, by incorporating a fluid stage into the microscope (**Figure 2**), we can evaluate the processes that occur in-situ in conditions as close to “live” as it is possible to get inside of a microscope. This stage in the DTEM essentially provides us with the flexibility of a confocal optical microscope with subnanometer and nanosecond resolution.

It is well understood that low-dose conditions are critical for successful bio-imaging and to eliminate the harmful effects of radiation damage on the specimen with the coinciding resolution degradation. On the most basic level, the DTEM allows the fundamental processes behind the requirements for low-dose imaging, i.e. beam-specimen interactions, to be examined using organic polymers as bio-mimetics (paraffin, catalase, etc) and simple viruses such as Tobacco Mosaic Virus (TMV) and bacteriophage MS2. Such studies can greatly increase our understanding and the potential spatial resolution in all electron beam methods. By using the stroboscopic capabilities of the DTEM we can investigate a wide range of biological processes, ranging from an analysis of the chronology and key-players in chromosome mechanics (maintenance and repair), mitosis and mitochondrial fusion/fission events, to the study of membrane pore formation by pentraxins or the detailed processes in membrane protein crystallization. As a long-term goal, we can even utilize the DTEM for visualizing the complex

molecular ballet that is protein folding, from the initial attachment of the messenger RNA (mRNA) molecule to the ribosome, through the fascinating process of translation, all the way to the final stages of product polypeptide folding up as it exits the ribosome.

This work performed under the auspices of the U.S. Department of Energy by Lawrence Livermore National Laboratory supported by the Office of Science, Office of Basic Energy Sciences, Division of Materials Sciences and Engineering, of the U.S. Department of Energy under Contract DE-AC52-07NA27344.

### References

- [1] Bostanjoglo, O. (2002) Advances in imaging and electron physics **121**, 1 - 51.
- [2] Bostanjoglo, O., Elschner, R., Mao, Z., Nink, T. & Weingärtner, M. (2000) Ultramicroscopy **81**, 141 - 147.
- [3] Zewail, A. H. (2005) Philosophical transactions **363**, 315-29.
- [4] Lagrange, T. B., et al. (2006) Applied Physics Letters **89**, 044105.
- [5] Armstrong, M. R., et al. (2007) Applied Physics Letters **90**, 114101.

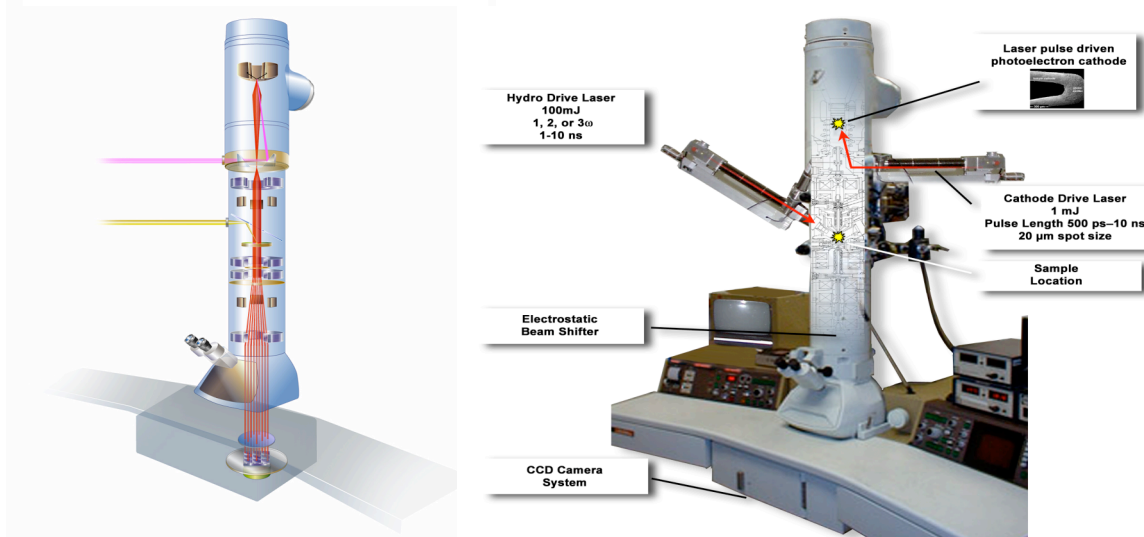


**Figure 1:** (a) The LLNL DTEM incorporates two high performance lasers directed inside the column. The cathode drive laser stimulates electron emission, while the drive laser stimulates a response in the specimen. The timing between the two lasers is controlled to achieve the pump – probe investigation. (b) The current DTEM is a modified JEOL 200FX.

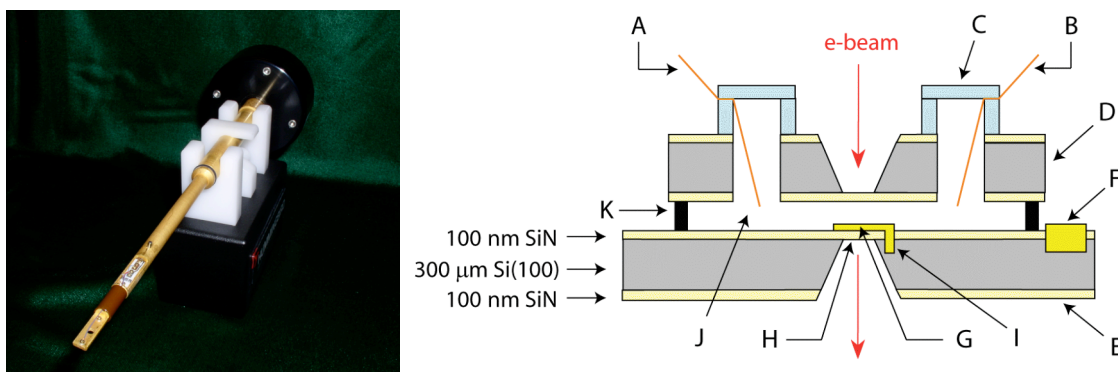


**Figure 2:** (a) The LLNL liquid TEM stage. (b) Schematic of the cell. A: Reference electrode, B: Counter electrode, C: Glass cap, D: Upper SiN<sub>x</sub>/Si(100)/ SiN<sub>x</sub> wafer, E: Lower wafer, F: Au contact to working electrode, G: 20 nm Au working electrode, H: 100 x 100 μm SiN<sub>x</sub> ‘window’, I: Electrical contact between Si(100) and Au, J: Solution reservoir, K: 200 nm SiO<sub>2</sub> spacer

## Molecularly Engineered Biomimetic Nanoassemblies

Andrew P. Shreve ([shreve@lanl.gov](mailto:shreve@lanl.gov)), Hsing-Lin Wang ([hwang@lanl.gov](mailto:hwang@lanl.gov)), Jennifer Martinez ([jenm@lanl.gov](mailto:jenm@lanl.gov)), Srinivas Iyer ([siyer@lanl.gov](mailto:siyer@lanl.gov)), Reginaldo Rocha ([rcrocha@lanl.gov](mailto:rcrocha@lanl.gov)), Los Alamos National Laboratory;  
James Brozik ([brozik@wsu.edu](mailto:brozik@wsu.edu)), Washington State University;  
Darryl Sasaki ([dysasak@sandia.gov](mailto:dysasak@sandia.gov)), Sandia National Laboratories;  
Atul N. Parikh ([anparikh@ucdavis.edu](mailto:anparikh@ucdavis.edu)), University of California, Davis.

### Program Scope

The program aims to develop self-assembly and biologically-assisted assembly methods for the incorporation of selected optical and electronically active nanoscale components into assemblies and the development of materials that produce functions related to the control of electronic energy flow through assemblies. Relevant functions include photo-induced charge separation, directed electronic energy transfer, and manipulation of biological energetics and signaling processes. Focus on these functions and on use of a few active components, selected to represent several different classes of important nanomaterials, is intended to also provide improved general understanding of structure and performance of the assembly types under study. The approach used includes a combination of materials synthesis and fabrication, static and time-resolved spectroscopies, optical and scanning probe microscopies, structural characterization, and modeling and analysis of electronic or optical responses. Our research team includes personnel with expertise in chemical and materials synthesis, self-assembly, electrochemistry, spectroscopy, molecular biology, and biochemistry.

### Recent Progress

Recently, we have addressed improved understanding of how interactions drive complex (bio)molecular assemblies and the interplay of structure, dynamics and function in such assemblies, with an emphasis on incorporation of optically or electronically active components. There has also been an effort to explore the synthetic development and characterization of different types of nanoscale components that could be incorporated into assemblies (*e.g.*, amphiphilic organic or organometallic molecular wire like compounds).

*Nanoscale components for assemblies.* We synthesized and studied the properties of amphiphilic phenylene acetylene derivatives, as both isolated molecules and assemblies of molecules. We determined the size-dependent electronic-state properties of the oligomers, and investigated how properties of the oligomers are modulated by incorporation into Langmuir-Blodgett assemblies. We also spectroscopically investigated the properties of surfactant-wrapped single-wall carbon nanotubes, which are soluble electronic and optically-active materials that can be incorporated into larger-scale assemblies. We demonstrated that resonance Raman spectroscopy allows quantitative determination of the weak exciton-phonon coupling strength in nanotubes, which is critical for understanding their performance in electronic and optical applications. Molecular components based on transition metal complexes were also studied for their potential role in mediating charge and energy transfer. An important issue in these types of systems is the role of symmetry breaking and energy localization. We synthesized and explored photophysical properties of multi-metal center complexes, oligomers and polymers using time-resolved infrared spectroscopy (TRIR), and studied the formation of localized charge-transfer excited states. Some of these compounds were also targeted for insertion into lipid bilayer membranes, and were synthesized with hydrophilic end groups to assist in assembly formation.

We have also developed other components that can be incorporated into assemblies for control of luminescence properties. As one example, metal nanoclusters consisting of small numbers of metal atoms exhibit strong size-dependent luminescence emission. We have developed methods for the aqueous production of homogeneous gold nanoclusters (e.g., Au<sub>8</sub>) using dendrimer templates, with discrete fluorescence emission, without production of non-fluorescent nanoparticles. Beyond Au<sub>8</sub>, we also developed methods to form larger gold clusters using a mild organic/biological reductant. In addition to the use of dendrimers for nanocluster synthesis, peptide templates were also developed using phage display methods. Three peptide templates were discovered that specifically catalyze the formation of fluorescent homogeneous gold nanoclusters.

We also demonstrated synthesis and characterization of two new water-soluble cationic poly (p-phenylenevinylene)s. Both polymers exhibit pH-dependent optical properties in aqueous solution, with luminescence quantum efficiencies of up to 14%. In addition, we synthesized a series of new water-soluble fullerene derivatives, including one highly symmetric compound with redox potential and optical properties similar to that of underivatized fullerene.

*Assemblies with optical or electronic responses.* Work aimed at characterizing the nature of assemblies formed in solution by conjugated polyelectrolytes was carried out. For a sulfonated water-soluble conjugated polymer we have demonstrated how time-resolved luminescence spectroscopy coupled with a maximum entropy analysis method allows for investigation of heterogeneous solution assemblies, and we have also explored how biochemical separation methods such as density gradient centrifugation can be used to separate assemblies by density. Overall, we determined that the conjugated polyelectrolyte/dendrimer assemblies exist in solution as mixtures of dense, non-luminescent aggregates, less dense somewhat luminescent complexes, and highly luminescent monomeric polymers, and that the observed luminescence of the mixture can be substantially modulated by changes in the relative population of these species as environmental conditions and solution composition are varied.

We have explored multi-layer and colloidal assemblies, developing, for example, several paths for incorporating fullerenes into such systems. Using synthesized amphiphilic fullerenes, we have made and characterized multi-component Langmuir-Blodgett (LB) films. In films with layers of amphiphilic phenylene-ethynylene oligomers and amphiphilic fullerenes prepared on substrates functionalized with conjugated polyelectrolytes, we have demonstrated very efficient luminescence quenching and inter-layer photo-induced charge separation. We have also shown formation of highly efficient (>99%) charge transfer assemblies using water-soluble, anionic fullerene and cationic PPV. This extremely high charge transfer efficiency is believed to be due to the enhanced miscibility between donor and acceptor species via electrostatic interaction. The PPV/fullerene complexes aggregate to form dispersible colloids smaller than 100 nm, which self-assemble into highly branched, fractal-like structures upon drying the solution.

Another approach toward larger-scale assemblies is provided by the development of patterned membrane assemblies on functional thick-film substrates (e.g., porous silica films with tunable luminescence properties). To this end, we produced films of mesostructured silica using an evaporation-induced self-assembly process, incorporated the pH sensitive fluorescent dye FITC into the silica, added a blocking layer of silane onto the surface of the film and then patterned these materials to produce patterned mesostructured regions (surfactant and FITC containing capped by silane) that surround mesoporous regions (water-filled accessible pores). We then formed supported phospholipid bilayers on these assemblies, and incorporated a functional proton-conductive peptide channel (gramicidin) in the membrane. The resulting architecture

consists of a functional region (bilayer containing gramicidin) that is surrounded by optical reporting regions (mesostructured material with FITC reporter dye). Upon change in solution pH, we observe changes in the FITC luminescence associated with proton transport through the functional gramicidin channels.

We have also begun to study strategies for the creation of controlled multilayer assemblies of phospholipids and other biologically compatible amphiphiles, providing a foundation for future integration of these assemblies with electronic or optically active components. One effort has involved the development of biotin-streptavidin linkage strategies to build up controlled numbers of phospholipid bilayers on surfaces. These systems have been characterized with atomic force microscopy, spectroscopic ellipsometry, and also fluorescence recovery after photobleaching to measure fluidity of bilayers. Some charged surfactants self-assemble into multi-bilayer architectures on surfaces, and we also have explored the use of these types of multi-layered membrane-mimetic assemblies as architectures for electrochemical studies of proteins, providing a measure of interfacial charge transfer from the assembly to the electrode. We have also demonstrated that this configuration provides for thin-layer UV-visible spectroelectrochemistry.

### **Future Plans**

Recent work on the development of molecular components and their integration into assemblies has provided methods of control of luminescence, photo-induced charge transfer, or electrochemical responses. Our future work will build upon these results to target development of higher-order assemblies that allow similar control of optical, ionic or electronic responses on larger scales and over larger volumes. We aim for improvement in general understanding of assembly methods, particularly methods appropriate for generation of larger-scale assemblies or even bulk or bulk-like materials. As active components, we will use representative members of different classes of nanomaterials, and by developing assemblies that incorporate these diverse materials, we hope to develop methods that are widely applicable. Targeted functions involving control of charge and energy flow, whether they derive from carbon-based materials, conjugated polymers, metallic nanoclusters, or proteins, are key to numerous specific applications. Characterization of assemblies and their functions using spectroscopic, scanning probe, electrochemical, imaging, and scattering methods will provide for improved general understanding of how multi-scale and multi-component functional assemblies can be produced using the tools of self-assembly and biologically-assisted assembly.

### **Publications (2005-2007)**

R.J. Magyar, S. Tretiak, Y. Gao, H.-L. Wang, A.P. Shreve, "A joint theoretical and experimental study of polyphenylene-acetylene molecular wires," *Chem. Phys. Lett.* **401** (2005) 149.

Y. Gao, Z. Tang, E. Watkins, J. Majewski and H.-L. Wang, "Synthesis and characterization of amphiphilic fullerenes and their Langmuir-Blodgett films," *Langmuir* **21** (2005) 1416.

M.C. Howland, A.R.S. Butti, S.S. Dixit, A.M. Dattelbaum, A.P. Shreve, A.N. Parikh, "Phospholipid morphologies on photochemically patterned silane monolayers," *J. Amer. Chem. Soc.* **127** (2005) 6752.

A.A. Levchenko, C.K. Yee, A.N. Parikh, A. Navrotsky, "Energetics of self-assembly and chain confinement in silver alkanethiolates: Enthalpy-entropy interplay," *Chem. Mater.* **17** (2005) 5428.

D.Y. Sasaki, T.A. Waggoner, J.A. Last, "Self-assembled lipid bilayer materials," U.S. Patent no. 6962747 (November 8, 2005).

Q.H. Li, M.L. Amweg, C.K. Yee, A. Navrotsky, A.N. Parikh, "Photochemical template removal and spatial patterning of zeolite MFI thin films using uv/ozone treatment," *Micropor. Mesopor. Mat.* 87 (2005) 45.

D.A. Doshi, A.M. Dattelbaum, E.B. Watkins, C.J. Brinker, B.I. Swanson, A.P. Shreve, A.N. Parikh, and J. Majewski, "Neutron reflectivity study of lipid membranes assembled on ordered nanocomposite and nanoporous silica thin films," *Langmuir* 21 (2005) 2865.

A.N. Parikh and J.T. Groves, "Materials science of supported lipid membranes," *MRS Bulletin* 31 (2006) 507-512.

Z.X. Tang, R.K. Hicks, R.J. Magyar, S. Tretiak, Y. Gao and H.-L. Wang, "Synthesis and characterization of amphiphilic phenylene ethynylene oligomers and their Langmuir-Blodgett films," *Langmuir* 22 (2006) 8813.

Z.X. Tang, P.A. Padmawar, T. Canteenwala, Y. Gao, E. Watkins, J. Majewski, L.Y. Chiang and H.-L. Wang, "Synthesis and characterization of monolayers and Langmuir-Blodgett films of an amphiphilic oligo(ethyleneglycol)-C<sub>60</sub>-hexadecaaniline conjugate," *Langmuir* 22 (2006) 5366.

W. Li, Q.X. Jia and H.-L. Wang, "Facile synthesis of metal nanoparticles using conducting polymer colloids," *Polymer* 47 (2006) 23.

T. Canteenwala, W. Li, H.-L. Wang and L.Y. Chiang, "Low multielectron reduction potentials of emerald green [60]fullerenes," *Chem. Lett.* 35 (2006) 762.

Y. Gao, L. Wang, C.C. Wang and H.-L. Wang, "Conjugated polyelectrolytes with pH-dependent conformations and optical properties," *Langmuir* 23 (2007) 7760.

A.P. Shreve, E.H. Haroz, S.M. Bachilo, R.B. Weisman, S. Tretiak, S. Kilina, and S.K. Doorn, "Determination of exciton-phonon coupling elements in single-walled carbon nanotubes by Raman overtone analysis," *Phys. Rev. Lett.* 98 (2007) 037405.

Y. Bao, C. Zhong, D.M. Vu, J.P. Temirov, R.B. Dyer and J.S. Martinez, "Nanoparticle free synthesis of fluorescent gold nanoclusters at physiological temperature," *J. Phys. Chem. C* 111 (2007) 12194.

W. Li and H.-L. Wang, "Electrodeless deposition of metals and metal nanoparticles using conducting polymers," *Chem. Materials* (2007) in press.

C.M. Yip, M.S. Kent and D.Y. Sasaki, "Protein-membrane interactions on supported lipid membranes," in *Soft Nanomaterials* (2007) in press.

T.-H. Yang, C.K. Yee, M.L. Amweg, S. Singh, E.L. Kendall, A.M. Dattelbaum, A.P. Shreve, C.J. Brinker and A.N. Parikh, "Optical detection of ion-channel induced proton transport in supported phospholipid bilayers," *Nano Letters* (2007) in press.

## Molecularly Organized Nanostructural Materials

Gregory J. Exarhos\*, Yongsoon Shin, Li Qiong Wang, William D. Samuels  
Pacific Northwest National Laboratory, P.O. Box 999, MS K8-93, Richland, WA 99352  
\*greg.exarhos@pnl.gov

### I. Program Scope

Homogeneous nanoscale architectures are prepared using an array of solution templated growth, molecular condensation, and post growth modification strategies that invoke chemical control of molecular self-assembly and disassembly. Uniform carbon-based structures derived from hydrothermal treatment of natural carbohydrate materials such as sugar or cellulose are readily obtained in high yields by means of two *green chemistry* routes. (1) In a closed system, aqueous solutions of simple or complex sugars including cyclodextrin fully condense into nanoscale carbon spheres. Incorporation of selected chemical groups into the structure is achieved through the use of appropriately functionalized sugar precursors. (2) At low pH, natural cellulose fibers (cotton) can be dissembled into amorphous and crystalline constituents. The nanocrystalline cellulose so obtained forms a reactive template that induces regio-specific reduction of metal cations to form catalytically active ordered arrays of metal nanoparticles or nanorods aligned along the resident pyranose units that comprise the structure. Materials are characterized with respect to phase composition and homogeneity by means of magnetic resonance spectroscopy and diffraction measurements that are complemented by traditional electron microscopy and scattering approaches.

### II. Recent Progress

#### A. Sugar Condensation

The remarkable transformation of carbohydrate molecules including sugars of general formula,  $[C(H_2O)]_x$ , to produce homogeneous carbon nanospheres readily occurs by means of a condensation mechanism and subsequent sequestering in aqueous sugar-containing solutions that are heated in pressurized vessels to temperatures between 125 and 180° C. At high temperature, the conversion occurs quickly and larger micron-size spheres are formed.<sup>1</sup> In this closed system, such molecules actually dehydrate even though they are dissolved in water. Competition between inter- and intra-molecular condensation affects the morphology of the evolving structure, the sphere diameter, and the overall reaction rate.

In this laboratory, uniform carbon spheres were readily formed upon heating an aqueous fructose solution in a closed vessel to temperatures between 120-140°C. During the initial dehydration reaction, *in situ* Raman and NMR measurements identified 5-hydroxymethyl-2-furaldehyde (HMF) that was generated by intra-molecular dehydration. At longer times, microscopic non-polar carbon-containing spheres spontaneously assembled in a manner analogous to the mechanism by which a detergent emulsifies a mixture of oil and water. Subsequent loss of water by these assemblies led to further coalescence of microscopic spheres to larger spheres thereby generating a grain-like surface morphology with attendant interconnected porosity. This reaction also was seen to occur in supramolecular cage structures such as the cyclodextrins<sup>2</sup> that are comprised of -1,4 glycoside-linked  $\beta$ -glucose units arranged in the shape of a conical basket as seen



in Figure 1. Upon hydrothermal treatment of  $\beta$ -cyclodextrin solutions, spheres with diameters of 50 nm were isolated. In contrast, hydrothermal treatment of the more soluble (6 glucose constituent)  $\alpha$ -cyclodextrin generated a carbon chain morphology.

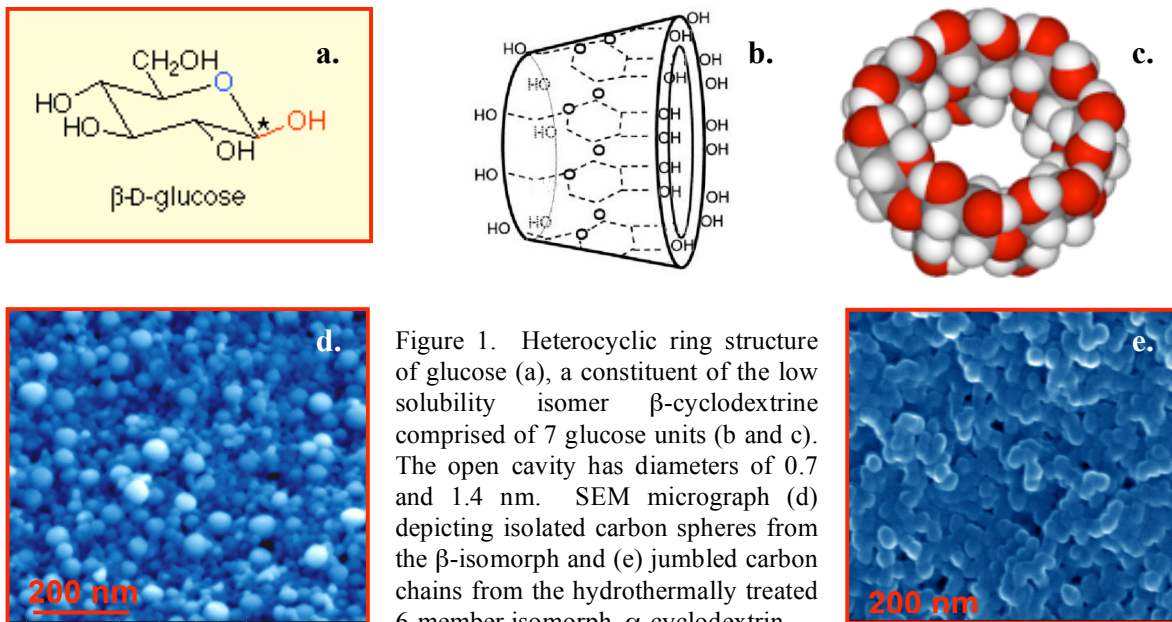


Figure 1. Heterocyclic ring structure of glucose (a), a constituent of the low solubility isomer  $\beta$ -cyclodextrine comprised of 7 glucose units (b and c). The open cavity has diameters of 0.7 and 1.4 nm. SEM micrograph (d) depicting isolated carbon spheres from the  $\beta$ -isomorph and (e) jumbled carbon chains from the hydrothermally treated 6-member isomorph,  $\alpha$ -cyclodextrin.

Earlier work in this laboratory that probed carbon sphere formation from hydrothermal dehydration of glucose (6-member ring) and fructose (5-member strained ring) suggested that the resulting sphere morphologies (smooth and orange peel respectively) resulted from a competition between inter- and intra-molecular dehydration. This competition may be the basis for the observed contrasting morphologies seen above.

### B. Starch Reduction

Cellulose fiber, a structural polysaccharide, may be described as a block copolymer that is comprised of acid-soluble (amorphous) and acid-insoluble (crystalline) blocks. Stable colloids comprised of rod-like cellulose nanocrystals (CNXL) 2-20 nm in diameter and hundreds to thousands of nanometers long are easily isolated from natural cellulose fibers like cotton by controlled acid hydrolysis. (Figure 2)

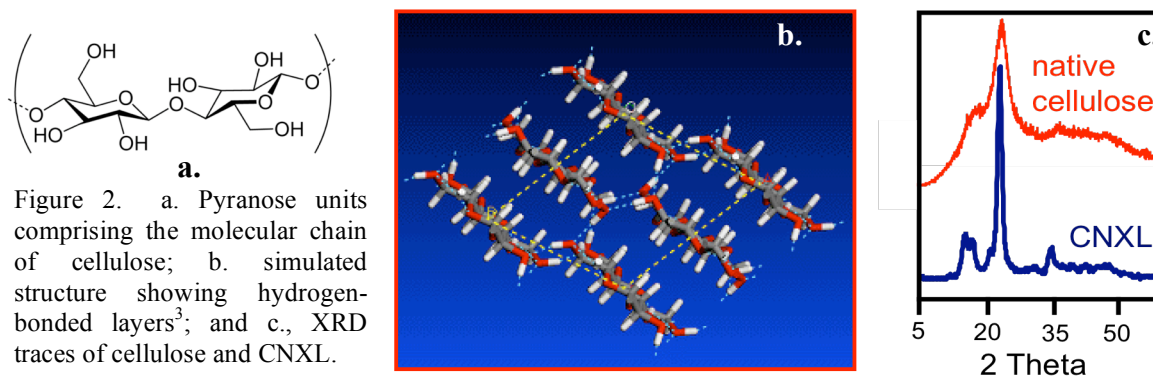


Figure 2. a. Pyranose units comprising the molecular chain of cellulose; b. simulated structure showing hydrogen-bonded layers<sup>3</sup>; and c., XRD traces of cellulose and CNXL.

The tendency of glucose to reduce certain metal cations is realized in both the Tollen's and Fehling's analytical tests for aldehyde. It is not surprising then, that cellulose also can behave as a reducing agent. Additionally, the presence of pyranose group orientation in CNXL suggests that ordered distributions of certain metal particles or nanostructures could result by a regio-specific reduction process. This, indeed, has been observed when CNXL's come into contact with  $\text{Au}^{+3}$ ,  $\text{Ag}^+$ ,  $\text{Pd}^{+2}$ ,  $\text{Pt}^{+4}$ , or  $\text{Cu}^{+2}$  containing solutions under hydrothermal conditions. In fact, even  $\text{Ni}^{+2}$  can be reduced albeit at higher temperatures.<sup>4</sup> Metal oxy-anions also are prone to reduction by CNXL as demonstrated by the formation of selenium nanoparticles upon hydrothermal treatment of  $\text{Na}_2\text{SeO}_3$  solutions at  $160^\circ\text{C}$ .<sup>5</sup> Figure 3 demonstrates a significant reduction in solution absorbance as a function of exposure time to light for methylene blue (MB) solutions containing dispersed, selenium-decorated CNXL colloids. MB solutions containing the same equivalent of dispersed selenium powder discolor at a markedly slower rate.

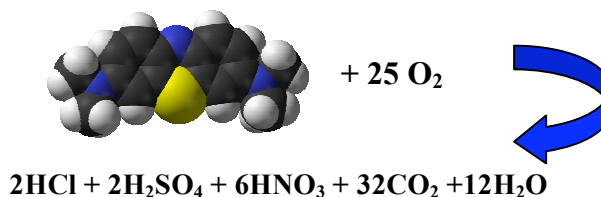
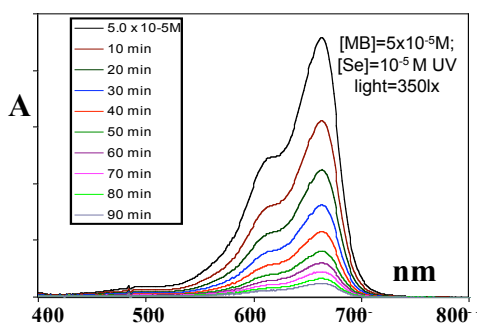


Figure 3. Kinetics of photo-oxidation of aqueous MB solutions containing a CNXL colloidal dispersion that shows enhanced catalytic efficiency.

### III. Future Work

The amphiphilic nature of the cyclodextrins resulting from inner hydrophobic regions and outer hydrophilic regions can be invoked to trap and nucleate non-polar species allowing formation of size-specific nanoparticles. Thiosulfate and its selenium analog decompose in aqueous solution to the element under mildly acidic conditions. The efficacy of using cyclodextrins as *getters* for various hydrophobic species as they are formed in solution will be investigated in order to identify processing conditions that promote trapping. Related investigations using *in situ* nucleated metal atoms to grow uniform sized metal clusters will follow.

Oriented platinum nanorods of 10 nm in diameter with an aspect ratio of 10 have been grown on CNXL surfaces in dilute solutions of the metal precursor. Understanding the chemical nature and reactivity of the nucleation sites will coordinate theoretical simulations with experimental measurements using atomic force microscopy<sup>6</sup>, and NMR.

### IV. References

1. Q Wang, H Li, L Chen, and X Huang, 2002. *Solid. State Ionics*. 152-153, 43 (2002).
2. Comprehensive Supramolecular Chemistry: Volume 3 – Cyclodextrins, J.-M. Lehn, Editor, Pergamon Press (1999), ISBN: 0-08-042715-4 (1999).
3. L.M.J. Kroon-Batenburg and J. Kroon, *Glycoconjugate Journal* 14(5):677 (1997)
4. Shin Y, JM Blackwood, I Bae, BW Arey, and GJ Exarhos. 2007. *Mater. Lett.* 61:4297 (2007).
5. Shin Y, I Bae, BW Arey, and GJ Exarhos. *Mater. Lett.* 64(14-15):3215 (2007).
6. A. A. Baker, W. Helbert, J. Sugiyama, and M. J. Miles, *Biophys. Jour.* 79:1139 (2000).

## V. Selected Sponsored Publications (2005-2007)

Shin Y, CM Wang, XS Li, and GJ Exarhos. 2005. "Synthesis of supported carbon nanotubes in mineralized silica-composites." *Carbon* 43(5):1096-1098.

Shin, Y, LQ Wang, GE Fryxell, and GJ Exarhos. 2005. "Hygroscopic Growth of Self-Assembled Layered Surfactant Molecules at the Interface between Air and Organic Salts." *J. Coll. and Interfac. Sci.* 284(1):278-281.

Shin Y, CM Wang, and GJ Exarhos. 2005. "Synthesis of SiC ceramics by the carbothermal reduction of mineralized wood with silica." *Adv. Mater.* 17(1):73-77.

Moudrakovski IL, CI Ratcliffe, JA Ripmeester, LQ Wang, GJ Exarhos, T Baumann, and JH Satcher. 2005. "NMR Studies of Resorcinol-Formaldehyde Aerogels." *J. Phys. Chem B* 109(22):11215-11222.

Chang, JH, GJ Exarhos, and Y Shin. 2005. "Biomimetic Catalysis of Tailored Mesoporous Materials with Self-Assembled Multifunctional Monolayers." *J. Ind. Eng. Chem.* 11(3):375-380.

Windisch CF, Jr, GJ Exarhos, and SK Sharma. 2005. "Viscosity by Fluorescence Depolarization of Probe Molecules. A Physical Chemistry Laboratory Experiment." *J. Chem. Ed.* 82(6):916-918.

Wang W, LQ Wang, BJ Palmer, GJ Exarhos, and AD Li. 2006. "Cyclization and Catenation Directed by Molecular Self-Assembly." *J. Am. Chem. Soc.*, 128 (34), 11150 -11159.

Huo Q, J Liu, LQ Wang, Y Jiang, TN Lambert, and E Fang. 2006. "A New Class of Silica Crosslinked Micellar Core-Shell Nanoparticles." *J. Am. Chem. Soc.* 128(19):6447-6453.

Pawsey S, IL Moudrakovski, JA Ripmeester, LQ Wang, GJ Exarhos, JL Rowsell, and OM Yaghi. 2007. "Hyperpolarized  $^{129}\text{Xe}$  Nuclear Magnetic Resonance Studies of Isoreticular Metal-Organic Frameworks." *Journal of Physical Chemistry* 11(16):6060-6067.

Wang LQ, GJ Exarhos, CF Windisch, Jr, C Yao, LR Pederson, and X Zhou. 2007. "Probing hydrogen in ZnO nanorods using solid-state H-1 nuclear magnetic resonance." *Appl. Phys. Lett.* 90(17):315-317.

Chang JH, ME Park, Y Shin, GJ Exarhos, KJ Kim, S Lee, and K Oh. 2007. "Functional Scaffolds of Bicontinuous, Thermoresponsive L3-phase Silica/Hydroxyapatite Nanocomposites." *Journal of Materials Chemistry* 17(3):238.

Shin Y, and GJ Exarhos. 2007. "Conversion of cellulose materials into nanostructured ceramics by biomineralization." *Cellulose* 14(3):269-279.

Shin Y, and GJ Exarhos. 2007. "Template synthesis of porous titania using cellulose nanocrystals." *Materials Letters* 61(11-12):2594-2597.

Shin Y, CM Wang, WD Samuels, and GJ Exarhos. 2007. "Synthesis of SiC nanorods from bleached wood pulp." *Materials Letters* 61(13):2814-2817.

Shin Y, JM Blackwood, I Bae, BW Arey, and GJ Exarhos. 2007. "Synthesis and stabilization of selenium nanoparticles on cellulose nanocrystal ." *Materials Letters*. 61 (2007) 4297-4300.

Shin Y, I Bae, BW Arey, and GJ Exarhos. 2007. "Simple preparation and stabilization of nickel nanocrystals on cellulose nanocrystal." *Materials Letters* 64(14-15):3215-3217.

Shin Y, GE Fryxell, W Um, KE Parker, and SV Mattigod. 2007. "Sulfur-Functionalized Mesoporous Carbon." *Advanced Functional Materials* (in press) DOI: 10.1002/adfm.200601230.

# Bio-Integration: Active assembly of dynamic and adaptable materials

George Bachand, Bruce Bunker, Erik Spoerke  
gdbacha@sandia.gov, bcbunke@sandia.gov, edspoer@sandia.gov  
Sandia National Laboratories, Albuquerque, NM 87185

## Program Scope

The Bio-Integration project involves fundamental materials science issues at the intersection of biology, nanomaterials, and integrated systems. Research activities in the *Active Assembly of Dynamic and Adaptable Materials* component of this project involves the exploitation of active biomolecules to perform tasks associated with living materials including the active transport, assembly, reconfiguration, healing, and disassembly of nanomaterials. Organisms utilize the cooperative interactions between motor proteins and microtubules for processes ranging from cell division to melanophore reorganization. Our work is focused on understanding how to exploit such energy-consuming proteins (i.e., tubulin and kinesin) for manipulating materials via mechanisms that are not constrained by limitations associated with standard diffusion or equilibrium processes. The overarching goal is to mimic phenomena such as the assembly of diatom skeletons and/or the reconfiguration of the color changing system of fish in integrated fluidic environments. This abstract will specifically discuss recent work in the area of *Active Transport*, which involves the engineering, control, and exploitation of biomolecular motors for the assembly of nanocomposite materials.

## Recent Progress

### *Controlling active transport through molecular switching*

Biological systems utilize a variety of complex mechanisms to control the functionality of motor protein-based transport.<sup>1,2</sup> Based on the inability to apply such mechanisms at nanoscale interfaces, control of kinesin transport in microfluidic systems has been primarily achieved by regulating the fuel source. For example, control of kinesin-based transport has been accomplished through

the light-induced release of caged ATP.<sup>3,4</sup> While useful for specific applications, the nature of this control mechanism does not enable independent control of different motor types within a single assembly or device. Thus, our work has focused on using genetic engineering techniques to introduce a secondary, allosteric regulation site into kinesin that essentially serves as a “chemical on/off switch” capable of controlling linear translation of the motor. A  $Zn^{2+}$ -binding

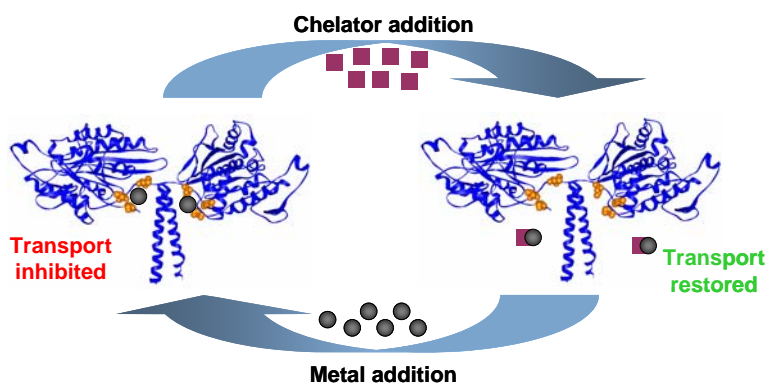


**Figure 1.** A zinc-binding site (amino acids shown in orange) was genetically engineered into the neck-linker region of kinesin motors, and used to control transport through sequential cycling of divalent metal ions and chelators.

site was engineered into the neck-linker region of kinesin (Figure 1); this domain is known to play a critical role in microtubule transport. Initially five different mutants were prepared and screened. Of these initial constructs, only one satisfied the baseline criteria that included (1) maintaining functionality and (2) responsiveness to zinc-dependent inhibition. The final switch mutant displayed on slight changes in transport velocity and microtubule affinity based on the introduction of zinc-binding site.

Microtubule transport by the mutant kinesin was successfully inhibited in the presence of 10  $\mu\text{M}$   $\text{ZnCl}_2$ , while the native kinesin maintained full motility at this concentration. Comparison of the concentration-dependent inhibition of the native and mutant kinesins demonstrated that the introduced zinc-binding site was responsible for the observed inhibition. The efficacy of other divalent metal ions was tested with respect to inhibiting microtubule transport. Overall, all metals tested inhibited transport with varying degrees of effectiveness:  $\text{Zn}^{2+} \approx \text{Cu}^{2+} > \text{Co}^{2+} > \text{Ni}^{2+} \geq \text{Mg}^{2+} \geq \text{Mn}^{2+}$ . Microtubule transport was successfully restored using a number of different chelators, including 1,10-phenanthroline (PNT), cysteine, and nitrilotriacetic acid. Lastly, sequential exchanges of  $\text{ZnCl}_2$  and PNT were used to demonstrate cyclic regulation of microtubule transport over four complete cycles.

#### *Dynamic assembly of nanocomposites through active transport*

Self-assembly of nano-structured materials through energy-dissipating process has been well-documented in biological systems. Recently, an interesting phenomenon in which motile microtubule filaments self-assembled into highly constrained spool-like nanocomposite structures was reported.<sup>5</sup> These composite structures consisted of streptavidin-coated quantum dots (SQDs) and biotinylated microtubules (bMTs). The assembly process of the composites mimics biological self-assembly, in which energy-dissipating and thermodynamic components drive the overall assembly. Under conditions of thermal equilibrium, mixtures of SQDs and bMTs self-assemble into disordered, aggregate structures.<sup>6</sup> However, when exploiting the energy-dissipating process of microtubule transport by kinesin motors, the introduction of the SQDs to actively moving bMTs leads to a balanced interaction between energy-dissipating (i.e., kinesin-based transport) and thermodynamic (i.e., biotin-streptavidin bond formation) processes. This interaction ultimately drives the assembly of the spool-like structures (Figure 2). The “phase” of the composite structure can be changed by varying the level of thermodynamic input (e.g., SQD concentration) while holding the energy-dissipating input constant.

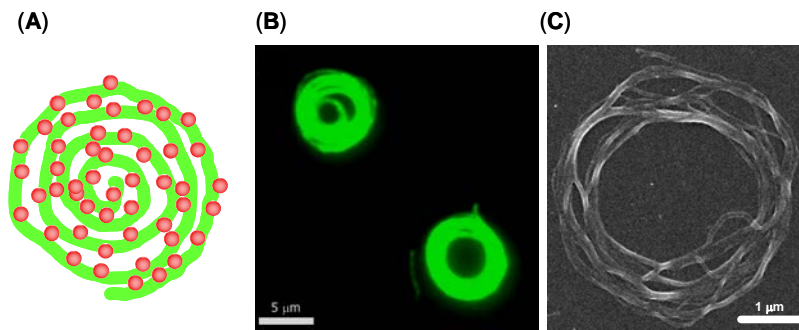


**Figure 2.** Artistic representation (A), and fluorescence (B) and scanning electron (C) photomicrographs showing the spool-like composite structures of quantum dots and microtubules assembled through active transport.

The spool-like composite structures are capable of storing considerable elastic energy. The microtubules are hollow cylinders with a diameter of  $\sim 25$  nm and possess a relatively high intrinsic rigidity ( $\kappa = 2.0 \times 10^{-24}$  N  $\text{m}^2$ ;  $L_p = \sim 500$   $\mu\text{m}$ ). The size of the spool-like structures ranged from 2.5 to 11  $\mu\text{m}$ , with an average inner and outer diameter ( $n = 86$  ring structures) of

$3.4 \pm 0.2 \mu\text{m}$  and  $5.2 \pm 0.2 \mu\text{m}$ , respectively. Using these values the elastic energy stored in a typical composite can be roughly estimated at  $\sim 33,000 K_B T$  (135 aJ).

Energy-dissipation also plays a key role in the disassembly of the composite structures. The fully assembled structures can remain stable for several hours when the energy-dissipating component (i.e., kinesin-based transport) is removed. However, if kinesin-based transport is maintained, the composites will spontaneously disassemble within 15 min after assembly. Structural defects and regions of high mechanical strain likely induce bMT breakage, which was noted by a significant decrease in the average length of the microtubules following disassembly. Such breakage enables kinesin motors to “unzip” individual and/or sections of several bMTs from the spool-like structures, and leads to complete disassembly of the composites. Once disassembly occurs, the SQD-bMTs do not reassemble into the composite structures again.

## Future Plans

The SDQ-bMT composites offer a unique system for studying the non-equilibrium assembly of nanostructured materials. We will continue studies of this model system to further understanding how the interaction of the thermodynamic and energy-dissipating components drives the various stages of assembly and disassembly. For example, the effects of the rate of energy-dissipation will be evaluated using the known enzyme kinetics of the motor protein. Another area of study will include the temperature-dependent effects on the assembly process. Altering the temperature will likely affect the assembly based on changes in the rate of energy-dissipation (i.e., microtubule transport), flexural rigidity of the bMTs, rate of SQD diffusion, and stability of the biotin-streptavidin bonds. We will also employ chemical and/or physical confinement<sup>7,8</sup> as a means of shifting the structural morphology of the composites. Finally, we will utilize the zinc-switch mutant kinesin to selectively start and stop the assembly/disassembly, and further examine the individual steps in these processes.

## References

1. Coy, D.L., Hancock, W.O., Wagenbach, M. & Howard, J. Kinesin's tail domain is an inhibitory regulator of the motor domain. *Nature Cell Biol.* **1**, 288-292 (1999).
2. Maniak, M. Organelle transport: A park-and-ride system for melanosomes. *Curr. Biol.* **2**, R917-R919 (2003).
3. Hess, H., Clemmens, J., Qin, D., Howard, J. & Vogel, V. Light-controlled molecular shuttles made of motor proteins carrying cargo on engineered surfaces. *Nano Lett.* **1**, 235-239 (2001).
4. Wu, D., Tucker, R. & Hess, H. Caged ATP - fuel for bionanodevices. *IEEE Trans Adv Pack* **28**, 594-599 (2005).
5. Bachand, M., Trent, A., Bunker, B. & Bachand, G. Physical factors affecting kinesin-based transport of synthetic nanoparticle cargo. *J. Nanosci. Nanotech.* **5**, 718-722 (2005).
6. Bachand, G.D., Rivera, S.B., Boal, A.K., Gaudioso, J., Liu, J. & Bunker, B.C. Assembly and transport of nanocrystal CdSe quantum dot nanocomposites using microtubules and kinesin motor proteins. *Nano Lett.* **4**, 817-821 (2004).
7. Boal, A.K., Bauer, J.M., Rivera, S.B., Manley, R.G., Manginell, R.P., Bachand, G.D. & Bunker, B.C. Monolayer engineered microchannels for motor protein transport platforms. *Abstracts of Papers of the American Chemical Society* **28**, U355-U355 (2004).

8. Clemmens, J., Hess, H., Lipscomb, R., Hanein, Y., Böhringer, K.F., Matzke, C.M., Bachand, G.D., Bunker, B.C. & Vogel, V. Mechanisms of microtubule guiding on microfabricated kinesin-coated surfaces: Chemical and topographic surface patterns. *Langmuir* **19**, 10967-10974 (2003).

#### **Recent BES-Sponsored Publications (2005-2007)**

- Rivera, S.B., Koch, S.J., Bauer, J.M., Edwards, J.M., & Bachand, G.D. (2007). Temperature dependent properties of a kinesin-3 motor protein from *Thermomyces lanuginosus*. *Fungal Genetics and Biology* (*in press*, [doi:10.1016/j.fgb.2007.02.004](https://doi.org/10.1016/j.fgb.2007.02.004)).
- Boal, A.K., Tellez, H., Rivera, S.B., Miller, N., Bachand, G.D., & Bunker, B.C. The stability and functionality of chemically crosslinked microtubules. *Small* **2**, 793-803 (2006).
- Boal, A.K., Bachand, G.D., Rivera, S.B., & Bunker, B.C. Interactions between cargo-carrying bio-molecular shuttles. *Nanotechnology* **17**, 349-354 (2006).
- Bachand, M., Trent, A.M., Bunker, B.C., & Bachand, G.D. Physical factors affecting kinesin-based transport of synthetic nanoparticle cargo. *J. Nanosci. Nanotech.* **5**, 718-722 (2005).
- Hess, H. & Bachand, G.D. Biomolecular motors to power nanotechnology. *Mater. Today*, **8**, 22-29 (2005).
- Bouchard, A.M., Warrender, C.E., & Obsourn, G.C. Harnessing microtubule dynamic instability for nanostructure assembly. *Phys. Rev. E*, **74**, 41902-1-16 (2006)

**Cell Directed Assembly of Novel Biotic/Abiotic Materials and Interfaces**  
**CJ Brinker (cjbrink@sandia.gov) Sandia National Laboratories, Molecular**  
**Nanocomposites Project - FWP Number 06-013370, Subtask 2 Complex Nanocomposites**  
 Team: Carnes, Eric; Singh, Seema; Lopez, DeAnna (UNM)

**Scope** - Immobilization of individual cells and collections of cells in well-defined, nano-to-microscale structures that allow structural and functional manipulation, interrogation, and fabrication of new bio/nano interfaces is important for developing new classes of biotic/abiotic materials and behaviors, for establishing the relationship between genotype and phenotype, and for elucidating complex pathways associated, for example, with the onset of disease or with energy storage, transduction and dissipation. Although there has been considerable recent progress in investigating the response of cells to chemical or topological patterns defined lithographically on two-dimensional (2D) surfaces, it is time to advance from 2D adhesion on dishes/fluidic devices to 3D architectures that better represent the natural nanoporous and 3D extracellular matrix (ECM). 3D immobilization in nanostructured hosts enables cells to be surrounded by other cells, maintains fluidic connectivity/accessibility, and allows development of 3D molecular or chemical gradients that provide an instructive background to guide cellular behavior. Although 3D cell immobilization in polymers, hydrogels, and inorganic gels has been practiced for decades, these approaches do not provide for bio/nano interfaces with 3D spatial control of topology and composition important to both the maintenance of natural cellular behavior patterns and the development of new non-native behaviors and functions. In particular for ALL previously reported approaches there was neither any apparent effect of the cell on the surrounding host nor any attempt to purposefully use the nanostructured host to develop new cellular behaviors. Here we show our recently discovered cell directed assembly (CDA) approach to be a unique distinguishing methodology to prepare new bio/nano interfaces and to develop new cellular behaviors.

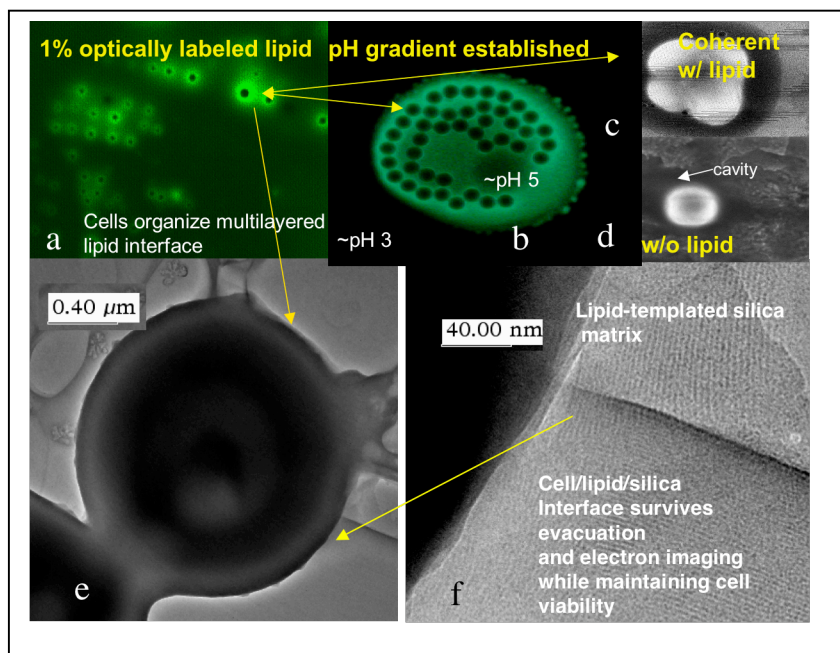


Fig. 1 – Essential features of CDA. a) lipid localization at yeast cell surface imaged using green labeled *diC<sub>6</sub>PC*, b) pH gradient imaged with pH sensitive dye, c) and d) SEM with and w/o *diC<sub>6</sub>PC*, showing shrinkage and cavity formation w/o lipid, e) and f) TEM images showing coherency of the nanostructured lipid/silica matrix at the cellular surface upon drying and evacuation without further fixation. Adapted from Baca, Brinker et al. *Science* 2006 [1].

**Background** – Cell-directed assembly [1,2] is an outgrowth of our prior work on evaporation-induced self-assembly (EISA) of ordered, periodic ‘so-called’ mesoporous silica films [3,4]. Starting with a dilute, homogenous solution of a hydrophilic silica precursor plus amphiphilic surfactant in alcohol/water solvent, sequential evaporation of alcohol and water, accompanying



dip-coating, spin-coating, ink-jet printing etc., drives the formation of micelles and their further organization into periodic mesophases. Association of the silica precursors with the hydrophilic interfaces of the surfactant mesophase in turn concentrates and condenses them to form a nanostructured silica matrix. In cell directed assembly normal surfactants are replaced with biocompatible short chain phospholipids (e.g.  $C_6$  phosphatidylcholines, abbreviated  $diC_6PC$ ) and the EISA process is carried out with added cells (initially yeast and bacterial cell lines and now also mammalian cells). Figure 1 shows the essential features of bio/nano interfaces formed by CDA with added brewer's yeast, *Saccharomyces cerevisiae*. Each yeast develops a lipid-rich interface (Panel a), which adjoins the surrounding lipid/silica mesophase (panels e and f). This interface remains coherent despite evacuation and electron imaging (Panels d and f), whereas cells introduced to a standard silica sol without surfactant (Panel c) undergo shrinkage and a cavity develops between the cell and the matrix. As revealed by inclusion of the pH sensitive indicator Oregon green (Panel b), yeast also develop a several unit gradient in pH ranging from  $\sim 5.5$  at the cell surface (bright green) to 3 in the silica matrix (black). As understood from studies with dead cells and cell surrogates, this unique interface does not form passively, rather we propose it results from the unique ability of living cells to sense and respond to their external environments. For example the increasing concentration of external osmolytes during evaporation may induce the high osmolarity glycerol (HOG) pathway in *S. cerevisiae*. HOG begins with an immediate brief expulsion of water that could establish the pH gradient. As would be expected on this premise, other cells exhibit different cell-specific responses and consequently unique cell-specific bio/nano interfaces.

**Progress - New Insights and Directions** – During the past year we have extended our original work on yeast to a wide variety of Gram positive and negative bacteria and several mammalian cells. Remarkably extended viability studies performed on numerous cell lines show that our lipid/silica matrix preserves cell viability under desiccating conditions (ambient NM exposure or evacuation), at high temperature ( $>40^\circ C$ ), and upon exposure to synchrotron radiation. In essence our immobilization scheme confers extremophile behavior to the guest cells. We hypothesize that this stems in part from lipid localization at the cellular surface. The coherent lipid reservoir prevents excessive drying, maintains fluidity, mediates stress, and may serve as a sort of repair kit, supplying lipid on demand to maintain the cellular membrane. The lipid interface provides additionally an opportunity to impart new functionality to the bio/nano interface. CDA performed with  $diC_6PC$  plus a longer chain lipid ( $diC_{14}PC$ , DMPC) introduced as a liposome preferentially localizes the longer chain DMPC lipid at the immediate cell surface (see Figure 2, Panel a). Because, to maintain their native conformations, transmembrane proteins require fluid, longer chain lipid bilayers to accommodate hydrophobic membrane-spanning domains, prioritized long chain lipid localization should allow the formation of an extracellular membrane bilayer/multilayer in which to incorporate transmembrane proteins with retained functionality. To demonstrate this concept, we used CDA to immobilize yeast plus bacteriorhodopsin (BR), a light-driven halophile transmembrane proton pump, introduced directly or in a DMPC liposome. Confocal fluorescence imaging (see Figure 2, Panels b and c) shows that BR introduced in a liposome is localized within regions adjacent to and conformal with the cellular surface. (Corresponding studies of BR added directly show a more diffuse localization). Figure 2, panels d-e show that BR introduced in a DMPC liposome dramatically influences/reduces the pH gradient. This result implies that some portion of the BR is incorporated within the localized DMPC bilayer where it can retain its native conformation and serve as a proton pump. Additionally it suggests that the radial asymmetry of the interface somehow serves to orient the BR causing proton pumping to result in a net change in the proton flux thereby changing the pH gradient. Overall this approach provides a new means to introduce to a cell surface new, arbitrary non-native functionality.

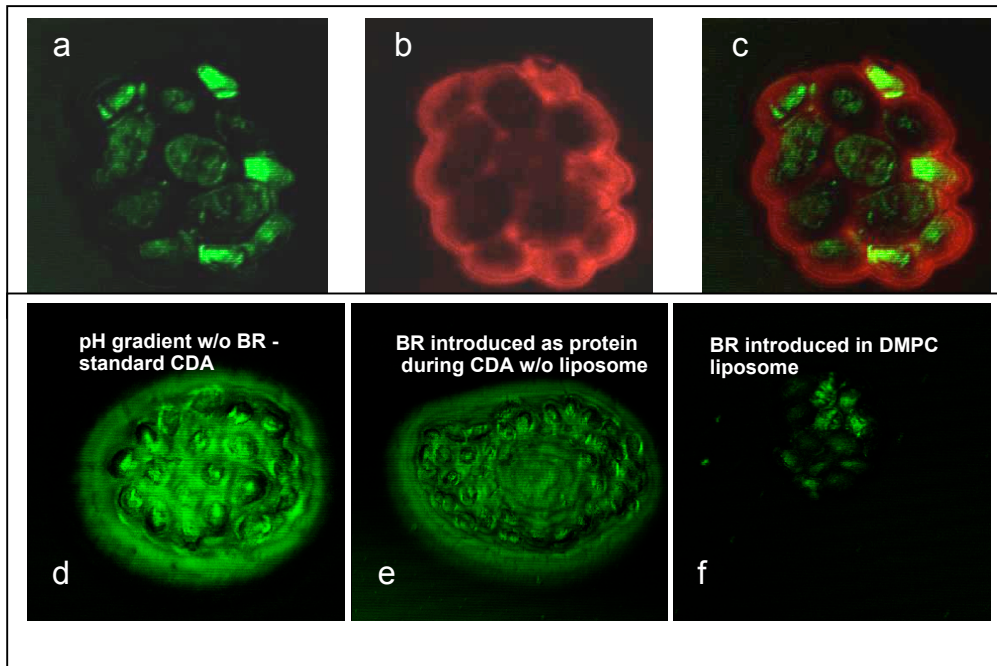


Fig 2. Confocal fluorescence images showing lipid/protein localization and pH gradient development at yeast surface after CDA. a) green labeled DMPC, b) red labeled BR, c) merged image, d) pH gradient imaged with Oregon green for standard CDA, e) pH gradient for BR added directly, and f) pH gradient for BR in DMPC liposome. For d-f, brighter green represents higher pH  $\sim 5.5$  at cell surface.

**A New Lithography with Life** – Cell directed assembly is cell-specific, meaning that different cell types direct differing amounts of lipid localization at the cell surface and establish different pH gradients. Despite these differences, all cells evaluated to date show some affinity for short chain PC lipids. This has enabled a new type of patterned cellular integration – achieved simply by deposition of cells onto pre-assembled lipid/silica mesophase films. Confocal scanning microscopy along with SEM/EDS analysis has confirmed that, within several minutes, yeast, bacterial, and mammalian cells deposited in buffer on the lipid/silica surface incorporate themselves through formation of a lipid localized interface similar to that of direct CDA. This is an active process - apoptotic cells (as well as colloidal cell surrogates) do not localize lipid/silica nor develop a pH gradient. It can be patterned by UV/ozone exposure of the lipid/silica surface prior to cell deposition. After cellular integration a second UV/ozone exposure can remove lipid, creating hydrophilic nanofluidic connections between cells. Within this construct we have preliminary evidence that we can follow the toll-like receptor 4 immune response pathway in mouse macrophage cells induced by addition of the model endotoxin lipopolysaccharide even after exposure of the cells for days to dry conditions. This patterned living cell-directed integration represents a new type of ‘lithography with life’ and should be of fundamental interest to understand the influence of nanoconfinement/nanostructuring on cellular behavior and communication.

#### **Immediate Questions being addressed in current research**

- What governs cell-specific lipid localization at cell surface?
- What is the metabolic state of the immobilized cells?
- What are associated cellular responses? Osmotic stress, adhesion, etc?
- Overall what is influence of nanoconfinement on cellular behavior?

## References

1. Cell-directed assembly of lipid-silica nanostructures providing extended cell viability, Baca, HK; Brinker, CJ, et al. **Science**, July 2006, **313**, p. 337-341.
2. Cell-directed assembly of bio/nano interfaces – a new scheme for cell immobilization Baca, Helen; Brinker, C. Jeffrey et al.. **Accounts of Chemical Research**, 2007, ASAP web Release date: August 03, 2007.
3. Continuous Formation of Supported Cubic and Hexagonal Mesoporous Films by Sol Gel Dip-Coating Lu, Y. F.; Brinker, C. J.; et al. **Nature** 1997, **389**, 364-368.
4. Evaporation-Induced Self-Assembly: Nanostructures Made Easy, Brinker, C.; Lu, Y.; Sellinger, A.; Fan, H..**Adv. Mater.** 1999, **11**, 579

## Selected Recent Publications

1. Cell-directed assembly of bio/nano interfaces – a new scheme for cell immobilization Baca, Helen; Carnes, Eric; Singh, Seema; Ashley, Carlee; Lopez, DeAnna; Brinker, C. Jeffrey. **Accounts of Chemical Research**, 2007, ASAP web Release date: August 03, 2007.
  2. Modulus/density scaling behavior and framework architecture of nanoporous, self-assembled silicas, Fan, Hongyou; Hartshorn, Christopher; Buchheit, Thomas; Tallant, David; Assink, Roger; Simpson, Regina; Kissel, Dave; Lacks, Daniel; Torquato, Salvatore; Brinker, C. Jeffrey, **Nature Materials**, June 2007, no. 6, p. 418-423.
  3. Optical Detection of Ion-Channel-Induced Proton Transport in Supported Phospholipid Bilayers, Tsung-Han (Calvin) Yang, Chanel K. Yee, Meri L. Amweg, Seema Singh, Eric L. Kendall, Andrew M. Dattelbaum, Andrew P. Shreve, C. Jeffrey Brinker, and Atul N. Parikh. **Nano Letters**; 2007; ASAP Web Release Date: 13-Jul-2007.
  4. Amphotericin B channels in phospholipid membrane-coated nanoporous silicon surfaces: Implications for photovoltaic driving of ions across membranes, Yilma, Solomon; Liu, Nangou; Samoylov, Alexander; Lo, Ting; Brinker, C. Jeffrey; Vodyanoy, Vitaly, **Biosensors and Bioelectronics**, Mar 15 2007, **22**, no.8, p.1605-1611.
  5. Nanometer-thick conformal pore-sealing of self-assembled mesoporous silica by plasma-assisted atomic layer deposition, Jiang, YB; Liu, NG; Gerung, H; Cecchi, JL; Brinker, CJ, **Journal of The American Chemical Society**, August 30, 2006, **128**, p. 11018-11019
  6. Drying transition of confined water, Singh, S; Houston, J; van Swol, F; Brinker, CJ, **Nature**, Aug 3 2006, **442**, p. 526
  7. Cell-directed assembly of lipid-silica nanostructures providing extended cell viability, Baca, HK; Ashley, C; Carnes, E; Lopez, D; Flemming, J; Dunphy, D; Singh, S; Chen, Z; Liu, N; Fan, HY, Lopez, GP; Brozik, SM; Werner-Washburne, M; Brinker, CJ, **Science**, July 2006, **313**, p. 337-341.
  8. Drag reduction on a patterned superhydrophobic surface, Truesdell, R; Mammoli, A.; Vorobieff, P; van Swol, F; Brinker, CJ., **Physical Review Letters**, July 28, 2006, **97**, p. 044504.
  9. Morphological control of surfactant-templated metal oxide films, Brinker, CJ; Dunphy, DR, **Current Opinion in Colloid & Interface Science**, Jun 2006, **11**, p. 126-132
  10. Investigating the interface of superhydrophobic surfaces in contact with water Doshi, DA; Shah, PB; Singh, S; Branson, ED; Malanoski, AP; Watkins, EB; Majewski, J; van Swol, F; Brinker, CJ, **Langmuir**; **21**, p.7805; 2005
- Neutron reflectivity study of lipid membranes assembled on ordered nanocomposite and nanoporous silica thin films, Doshi, DA; Dattelbaum, AM; Watkins, EB; Brinker, CJ; Swanson, BI; Shreve, AP; Parikh, AN; Majewski, J, **Langmuir**; **21**, p.2865; 2005.

## **Program Title: Optical Techniques for Studying Novel Biomaterials**

Principal Investigator's

P. L. Gourley, Dept. 8331, MS1413, SNL, Albuquerque, NM 87185

[plgourl@sandia.gov](mailto:plgourl@sandia.gov),

D. Y. Sasaki, Dept. 8331, MS 9292, SNL, Livermore, CA 94550

[dysask@sandia.gov](mailto:dysask@sandia.gov)

M. B. Sinclair, Dept. 1824, MS 1411, SNL, Albuquerque, NM 87185

[mbsincl@sandia.gov](mailto:mbsincl@sandia.gov)

**Scope:** This program investigates optical techniques for probing novel biomaterials structures on the micro to nanoscale. The techniques include linear and nonlinear optical microscopy, nanolaser spectroscopy, light scattering, and time-resolved imaging, as well as micro/nanofabrication of environmentally controlled optical cavities/platforms for flowing and containing biomaterials under study.

### **Progress**

Recently, we completed a study of biophotonic properties of organelles (mitochondria of few hundred nm in size) isolated from yeast cells. The nanolaser measures a quantity called  $\Delta\lambda$  that is a function of the refraction index, a quantity that is closely related to the cell biomolecular composition, concentration, and particle size. We measured the refractive index of each organelle in a large population ( $\sim 10^4$ ) for the first time. The results show that the biomolecular changes in bioparticles can be effectively probed by optical measurements. For this study, we developed a nanolaser spectroscopic technique that has two important features. First, it is sensitive to very small changes in biomolecular composition of small particles. These changes result in small shifts in the nanolaser wavelength that can be detected to about  $10^{-5}$  times the laser wavelength. Second, the laser is sensitive to very small objects like mitochondria and exploits a newly discovered nano-optical transduction method called "nano-squeezing" of light whereby photon modes are imposed by the ultrasmall dimensions of the nanoparticles in a submicron laser cavity. The condition for nano-squeezing is that the particle must be approximately smaller than the wavelength of light. With these conditions met, the laser signal simplifies to a single intense optical mode. This is a critical advantage of the biocavity laser. Because the mitochondria are small, it has been difficult to study them using standard light microscope or flow cytometry techniques. And, electron or atomic force microscopies are limited to nonviable, fixed organelles so they cannot reproduce physiologic measurements. Thus nanolaser spectroscopy is an ideal tool for studying biomolecular changes in bioparticles.

We also conceived of a novel way to image and study motion of virus particles. The small virus size (~20 to 100 nm) requires new spectroscopic and imaging techniques for detection and differentiation. We fabricated nanochannels to transport virus particles through ultrashort laser cavities and measured the lasing output as a sensor for virions. We used a type of bacterial virion having relatively large diameter of 100 nm (*Bacillus megaterium* virus). The virions were flowed through the laser cavity and spectra were recorded. We investigated two types of intracavity quantum photonics: the first is direct pathogen-supported lasing modes and the second is indirect modulation of the modal noise in stimulated emission from the laser cavity. Though we did not observe the first quantum photonic effect, we did observe the second effect. We found that the bacterial virion could modulate the noise spectrum of the cavity modes as measured with a spectrum analyzer. To further investigate the optical measurements of these bioparticles, we also studied light scattering from virions, both to determine the magnitude of the scattered signal and to use it to investigate the motion of virions. We observed the motion of virions in transparent dielectric nanocavities using ultra dark field scattering. It was possible to directly observe scattered light from virions and their Brownian movement with these techniques, despite the fact that the virions are nearly five to ten times smaller than the wavelength of light used. By using laser scanning microscopy, it was possible to record movies of the virion motion and indirectly determine the size of the virion by kinetic studies. We used a large virion *Bacillus megaterium* (about 100 nm in diameter) and a small virion (*Pseudoalteromonas espejiana* phage about 50 nm in diameter). From the framing images (taken every 34 ms) we constructed histograms of virion step size. The histograms were Poissonian-like for the *Bacillus megaterium* virus and more Gaussian for the smaller *Pseudoalteromonas espejiana* phage.

Bioparticles can be found as isolated species both in nature and in synthetic formulations. In many biological systems of interest, bioparticles often occur in higher concentrations in which the bioparticle can interact and influence the collective properties of the ensemble. It is of considerable interest to measure many-body effects in biomaterials as they are expected to be particularly sensitive to environmental changes and may serve as a useful marker for the presence of pathogens, toxins, or other biomolecules. One such system is the mitochondrial network in mammalian cells. The morphology of mitochondria is highly variable where the organelle can switch between a fragmented morphology with many ovoid-shaped particles to a reticulum in which the organelle is a single, many-branched structure. We used two laser-scanning microscopic techniques. The first is spatial auto-correlation of fluorescent bioprobes attached to the network. The second is cross-correlation of the fluorescence signal with an ultra-darkfield signal. Both techniques showed that the normal, actively respiring network gave very high correlation images. In contrast, a modified network with low respiration activity (induced by a chemical modification) gave much lower correlation. The results indicate that optical

image correlation methods are effective for studying many-body effects in multiparticle biomaterials.

## **Future**

### Nonlinear Optical Imaging Microscope

The recent appearance of nonlinear, multi-photon, and coherent light imaging techniques, as well as the emergence of sophisticated imaging techniques such as  $4\pi$  confocal imaging, and new developments in high sensitivity detector arrays and optical engineering of extremely low aberration, high numerical aperture objective lenses, provide the impetus for systematic, thoughtful designs for integrating these novel methods into mid-scale microscopic instruments for biomaterial sciences. The microscope could possibly integrate multiple ultrafast (picosecond and femtosecond) laser sources, advanced high resolution imaging techniques such as  $4\pi$  confocal microscopy, nonlinear optical techniques such as Coherent anti-Stokes Raman Spectroscopy (CARS) and spectral imaging techniques, to provide an unprecedented ability to acquire high resolution images containing molecularly specific information. These powerful nonlinear imaging modalities for biomaterials offers chemically selective contrast based on vibrational sensitivity. This new instrument would represent a versatile new tool for exploration and discovery in nano- and soft matter material systems.

This instrument is timely due to recent advances in fiber, solid state and semiconductor laser sources. At the same time, emerging micro- and nanofabricated optics offer the possibilities of resonant light confinement, surface-enhanced scattering, phase matching and detection, and microfluidic handling of specimens. Thus, simultaneous physics on the mid-, macro-, micro- and nano- scales offers ultrahigh sensitivity, high throughput, and statistical analyses not currently available in commercial instruments. In addition, both inelastic Raman scattering and elastic light scattering could be integrated into the same microscope. The latter has the advantage of being highly sensitive and selective for nanoparticles when ultra-dark field (extreme wide angle scattering) is employed. In a resonant cavity where the optical field is a standing wave, it is possible to perform 3D imaging by spatially resolving scattered light in the vertical axis without mechanical scanning of the specimen. It results in considerable advantage for ultra high speed 3D probing of Brownian motion (translational and rotational) of nanoparticles for characterizing size, mass and morphology. Under high field conditions, the field can also act as a periodic optical trap to contain small particles for subsequent motional study or spectroscopy.

## Recent Publications Resulting from BES support

1. **Biocavity Laser Spectroscopy of Genetically-altered Yeast Cells and Isolated Yeast Mitochondria**, P. L. Gourley, J. K. Hendricks, A. E. McDonald, R. G. Copeland, R. K. Naviaux, M. P. Yaffe, *J. Biomedical Optics*, accepted March 2006
2. **Optical Phenotyping of Human Mitochondria in a BioCavity Laser**, P. L. Gourley and R. K. Naviaux, *Special Issue on Biophotonics, IEEE J. of Selected Topics in Quantum Electron.* **11**, July/August 2005, p. 818-826.
3. **Mitochondrial Correlation Microscopy and Nanolaser Spectroscopy – New Tools for Biophotonic Detection of Cancer in Single Cells**, P. L. Gourley, J. K. Hendricks, A. E. McDonald, R. G. Copeland, K. E. Barrett, C. R. Gourley, K. K. Singh, R. K. Naviaux, *Technology in Cancer Research & Treatment* **4**, Adenine Press (2005), p. 585-592.
4. **Brief Overview of BioMicroNanoTechnologies**, P. L. Gourley, *Biotechnology Progress*, Am. Chem. Soc. Feb 2, 2005.
5. **Poly(dimethylsiloxane) thin films as biocompatible coatings for microfluidic devices: Cell culture and flow studies with glial cells**, S. L. Peterson, A. E. McDonald, P. L. Gourley, D. Y. Sasaki, *J. Biomed. Mater. Res.* 2005, 72A, 10 - 18.

## Adaptive and Reconfigurable Nanocomposites

### Molecular Nanocomposites Project - FWP Number 06-013370, Subtask 1

Bruce C. Bunker ([bcbunke@sandia.gov](mailto:bcbunke@sandia.gov)), Todd M. Alam ([tmalam@sandia.gov](mailto:tmalam@sandia.gov)),  
David R. Wheeler ([drwheel@sandia.gov](mailto:drwheel@sandia.gov)), Dale L. Huber ([dlhuber@sandia.gov](mailto:dlhuber@sandia.gov)),  
Chris Orendorff ([corendo@sandia.gov](mailto:corendo@sandia.gov)), Mark J. Stevens ([msteve@sandia.gov](mailto:msteve@sandia.gov)),  
and Darryl Y. Sasaki ([dysasak@sandia.gov](mailto:dysasak@sandia.gov))

Sandia National Laboratories, P.O. Box 969, Livermore, CA 94551  
& P.O. Box 5800 Albuquerque, NM 87185

### Program Scope

The aim of this project is to explore the basic science associated with the use of energy consuming, switchable, and/or responsive components to create programmable and/or reconfigurable nanocomposites. As biological systems employ such schemes to initiate new/altered function in nanoscale self-organizing assemblies, we are exploring simplified versions of these nanomaterials to understand the molecular and supramolecular interactions that lead to component organization upon switching through external activation sources, such as heat, light, electric fields, and host-guest complexation. Our activities include 1) synthesis of molecular building blocks with programmed function, 2) assembly of the building blocks into films and 3D structures, 3) stimulation and characterization of phase transitions and reconfigurations, and 4) modeling of component interactions to aid in design and visualization of reconfigurable phenomena.

### Recent Progress

The presented work will describe our past and recent efforts that utilize host-guest interactions to modulate nanoscale structure and generate 3D architectures in self-organizing media, specifically lipid membranes. Binding events located at the surface of lipid membranes actuates rapid and dynamic structural changes that occur at the nanometer to micron scale to create reversible domain formation and hierarchical bilayer assemblies.

The binding of metal ions to recognition sites provides a selective toggle that induces attractive as well as repulsive interactions within molecular and supramolecular systems. A sample of synthetic lipids with metal ion receptors at the headgroup position, shown in Figure 1, were prepared for the selective binding of  $\text{Cu}^{2+}$  (PSIDA, PSBiPy) and for  $\text{Pb}^{2+}$  (PS18C6).<sup>1</sup> Bilayers of distearoyl phosphatidylcholine (DSPC) containing small amounts of these lipids perform as optical sensor materials for their

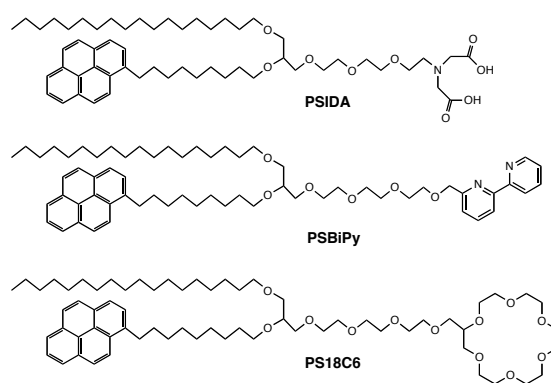


Figure 1. Metal ion receptor lipids.



target metal ions with < ppb sensitivity.

The optical detection scheme relies on the aggregation/dispersion of the receptor lipids as they respond to metal ion recognition. Aggregation of the receptor lipids produces a high local concentration of pyrene fluorophores resulting in pronounced excited dimer (excimer) emission and reduced emission from the monomer. Dispersion, on the other hand, decreases the local concentration resulting in a reversal of the excimer to monomer ratio. The fluorescence experiments indicated that the receptor lipids strongly aggregate in the DSPC bilayers, but then disperse upon recognizing specific metal ions.

Control over this process

was programmed into the lipid molecule utilizing specific molecular features. For example, by designing the receptor lipid to exist in the fluid phase at room temperature spontaneous phase separation from the gel phase DSPC matrix was expected. Metal ion recognition of divalent metal ions then produces a charged headgroup that becomes electrostatically repulsive of other metal-bound headgroups, thus inducing dispersion. Through atomic force microscopy (AFM) we were able to observe and follow the reversible changes in nanoscale domain formation in the lipid membrane with repeated metal ion addition and subsequent removal by ethylene diaminediacetic acid (EDTA) (Figure 2).<sup>2</sup>

Chemical recognition also enables the generation of unique supramolecular architectures through host-guest interaction. Binding of iminodiacetic acid to  $\text{Cu}^{2+}$  can occur in a 2:1 octahedral-like complex promoting attractive interactions between opposing bilayers containing PSIDA lipid. Such interactions have led to the chemical recognition-driven formation of stacked lipid bilayers reminiscent of bilayer architectures found in light harvesting cells (Figure 3a).<sup>3</sup> Recent studies have found that the bilayer stacking process begins with individual liposomes that first collapse and then fold in half to produce a stacked bilayer unit composed of four bilayer sheets. Stacking of the units subsequently generates the larger assemblies.

Another example of a hierarchical bilayer structure employs the criss-cross geometry of bipyridine- $\text{Cu}^{2+}$

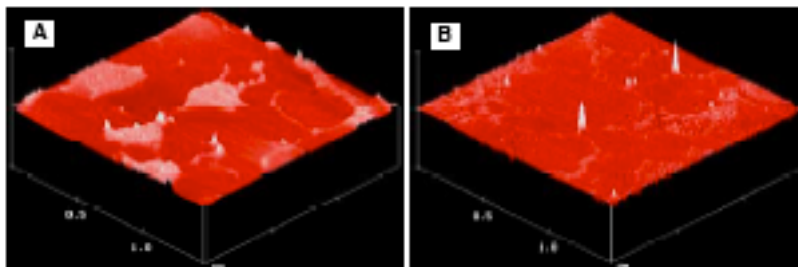


Figure 2. Oblique AFM images of 20% PS18C6/DSPC bilayers A) before and B) after addition of  $\text{Pb}^{2+}$  ( $1.0 \mu\text{M}$ ). Areas rich in PS18C6 (lighter regions) are  $\sim 11 \text{ \AA}$  taller than the DSPC membrane, consistent with molecular models (image edge length =  $1.5 \mu\text{m}$ ).

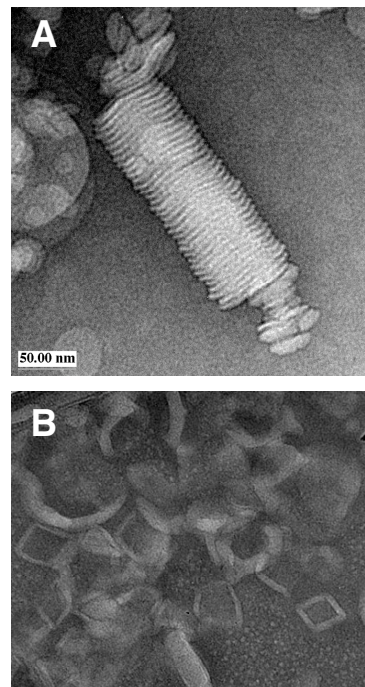


Figure 3. TEM images of  $\text{Cu}^{2+}$ -induced formation of A) stacked lipid bilayers from liposomes of PSIDA/DSPC, and B) rhombi from liposomes of PSBiPy/DSPC.

interactions with the PSBiPy lipid to direct the formation of rhombohedral structures from DSPC bilayers (Figure 3b).<sup>4</sup>

## Future Plans

A couple of examples of new directions being pursued to further understand methods to control the structure of lipid membrane assemblies and nanocomposites utilizes metal nanoparticles and temperature-sensitive polymers. The first employs some of the concepts described above to control phase separation and interfacial interactions to direct the formation of complex nanocomposite constructs. A particularly unique aspect of this work will be the utilization of induced membrane curvature to dictate the location of phase-separated domains. The geometry of a lipid or membrane protein defines a packing order that partitions molecules to a specific membrane curvature.<sup>5</sup> Conical shape molecules, for example, favor convex structures whereas cylindrical shapes favor planar structures. In a current investigation we are preparing lipid membrane coatings on gold nanorods and utilizing the distinct curvatures existing on the side and ends of the nanorod to direct asymmetric functionalization (Figure 4).<sup>6</sup> By coupling the asymmetric functionalization with lipid dispersion via host-guest complexation, reversible formation of novel gold nanorod assemblies that yield new optical and electronic behavior may be possible.

The second direction is focused on the development of temperature-actuated lipid assemblies to enable multi-level transformation of defined membrane architectures. Our approach is to prepare poly(N-isopropylacryl amide) (PNIPAM)<sup>7</sup> functionalized lipids that can change their structural geometry in response to temperature. As the solution temperature changes, the PNIPAM headgroup accordingly shrinks or swells leading to a spectrum of lipid geometries resulting in membrane architectures from stacks and vesicles to tubules and cubic assemblies.

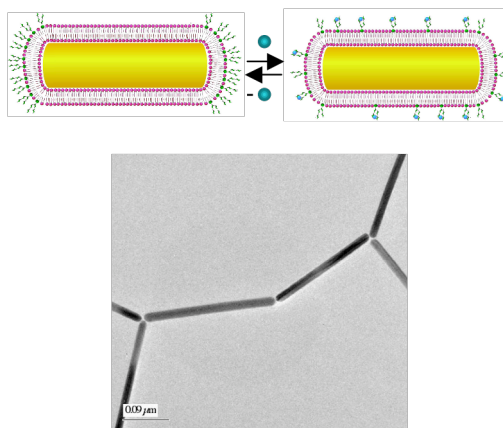


Figure 4. Schematic of reversible curvature-induced lipid assembly on Au nanorod (above). TEM image of assembling Au nanorods (below).

## References

- 1) D. Y. Sasaki, *Cell Biochem. Biophys.* **2003**, *39*, 145.
- 2a) D. Y. Sasaki, T. A. Waggoner, J. A. Last, T. M. Alam, *Langmuir* **2002**, *18*, 3714. b) J. Gaudio, D. Y. Sasaki, in *Encyclopedia of Nanoscience and Nanotechnology* (Eds.: J. A. Schwarz, C. I. Contescu, K. Putyera), Marcel Dekker, Inc., New York, **2004**, pp. 2507.
- 3a) T. A. Waggoner, J. A. Last, P. G. Kotula, D. Y. Sasaki, *J. Am. Chem. Soc.* **2001**, *123*, 496. J. L. b) D. Y. Sasaki, M. J. Stevens, *MRS Bulletin* **2006**, July, p. 521.
- 4) Pincus, C. Jin, W. Huang, H. K. Jacobs, A. S. Gopalan, Y. Song, J. A. Shelnett, D. Y. Sasaki, *J. Mater. Chem.* **2005**, *15*, 2938.
- 5) J. N. Israelachvili, *Intermolecular and Surface Forces*, 2nd ed., Elsevier Academic Press,

San Diego, **1992**.

- 6) C. J. Orendorff, P. L. Hankins, C. J. Murphy, *Langmuir* **2005**, *21*, 2022.
- 7) D. L. Huber, R. P. Manginell, M. A. Samara, B.-I. Kim, B. C. Bunker, *Science* **2003**, *301*, 352.

### **Acknowledgements**

This research was supported by the Division of Materials Science and Engineering in the Department of Energy Office of Basic Energy Sciences. Sandia is a multiprogram laboratory operated by Sandia Corporation, a Lockheed Martin Company, for the United States Department of Energy under Contract DE-AC04-94AL85000.

### **Publications resulting from this subtask (2005 – 2007)**

Bunker, B. C., Huber, D. L., Kushmerick, J. G., Dunbar, T., Kelly, M., Matzke, C., Cao, J., Jeppesen, J. O., Perkins, J., Flood, A. H., Stoddart, J. F., “Switching surface chemistry with supramolecular machines” *Langmuir*, **2007**, *23(1)*, 31 – 34.

Farrow, M. J., Zavadil, K. R., Pile, D. L., Yelton, W. G., Bunker, B. C., “Reversible electrochemical patterning of antibodies at self-assembled monolayers of beta-cyclodextrin” submitted to *Langmuir*.

Sasaki, D. Y., Stevens, M. J., “Stacked, Folded, and Bent Lipid Membranes” *MRS Bulletin* **2006**, July issue, 521 – 526 (invited review article).

Yim, H., Kent, M. S., Sasaki, D. Y., Polizzotti, B. D., Kiick, K. L., Majewski, J., Satija, S., “Rearrangement of Lipid Ordered Phases Upon Protein Adsorption Due to Multiple Site Binding” *Phys. Rev. Lett.*, **2006**, *96(19)*, 198101/1 – 4.

Zeineldin, R., Last, J. A., Slade, A. L., Ista, L. K., Bisong, P., O’Brien, M. J., Brueck, S. R. J., Sasaki, D. Y., Lopez, G. P., “Using Bicellar Mixtures to Form Supported and Suspended Lipid Bilayers on Silicon Chips” *Langmuir* **2006**, *22*, 8163 – 8168.

Song, Y., Steen, W. A., Peña, D., Jiang, Y.-B., Medforth, C. J., Huo, Q., Pincus, J. L., Qiu, Y., Sasaki, D. Y., Miller, J. E., Shelnutt, J. A., “Foamlike Nanostructures Created from Dendritic Platinum Sheets on Liposomes” *Chem. Mater.* **2006**, *18*, 2335 – 2346.

Kent, M. S., Yim, H., Sasaki, D. Y., Satija, S., Seo, Y.-S., Majewski, J., “Adsorption of Myoglobin to Cu(II)-IDA and Ni(II)-IDA Functionalized Langmuir Monolayers: Study of the Protein Layer Structure during the Adsorption Process by Neutron and X-Ray Reflectivity” *Langmuir*, **2005**, *21*, 6815 – 6824.

Pincus, J.L., Jin, C., Huang, W., Jacobs, H. K., Gopalan, A. S, Song, Y., Shelnutt, J. A., Sasaki, D. Y., “Selective fluorescence detection of divalent and trivalent metal ions with functionalized lipid membranes” *J. Mater. Chem.*, **2005**, *15*, 2938 – 2945 (invited article in Special Issue of Fluorescence Sensors).

## Metal-Lipid Nanocomposites from Reconfigurable Bicellar Structures

John A. Shelnutt

Sandia National Laboratories

Molecular Nanocomposites Project

FWP Number 06-013370, SCW93223, KC 0203010 Subtask 2 Complex Nanocomposites

Team: Yujiang Song; Darryl Y. Sasaki; Frank van Swol; Sivakumar Challa; Rachel Dorin; Robert Garcia

**Motivation** – Our goal is to develop nano-to-microscale structures that allow structural and functional manipulation, interrogation, and fabrication of new bio/nano composites and interfaces. The ability to *in situ* reconfigure or adapt structure and thereby control function is important for developing new classes of bioinspired nanomaterials and functional behaviors. The overall objective is the development of new methods for materials design, development of new building blocks, and organization of the building blocks by self-assembly, directed assembly, templating, and non-covalent interactions. Ultimately these new functional nanocomposites will be integrated into platforms allowing their structural and functional characterization, establishment of structure-property relationships, and incorporation in bio/nano devices for diverse applications. One aspect of our research involves reconfigurable and adaptable lipid assemblies, which respond to differing solution conditions by altering the structure of the lipid assembly or by forming hierarchical superstructures. These reconfigurable assemblies can then be used as templates for the growth of metal nanostructures and metal-lipid nanocomposites. Liposomes and bicelles are lipid structures that can be altered by changes in solution conditions, relative lipid concentrations, presence or absence of metal ions, temperature, and other factors. In addition, they can serve as templates for metal growth to produce metal structures that reflect the present morphology of the lipid assemblies. Our current efforts are directed toward establishing control over these reconfigurable lipid structures and utilizing them to template the growth of catalytic metal nanomaterials and nanocomposites.

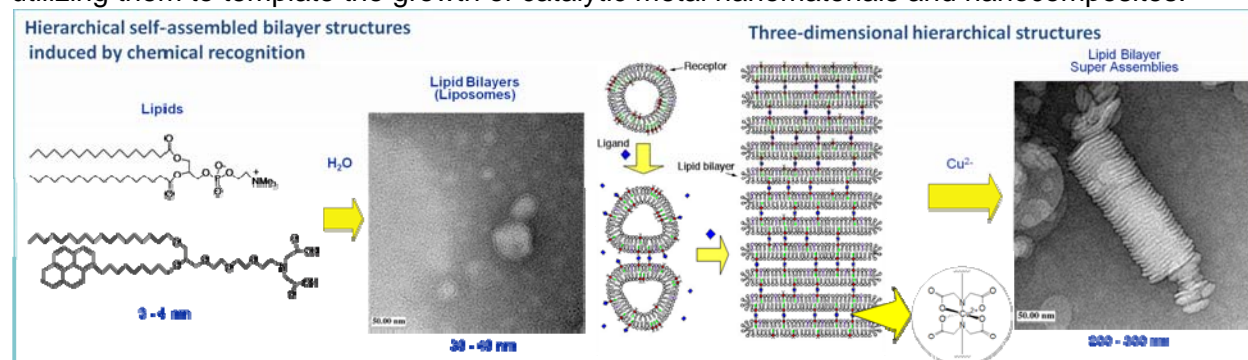


**Fig. 1.** Lipids used to form metal-sensitive liposomes and their conversion to stacks of lipid bicelles.

**Background** – Our use of reconfigurable lipid assemblies as templates for directed synthesis of metal nanomaterials is an outgrowth of our prior work in two areas—the dendritic growth and photocatalytic control of metal nanostructures [1-5] and the structural control of liposomes and bicelles [6,7]. Fig. 1. illustrates the use of lipids that bind metal ions to control the interconversion of liposomes into bicelles and their hierarchical self-organization into bicellar stacks. Metal ion binding can also cause the differential aggregation of metal-bound and unbound lipid molecules in the liposomes, which can be used as a sensing mechanism and as a means of controlling the morphology of the lipid structures. Fig. 2. illustrates our use of various lipid assemblies as templates to control the dendritic growth of platinum metal to produce a wide variety of metal nanostructures, including globular Pt nanodendrites, flat dendritic nanosheets, foam-like nanospheres, nanocages, and nanowire networks.

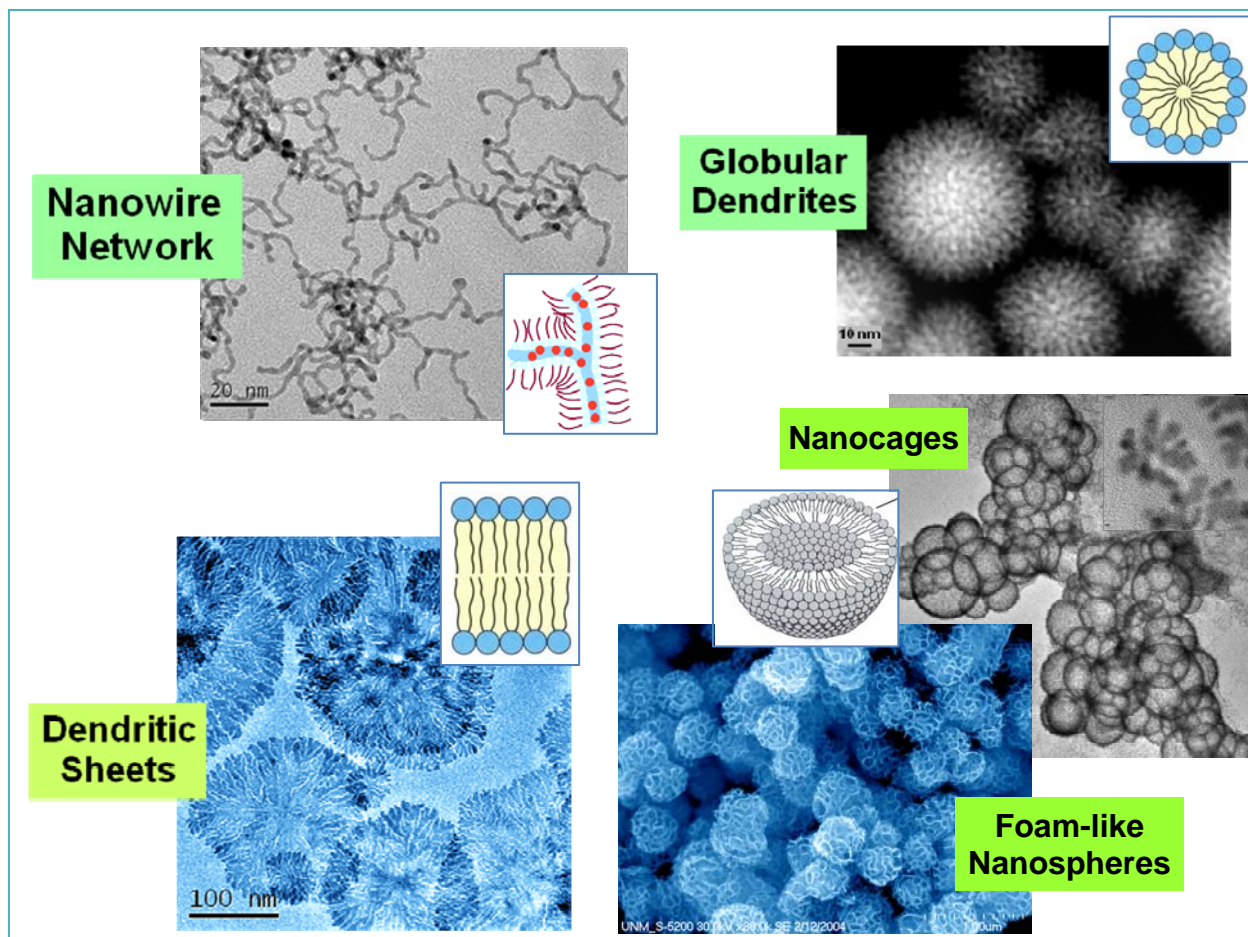


**Fig. 2.** Platinum nanomaterials produced with various templates obtained from lipid assemblies: (a) worm-like micellar networks, (b) micelles, (c) large liposomes or vesicles, and (d) unilamilar liposomes.

Platinum has technological applications in sensors, biosensors and other devices, and as catalysts and electrocatalysts for reduction of tailpipe emissions, polymer electrolyte membrane (PEM) fuel cells, and solar water-splitting devices. Because of the limited supply and high cost of platinum, researchers are developing methods for reducing the precious metal content in these applications. One way to minimize Pt usage is to increase catalytic efficiency by nanostructuring high-surface-area morphologies that are resistant to sintering/ripening processes. Our recent studies of bicelles and bicelle stacks aid in understanding the interactions of various lipid assemblies as well as their metal-templating properties that lead to formation of some extraordinary metal nanostructures using these bio-inspired templates.

**New Insights and Directions** – During the past year we have extended and combined our original work in these two research areas of reconfigurable lipid assemblies and templated growth of dendritic metal nanostructures. In the area of reconfigurable and responsive lipid assemblies, we have investigated the multi-component system involving two lipids, one of which binds metal ions, by varying the concentrations of lipids and metal ions to determine the amounts of each component necessary to induce stacking as shown on the right in Fig. 1. In the TEM study of the resultant lipid assemblies, we also discovered a liposomal folding mechanism by which the stacks of bicelles may form, which might also play a role in biology.

Remarkable new platinum nanomaterials have resulted from the combined use of bicelles and

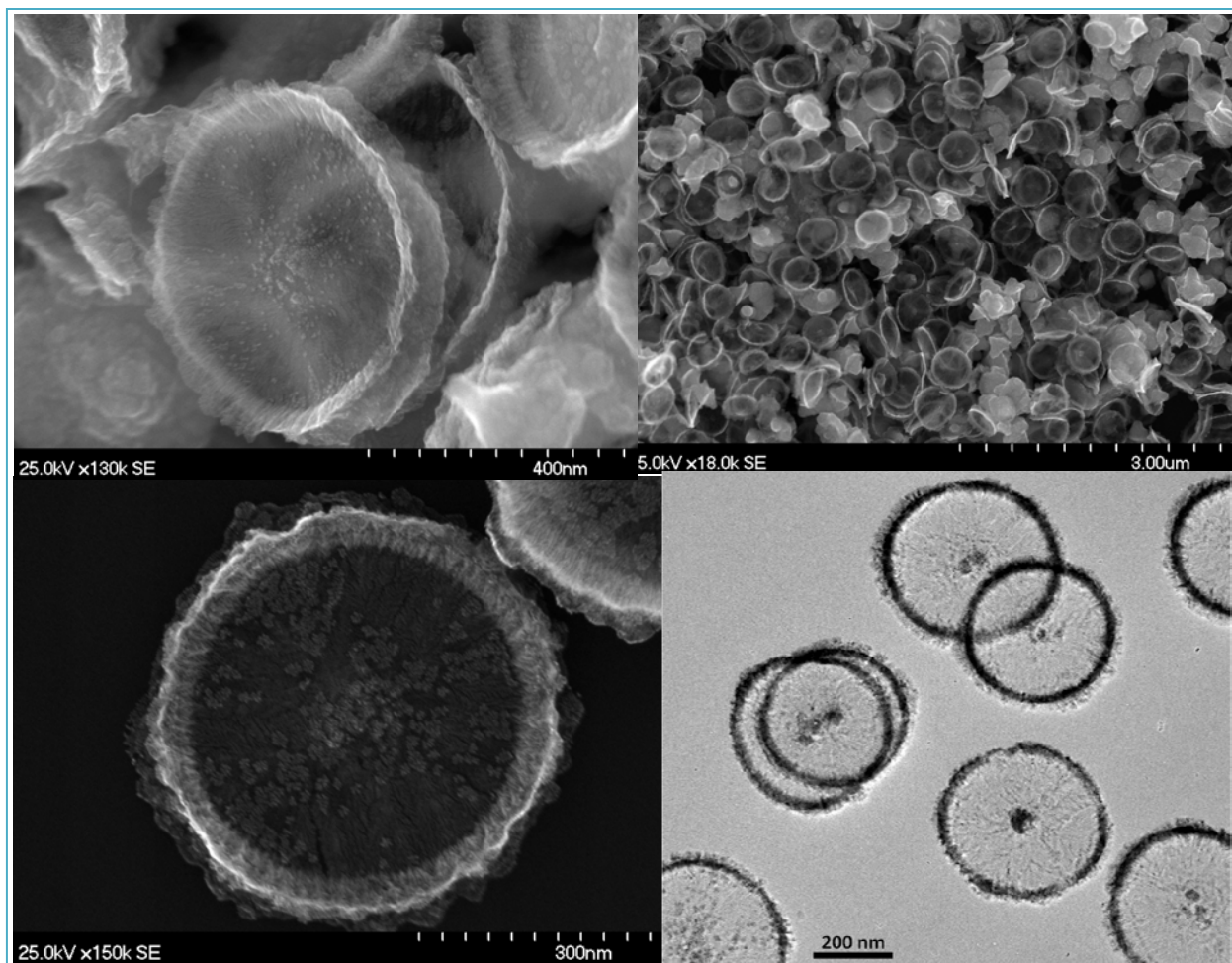


**Fig 3.** SEM images of platinum nano-coins produced by dendritic growth of metal with lipid bicelles composed of the two surfactants shown in Fig. 4.

dendritic metal growth in these lipid assemblies. Using lipid bicelles as templates for dendritic platinum growth, we produced the wheel-shaped nano-coins shown in the scanning electron microscopy (SEM) and transmission electron microscopy (TEM) images of Fig. 3. The lipids and reactants used to synthesize the Pt nano-coins are illustrated in Fig. 4.

The stacking of bicelle disks was also investigated by Monte Carlo simulation of hard circular cylinders. Simulations at various packing fractions (not shown), demonstrate the oriented ordering characteristic of hard coins. Hard coins do not overlap and have no short-range and no long-range interactions. The simulations provide an understanding of the super-stacks of Pt coins and bicelles and verify that interaction between bicelles must play a role in their stacking.

TEM studies and Monte Carlo simulations of

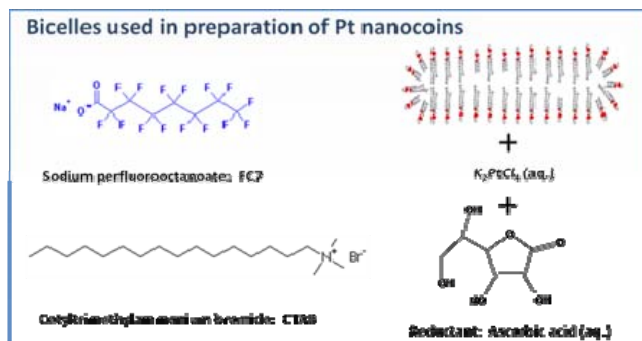


**Fig 4.** Surfactants and reactants used in producing the platinum nano-coins by dendritic growth of metal with lipid bicelles composed of the two surfactants shown.

the sintering process of platinum dendritic nanosheets demonstrate the formation of persistent nanopores during sintering and the formation of sintering-resistant holey sheets (Fig. 5). This study illustrates one of the unique properties of these new bionanomaterials, which is of particular importance for catalysis. The nanopores form quickly and their diameters is close to a critical value related to the sheet thickness at which they persist for long times during sintering. In the present case, the persistent pores also form in the thinnest possible Pt sheet (2-3 nm) to give the highest surface area possible in a sintering-resistant holey sheet morphology.

In conclusion, lipid bicelles have successfully used as soft-templates for the first time for the growth of dendritic platinum nano-coins. The lipid stacks of bicelles were prepared via chemical recognition and these will be platinized to form nanoscale Pt nano-coin stacks. Monte Carlo simulations aid in understanding for the assembly and organization of both the Pt coins and the lipid stacks. In addition, *in situ* TEM studies and Monte Carlos simulations of the dendritic Pt nanosheets show that they for holey nanosheets that are resistant to further sintering, indicating that the Pt nano-coins may also have similar sintering-resistant properties due to their similar dendritic and sheet-like structural features.

Sandia is a multiprogram laboratory operated by Sandia Corporation, a Lockheed Martin Company, for the United States Department of Energy's National Nuclear Security Administration under Contract DEAC04-94AL85000.

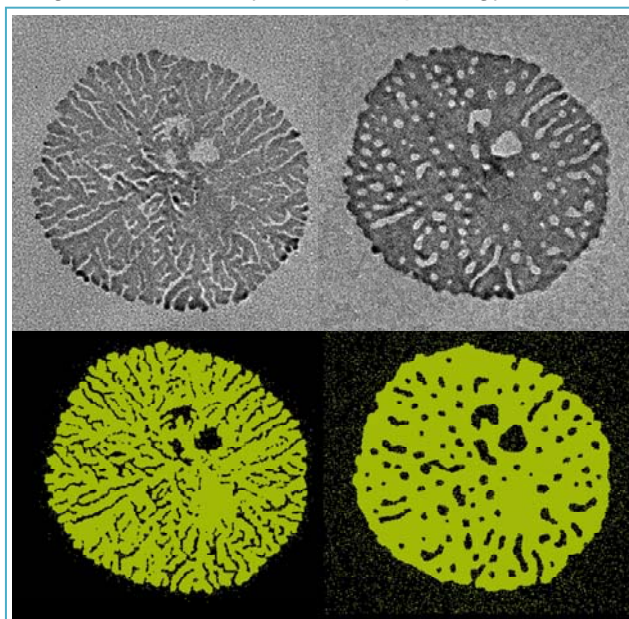


**Fig 5.** Sintering of Pt dendritic sheets like that forming the 'spokes' of the platinum nano-coins in the electron beam for 0 and 40 minutes (top) and Monte Carlo simulations of the sintering process showing the conversion of the dendrites to the sintering-resistant holey nanosheet.

## References and Selected Recent Publications

1. *Synthesis of Platinum Nanocages Using Liposomes Containing Photocatalyst Molecules*, Song, Y. J.; Garcia, R. M.; Dorin, R. M.; Wang, H. R.; Qiu, Y.; Shelnutt, J. A., *Angew. Chem. Int. Ed.* 2006, 45, 8126-8130.
2. *Controlled Synthesis of 2-D and 3-D Dendritic Platinum Nanostructures*, Y. J. Song, Y. Yang, C. J. Medforth, E. Pereira, A. K. Singh, H. F. Xu, Y. B. Jiang, J. Brinker, F. van Swol, J. A. Shelnutt, *J. Am. Chem. Soc.* 2004, 126, 635-645.
3. *Foamlike Nanostructures Created from Dendritic Platinum Sheets on Liposomes*, Song, Y.; Steen, W. A.; Peña, D.; Jiang, Y.-B.; Medforth, C. J.; Huo, Q.; Pincus, J. L.; Qiu, Y.; Sasaki, D. Y.; Miller, J. E.; Shelnutt, J. A., *Chem. Mater.* 2006, 18, 2335-2346.
4. *Platinum Nanodendrites*, Song, Y.; Jiang, Y.-B.; Wang, H.; Pena, D. A.; Qiu, Y.; Miller, J. E.; Shelnutt, J. A., *Nanotechnology* 2006, 17, 1300-1308.
5. *Interfacial Synthesis of Dendritic Platinum Nanoshells Templated on Benzene Nanodroplets Stabilized in Water by a Photocatalytic Lipoporphyrin*, Wang, H.; Song, Y.; Medforth, C. J.; Shelnutt, J. A., *J. Am. Chem. Soc.* 2006, 128, 9284-9285.
6. *Self-assembled Columns of Stacked Lipid Bilayers Mediated by Metal Ion Recognition*, Waggoner, T. A.; Last, J. A.; Kotula, P. G.; Sasaki, D. Y., *J. Am. Chem. Soc.* 2001, 123, 496 - 497.
7. *Selective Fluorescence Detection of Divalent and Trivalent Metal Ions with Functionalized Lipid Membranes*, Pincus, J. L.; Jin, C.; Huang, W.; Jacobs, H. K.; Gopalan, A. S.; Song, Y.; Shelnutt, J. A.; Sasaki, D. Y., *J. Mater. Chem.* 2005, 15, 2938-2945.

# Artificial Microtubule Organizing Centers: Reconstructing Natural Architectures

Erik D. Spoerke, Andrew K. Boal, George D. Bachand, Ann Bouchard,  
Gordon Osbourn, and Bruce C. Bunker

Bio-Integration Program (Active Assembly of Dynamic and Adaptable Materials)  
Sandia National Laboratories, P.O. Box 5800, MS 1411, Albuquerque, NM, 87185-1411  
Author: [edspoer@sandia.gov](mailto:edspoer@sandia.gov), PI: [bcbunke@sandia.gov](mailto:bcbunke@sandia.gov)

Sandia is a multiprogram laboratory operated by Sandia Corporation, a Lockheed Martin Company, for the United States Department of Energy's National Nuclear Security Administration under Contract DE-AC04-94AL85000.

## Program Scope

The Bio-Integration project focuses on materials science issues critical to the intersection of biology, nanomaterials, and integrated systems. One key focus within the program is on the active assembly of dynamic and adaptable materials. Working specifically with energy-consuming proteins such as tubulin and motor proteins, we aim to understand how these biological tools drive biological organization and assembly while seeking to exploit these biological concepts and agents to develop unique synthetic nanomaterials assembly strategies. In the present work, this objective will be discussed in the context of artificially recreating biological architectures known as microtubule organizing centers (MOCs).

Microtubules (MTs) are polymeric protein filaments that, along with intermediate filaments and actin compose the cytoskeleton of eukaryotic cells.<sup>1, 2</sup> Hollow cylinders, roughly 25 nm in diameter and microns long, MTs are polymerized from dimers of  $\alpha$  and  $\beta$ -tubulin. This polymerization produces MTs whose ends terminated with either  $\alpha$ -tubulin (the "minus" end) or  $\beta$ -tubulin (the "plus" end), resulting in a biochemical polarity of the MTs. The polar nature of these bio-supramolecular assemblies enables them to perform a number of critical, orientation-dependent functions in the cell, ranging from chromosome separation during cell division to directing motor-protein based cargo trafficking within the cell. In order to effectively perform these complex tasks, however, the MTs are carefully organized to form microtubule organizing centers. These MOCs, commonly known as centrosomes in mammalian cells, are sophisticated, aster-like constructs of microtubules. We have recently demonstrated several methods to assemble artificial organizing centers, and predictively modeled the behavioral interactions between such organizing centers and motor protein cargo transporters.

## Recent Progress

### *MOC Assembly using Microtubule Associated Proteins (MAPs)*

Microtubule associated proteins are a collection of proteins that bind to the exterior of MTs and serve to stabilize the MTs and negotiate interactions of the MTs with other structures and agents within the cell.<sup>3, 4</sup> We have developed an assembly approach in which MAPs are used to bind MTs to functionalized microspheres. By covalently linking the MAPs to the microspheres, we impart a strong MT-binding functionality to the spheres. When tubulin is then polymerized in the presence of these functionalized particles, the growing MTs have a strong affinity for the spheres, nucleating and growing densely around the particles. In addition, the MAPs serve to



stabilize the MTs grown around the synthetic microspheres. The resulting aster-like structures (figure 1) are three-dimensional assemblies of MTs, organized around a synthetic particle.

In this stabilizing environment, the length of the polymerizing MTs can be controlled by the adjusting duration of polymerization. Short polymerization times produce MTs only a few microns long, while polymerization of 30 minutes or more may produce MTs tens of microns in length. In addition, these artificial assemblies demonstrate a key trait of natural systems in that they can be recycled. MTs in natural MOCs can be polymerized and depolymerized (a process known as dynamic instability) to accommodate changing organizational requirements within a living cell. In our synthetic system, we take advantage of MT instability at low temperatures to disassemble these artificial organizing centers. By properly cycling the MOC solution temperature, it is possible to disassemble and subsequently reconstitute these MAP-based MOCs.

This approach to artificial microtubule organization enables us to produce dense, dynamic, three-dimensional MT asters, which may serve as biochemical templates for non-biological materials growth, mesogens for subsequent levels of dynamic materials assembly, or platforms for the study of MTs properties such as dynamic instability.

#### *Assembly of Polar Oriented Synthetic Microtubule Organizing Centers (POSMOCs)*

The MAP-based assembly of MOCs described above provides dense aster-like structures, but the polar orientation of MTs on these structures is not directed. We have developed an alternative approach to aster formation that enables us to control the polar orientation of the MTs as they assemble into aster form. The key to forming these polar oriented synthetic microtubule organizing centers (POSMOCs) lies in the formation of functionally-segmented microtubules. In a controlled, multi-step polymerization process, we create MTs whose “plus” and “minus” ends are chemically distinct from one-another. These hybrid MTs are created by first ensuring that polymerization of the MTs predominantly occurs in the “plus” direction.<sup>5</sup> We can then take advantage of the concentration-dependent nature of tubulin polymerization to either “homogeneously” nucleate MT “seeds” or “heterogeneously” grow functionalized regions of the MTs.<sup>6</sup> In this way, we can produce MTs where only the “plus” end would contain tubulin functionalized with biotin, for example.

When such partially-biotinylated MTs are introduced to streptavidin-coated microspheres, only the functionalized “plus” ends of the MTs bind to the microspheres. The resulting aster assemblies are consequently organized such that MTs bound within this organizing center are all oriented with the “plus” end directed centrally. This straightforward approach can also be reversed to produce asters where the “minus” end is directed centrally, simply by reversing the order in which the biotinylated tubulin is introduced in the polymerization process. This assembly strategy not only enables us to produce these organizing centers, but also demonstrates one of the uniquely valuable traits of MTs as supramolecular constructs. Among synthetic or natural supramolecular

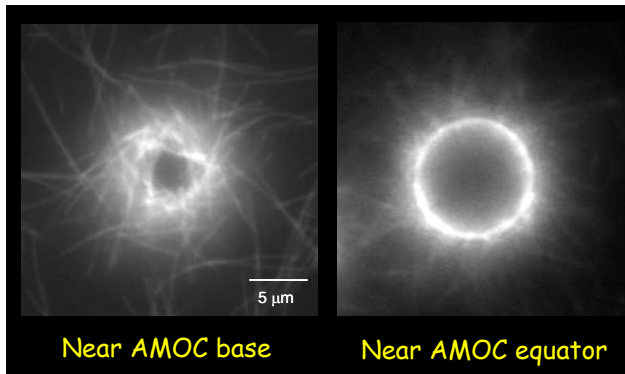


**Figure 1:** Planar fluorescence images of a 3-dimensional artificial microtubule aster, formed around a functionalized microsphere. Images from the base and the equator of the particle show the 3-dimensional nature of MT organization.

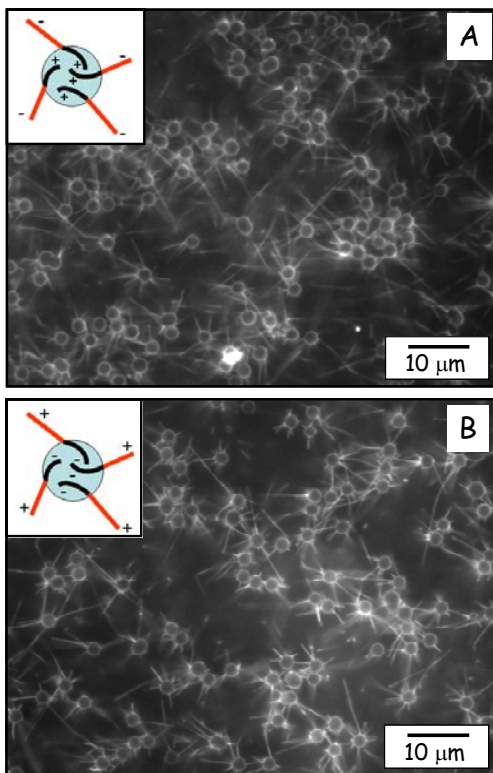


**Figure 2:** Fluorescence images of POSMOCs assembled with MT plus ends directed “in” (A) or “out” (B).

model capable of simulating processes such as dynamic instability, motor protein-binding to microtubules, and the motor-protein based transport of cargo on MOCs. These simulations have helped us understand how these biological agents may be able to sort, organize, and transport cargo. For example the simulation summarized in figure 3 illustrates how activating or deactivating cargo-carrying motor proteins on a model POSMOC can simulate the concentration or dispersion of cargo. The results of this simulation indicate that this designed process resembles, at least phenomenologically, processes that produce the color changing effect in some amphibians and fish.<sup>10</sup> In other cases, where MT dynamic instability was added to the model, these active systems were shown to effectively perform functions such as particle sorting. These models have provided valuable predictive insight into how our synthetic designs may behave in complex scenarios involving multiple interactive agents.

assemblies, few systems display an inherent, functional polarity. In our approach, we demonstrate not only that the inherently polar MTs can be synthetically assembled, but also that we can control the orientation of this polarity when organizing the MTs. Understanding this system and how it can be employed may have tremendous implications for future efforts advancing supramolecular chemistry.

### *Simulations of Motor Protein Cargo Transport on Organizing Centers*

Computer simulations are widely utilized as tools to predict the behavior of cellular processes and interactions between biological agents.<sup>7</sup> We have utilized stochastic, agent-based simulations<sup>8</sup> to predict how cargo-laden motor proteins may be able to direct materials organization on MOCs such as those synthesized above.<sup>9</sup>

The kinetics of component interactions (largely protein-protein interactions) are modeled to be consistent with the statistical and temporal properties observed experimentally. By breaking down each interaction into a series of “events,” it is possible to construct a dynamic

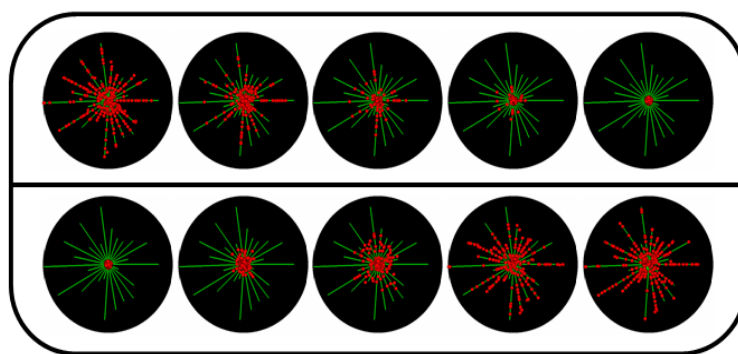


**Figure 3:** Image series (left to right) from a simulation of motor protein-based cargo (red) concentration (top) and dispersion (bottom) on a POSMOC-like structure (green MTs). Top: Cargo decorated with both fast outward-walking motors and slow inward-walking motors. Initially, both motors are “on” creating dispersed cargo. When the fast motor is turned “off” the inward-walking motors concentrate the cargo. Bottom: After concentrating cargo, the fast, outward-walking motors are turned back “on,” resulting in rapid dispersion of the of the cargo.

## Future Plans

Our research focus on microtubule assembly will take us forward in a number of new directions. One area of interest will involve integrating the two types of organizing centers described here to create polar organized systems that will demonstrate the dynamic character of the MAP-assembled MOCs. In addition, we will explore the incorporation of motor protein-based cargo transport on these organized superstructures. The ability to direct active cargo transport using these engineered architectures would represent a significant advance in bio-mediated materials assembly. In addition, the computer modeling described above predicts that the phenomenological cargo-organizing behavior that emerges from the integration of motor proteins with dynamic, polar assemblies will be a rich area of active materials research.

## References

1. Holy, T.; Dogterom, M.; Yurke, B.; Leibler, S., Assembly and positioning of microtubule asters in microfabricated chambers. *Proc. Natl. Acad. Sci. USA* **1997**, 94, 6228-6231.
2. Lodish, H.; Berk, A.; Zipursky, S.; Matsudaira, P.; Baltimore, D.; Darnell, J., Cell Motility and Shape II: Microtubules and Intermediate Filaments. In *Molecular Cell Biology*, 4th ed.; W.H. Freeman and Co.: New York, NY, 1999; pp 795-836.
3. Al-Bassam, J.; Ozer, R. S.; Safer, D.; Halpain, S.; Milligan, R., MAP2 and tau bind longitudinally along the outer ridges of microtubule protofilaments. *J Cell Biol* **2002**, 157, (7), 1187-1196.
4. Cleveland, D. W.; Hwo, S. Y.; Kirschner, M., Purification of Tau, a microtubule-associated protein that induces assembly of microtubules from purified tubulin. *J Mol Biol* **1977**, 116, (2), 207-225.
5. Phelps, K.; Walker, R., NEM Tubulin Inhibits Microtubule Minus End Assembly by a Reversible Capping Mechanism. *Biochem* **2000**, 39, 3877-3885.
6. Fygenson, D.; Braun, E.; Libchaber, A., Phase diagram of microtubules. *Phys. Rev. E* **1994**, 50, (2), 1579-1588.
7. Endy, D.; Brent, R., Modeling cellular behaviour. *Nature* **2001**, 409, 391.
8. Gillespie, D. T., A general method for numerically simulating the stochastic time evolution of coupled chemical reactions. *J Comput Phys* **1976**, 22, 403.
9. Bouchard, A. M.; Warrender, C. E.; Osbourn, G. C., Harnessing Microtubule Dynamic Instability for Nanostructure Assembly. *Phys. Rev. E* **2006**, 74, 041902.
10. Haimo, L.; Thaler, C., Regulation of organelle transport - Lessons from color-change in fish. *BioEssays* **1994**, 16, (10), 727-733.

## Recent BES-Sponsored Publications (2005-2007)

- S.B. Rivera, S.J. Koch, J.M. Bauer, J.M. Edwards, and G.D. Bachand. "Temperature dependent properties of a kinesin-3 motor protein from *Thermomyces lanuginosus*." *Fungal Genetics and Biology*. **in press**, [doi:10.1016/j.fgb.2007.02.004](https://doi.org/10.1016/j.fgb.2007.02.004)
- A.K. Boal, H. Tellez, S.B. Rivera, N. Miller, G.D. Bachand, and B.C. Bunker. "The stability and functionality of chemically crosslinked microtubules." *Small*. **2**, 793- 803 (2006).
- A.K. Boal, G.D. Bachand, S.B. Rivera, and B.C. Bunker. "Interactions between cargo- carrying biomolecular shuttles." *Nanotechnology*. **17**, 349-354 (2006).
- A.M. Bouchard, C.E. Warrender, and G.C. Osbourn. "Harnessing Microtubule Dynamic Instability for Nanostructure Assembly." *Phys Rev E*, **74**, 041902 (2006)
- M. Bachand, A.M. Trent, B.C. Bunker, and G.D. Bachand. "Physical factors affecting kinesin-based transport of synthetic nanoparticle cargo." *J Nanosci. Nanotech.* **5**, 718-722 (2005).
- H. Hess and G.D. Bachand. "Biomolecular Motors to Power Nanotechnology." *Materials Today*, **8**, 22 (2005)

***UNIVERSITY GRANT  
PROJECTS***

# Structure-Property Relationships of Polymer Brushes in Restricted Geometries and their Utilization as Ultra-Low Friction Lubricants

PI: Tonya Kuhl  
University of California, Davis  
Department of Chemical Engineering and Materials Science  
One Shields Avenue  
Davis, CA 95616  
tkuhl@ucdavis.edu

## Program Scope or Definition:

Though polymer films are widely used to modify or tailor the physical, chemical and mechanical properties of interfaces in both solid and liquid systems, the rational design of interface- or surface-active polymer modifiers has been hampered by a lack of information about the behavior and structure-property relationships of this class of molecules. This is especially true for systems in which the role of the polymer is to modify the interaction between two solid surfaces in intimate contact and under load, to cause them to be mechanically coupled (e.g. to promote adhesion and wetting) or to minimize their interaction (e.g. lubrication, colloidal stabilization, etc.). Detailed structural information on these systems has largely been precluded by the many difficulties and challenges associated with direct experimental measurements of polymer structure in these geometries. As a result, many experimenters have been forced to employ indirect measurements or rely wholly on computer simulation. This has resulted in an incomplete understanding of the structure-property relationships, which are relied upon for the rational design of improved polymer modifiers.

We have recently demonstrated that we can overcome many of these difficulties using a newly developed instrument that permits direct measurements of the structure of polymers at the interface between two solid surfaces under confinement (load) and shear. This instrument, which we refer to as the Neutron Confinement Shear Cell (NCSC), employs a specularly reflected neutron beam to non-destructively probe the polymer structure with sub-nanometer resolution (Fig. 1). We will show preliminary experimental results that demonstrate the capability of the NCSC under shear as well as more complete characterization of the structure of polymer brushes as a function of confinement. In tandem with these experimental studies, we are carrying out complementary computer simulations – atomistic and course grained. The atomistic simulations allow us to

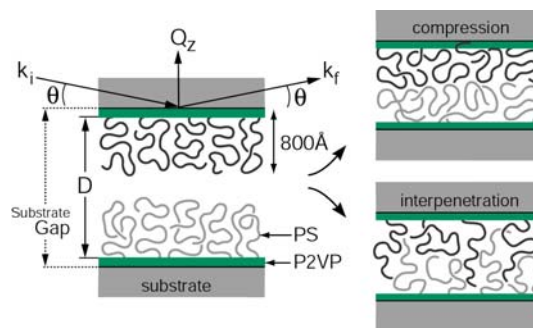


**Fig. 1.** (Left) Geometry of the neutron reflectivity measurements and experimental system. (Right) two structural rearrangements of grafted polymer brush layers in contact, illustrating brush compression and brush interpenetration.

develop models and force fields that accurately reflect the true experimental system, while the course grained simulations allow us to access more realistic polymer lengths and time scales. By combining these novel tools, we will be able to obtain a higher level of information and predictive capabilities that will provide the basis for the rational design of new materials.

### Recent Progress:

Over the past year, we have been investigating and characterizing the structure of high density polymer brushes under good and theta solvent conditions. To create high density polymer brushes amenable for experimental confinement studies, we used 50:50 diblocks of polystyrene-poly-2-vinylpyridine (PS-P2VP) (28). The polystyrene portion of the diblock was either hydrogenated (hPS, MW 122k) or deuterated (dPS, MW 136k)<sup>1</sup>. The films were deposited on silicon and sapphire substrates by spin coating and annealed. The P2VP layer prefers to wet the substrates while the PS segregates to the air interface. The polymer layers were first characterized in the dry state. Typically films of 250-300Å were used. In a selective solvent, the P2VP block anchors the chain to the substrate while the PS extends away from the interface into the solution. For polymer brushes of moderate grafting density both theory and simulations predict a parabolic density profile away from the surface in good solvent (Eq 1, n=2). With increasing grafting density, the profile is predicted to flatten and follow a higher order power law, (n>2),

$$\phi(z) = \phi_0 \left( 1 - \left( \frac{z}{h_0} \right)^n \right) \quad \text{Eq 1}$$

where  $\phi_0$  is the volume fraction of the brush at the interface and  $h_0$  is the unconfined, equilibrium extension of the brush perpendicular to the interface. Surprisingly, even for very high grafting coverages, here up to 29 times the overlap concentration,  $\sigma^*$ , the unconfined brush density profile was parabolic.

The effect of confinement and compression of two opposing PS polymer brushes was then investigated using the Neutron Confinement and Shear Cell (NCSC). The NCSC allows control of the surface separation and parallel alignment of the substrates under applied loads – with *in situ* structural characterization of the intervening material via neutron reflectivity measurements (Fig. 1)<sup>2</sup>. Fig. 2A shows the neutron reflectivity profile for opposing, symmetric, deuterated PS brushes for three different levels of confinement. The low  $Q_z$  oscillations in the reflectivity profile correspond to the substrate gap spacing (Fig 1,  $D \approx 1000, 960, \text{ and } 930\text{\AA}$ ). For these separations, the confinement of the brushes is significant and can be described in terms of a reduced separation,  $\tilde{u} = D/2h_0 \cong 0.6$ .

The best fit to the reflectivity data are the solid curves in Fig 2A. Robust fits were obtained by simultaneously modeling all three curves. In each case, the quality of fit was very good with  $\chi^2 < 3$ . To obtain the polymer brush density distribution, the SLD profiles (Fig 2B) were converted to volume fraction

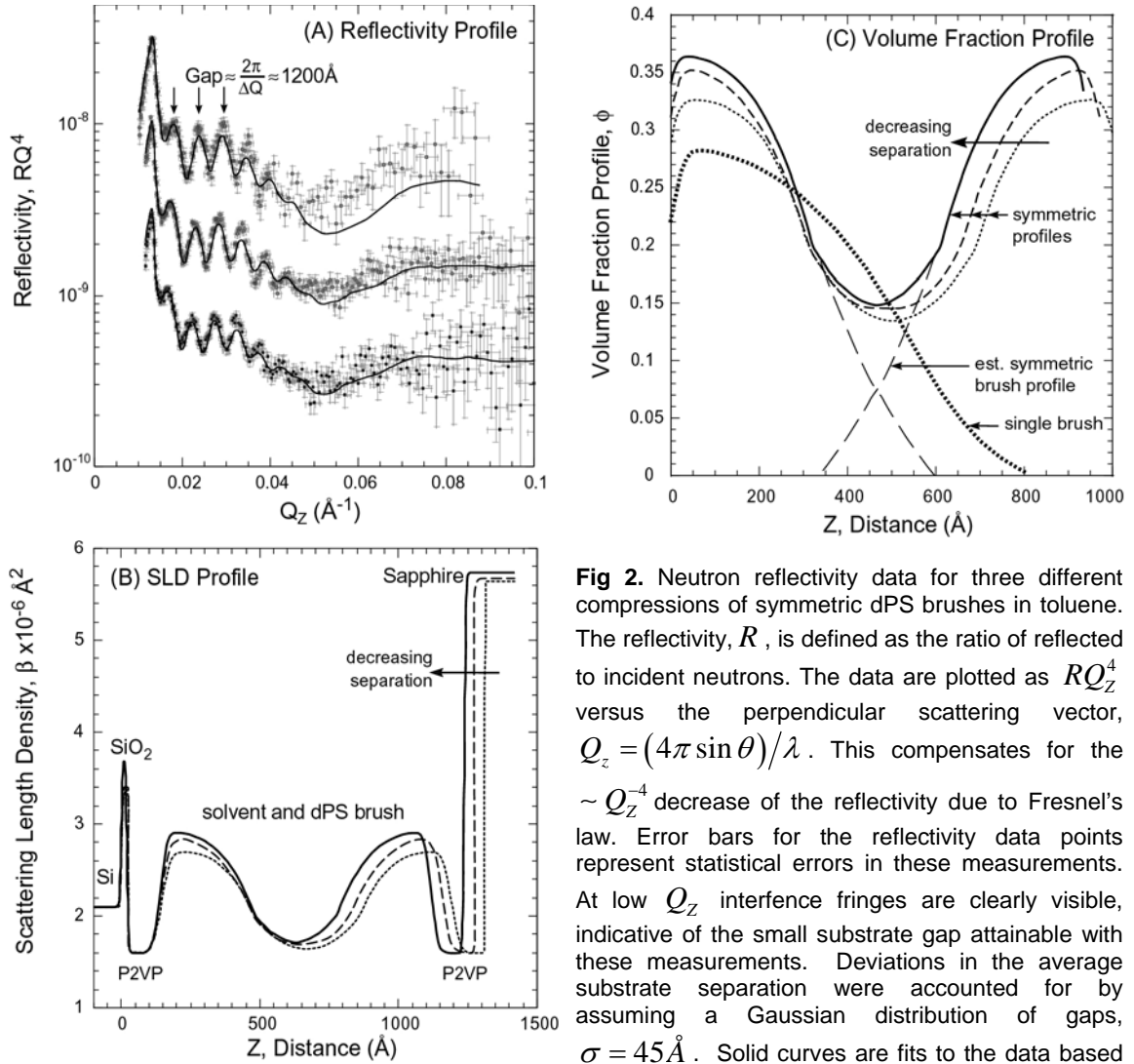


**Fig 2.** Neutron reflectivity data for three different compressions of symmetric dPS brushes in toluene. The reflectivity,  $R$ , is defined as the ratio of reflected to incident neutrons. The data are plotted as  $RQ_Z^4$  versus the perpendicular scattering vector,  $Q_Z = (4\pi \sin \theta)/\lambda$ . This compensates for the  $\sim Q_Z^{-4}$  decrease of the reflectivity due to Fresnel's law. Error bars for the reflectivity data points represent statistical errors in these measurements. At low  $Q_Z$  interference fringes are clearly visible, indicative of the small substrate gap attainable with these measurements. Deviations in the average substrate separation were accounted for by assuming a Gaussian distribution of gaps,  $\sigma = 45 \text{ \AA}$ . Solid curves are fits to the data based on the scattering length density (SLD) profiles shown in (B). (C) The corresponding volume fraction profiles for the three compressions. The long dashed lines are estimated extensions of the individual brushes. The heavy dotted line is the measured profile for an unconfined brush at a single surface.

profiles using  $SLD_{fitted} = \phi_{PS}(SLD_{PS}) + (1 - \phi_{PS})SLD_{toluene}$  (Fig 2C). Notably, the PS volume fraction at the interface remains higher than that of the gap and *increases* as the brushes are compressed. Clearly, squeezing two opposing brushes causes the density of the brush at the anchor interface to increase continuously as a function of confinement. The profile remained parabolic ( $n_1=2\pm 0.1$ ) and only modest changes in concentration at the midpoint between the brushes were observed. In contrast to these experimental findings, previous theory and simulations have predicted that the density profile will flatten at the midpoint before increasing at the anchor interface<sup>3-5</sup> and dramatically demonstrate the need for continued simulations that more accurately model a real experimental system. The difference between

the experiments and previous theoretical work suggests that the PS brushes compress against the anchor surface with confinement resulting in less interpenetration. The interpenetration was estimated by extrapolating the brush profile yielding 3.8% for  $D=930\text{\AA}$ . For comparison, the measured profile of a brush at a single interface (no confinement) is shown (Fig 2C).

Experiments on asymmetric brushes -with one side dPS and the other side hPS- provide contrast to determine extension and interpenetration of the brushes under confinement. A summary of recent measurements with various contrasts will be highlighted.

On the simulation side, the focus over the past year has been to establish the simulation method to model PS brushes of variable grafting density in solvents of varying quality. A key goal is to map as closely as possible to the experimental system. Preliminary atomistic studies are highlighted in a poster presented by Dr. Petra Traskelin.

#### **Future Plans:**

We have been developing "grafting-from" procedures based on Atom Transfer Radical Polymerization (ATRP) to grow PS brushes directly from our substrates<sup>7</sup>. Importantly ATRP formed brushes have been found to have much better lubrication properties compared to brushes formed by "grafted-to" approaches including lower friction coefficients and increased wear resistance. These enhanced properties have been attributed to the extremely high grafting density and strong anchoring of ATRP grown layers. However, the structure of solvated ATRP brushes has not been extensively studied. Most of the current structural information on ATRP films has come from ellipsometry and atomic force microscopy. While these techniques are useful for estimating total thicknesses, they do not provide a detailed structural profile. We have begun extensive studies on characterizing PS brushes grown via ATRP and are particularly keen to continue with these studies as they map onto our synergistic simulation work more directly than the PS-PVP diblock studies.

#### **Publications sponsored by this grant:**

Laub, C. F. and Kuhl, T.L. "Fitting a free-form scattering length density profile to reflectivity data using temperature-proportional quenching," *J. Chem. Phys.* 125:244702 (8pgs) (Dec. 28, 2006).

#### **References:**

1. R. Levicky, N. Koneripalli, M. Tirrell, S. K. Satija, *Macromolecules* **31**, 3731-3734 (1998).
2. T. L. Kuhl, G. S. Smith, J. N. Israelachvili, J. Majewski, W. Hamilton, *Review of Scientific Instruments* **72**, 1715-1720 (2001).
3. G. S. Grest, *Polymers in Confined Environments* **138**, 149-183 (1999).
4. J. I. Martin, Z. G. Wang, *Journal of Physical Chemistry* **99**, 2833-2844 (1995).
5. I. M. Neelov, O. V. Borisov, K. Binder, *Journal of Chemical Physics* **108**, 6973-6988 (1998).
6. M. D. Whimore and R. Baranowski, *Macromolecular Theory and Simulations* **14**, 75-95 (2005).
7. K. Matyjaszewski, P. Miller, N. Shukla, B. Immaraporn, A. Gelman, B. Luokala, T. Siclovan, G. Kickelbick, T. Vallant, H. Hoffmann, T. Pakula, *Macromolecules* **32**: 8716-8724 (1999).



## Dynamic Self-Assembly: Functional Reorganizations in Biomembranes

Atul N. Parikh and Sunil K. Sinha, University of California, Davis and San Diego, CA

[anparikh@ucdavis.edu](mailto:anparikh@ucdavis.edu), [ssinha@physics.ucsd.edu](mailto:ssinha@physics.ucsd.edu)

**Program Scope** This program seeks to explore dynamical self-assembly processes within the quasi-two dimensional, fluid phospholipid membrane media. Of particular interest to this program are biologically important reactive-diffusive processes including (1) spreading dynamics of lipids at surfaces; (2) lipid-lipid mixing and phase separation such as occurs in lipid rafts; (3) dynamic reorganizations of phase separated lipid mixtures following a biologically relevant chemistry (e.g., selective lipid oxidation); (4) membrane dynamics following extraneous physical interactions (e.g., adhesion and fusion); (5) curvature-mediated dynamics; (6) membrane receptor-clustering and pattern formation following a protein recognition or a binding event; and (7) protein-protein clustering mediated by the intrinsic lateral mobilities of membrane lipids. Our strategy involves the design of simple membrane models suitable for such studies and their implementation using biomimetic systems to generate fundamental design rules that can be used to synthesize novel materials based on biologically inspired principles of dynamic self-assembly.

**Recent Progress.** Over the past two years (2005-2007), we have been advancing along all major fronts. Earlier, during the first year of the grant, we developed a variety of model membrane configurations, developed characterization tools, and began investigating dynamic processes induced by a variety of external stimuli and recognition events. An overview of opportunities and challenges associated with the development of a materials science based understanding of lipid membranes was recently provided in a recent guest editorial (Parikh & Groves, MRS Bulletin, 2006). Key accomplishments were described in a series of publications (and several in preparations). Below, we highlight some of our key recent achievements.

An essential property of lipid bilayers which allows for dynamic reorganizations is the lateral and transverse mobility of lipids and proteins comprising the bilayer. It is well appreciated that that these lipids and proteins display a broad variation in molecular diffusivities, determined by membrane heterogeneities (e.g., proteins, multiprotein aggregates, and cytoskeleton-binding proteins) and membrane compartmentalization. Moreover, these heterogeneities (and compartments) themselves rearrange further complicating molecular mobilities within membranes. How the presence, distributions, and dynamics of diffusional barriers influence Brownian motions of lipids and proteins, however, remains poorly understood. To systematically study these processes, we have developed a variety of tools to engineer diffusion barriers within supported bilayers. Briefly, we have demonstrated that spatially defined illumination of supported bilayers using short-wavelength ultraviolet (or near-infrared multiphoton absorptions) allows for membrane compartmentalization and the creation of pre-determined geometries of diffusional barriers. We have also shown that these barrier regions can be conveniently healed by thermal effects. Together these tools allow for dynamic recompartimentalization at the timescales comparable to diffusional timescales for lipids and proteins. *These abilities to (dynamically) alter molecular motions in membranes provide new synthetic material constructs to engineer diffusional motions and may provide new routes for sorting, separating and chasing biomolecules.*

The membrane lithography methods developed above provide diffusional barriers which can be backfilled thus providing a simple means to study *compositional dynamics* and lipid-lipid intermixing. These secondary intercalants selectively fuse within the barrier regions and become contiguous with the existing membrane. When the secondary intercalants are lipids of comparable structure and fluidity to those of the primary matrix, they erase patterns by thermal mixing or Brownian dynamics. On the other hand, the introduction of liquid-ordered or gel phase lipids or their mixtures lead to phase-separated, metastable membrane environments stable for several hours. The stability or lifetime of these metastable domains appears to be determined by the size of the imposed phase-separation and the nature and extent of disparity (e.g., fluidity, transition temperatures, charge differences, etc) between the juxtaposed membrane phases. Using these approaches, we demonstrated the ability to engineer patterns of

cholesterol-rich (raft-like) membrane heterogeneities for localization of raft-dependent membrane functions. Additional studies employing these compositional micro-arrays in parallel experiments are currently underway to develop elemental phase diagrams for binary and ternary lipid mixtures in supported bilayer configurations.

Toward developing useful model systems for studies of *membrane dynamics associated physical curvatures*, we developed a new class of supported bilayers which exhibit pre-determined (and in one case switchable) patterns of 1D and 2D curvatures. Using well-ordered, self-assembled colloidal crystal substrates (colloidal dimensions 100-500 nm), we demonstrated the formation of compliant lipid bilayers provide a unique opportunity to impose tunable curvatures (Gaussian) onto lipid bilayers thereby allowing for a study of curvature-induced dynamic reorganizations within bilayer membranes. Because colloidal crystals offer unique photonic properties, they afford new opportunities to integrate functions associated with lipid membranes with optical properties of the substrates. More recently, we demonstrated that surface wrinkling of polymeric and elastomeric surfaces provide novel classes of substrates dynamically impose and remove one-dimensional curvatures on fluid membranes. These studies are being vigorously pursued toward future accomplishments (See below).

These platform systems were also used to decipher how membrane organizations are perturbed while responding to *external stimuli* inducing functional reorganizations within bilayers. In particular, we studied (1) how selective oxidation of sphingolipids perturbs the cholesterol-rich sphingolipid domains; (2) how adhesion of beads (and nanoparticles) gives rise to mechanical and chemical reorganizations within lipid bilayers; and (3) how local protein-binding processes induces large-scale, highly amplified phase-change in lipid bilayers.

*In the middle of the second year of this grant (Oct. 2005)*, we launched a collaboration with Prof. Sunil Sinha (UCSD) (now a co-investigator) to initiate a complementary set of neutron (LANSCE) and x-ray (APS) scattering based structural studies to characterize membrane heterogeneities organized below the diffraction limit of visible light. It is now well-established that neutron and X-ray specular reflectivity of single (or multi-) bilayers supported on a smooth flat substrate such as silicon can be used to determine, with high z-resolution (angstrom scale), the profile of the molecular density normal to the plane of the membrane, including the thin cushioning water layer between the substrate and the membrane. These studies are being elaborated to focus on membrane undulations and compositional fluctuations which result due to imposition of curvatures, for example, using X-ray photocorrelation spectroscopy.

**Future Plans.** Our future activities will build on the accomplishments highlighted above. In particular, we will focus our primary activities on addressing curvature-related physical and compositional dynamics within membranes. We have recently shown that single supported phospholipid bilayers form at the interfaces between deformable, oxidized PDMS elastomers and aqueous phases, and are coupled to the substrate topography. Real-time variations in substrate topography trigger spatially patterned mesoscale reorganization of the bilayer accompanied by curvature-dependent molecular reorganization. This ability to dynamically impose curvatures on supported bilayers and their attendant re-equilibration promises fundamental studies of a range of curvature-induced dynamic reorganization and its functional consequences in a massively parallel fashion. Because patterns of curvatures can stabilize heterogeneous distribution of molecules within fluid membranes, these model membranes provide a generic means to create sustained molecular gradients and carry out spatial separation of membrane-compatible amphiphiles of varying intrinsic molecular curvatures. Key questions we will investigate include:

*Deciphering relations between membrane curvature, molecular shapes, and their effects on phase separation and dynamics of multicomponent fluid supported bilayers at structured surfaces:*

1. determine the relations between induced membrane curvatures, molecular shapes, and curvature-dependent phase separations in lipid bilayer membranes;
2. explore how switchable surface curvatures dynamically reorganize membrane phases and domains in lipid bilayers;

3. Characterize the role of induced membrane curvatures on membrane dynamics and fluctuations using x-ray and fluorescence techniques. From the technique development point of view, this will require developing X-ray photoelectron correlation spectroscopy for applications in interfacial membrane configurations.

*Characterization of the structurally and compositionally distinct dynamic self-assemblies (or micro-heterogeneities) and their mesoscale ordering within fluid phospholipids bilayers at chemically and topographically structured (including curved) surfaces:*

4. Study non-equilibrium and kinetic traps in the equilibration of phase separating morphologies in supported membranes;
5. Determine the role of inter-layer coupling in controlling intralayer phase separation and raft formation;
6. Characterize nanoscale bilayer heterogeneities using X-ray and neutron scattering methods.

We expect that a successful completion of these studies will further help determine design rules for dynamic reorganizations within the membrane media which will then be used to design active and dynamic biomimetic materials such as needed for biomimetic conversion of optical to electrical energy.

## **Publications Resulting From The Grant (2005-2007)**

### **1.1. Peer-Reviewed Papers.**

- 1) Phospholipid Bilayers at Photochemically patterned silane monolayers, M. C. Howland, A. R. Sapuri-Butti, S. S. Dixit, A. M. Dattelbaum, A. P. Shreve, A. N. Parikh, **J. Amer. Chem. Soc.** 126, 13963-13972, 2005.
- 2) Direct Patterning of Membrane-Derivatized Colloids Using in situ UV-Ozone Photolithography, C. -H. Yu, A. N. Parikh, J. T. Groves, **Adv. Mater.**, 17, 1477-1480, 2005.
- 3) Interferometrically Induced 190 nm grating formation in azo-dye-labeled phospholipid thin films using 244 nm light, A. Sharma, M. Dokhanian, A. Sileshi, A. N. Parikh, **Optics Lett** 30 (5): 501-503, 2005.
- 4) Transition from Homogeneous Langmuir-Blodgett Monolayers to Striped Bilayers Driven by a Wetting Instability in Octadecylsiloxane Monolayers, M. C. Howland, M. S. Johal, A. N. Parikh, **Langmuir** 21, 10468-10474, 2005.
- 5) Formation of Spatially-Patterned Colloidal Photonic Crystals Through a Control of Capillary Forces and Template Recognition, A. M. Brozell, M. A. Muha, A. N. Parikh, **Langmuir** 21, 11588-11591, 2005.
- 6) A New Class of Supported Membranes: Bilayers on Photonic Band-gap Colloidal Crystals, A. M. Brozell, M. A. Muha, B. Sanii, A. N. Parikh, **J. Amer. Chem. Soc.**, 128, 62-63 2006
- 7) Non-equilibrium patterns of Cholesterol-rich membrane Heterogeneities, A. R. Sapuri-Butti, Q. Li, J. T. Groves, A. N. Parikh, **Langmuir** 22, 5374-5384, 2006.
- 8) Glass Bead Probes of Local Morphological and Mechanical Properties of Supported Membranes, S. S. Dixit, A. W. Szmodis, A. N. Parikh **Chem Phys Chem**, 7, 1678-1681, 2006 (Journal Cover).
- 9) Lipid Lateral Mobility and Membrane Phase Structure Modulation by Protein Binding, Martin B. Forstner, Chanel K. Yee, Atul N. Parikh, Jay T. Groves, **J. Amer. Chem. Soc.** 128, 15221-15227, 2006.
- 10) Membrane Materials Science, A. N. Parikh and J. T. Groves, **MRS Bulletin**, GUEST EDITORIAL, July 2006. (Journal Cover)
- 11) Characterization of Physical Properties of Supported Membranes Using Quantitative Imaging Ellipsometry at Optical Wavelengths, M. Howland, A. W. Szmodis, B. Sanii, A. N. Parikh, **Biophys J**, 92, 1306-1317 2007 . (Journal Cover)
- 12) Dynamic re-compartmentalization of Lipid Membranes Using Femtosecond Pulses, A. M. Smith, T. R. Huser, A. N. Parikh, **J. Amer Chem. Soc.**, 129, 2422-2423, 2007.

- 13) Optical Transduction of Ion-Channel Mediated Proton Transport, T.-H. (Calvin) Yang, C. K. Yee, M. L. Amweg, E. L. Kendall, S. Singh, A. M. Dattelbaum, A. P. Shreve, C. J. Brinker, A. N. Parikh, **Nano Letters**, in press, 2007.
- 14) Surface Energy Dependent Spreading of Lipid Monolayers and Bilayers, Babak Sanii and Atul N. Parikh, **Soft Matter**, in press, 2007.
- 15) Characterization of Supported Membranes on Topographically Patterned Polymeric Elastomers and Their Applications in Micro-Contact Printing, A. R. S. Butti, R. Butti, A. N. Parikh, **Langmuir**, in press, 2007
- 16) X-ray Reflectivity Studies of cholesterol-Dependent Phase Separation in Phospholipid Sphingolipid Mixtures, J. Zhang, A. W. Szmodis, A. N. Parikh, S. K. Sinha, Unpublished material, 2007.

## 1.2. Invited Reviews and Perspectives

- 17) Patterning Material Surfaces Using Photo-generated reactive oxygen Species, B. Sanii and A. N. Parikh, Annual Rev. of Physical Chemistry, in press, July 2008.
- 18) Materials Science of Supported Membranes, A. N. Parikh and J. T. Groves, MRS Bulletin, Editorial Introduction, July 2006. (Cover)

## 1.3. Invited Presentations

- |      |   |
|------|---|
| 2007 | American Vacuum Society, Biomaterials Interfaces, Seattle, WA Oct. 18   |
| 2007 | Workshop on Novel Model Systems for the Bimolecular Lipid Membranes, Max-Planck Institute Workshops, Schloss Ringberg, Tegernsee, Germany, Sept. 20, 2007   |
| 2007 | Challenges in Membrane Biophysics, Park City, UT June 15  |
| 2007 | Emergence in Complex Functional Systems, ACS Annual Meeting, Boston   |
| 2007 | Membrane Biosensors, PittCon Meeting, Chicago, Mar 1  |
| 2007 | Biological Surface Chemistry, ACS Chicago, March 22   |
| 2006 | ACS National Meeting, San Francisco, Sept 12  |
| 2006 | American Association for Nanomedicine, National Academy of Sciences, Washington, D.C., Sept. 10   |
| 2006 | International Conference on Nanotechnology ICN+T 2006 Conference, Basel, Switzerland, August  |
| 2006 | Research Infrastructure in Science and Education (RISE) Sensors Workshop, HBCU/Minority Serving Institutions Collaboratory, Alabama, AL, July 2006  |
| 2006 | AAAS Annual Meeting, Nanotechnology, St. Louis, MO February 2006  |
| 2005 | Pacificchem, Hawaii, December   |
| 2005 | Second Annual Biophotonics Symposium, San Antonio, TX   |
| 2005 | Materials Research Society, San Francisco, Annual Meeting, (2 invited talks)  |
| 2005 | National Meeting of The American Chemical Society, Washington, D. C.  |
| 2005 | Center for Integrated Nanotechnologies Users Workshop, Albuquerque, NM  |
| 2005 | Next Generation Neutron Source Workshop, San Diego, CA  |
| 2007 | Department Seminars, Princeton Institute for Science of Materials, Princeton University, April 15; 2007 Illinois Institute of Technology, April 8, University of Nevada, Reno, April 14, 2006, Rensselaer Polytechnic, March 2006 |

These accomplishments document (1) Ph. D. dissertation opportunities for several graduate students spanning many departments (Michael Howland, Materials Science; Babak Sanii, Applied Physics; Alan W. Szmodis, Biophysics; Michelle Smith, Biophysics; Adrian Brozell, Biophysics); Jiang Zhang (Physics, UCSD) (2) post-doctoral training for Dr. Sanhita Dixit (Ph. D. Physics, now at SRI), Dr. Ann Oliver, and Dr. Chanel Yee (Ph.D. Materials, now at Amgen); and (3) several summer undergraduate researchers. They also document our strong collaborations with other complementary efforts including some BES-supported such as those led by Prof. Jay Groves (UC Berkeley) and Dr. Andy Shreve (LANL/CINT). Furthermore, the effort benefits strongly from many successful user proposals at Los Alamos Neutron Science Center (LANSCE), Advanced Photon Source at Argonne, and Center for Integrated Nanotechnology (CINT) at Sandia/Los Alamos.

## **Biological and Biomimetic Low-Temperature Routes to Materials for Energy Applications**

Daniel E. Morse

California NanoSystems Institute, University of California, Santa Barbara, CA 93106-6105;  
d\_morse@lifesci.ucsb.edu

### **Program Scope; Synopsis:**

Biological systems fabricate multifunctional, high-performance materials at low temperatures and near-neutral pH with a precision of three-dimensional nanostructural control that exceeds the capabilities of present human engineering. We discovered the mechanism governing the nanofabrication of silica in a biological system, and translated this mechanism to develop a new low-temperature route for the synthesis of a wide range of nanostructured metal oxide, -hydroxide and -phosphate semiconductor thin films and perovskite nanoparticles without the use of organic templates, producing many with forms and properties that could not be attained by conventional syntheses. Because no organics are used, the resulting products exhibit high purity, making this process compatible with MOCVD manufacturing. The electronic properties of several of these novel materials suggest strong advantages for energy applications.

### **Recent Progress:**

#### **1. Biological Mechanism of Low-temperature, Catalytic, Structure-Directed Nanofabrication of Inorganic Materials; Confirmation with Biomimetics:**

We discovered that the silicateins, a family of enzyme proteins we found occluded within the silica needles made by a marine sponge, can catalyze and structurally direct the polymerization of silica, silsesquioxanes, organometallics and a wide range of metal oxide semiconductors from the corresponding molecular precursors at neutral pH and low temperature. These were the first reported examples of enzyme-catalyzed, nanostructure-directed synthesis of semiconductors. Interaction with the template-like protein surface stabilizes polymorphs of these materials (e.g., the anatase form of titanium dioxide and the spinel polymorph of gallium oxide) otherwise not formed at low temperatures. This observation and the preferential alignment of the Ga<sub>2</sub>O<sub>3</sub> nanocrystallites suggested a pseudo-epitaxial relationship between the mineral crystallites and specific functional groups on the templating protein surface. Genetic engineering of the protein, in conjunction with diffraction studies of the semiconductor products and the templating surface, confirmed the proposed mechanism of action and identified the functional groups responsible for catalysis and templating. This mechanistic understanding was confirmed and extended through the synthesis of a series of "biomimetic" peptides, polymers, small bifunctional organics and multifunctional self-assembled monolayers displaying the functionalities identified by genetic engineering to be required for catalysis and templating, thus yielding new structure-directing catalysts of siloxane and metallo-oxane polycondensation from the corresponding molecular precursors at low temperature and neutral pH. The success of these results permitted us subsequently to translate the fundamental mechanisms underlying silicatein-mediated catalysis and templating to a process wholly controlled by chemistry and physics, without the use of any biochemical or organic molecules.

#### **2. Low-Temperature Catalytic Nanofabrication of Metal Oxides, Hydroxides, Phosphates, Nitrides and Sulfides:**

The method we developed uses vapor diffusion of acid, alkaline or aqueous catalysts through a gas-liquid interface into a solution of molecular precursor to provide vectorial and kinetic control of catalysis, at low-temperature, of synthesis of a wide range of inorganic materials. The result is a novel, highly generic, low-temperature and environmentally benign method for the nanofabrication of a wide range of more than 35 different nanostructured thin films and nanoparticles of metal oxides, hydroxides, phosphates and perovskites, many with unique and potentially useful morphologies and properties not attainable by conventional high-temperature routes. The method uses no biochemicals, biologicals or organic materials. Post-synthesis conversion to the nitrides and sulfides has been demonstrated.

The resulting materials were characterized XRD, SEM, TEM, X-ray photoelectron spectroscopy, X-ray absorption near edge structure and various chemical and electronic analytical techniques. For the first time the electronic properties and crystal structures of some of these materials could be studied in thin films not influenced by the presence of an underlying substrate. Thus, for the  $\text{Co}_5(\text{OH})_8(\text{NO}_3)_2 \cdot 2\text{H}_2\text{O}$  films, which crystallized in a layered hydroxalcalite-like structure that proved homogeneous from the nanoscale to macroscale, unanticipated photoconductivity was observed. We found that this material is a p-type semiconductor with an unusually long minority carrier lifetime, high carrier density, high surface area and strong absorption in the visible, making it potentially attractive for photovoltaic applications. Doping with high levels of lithium ions has been achieved, making this material potentially useful for improvements in lightweight batteries.

### **3. Low-Temperature Catalytic Synthesis of $\text{BaTiO}_3$ Nanoparticles:**

Combining the advantages of a unique bimetallic precursor molecule with the gentle, low-temperature and vectorially controlled catalysis method described above makes it possible to produce highly crystalline  $\text{BaTiO}_3$  nanoparticles (6 nm diam.) with low polydispersity, good control over the stoichiometry and atomic-scale geometry of the two metal centers, and without the complications of phase-segregation and degradation of properties typical of high-temperature methods. When these nanoparticles were doped with La to provide good conductivity and sintered, the resulting fine-grained (nanoparticulate) ceramic exhibited a strong positive thermal coefficient of resistance (PTCR), with a ca. 10,000-fold increase in electrical resistance over a narrow range of heating above 130 °C ( $T_C$ ), making this material potentially useful for fireproof Li ion batteries. (Other potential applications include improved magnetic information storage, piezoelectric and IR detectors.)

### **Future Plans: Genetic Engineering and Analyses of Self-Assembly for Further Insights:**

We are continuing our molecular and genetic analysis of the biomolecular mechanisms governing hierarchical self-assembly, catalysis and templating of inorganic materials synthesis to gain further insights for ultimate translation into new methods of controlled nanofabrication. Because living cells may be killed by the inorganic materials that are the focus of our interest, we are using a new system for genetic engineering known as In Vitro Gene Expression, in which the biomolecules required for gene expression produce the target enzyme molecules from recombinant DNA molecules carried in single copy in each of millions of micron-sized vesicles dispersed in suspension. These vesicles thus function as more readily manipulated analogs of living cells. When the DNA coding for a material-synthesizing enzyme is first mutagenized or combinatorially scrambled before encapsulation in the vesicles, the resulting vesicles can subsequently be screened with a high-throughput Fluorescence Activated Cell Sorter, at the rate of millions per minute, to identify those carrying any rare mutant DNAs that encode the synthesis of mutationally altered enzymes that either produce greater quantities of the target material (identified by its characteristic fluorescence), or new structures of that material.

We first established proof of principle by starting with the cloned, recombinant DNA that codes for the enzyme, silicatein (the enzyme we had discovered that catalyzes the low-temperature synthesis of silica and various metal oxide semiconductors). We mutagenized the silicatein DNA at random, packaged the resulting "mutant silicatein DNA library" in the vesicles, and provided a molecular precursor of silica synthesis, enabling us to discover a rare mutant DNA that codes for the synthesis of a novel, mutationally altered variant of the silicatein enzyme that catalyzes the formation of crystalline Cristobalite (a quartz-like form of silica, normally produced geologically only at very high temperatures). The normal form of silicatein is capable of producing only amorphous (non-crystalline) silica. Using this method, we were able to identify a rare mutant form of the enzyme that can now catalyze and structurally direct the synthesis of the crystalline Cristobalite at 16 oC!

Extending this proof of principle, we now are using this and related methods to further characterize and manipulate those parts of the protein that govern the specificity of mineral synthesis and structure, and the hierarchical assembly of the protein template.

**Figures:**

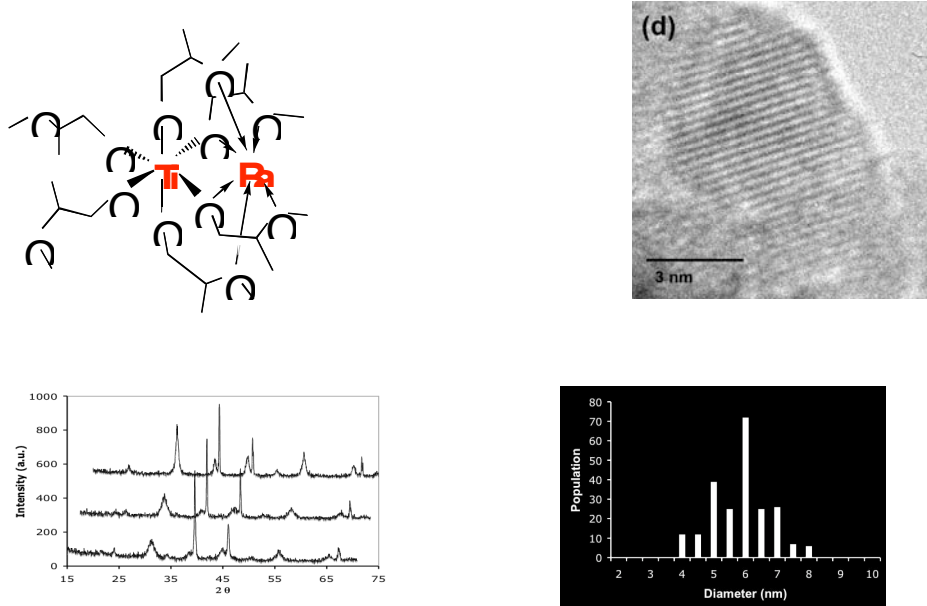


**Figure 1.** Bio-inspired, low-temperature synthesis of high-quality BaTiO<sub>3</sub> nanoparticles. (Upper left) bimetallic unimolecular precursor used in conjunction with low-temperature vapor-diffusion catalysis yields highly crystalline, ultrapure BaTiO<sub>3</sub> nanoparticles 6 nm in diameter (upper middle). High resolution TEM (upper right) shows high degree of crystallinity without phase segregation. (Lower left) X-ray diffraction traces reveal that the as-made cubic polymorph nanoparticles (lower trace) are progressively converted to the tetragonal polymorph upon heating. (Lower right) narrow size-distribution of the as-made nanoparticles.

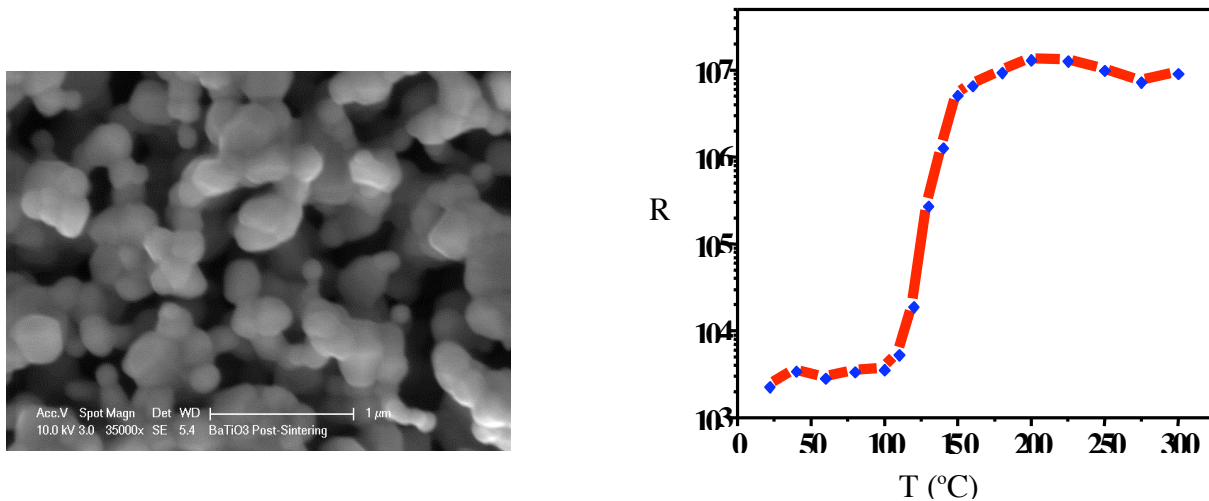


**Figure 2.** (above, left) Sintered nanoparticles of La-doped barium titanate.

**Figure 3.** (above, right) Strong positive thermal coefficient of resistance (PTCR) of the new material described above. As the sample is heated above the Curie temperature (130 °C), resistance increases by nearly 4 orders of magnitude, from ca. 10<sup>3</sup> ohms to ca. 10<sup>7</sup> ohms.

## References:

- Curnow, P., P.H. Bessette, D. Kisailus, M. M. Murr, P. S. Daugherty and D. E. Morse. 2005. Enzymatic synthesis of layered titanium phosphates at low temperature and neutral pH by cell-surface display of silicatein-a. J. Amer. Chem. Soc. 127: 15749-15755.
- Roth, K.M., Y. Zhou, W. Yang and D.E. Morse. 2005. Bifunctional small molecules are biomimetic catalysts for silica synthesis at neutral pH, J. Amer. Chem. Soc. 127: 325 - 330.
- Kisailus, D., J.H. Choi, J. C. Weaver, W. Yang and D.E. Morse. Enzymatic synthesis and nanostructural control of gallium oxide at low temperature. 2005. Advanced Materials 17: 314-318.
- Kisailus, D., M. Najarian, J. C. Weaver, and D.E. Morse. 2005. Functionalized gold nanoparticles mimic catalytic activity of a polysiloxane-synthesizing enzyme. Advanced Materials 17 [10]: 1234-1239 (+ cover).
- Aizenberg J., J. C. Weaver, M. S. Thanawala, V. C. Sundar, D. E. Morse and Peter Fratzl. 2005. Skeleton of *Euplectella sp.*: Structural hierarchy from the nanoscale to the macroscale. Science 309: 275-278 (+ cover).
- Murr, M. and D.E. Morse. 2005. Fractal Intermediates in the self-assembly of silicatein filaments. Proc. Natl. Acad. Sci. USA 102: 11657-11662.
- Fu, G., S.R. Qiu, C.A. Orme, D.E. Morse, and J.J. De Yoreo. 2005. Shifting crystal growth into high gear: Acceleration of calcite kinetics by abalone nacre proteins. Advanced Materials 17: 2678-2683 (+cover).
- Schwenzer, B., K.M. Roth, J. R. Gomm, Meredith Murr & D. E. Morse. 2006. Kinetically controlled vapor-diffusion synthesis of novel nanostructured metal hydroxide and phosphate films using no organic reagents. J.Mater. Chem. 16: 401 - 407.
- Kisailus, D., Y. Amemiya, J. C. Weaver, Q. Truong and D.E. Morse. 2006. Self-assembled bi-functional surface mimics an enzymatic and templating protein for low-temperature synthesis of a metal oxide semiconductor. Proc. Natl. Acad. Sci. USA 103: 5652-5657.
- Brutchey, R.L., E. S. Yoo, and D. E. Morse. 2006. Biocatalytic synthesis of a nanostructured and crystalline bimetallic perovskite-like barium oxofluorotitanate at low temperature. J. Amer. Chem. Soc. 128: 10288-10294.
- Kisailus, D. J., B. Schwenzer, J. Gomm, J. C. Weaver and D. E. Morse . 2006. Kinetically controlled nucleation of zinc oxide thin films at low temperatures. J. Amer. Chem. Soc. 128: 10276-10280.
- Brutchey, R.L. and D.E. Morse. 2006. Template-free, low-temperature synthesis of crystalline barium titanate nanoparticles under bio-inspired conditions. Angewandte Chemie Intl. Ed. 45: 6564-6566.
- Curnow, P., D. Kisailus and D.E. Morse. 2006. Biocatalytic synthesis of poly(L-lactide) by native and recombinant forms of the silicatein enzymes. Angewandte Chemie Intl. Ed. 45: 613-616.
- Woesz, A., J. C. Weaver, M. Kazanci, Y. Dauphin, J. Aizenberg, D.E. Morse and P. Fratzl. 2006. Micromechanical properties of biological silica in skeletons of deep-sea sponges. J. Mater. Res. 21: 2068-2078.
- Schwenzer, B., J.R. Gomm and D.E. Morse. 2006. Substrate-induced growth of nanostructured zinc oxide films at room temperature using concepts of biomimetic catalysis. . Langmuir 22: 9829-9831.
- Weaver, J.C., J. Aizenberg, G. E. Fantner, D. Kisailus, A. Woesz, P. Allen, K. Fields, M. J. Porter, F. W. Zok, P.K.Hansma, P. Fratzl and D. E. Morse. 2007. Hierarchical Assembly of the Siliceous Skeletal Lattice of the Hexactinellid Sponge *Euplectella aspergillum*. J. Structural Biology 158: 93-106 (+ cover).
- Gomm, J.R., B.Schwenzer and D. E. Morse. 2007. Textured films of chromium phosphate synthesized by low-temperature vapor diffusion catalysis. Solid State Science 9: 429-431.
- Adamson, D.H., D.M. Dabbs, C. Pancheco, M.V. Giotto, D.E. Morse and I.A. Aksay. 2007. Non-peptide polymeric silicatein alpha mimic for neutral pH catalysis of silica condensation. Macromolecules (in press).
- Brutchey, R. L., G. Cheng, Q. Gu, and D. E. Morse. (2007). Positive temperature coefficient of resistivity in donor-doped BaTiO<sub>3</sub> ceramics derived from nanocrystals synthesized at low temperature, Adv. Mater. (in press)



## **Program Title: Miniaturized Hybrid Materials Inspired by Nature**

**Principle Investigator: C. R. Safinya; Co-PIs: Y. Li and K. Ewert**

**Mailing Address: Materials Department, University of California at Santa Barbara  
Santa Barbara, CA 93111**

**E-mail: safinya@mrl.ucsb.edu**

### **Program Scope:**

The broad aim of the project is to develop a fundamental understanding of the mechanisms underlying lipid and protein based nanometer scale self-assembly. The understanding will lead to the development of nanometer scale materials with distinct properties important both from a scientific and technological perspective. For example, nanometer scale tubules and their assemblies are of interest as miniaturized materials with applications as circuitry components, enzyme encapsulation systems and biosensors, and vehicles for chemical delivery.

The principle strategy that we will use to achieve our goals consists of learning from, and building upon, the many illuminating examples of (out-of-equilibrium) assembly occurring *in vivo*. For example, the nerve cell cytoskeleton provides a rich variety of highly ordered bundles and networks of interacting neurofilaments, microtubules (MT), and filamentous actin, where the nature of the interactions, structures, and structure-function correlations remain poorly understood. In recent work in far simpler reconstituted protein systems in the presence of counter-ions, (using a combination of synchrotron x-ray diffraction, electron microscopy, and optical imaging data), we have demonstrated how MT bundles and network-like necklaces may be assembled *in vitro* revealing unexpected structures not predicted by current electrostatic theories of polyelectrolyte bundling. In another set of experiments we are currently developing lipid-protein and lipid bio-nanotubes through membrane shape evolution processes involving protein templates and curvature stabilizing lipids. Indeed, similar membrane shape changes, occurring *in vivo* for the purpose of specific cellular functions, are often induced by protein scaffold recruitment through interactions between membranes and proteins (e.g. in endocytosis involving clathrin covered vesicles, the protein dynamin is recruited and assembled into rings (or stacks of rings) in the negative curvature region of the invaginated membrane vesicle forcing dynamical lipid shape changes where a transient tubular neck formation is followed by membrane fission).

The projects involve both custom synthesis of novel lipids, peptide-lipids, and PEG-lipids with or without functional end groups, and purification of biological molecules. In some instances the enhanced stability of the lipid assemblies will be achieved by lipids with polymerizable chains. The higher order assembly of the building blocks will be achieved via competing interactions, where end-functionalized PEG-lipids may play an important role.

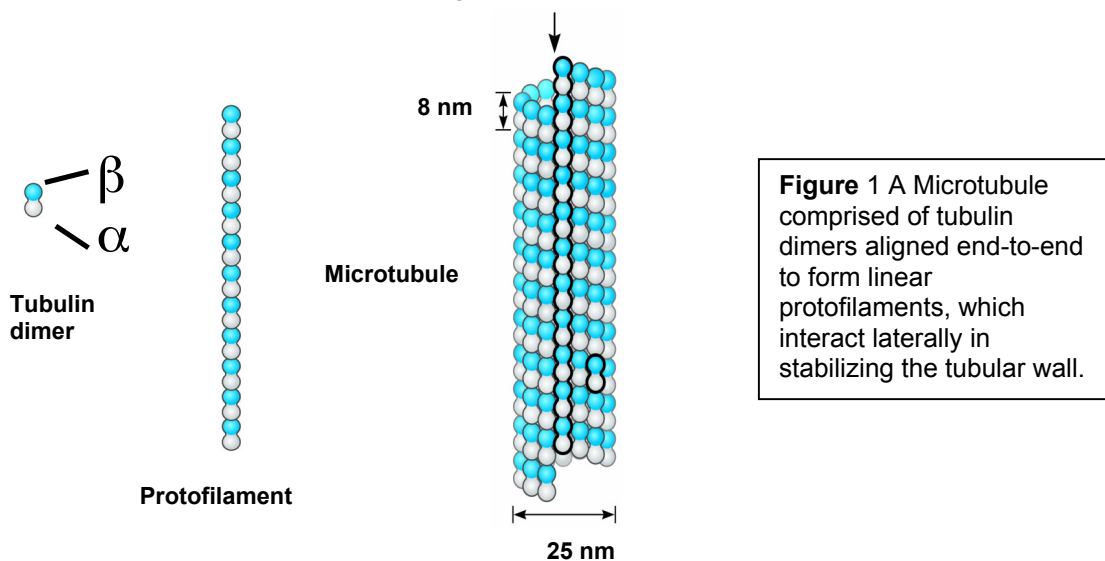
The projects utilize the broad spectrum of expertise of the group members in biomolecular self-assembling methods, synchrotron x-ray scattering and diffraction, electron and optical microscopy characterization techniques. The miniaturized hybrid biomaterials resulting from this research program should be of high interest in a broad range of industries from chemical, pharmaceutical and biotechnology, to semiconductors.

## Recent Progress

### (A) Stepwise Nanometer Scale Changes in the Diameter of Microtubule-based Lipid-Protein Nanotubes by the Charge Density of an Enveloping Lipid bilayer

#### Background

Microtubules (MTs) are nanometer scale hollow cylinders derived from the eukaryotic cell cytoskeleton. The hollow cylinders are comprised of globular tubulin subunits, which align end-to-end to form linear protofilaments. The lateral interactions between protofilaments stabilize the tubular wall (see figure 1). In vivo, MTs and their assembled structures (most of which remain to be identified) are key components in a broad range of cell functions from providing tracks for the transport of cargo (organelles, vesicles, neurotransmitters, etc.) to forming the spindle structure in cell division. Nevertheless, precisely because of their biological origin MTs may also be considered as model nanotubes with a well-defined inner ( $\approx 15$  nm) and outer ( $\approx 25$  nm) diameter, which can be fine-tuned depending on the solution conditions. Nanotubes and bundles of nanotubes are currently being explored for technological, biomedical, and biotechnological applications. (See e.g. Scientific American, September 2001, Special Issue on Nanotech: the science of the small gets down to business".).



#### Highlights of 2007 Biophysical Journal [1]

In an earlier study by our group we reported on a new paradigm for lipid self-assembly leading to nanotubule formation in mixed charged systems. (U. Raviv, et. al *Proceedings of the National Academy of Sciences of the USA*, **102**, 11167-11172 (2005)). We looked at the interaction between negatively charged Microtubules, and cationic lipid vesicles and discovered, under the appropriate conditions, spontaneously forming lipid protein nanotubes (LPNs). The LPNs exhibit a rather remarkable architecture with the cylindrical Lipid-bilayer sandwiched between the microtubule and an outer tubulin oligomer. The new type of self-assembly arises because of an extreme mismatch between the charge densities of microtubules and cationic lipid. This is a novel finding in equilibrium self-assembly. The nanotube consisting of a three-layer wall appears to be the best the system can do in compensating for this charge density mismatch. Interestingly, we found that by controlling the degree of overcharging of the lipid-protein nanotube enables us to switch between two states of nanotubes with either closed ends (positive overcharged) or open ends (negative overcharged) with lipid caps, which forms the

basis for controlled chemical and drug encapsulation and release.

In this most recent work [1] a physical interaction method was developed where by the inner diameter of the lipid-protein nanotube - a key parameter in chemical encapsulation and templating applications - may be controlled and varied in a step-wise fashion in response to changes in the membrane charge density of the enveloping cylindrical lipid bilayer (Figure 2).



**Figure 2** Lipid protein nanotubes made of microtubule protein (protein subunits shown as red-blue-yellow-green objects) that is coated by a mixture of cationic and neutral lipid bilayer membrane (drawn with yellow tails and green (cationic) and white (neutral) spherical heads), which in turn is coated by tubulin protein rings or spirals. A top view of the nanotubes is shown on the right. Changes in the membrane-charge-density modify - in a step-wise fashion - the inner diameter of the microtubule lumen. U. Raviv et al. *Biophysical Journal*, 2007, **92**, 278-287

## **(B) The Development of a New AFM-Based Molecular Scale Imaging of F-actin Assemblies Immobilized on a Photopolymer Surface.**

### Highlights of 2007 Physical Review Letter [2]

Although atomic force microscopy (AFM) has become an established technique for imaging biological macromolecules including single filamentous proteins, imaging protein assemblies in native aqueous environments presents special challenges, in particular, due to thermal fluctuation effects, which tend to smear out important molecular level structural details. In this work we developed a new method that can be effectively used to image a wide range of supramolecular assemblies in native environments with molecular resolution. A recently developed photo-immobilization based process was used for direct imaging of hierarchical assemblies of biopolymers using AFM. The new technique was used to investigate the self-assembled structures of filamentous (F)-actin aggregates as a function of concentration of the divalent cation  $Mg^{2+}$ . The data provided the first direct experimental evidence of a coil-on-coil (braided) structure of F-actin bundles formed at high  $Mg^{2+}$  concentrations. This braided structure may be an important basic unit of hierarchical assembly in filamentous protein systems.

## **Future Plans**

### **(1) Lipid-based Liquid Nanotubes**

Nanotubes are indispensable components in the development of future miniaturized materials. They have applications in diverse areas from uses as chemical encapsulation vehicles, to biosensors and circuitry components. Thus, an area of intense current research in nanoscience is in elucidating the key parameters, which control the self-assembling properties of nanometer scale tubules. In this next period we will investigate the development of liquid phase lipid nanotubes using curvature stabilizing lipids, which mimic curvature stabilizing proteins used in nature [3]. The experiments will involve at least a two-component lipid mixture, which on theoretical grounds should allow us to achieve our goal. The key lipids (custom synthesized in our laboratory [4,5]) will consist of conically shaped molecules where the head-group is comprised of charged dendrimers. The lipids have been designed to give rise to membranes with a positive spontaneous curvature on the nanometer scale because of the highly asymmetric conical shape of the lipid (with extreme mismatch in headgroup area versus tail area), and the unprecedented large charge of the lipid headgroup. The second lipid will have

a cylindrical shape, which is expected to give rise to zero curvature flat membranes. On theoretical grounds we expect that the lipid mixture may give rise to liquid phase lipid nanotubules, i.e. liquid nanotubes, (where the lipid molecules remain in their chain-melted state), if a spontaneous breaking of compositional symmetry occurs between the inner and outer monolayers of the lipid bilayer. The liquid nanotubes should be desirable candidates for drug/gene delivery applications or as template for nanostructures such as wires or needles. The incorporation of functional biomolecules, which typically require the membrane to be in the liquid state to retain their full biological activity, would lead to bioactive liquid nanotubes for a range of applications including sensing and chemical delivery.

The first system that we are exploring and will continue to do so are membranes comprised of mixtures of MVLBG2 and 1,2-dioleoyl-*sn*-glycero-3-phosphocholine (DOPC). MVLBG2 is a multivalent cationic lipid with di-oleyl tails and a dendritic headgroup based on ornithine and carrying a colossal charge of +16 e at full protonation [4]. Both lipids are in their chain-melted state at room temperature due to the presence of a *cis* double bond in their oleoyl chains. The MVLBG2 system has led to the discovery of a remarkable new class of vesicles containing tubular vesicles in the chain-melted liquid phase with the inner lumen in the true nanometer scale range. To further gain insight into the separate contributions of electrostatics and  $C_0$  on the formation of nanotubes, we will study vesicle shape behavior in charged membranes comprised of mixtures of DOPC with the cationic univalent lipid 1,2-dioleoyl-3-trimethylammonium-propane (DOTAP), which has a cylindrical molecular shape favoring  $C_0 = 0$ . Future studies involving systematic variations in the shape, size and charge of the curvature-stabilizing lipid (which mimics curvature stabilizing proteins *in vivo* [3]) will lead to optimal control of the tubule diameter distribution. In particular, we will explore recently synthesized multivalent lipids, which span +2, +4, +6, +8, +16, and +32.

## **(2) Neurofilaments as models of biopolymer liquid crystalline networks with tunable interactions**

Understanding the fundamental interactions underlying the self-assembly of hierarchical structures with distinct properties is important from a scientific and technological perspective. As a model system we are studying neurofilaments, to elucidate and differentiate between, the distinct interactions (including, electrostatics, van der Waals, hydrogen bonding and hydrophobic interactions) responsible for their hierarchical assembly.

## **References (which acknowledge DOE support)**

1. Microtubule Protofilament Number is Modulated in a Stepwise Fashion by the Charge Density of an Enveloping Layer. U. Raviv, T. Nguyen, R. Ghafouri, D. J. Needleman, Y. Li, H. P. Miller, L. Wilson, R. F. Bruinsma, C. R. Safinya, *Biophysical Journal* **92** (1): 278-287, (2007)
2. Molecular scale imaging of F-actin assemblies immobilized on a photopolymer surface T. Ikawa, F. Hoshino, O. Watanabe, Y. Li, P. Pincus, C. R. Safinya, *Physical Review Letters* **98** (1): 018101, (2007)

## **Other References**

3. McMahon, H. T. & Gallop, J. L. Membrane curvature and mechanisms of dynamic cell membrane remodelling. *Nature* **438**, 590-596 (2005).
4. A Columnar Phase of Dendritic Lipid-Based Cationic Liposome-DNA Complexes for Gene Delivery: Hexagonally Ordered Cylindrical Micelles embedded in a DNA Honeycomb Lattice. K. Ewert, H. Evans, A. Zidovska, N. F. Buxsein, A. Ahmad, C. R. Safinya, *J. Am. Chem. Soc.* **128**, 3998-4006 (2006)
5. Dendritic Cationic Lipids with Highly Charged Headgroups for Efficient Gene Delivery. K. Ewert, H. Evans, C. R. Safinya, *Bioconjugate Chemistry*, **17** (4), 877-888 (2006).

## RNA Mediated Assembly of Inorganic Metal and Metal Oxide Nanoparticles

Dan Feldheim, Lina Gugliotti, Magda Dolska, J' aime Manion, Jessica Rouge and Bruce Eaton\*

Department of chemistry and Biochemistry  
University of Colorado at Boulder  
Boulder, Colorado, 80309  
(bruce.eaton@colorado.edu)

The Eaton has successfully used chemically modified RNA<sup>1,2</sup> in vitro selection methods to discover several new organic<sup>3-7</sup> and with Feldheim inorganic<sup>8,9</sup> reactions and is now accelerating nanoparticle discovery by replacing the traditional serial synthesis approach with one that mimics biological selection. For example, the Eaton and Feldheim groups have shown that using RNA in vitro selection in a magnetic field that it is possible to isolate new magnetic oxide nanoparticles. In contrast to conventional magnetic nanoparticle preparations, these materials were formed at room temperature and pH 7. In a separate in vitro selection, RNA sequences were isolated that mediate the formation of large (1 micron) hexagonal palladium platelets (<20 nm thick, Figure 1). In addition, these same RNA sequences were shown to be catalysts for the assembly of platinum nanoparticles. Platinum nanoparticles are well known as methanol oxidation catalysts. When we compared electrochemically the catalytic activity of the platinum particles formed by RNA to the conventional platinum used for methanol oxidation we found them to be significantly more efficient. This highlights the remarkable ability of biomolecule catalysts to control materials size, shape, and kinetic parameters. Our goal is to advance RNA-Mediated Evolutionary Materials Chemistry to the point where it is a valuable tool for high-throughput discovery.

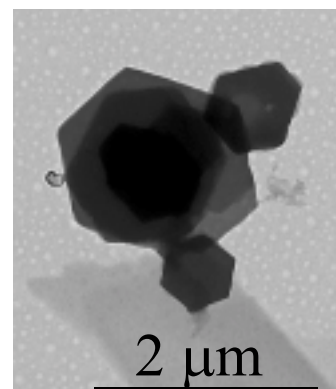


**Figure 1.** Palladium particles assembled by a single RNA sequence

RNA catalysis to assemble nanomaterials could provide major benefits in the synthesis of well-defined particle shapes, compositions and functions. RNA may also be able to play a role in affinity purification or assembly of specific nanoparticles with desired properties, including the discovery of new catalytic nanoparticles. Some of the attributes of RNA in vitro selection techniques are:

1. A large library of RNA sequences ( $10^{14}$ ) can be used to select for new nanoparticle catalysts not readily synthesized by conventional methods;
2. Multiple metal precursors may be tested simultaneously and selected;
3. Modification of the RNA to include new functional groups important for catalysis and metal ion binding are easily accomplished. These modifications are compatible with enzymatic processes such as PCR amplification, thus, a catalytically active RNA sequence, even if extremely rare, can be amplified and identified. This is a distinguishing feature as compared to in vitro protein evolution techniques;

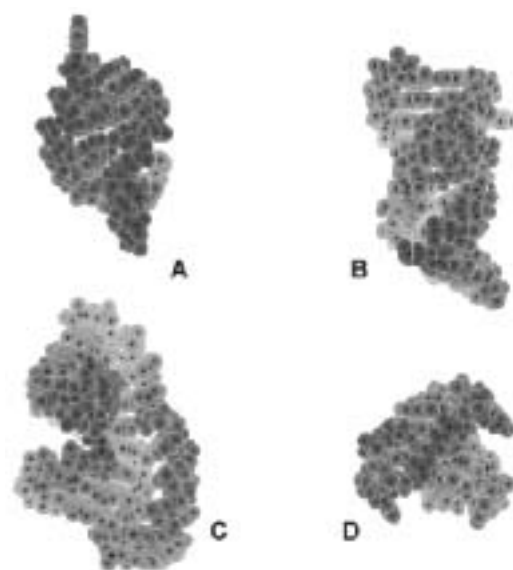


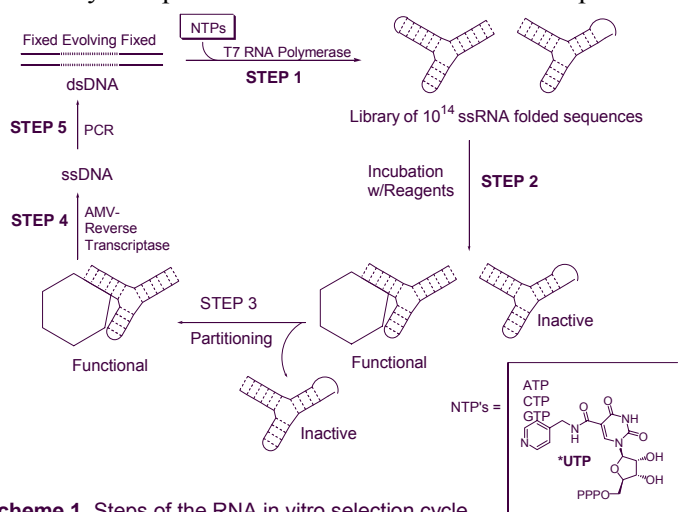
**Figure 2.** Some common ssRNA structural motifs

- High selectivity may be achieved for specific structures or properties;
- A complex mixture of metal ions can be used to discover new materials and nanoparticle catalysts.

RNA *in vitro* selection can be used to explore a wide range of inorganic material compositions. In contrast to all other materials discovery methods, RNA mediated materials synthesis has the benefit of evolution. Even if extremely rare, materials composition, crystal type and physical properties can evolve in response to selection pressures.

The first consideration in understanding the utility of RNA-based synthesis is that single stranded RNA (ssRNA) can fold up in complex 3D shapes with intricate binding pockets. The number and potential structures possible to bind large molecules or catalyze reactions is unknown. Some models of typical folded RNA motifs are shown in Figure 2. These examples include hairpin stem (**A**), symmetric bulge (**B**), pseudoknot (**C**) and G-quartet (**D**). There are many more diverse motifs possible for RNA and we have much to learn about these different folded RNA structures and their ability to assemble other macromolecules. Some RNA sequences will form catalytic pockets and some may only bind proteins, surfaces, etc. Indeed, most RNA structures in a random population of sequences will not do anything specific.

By the process of *in vitro* selection it is possible to test a hypothesis about a range of metal



**Scheme 1.** Steps of the RNA *in vitro* selection cycle

colloids or metal ion compositions that could lead to important new materials or catalysts. The generic *in vitro* selection cycle used for discovering RNA catalysts is shown in Scheme 1. The process begins with a ssDNA library of  $10^{14}$  sequences made on an automated DNA synthesizer. A starting dsDNA template for enzymatic transcription is made by 2-cycle PCR of this ssDNA library. The ends of the dsDNA template contain fixed regions required for the enzymes used in amplification and the center region (40 nucleotides long) contains random sequence (ca. 1 nmole of RNA  $\approx 10^{14}$  sequences). STEP 1 involves T7 RNA

polymerase transcription of this dsDNA library to produce a new ssRNA library of  $10^{14}$  folded sequences. During STEP 1 it is possible to incorporate additional functional groups into the RNA by using modified UTP or CTP (not shown in Scheme 1) analogs. In Step 2 the RNA library can be incubated with chemical reagents consisting of metal ions, organic and organometallic compounds. Functional RNA sequences that either bind to the reagents, or catalyze reactions between reagents and remain bound to the product, have a selection advantage as they become amplified (STEPS 4 and 5). The Functional RNA is then partitioned in STEP 3 from the Inactive RNA by either electrophoresis gel-mobility shift, HPLC, GPC, membrane size exclusion, dialysis, magnetic force, or a chemical transformation. After isolation and concentration the Functional RNA is then reverse transcribed (STEP 4) by AMV reverse transcriptase to give a cDNA copy of the “winning” sequences from the starting library of  $10^{14}$ . Only a small fraction (ca. 100s) of the starting  $10^{14}$  RNA sequences are Functional making it likely that some Inactive RNA sequences will be carried along in STEP 3. For this reason the cycle must be repeated several times. STEP 5 is PCR, used to give multiple copies (1,000s) of the winning sequences as dsDNA templates for T7 RNA polymerase ready to enter the next cycle of selection at STEP 1. For successful RNA *in vitro* selection experiments, repeating this amplification cycle 8 – 16 times gives a convergence on the functional sequences. After convergence the RNA library will consist of approximately 10 to 100 sequences that are functional.

To isolate the individual Functional RNA sequences, the DNA PCR product from Step 5 of the last cycle is used in standard plasmid cloning procedures, which allows for the isolation of *E. coli* colonies containing individual catalyst sequences. Sequencing is performed on the isolated DNA from the colonies. The sequence data is aligned and the isolates grouped into families for characterization. Using the plasmid DNA and the correct primers, PCR amplification yields a dsDNA template that can be used to perform T7 transcription to provide a single RNA sequence for study. Typically, highly conserved sequence regions are found. This sequence information can be used to construct phylogeny relationships within and between the RNA families. The sequences of the families also provide indirect activity information about the RNA.

Over the last couple of years we have shown that specific RNA sequences can be selected that make metal and organometallic particles of defined shape. Our initial results on palladium<sup>8,9</sup> prompted us to explore the synthesis of Pt containing nanoparticles (Figure 3). These metals are of obvious interest as catalytic materials in fuel cells and as islands on semiconductor particles for water splitting. We wanted to better understand if the choice of the organometallic precursor mattered in determining the shape and concomitant sequence of the RNA. We first used RNA sequences selected for the formation of Pd containing nanoparticles from Pd<sub>2</sub>(DBA)<sub>3</sub> to determine if these RNA sequences could make Pt particles. These particles could indeed in the presence of these sequences but control of shape was significantly less than that observed previously. A new in vitro selection was performed for Pt particle formation. The organometallic precursors Pt<sub>2</sub>(DBA)<sub>3</sub> and Pt(PPh<sub>3</sub>)<sub>4</sub> were used in separate RNA in vitro selections. The selections resulted in convergence of RNA sequences and analysis of the shape control achieved is summarized in Table 1.

**Table 1.** Shape and Size Distribution of Pt Particles Formed by  
In vitro selected RNA Sequences

RNA Sequence #	Particle Shape	Size (μm)	% Population
2	hexagonal	0.14 ± 0.05	100
12	hexagonal	0.16 ± 0.08	100
18	spherical	0.023 ± 0.008	73
	hexagonal	0.22 ± 0.14	17
	cubic	0.07 ± 0.02	10
21	hexagonal	0.13 ± 0.04	100
32	hexagonal	0.18 ± 0.09	100

As can be seen from Table 1 many of the isolated sequences showed excellent shape control (Sequences 2, 12, 21 and 32). Even alternative shapes (Sequence 18) were demonstrated using the identical reaction conditions using Pt<sub>2</sub>(DBA)<sub>3</sub> as the zero-valent metal precursor. It should be noted that the average size of these Pt particles was significantly smaller than those observed from RNA mediation with Pd<sub>2</sub>(DBA)<sub>3</sub> and the distribution of particle sizes observed was also narrower.

To be able to split water photochemically two catalyst materials are required. A catalyst that can accept electrons, such as Pt, and reduce protons to hydrogen, and a separate (physically?) catalysts that will accept holes and oxidize water to oxygen. Metal oxides are perhaps one of the best known classes of structures known to be capable of this water oxidation reaction. We are in the process of completing a selection for a mixed metal oxide derived from a mixture of early and late transition metal precursors to form mixed metal oxide nanoparticles. We have worked out selection conditions for RNA in the presence of a diverse mixture of metal precursors. Following our success with binary mixtures of iron and cobalt we have now worked out conditions for ternary and quaternary mixtures of Platinum (0), Titanium (IV), Copper (I),

and Iron (II). Compatibility of RNA in these solutions was demonstrated and several cycles of invitro selection have been completed using a size based partitioning scheme.

An inorganic selection of this complexity has never been attempted before while previous selections used a 87 mer RNA with a 40 nucleotide random region, there was concern based on previous experience in the Eaton group, that greater RNA structure could be required for the formation of these mixed metal oxides. that this that. Consequently, we have designed two RNA templates with different lengths (40 and 80 nucleotides) for the random regions. These two different lengths of random template may allow us to see if the evolved RNA sequences will be able to create mixed metal oxides with a smaller random region or if the system requires the greater structural capabilities of the longer random region. Preliminary results are encouraging with regard to RNA dependent formation of nanoparticles under these mild reaction conditions. It remains to be seen if any catalytic activity will be observed from these selected particles.

#### Reference List

1. T. M. Dewey, A. A. Mundt, G. J. Crouch, M. C. Zyzniewski, B. E. Eaton, *Journal of the American Chemical Society* 117, 8474-8475 (1995).
2. J. D. Vaught, T. Dewey, B. E. Eaton, *Journal of the American Chemical Society* 126, 11231-11237 (2004).
3. T. M. Tarasow, S. L. Tarasow, B. E. Eaton, *Nature* 389, 54-57 (1997).
4. T. W. Wiegand, R. C. Janssen, B. E. Eaton, *Chemistry & Biology* 4, 675-683 (1997).
5. T. M. Tarasow, S. L. Tarasow, C. Tu, E. Kellogg, B. E. Eaton, *Journal of the American Chemical Society* 121, 3614-3617 (1999).
6. T. M. Tarasow, S. L. Tarasow, B. E. Eaton, *Journal of the American Chemical Society* 122, 1015-1021 (2000).
7. D. Nieuwlandt, M. West, X. Q. Cheng, G. Kirshenheuter, B. E. Eaton, *Chembiochem* 4, 651-654 (2003).
8. L. A. Gugliotti, D. L. Feldheim, B. E. Eaton, *Science* 304, 850-852 (2004).
9. L. A. Gugliotti, D. L. Feldheim, B. E. Eaton, *Journal of the American Chemical Society* 127, 17814-17818 (2005).



Bio Molecular Materials Contractor's Meeting, Aerial Conference Center, Warrenton, Virginia, MA, November 4-7, 2007

Research Project Title: "Influence of Surface Chemistry and Folding Free Energy on Protein Adsorption"

Researchers and address:

Sanat Kumar

Department of Chemical Engineering, Columbia University, New York, NY.

Georges Belfort

Howard P. Isermann Department of Chemical and Biological Engineering, Rensselaer Polytechnic Institute, Troy, NY 12180-3590, USA, and

Program Title: Materials Discovery. Design and Synthesis, Material Science and Engineering Division, Office of Basic Energy Science, US Department of Energy.

Project Monitor: Dr Aravinda M. Kini.

### **Scope of Work**

There is an increasing interest in revealing and controlling the structural behavior of adsorbed and covalently-bound or tethered proteins at solid surfaces. Protein adsorption on solid substrates has been extensively studied, however, little, if any, work has been conducted to understand the stability of surface-tethered proteins. For certain protein surface applications like pattern recognition, protein micro-arrays, biosensors, and biophysical studies, it is critical that the native state of the protein on the surface remains stable. The stability of tethered proteins can be affected by the presence of solid substrates and can depend on the site of tethering, entropic loss upon tethering and energetics. In this work we shall combine experiments and theory to understand the effect of surfaces on protein behavior, especially focusing on their adhesion behavior.

### **Stability of proteins tethered to solid substrates: Chemical and thermal excursions**

Surface properties, such as exposed functional groups, surface restructuring and surface topology, affect thermodynamic stability of tethered proteins. There exist many well-developed techniques to monitor protein unfolding in solution. There are hardly any methods to monitor unfolding of surface-tethered proteins in solution. This is likely due to the low concentrations of tethered proteins and the opaque natures of substrates.

In our work experimental observations and theoretical predictions are compared for unfolding of surface-tethered proteins. We probe the adhesion behavior of model proteins (hen egg lysozyme and ribonuclease A) covalently tethered to a gold surface through an alkanethiol self-assembled monolayer by exposing them to a hydrophobic-coated probe under increasing temperature or denaturant concentrations. The experiments were conducted with an atomic force microscope in force-mode by attaching a 10 mm diameter borosilicate sphere to the cantilever tip, so as to measure the adhesion energy between the protein and various functionalized surfaces. Using adhesion energy as a function of concentration of chemical denaturant or temperature, we were able to follow the unfolding process of tethered proteins. The temperature dependence of adhesion energy with tethered proteins passes through a maximum. The drop in the adhesion energy beyond the adhesion maxima is attributed to dominant protein-protein interactions just after the proteins unfold. Once the proteins unfold, there is a propensity for the unfolded domains to aggregate via hydrophobic or other interactions. We also show that the drop in the adhesion energy beyond the maxima is irreversible. The results were also compared with those in free

solution (*sans* surfaces). To understand the observed behavior, computer simulations of simple lattice proteins which are grafted to a surface were conducted.

The RPI group (Dr. G. Belfort and PhD student, Gaurav Anand) will continue to focus on the experimental aspects of the grant and (i) measure the amount of protein adsorption and protein-surface adhesion for three different model proteins on a variety of surfaces, varying from ones with well defined surface chemistries to ones which are relevant to practice, and (ii) measure the changes in protein conformation on adsorption and understand how these are affected by chain conformation in the bulk solution. The Columbia group (Dr. S. Kumar and PhD student, Sumit Sharma) will couple these experimental ideas to theoretical models with hierarchically increasing levels of complexity so as to predict the relative importance of folding thermodynamics and surface energetics during adsorption, and surface induced conformational changes.

### **Future Plans**

Looking out we find it very interesting that the adhesion is maximized, not at the bulk melting temperature, but rather at some lower temperature. We speculate that this reflects the fact that proteins tend to unfold more readily at surfaces than in the bulk. Under conditions where the proteins is unfolded, there is a competition between protein aggregation and adhesion: in contrast, when folded the only dominant mechanism is the adhesion. While this argument qualitatively rationalizes the measured adhesion trends, to understand this issue in more detail we shall conduct circular dichroism experiments to examine if indeed chain conformations correspond to more unfolded ones at the onset of the adhesion “transition”. (In this context it is unclear if CD can be used under such conditions, but this is an issue we are focusing on currently). A second aspect we shall also study is the role of the exposure time (i.e., the contact time between the AFM tip and the protein) on the location of this adhesion maximum. It is precisely in this context that theory will play a crucial role: we are currently simulating the behavior of proteins under such situations to examine how these different variables affect the measured adhesion.

# Interfacial Friction of Multi-tiered Thin Films

Lynden A. Archer

School of Chemical and Biomolecular Engineering

Cornell University, 14850

## Introduction

In a series of recent studies, Zhang and Archer investigated interfacial friction and adhesion characteristics of one and two-component mixed alkylsilane self-assembled monolayers (SAMs) tethered to oxidized silicon. The goal of this work was to determine the effect of molecular-level disorder in the outermost, *canopy*, layer of the films on their interfacial properties.<sup>1-3</sup> We found that provided the packing density is kept the same, mixed SAMs comprised of a blend of short and long chains manifest lower friction coefficients, and better wear characteristics than pure, single-component SAMs. This finding has been rationalized using a simple Eyring model for the friction force,  $f$ , produced by a thin, viscoelastic lubricant film at an interface. Specifically, this model predicts that the friction force between surfaces grafted with a polymer layer with characteristic relaxation time  $\tau_0$ , moving at relative velocity  $V$ , under a normal load  $N$ , can be predicted using the formula,<sup>1</sup>

$$f = \frac{A}{\phi} [kT \ln(v/V_0) + Q] + \frac{N\Omega}{\phi} \quad (1)$$

Here the macroscopic sliding velocity  $V$  and microscopic or local exchange velocity  $v$  of species in the thin film are related by,  $v = V(1 - \exp[-\delta/V\tau_0])$ ;  $Q$  is the potential barrier neighboring molecules exert on a test molecule in the film. It quantifies restrictions imposed by the neighbors on motion of the test molecule;  $\Omega$  and  $\phi$  are respectively, the pressure and stress activation volumes; and  $A$  is the “real” contact area between the surfaces. It is therefore a function of  $N$ . As is the case for any Eyring-type models,  $\phi$  is a coarse grained quantity and therefore lacks a precise molecular definition. It can be roughly thought of as the volume of the fundamental fluid units that move in response to an applied shear stress. Whether this volume is the actual volume occupied by single molecules in the lubricant film, or of subsections (chain segments), it is anticipated to be larger in materials with less interfacial crowding and higher free volume.

The combination of surface protection provided by a well-ordered SAM under-layer tethered to the substrate, and the higher mobility of molecular segments in the canopy of the mixed SAMs, points to a potential general strategy for designing low-friction coefficient lubricant coatings for nano- and micron-scale interfaces. Coatings should possess a two-layer structure: an inner densely packed sublayer, which protects against asperity penetration and direct contact between surfaces, and an outer canopy layer possessing high, liquid-like mobilities and low shear resistance, serving as the effective lubricant.<sup>4</sup> Figure 1 illustrates the general configuration of the proposed

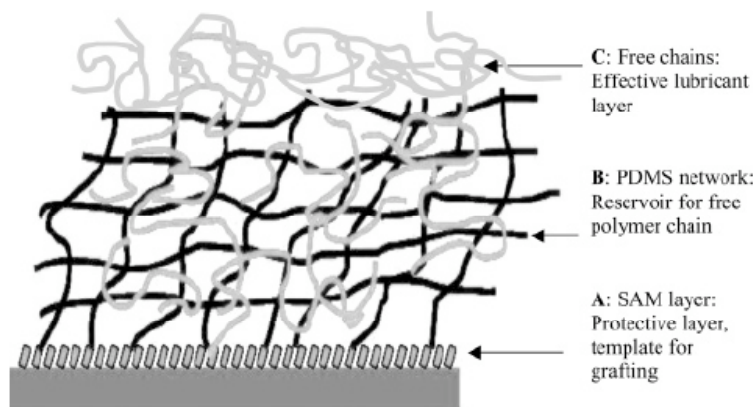
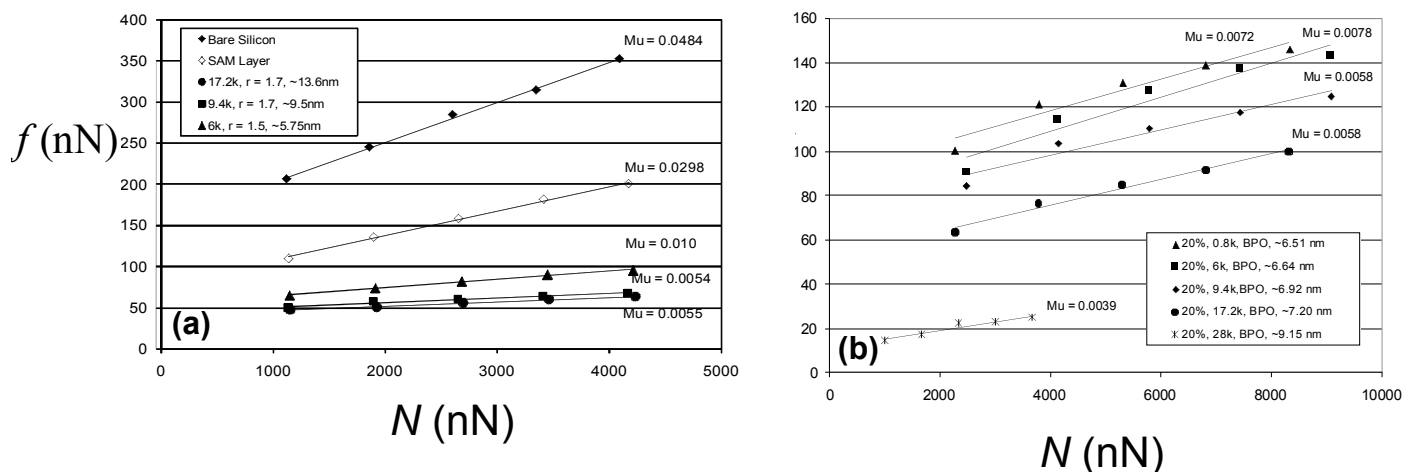


Figure 1. Schematic of tethered, three-tiered, thin film lubricant.

lubricant systems. Component A is a densely packed SAM with reactive terminal functional groups. This SAM *underlayer* simultaneously acts as a protective barrier to asperity and/or moisture penetration and provides the template for chemical tethering of subsequent tiers of the coating. The second component (B) is a thin film comprised of a cross-linked polymer network, which is chemically tethered to the SAM surface. This network layer is designed to function as a container or reservoir for free, mobile polymer chains (component C in this model). These chains are anchored to the substrate by physical, secondary bonds they form with the network, but are otherwise free to diffuse. Their relatively high mobility in the network is expected to simultaneously enhance the lubrication properties of the coating and to permit continuous replenishment of lubricant (*self-healing*) at the network surface. Some features of the proposed lubricants are similar to biological lubricants in synovial fluid. Specifically, these materials also combine high mobility of polymer chains, such as the sodium salt of hyaluronic acid, with mechanical reinforcement provided by transiently coordinated proteins, e.g. albumin and globulins, and a porous, tethered collagen layer, to provide exceptional lubrication ( $\mu = 0.002-0.01$ ) in bone joints.<sup>5-6</sup> I will show that without efforts to optimize their performance, tethered lubricants with the structure depicted in Fig. 1 manifest friction coefficients  $\mu$  that approach those reported from canine bone-joint studies of synovial fluid.<sup>6</sup>

### Friction Coefficient of Thin Cross-linked Polymer Films

The interfacial friction force measured using cross-linked poly(dimethyl-siloxane) (PDMS) networks tethered to a vinyl terminated SAM layer are reported in Figures 2(a) and 2(b). Friction force measurements were performed in a controlled-humidity, clean-room environment using a Dimension 3100 (Digital Instruments) atomic force microscope operated in the so-called lateral force microscopy (LFM) mode, and outfitted with a 5  $\mu\text{m}$  spherical bead probe. PDMS networks were formed by chemically cross-linking vinyl capped difunctional PDMS chains spin coated from a 20 weight percent solution in toluene onto a vinyl terminated SAM layer tethered to the substrate. Figure 2(a) summarizes results for PDMS molecular weights ranging from 6,000 to 28,000 g/mol, cross-linked using tetrakis(dimethylsiloxy) silane in the presence of a platinum-based catalyst.<sup>7</sup> The ratio  $r$  of cross-linker to PDMS chains used to prepare the respective film specimen is an important characteristic of this chemistry and are provided in the legend. A free radical chemistry, based on benzoyl peroxide (BPO), was used to cross-link the networks used for friction measurements reported in Figure 2(b).<sup>5</sup> To facilitate comparisons, the friction coefficients,  $\mu$ , extracted from the slope of straight line fits to the  $f$  versus  $N$  data are provided.  $\mu$  values for the bare substrate and for the substrate after functionalization



**Figure 2.** Friction force vs. normal load for a PDMS network tethered to a vinyl terminated SAM. (a) Tethered polymer networks prepared using tetrakis(dimethylsiloxy) silane; (b) Networks prepared using benzoyl peroxide.

with the SAM layer are also provided in the figure. Thickness of the lubricant films was characterized by ellipsometry, this data is provided in the figure legends.

It is apparent from the results in both figures that quite low friction coefficients can be achieved using multi-tiered coatings, even without the free chains. It is also observed that the cross-linking chemistry has only a small effect on the interfacial friction coefficient and that the networks with the highest molecular weight between entanglements (i.e. the lower modulus) generally yield lower friction coefficient values. It is possible to quantify the degree of cross-linking in the networks from swelling and nanoindentation studies utilizing an oligomer of the cross-linked polymer or a low-volatility solvent such as toluene. These studies are currently underway and are expected to provide important insight into the physical processes responsible for the exceptionally low friction coefficients observed.

### Friction Coefficient of Thin Cross-linked Polymer Films Containing Free Chains

Both chemistries described in the previous section can be performed using mixtures of unreactive and reactive vinyl-capped, difunctional PDMS. This procedure yields a surface tethered network containing a predetermined fraction of free molecules. Furthermore, if some fraction of the reactive molecules are deliberately chosen to be mono-functional, it is also possible to create networks with controlled levels of disorder or dangling chains.<sup>7</sup> We have used the first approach to create surface

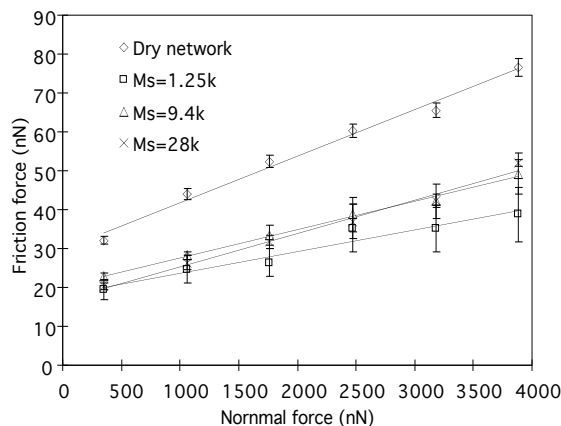


**Figure 3.** Friction force vs. normal load for a PDMS network ( $M_c = 9400\text{g/mol}$ ) swollen by free PDMS chains with different  $M_s$ .

tethered BPO cross-linked PDMS networks containing free PDMS chains of controlled molar mass. Figure 3 summarizes the friction force versus normal load data for one such system. In this case, the molecular weight and volume fraction of the difunctional chains is fixed ( $M_c = 9,400\text{ g/mol}$ ; thickness  $50 \pm 5\text{ nm}$ ), and the molecular weight of the non-reactive, free chains is varied. By comparing the  $f$  versus  $N$  plots for the unswollen (dry) network film with those for films swollen with free chains, it is apparent that the free chains have a profound effect. The friction coefficients are provided in Table 1 to facilitate the comparisons. It is evident from these results that the free chains with the lowest molecular weight produce the greatest reduction in friction coefficient. However, the differential change in friction coefficient achieved

with the free chains is weaker than expected from their bulk viscosities, indicating that their role at the surface is more complex. I will discuss this role using an analysis based on classical lubrication theory.

**Table III** Friction coefficients for samples in Figure 3

Samples	Dry network	$M_s = 1.25\text{ k}$	$M_s = 9.4\text{ k}$	$M_s = 28.0\text{ k}$
Friction coefficient	$0.012 \pm 0.0021$	$0.0052 \pm 0.0013$	$0.0071 \pm 0.0015$	$0.0085 \pm 0.0015$

## Friction Coefficient of Thick Cross-linked Polymer Films

The silane-based cross-linking procedure can be used to create so-called optimal/model networks if the concentration of vinyl-capped chains used in the cross-linking reaction is large. This can be achieved by spin-coating the precursors in a volatile solvent that evaporates on timescales that are short relative to the cross-linking process. This approach leads to much thicker network films, but more precise control over the cross-linking process. Indeed the much greater thicknesses of these networks can facilitate characterization of their structure (from swelling and nanoindentation measurements). Furthermore, by selectively seeding the precursor mixture with monofunctional or unreactive chains these materials can be used to create cross-linked polymer systems with well-defined features for in-depth studies. Finally, using simple chemistries it is possible to introduce ionic side groups into the PDMS to explore the effect of charges on interfacial friction behavior.

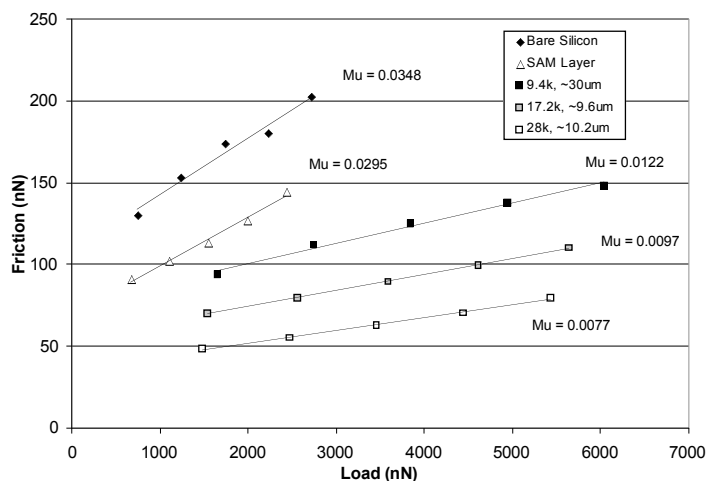


**Figure 4.** Friction force versus load for thick network films.

Interfacial friction data obtained using model PDMS networks synthesized in this manner are provided in Figure 4. Again the friction coefficient  $\mu$  and thickness of the coatings are provided to facilitate comparisons of results obtained using multiple polymer molecular weights. It is apparent from the figure that even these relatively thick networks yield significantly lower interfacial friction coefficients than a SAM layer alone. The friction coefficient values are also generally larger than those found using the thin networks, but considering the large difference in thickness, the effects are relatively small. As was the case for the thin networks, we again observe that the lowest friction coefficients are achieved in networks

with the highest molecular weight strands between cross-links or lower modulus. This means that the multi-tiered coating approach should prove effective for lubricating both small (where ultra thin films are required) and large devices.

## References Cited

- (1) Zhang, Q.; Archer, L. A. *J. Phys. Chem. B.*, **2003**, *107*, 13123.
- (2) Zhang, Q.; Archer, L. A. *Langmuir*, **2005**, *21*, 5405
- (3) Zhang, Q.; Archer, L. A. *Langmuir*, **2006**, *22*, 717
- (4) Zhang, Q.; Archer, L. A. *Langmuir*, **2007**, *23*,
- (5) Linn, F.C. *J. Biomech.* **1968**, *1*, 193
- (6) Mabuchi, K.; Tsukamoto, Y.; Obara, T.; Yamaguchi, T. *J. Biomed. Mater. Research* **1994**, *28*, 865
- (7) Batra, A.; Cohen, C.; Archer, L.A. *Macromolecules*, **2005**, *38*, 7174

## Hyperbranched Conjugated Polymers and Their Nanodot Composites as Universal Bioinspired Architectures (DE-FG02-04ER46141; 2007-2010)

### Sugar-Substituted Poly(*paraphenyleneethynylene*): “Molecular Ropes” for Sensing of Bioterrorist and Disease Related Toxins (DE-FG02-04ER46141; 2004-2007)

PI Uwe H. F. Bunz,<sup>1</sup> Co-PI Mohan Srinivasarao,<sup>2</sup> Co-PI Vincent M. Rotello,<sup>3</sup>

<sup>1</sup>) School of Chemistry and Biochemistry, Georgia Institute of Technology, 901 Atlantic Drive, Atlanta, GA 30332, E-mail: [uwe.bunz@chemistry.gatech.edu](mailto:uwe.bunz@chemistry.gatech.edu)

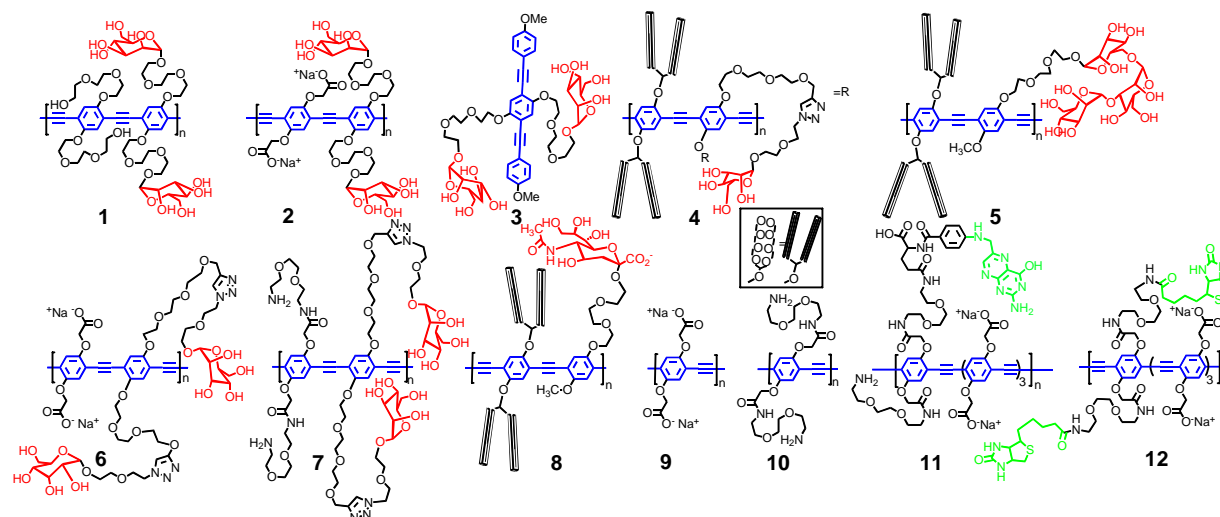
<sup>2</sup>) School of Polymer Textile and Fiber Engineering, Georgia Institute of Technology, 901 Atlantic Drive, Atlanta, GA 30332, E-mail: [mohan@ptfe.gatech.edu](mailto:mohan@ptfe.gatech.edu) (Co-PI 2004-2007)

<sup>3</sup>) Department of Chemistry, University of Massachusetts at Amherst, 910 North Pleasant Street, Amherst, MA 01003, E-mail: [rotello@chem.umass.edu](mailto:rotello@chem.umass.edu) (Co-PI 2007-2010)

## Program Scope

Our program has dealt with the synthesis and property evaluation of water soluble, sugar substituted conjugated fluorescent polymers of the poly(*paraphenyleneethynylene*) (PPE) type. We have harnessed the superb property profile of PPEs resulting from a polymeric fluorescent backbone capable of supporting multiple recognition elements as side chains. In the last two years we have investigated polyvalent interactions of these multiply substituted PPEs with analytes of biological interest, including different proteins and metal cations.<sup>2-10</sup>

For the current funding period (2007-2010) we have shifted our focus towards the the interaction of PPE-types with metal nanoparticles to a) investigate and evaluate the factors determining extent and mechanism of the interaction of the organic semiconductor with the metal nanoparticles, b) use biomimetic principles to design hyperbranched PPEs that show increased “wraparound” interactions with metal nanoparticles in organic and aqueous solution as well as in the solid state, and c) use the formed biomimetic composite materials as probes for bioanalytical purposes and in organic electronics, such as in thin film transistors and photovoltaic devices.

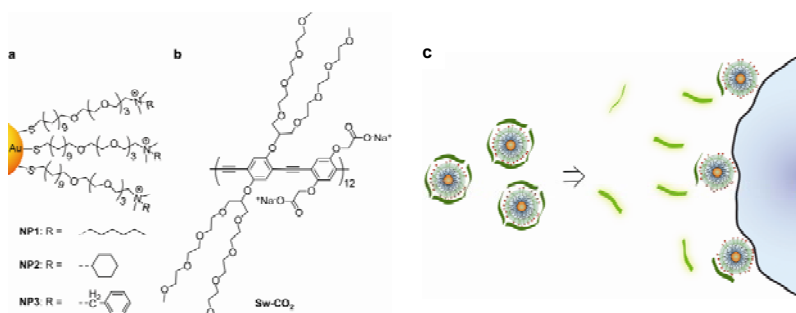


Panel 1. Selection of PPEs with sugar and folate substituents that have been prepared.

## Recent Progress

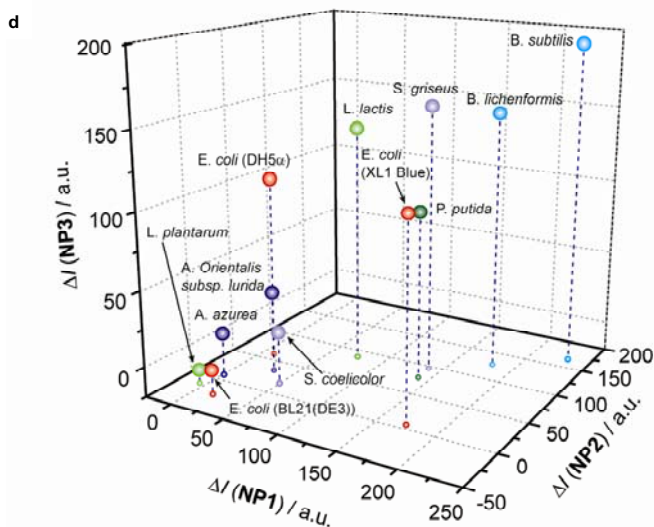
### 1) Metal-Nanoparticles and Conjugated Polymers

Gold nanoparticles efficiently quench the fluorescence of conjugated polymers as the plasmon absorption of the gold nanoparticles overlaps with the emission features of most conjugated polymers, allowing quenching via an energy transfer mechanism. We found that negatively charged proteins but also bacteria can disrupt the preformed nanoparticle-PPE conjugates; PPE is released and differential fluorescence recovery results. The degree of recovery is dependent both upon the chemical structure of the monolayers that protect the nanoparticles as well as upon the identity of the added protein or bacterium. This scheme, utilizing three differently functionalized, positively charged, monolayer-protected gold nanoparticles, allows to easily discern 20 different microorganisms. More importantly, not only different bacteria but as well *different strains of the same bacterium (E. coli) were discerned with this simple but powerful approach through evaluation of the differential fluorescence recovery (Figure 1). Applications are imminent.*



*Applications are imminent.*

**Figure 1.** Detection of pathogens using gold-nanoparticle constructs. a) Structure of the three utilized hydrophobically functionalized gold nanoparticles. b) Structure of the used PPE c) Schematic mechanism of the displacement assay using PPE-gold-nanoparticle constructs d) Three-dimensional plot of the fluorescence increase of the three nanoparticle-PPE constructs upon exposure to different bacteria. All twenty bacteria can be discerned.



### 2) Polyvalent Interactions Mediated by PPEs

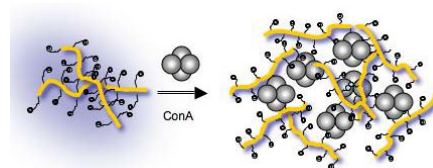


**Figure 2.** Cartoon for the interaction of sugar-substituted PPEs with ConA. In the case of low concentrations a 1:1 complex of ConA and one polymer chain is formed.

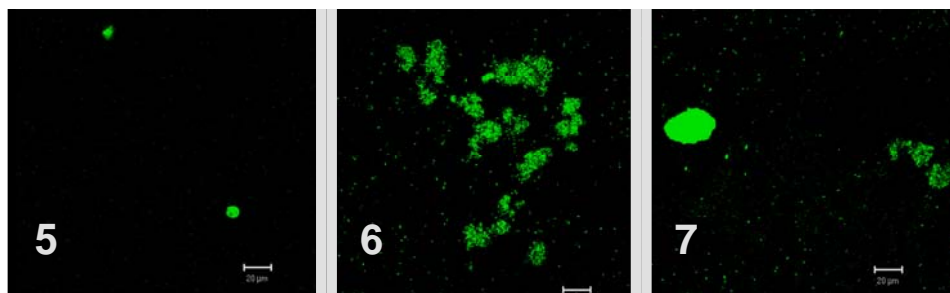


**Figure 3.** Interactions of sugar-substituted PPEs 5-7 with mannose-binding *E. coli* ORN 178; 5 is the most effective polymers in the agglutination of the bacteria.



Sugar substituted PPEs interact strongly with lectins: The polyvalent interactions of the sugar-side chains with Concanavalin A led to efficient quenching of the PPE's fluorescence. Different PPE-ConA complexes form, depending upon the concentration of the PPE and the protein and all show quenched fluorescence. This study aided understanding the interaction of mannose-substituted PPEs with wild-type *E. coli* with the possibility of constructing differential *E. coli* sensor. Figure 3 shows that agglutination of *E. coli* by PPEs is dependant upon the polymer's structure. The ability of a specific PPE to agglutinate *E. coli* is strongly correlated to its propensity to being quenched by Con A.

Combination of PPEs with proteins unlocks powerful synergies in the construction of novel sensory materials, harnessing the fluorescence of the PPE and the specific interactions that proteins feature. We investigated the self-assembly of the carboxylate-PPE **9** and a thiol protease, papain, commercially available on a 100-g-scale. Upon combination of **9** and papain, a protein-PPE complex with slightly decreased fluorescence formed. This complex was very, i.e. by a factor of 10, more sensitive towards the exposure of mercury salts than **9** itself. The recognition of the mercuric ions was selective as shown in Figure 4. Figure 5 shows the proposed mechanism of action.

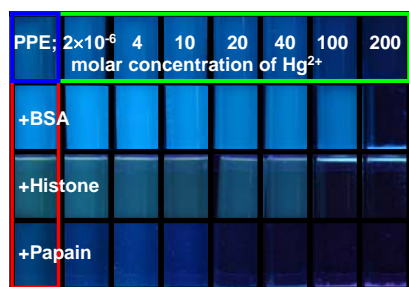


**Figure 4.** Left: Addition of increasing concentrations of  $\text{Hg}^{2+}$  (mol/L) to **9** ( $5 \mu\text{M}$ ) and its protein and polymer complexes ( $5 \mu\text{M}$  protein). Green box: PPE **9**+increasing concentration of  $\text{Hg}^{2+}$ . Red box: **9**•protein complexes. Blue box: PPE **9** alone. All boxed data are controls. The picture shows the fluorescence of the samples under a hand held UV-light ( $\lambda_{\text{max}}$  365 nm). A) PPE **9**•papain complex (**9**:  $5 \mu\text{M}$ ; papain  $5 \mu\text{M}$ ), B) all ten metals added to **9**•papain complex (each metal: 0.4 mM), C) same without  $\text{Hg}$ -ions. Picture shows fluorescence and was taken under a hand-held UV light (excitation wavelength 365 nm).

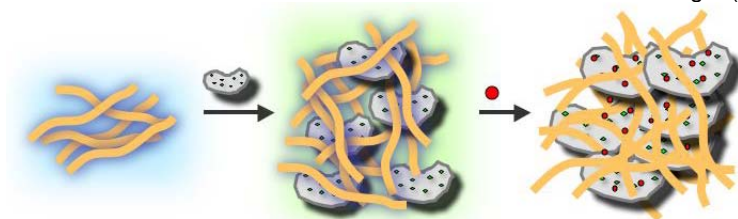
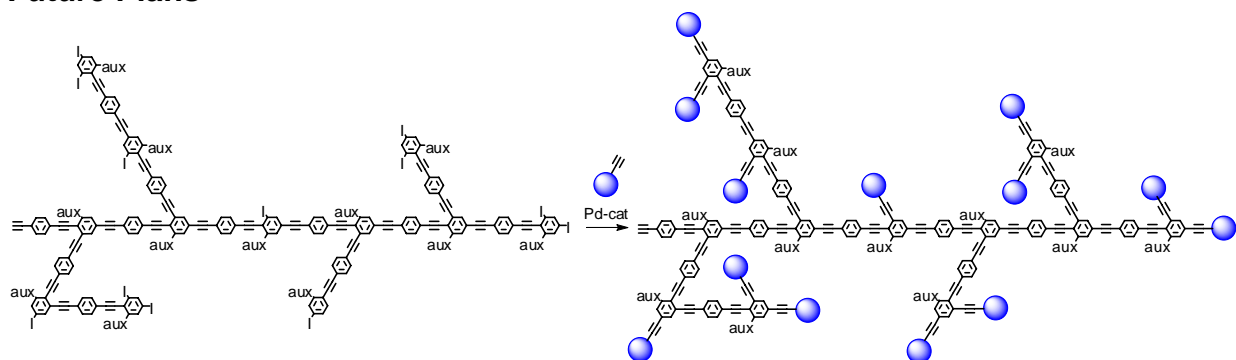


**Figure 5.**  $\text{Hg}^{2+}$  induced agglutination of the **9**•papain. Left: **9** alone. Middle: Electrostatic complex from **9**•papain. Right: The addition of  $\text{Hg}^{2+}$  to **9**•papain leads to its precipitation by crosslinking of papain through  $\text{Hg}^{2+}$ .

## Future Plans



**Scheme 1.** Synthesis of a hyperbranched PPE containing binding elements (blue spheres) for gold nanoparticles.

We plan to synthesize a series of hyperbranched PPEs (Scheme 1) containing iodine end groups; these PPEs will be post-functionalized by coupling to different alkynes carrying functional groups such as nitriles, isonitriles, pyridines, etc interacting with the gold surface.

We will evaluate the strength of the interaction of the hyperbranched PPE with gold nanoparticles to find out which functional group promotes the highest degree of interaction between gold and PPE. We will then compare the magnitude of the interaction of gold-nanoparticles with hyperbranched PPE with the magnitude of the interactions observed in linear and small molecule fluorophores featuring identical ligating substituents or binding elements. We will investigate the strength of the interaction between gold nanoparticle and chromophore by the former's ability to quench the fluorescence of the latter. We will use the Stern-Volmer formalism to quantify the nanoparticle fluorophore interactions in solution and derive meaningful binding constants from these experiments.

## References of DOE sponsored research

- 1) Array-based sensing of proteins using conjugated polymers  
Miranda OR, You C.-C, Phillips R, Kim IB, Ghosh PS, Bunz UHF, Rotello VM, *J. Am. Chem. Soc.* 2007, 129, 9856-9857.
- 2) Detection and identification of proteins using nanoparticle-fluorescent polymer 'chemical nose' sensors  
You CC, Miranda OR, Gider B, Ghosh PS, Kim IB, Erdogan B, Krovi SA, Bunz UHF, Rotello VM, *Nature Nanotech.* 2, 318-323, 2007
- 3) Carboxylate group side-chain density modulates the pH-dependent optical properties of PPEs  
Kim IB, Phillips R, Bunz, UHF *Macromolecules* 2007, 40, 5290-5293
- 4) Use of a folate-PPE conjugate to image cancer cells in vitro  
Kim IB, Shin H, Garcia AJ, Bunz UHF, *Bioconjugate Chem.* 2007, 18, 815-820,
- 5) Reduced fluorescence quenching of cyclodextrin-acetylene dye rotaxanes  
Park JS, Wilson JN, Hardcastle KI, Bunz UHF, Srinivasarao M, *J. Am. Chem. Soc.* 128, 7714-7715, 2006
- 6) Forced agglutination as a tool to improve the sensory response of a carboxylated poly(p-phenyleneethynylene)  
Kim IB, Phillips R, Bunz UHF, *Macromolecules* 40, 814-817, 2007.
- 7) Poly(aryleneethynylene)s with orange, yellow, green, and blue solid-state fluorescence  
Wang Y, Park JS, Leech JP, Miao S, Bunz UHF, *Macromolecules*, 40, 1843-1850, 2007.
- 8) Modulating the sensory response of a conjugated polymer by proteins: An agglutination assay for mercury ions in water  
Kim IB, Bunz UHF, *J. Am. Chem. Soc.* 128, 2818-2819, 2006
- 9) 1,3-Dipolar cycloaddition for the generation of nanostructured semiconductors by heated probe tips,  
Bakbak S, Saxena S, Carson BE, Leech JP, King WP, Bunz UHF, *Macromolecules* 2006, 39, 6793-6795
- 10) Nonspecific interactions of a carboxylate-substituted PPE with proteins. A cautionary tale for biosensor applications  
Kim IB, Dunkhorst A, Bunz UHF, *Langmuir* 21, 7985-7989, 2005
- 11) Sensing of lead ions by a carboxylate-substituted PPE: Multivalency effects  
Kim IB, Dunkhorst A, Gilbert J, Bunz UHF, *Macromolecules* 38, 4560-4562, 2005
- 12) Mannose-substituted PPEs detect lectins: A model for Ricin sensing  
Kim IB, Wilson JN, Bunz UHF, *Chem. Commun.* 1273-1275, 2005
- 13) Click chemistry as a powerful tool for the construction of functional poly(p-phenyleneethynylene)s: Comparison of pre- and postfunctionalization schemes,  
Englert BC, Bakbak S, Bunz UHF, *Macromolecules* 2005, 38, 5868-5877.

# Structured, Stabilized Phospholipid Vesicles

Steve Granick and Erik Luijten

University of Illinois  
Department of Materials Science and Engineering  
1304 West Green St.  
Urbana, IL 61801  
[sgranick@uiuc.edu](mailto:sgranick@uiuc.edu)  
[luijten@uiuc.edu](mailto:luijten@uiuc.edu)

**Program Scope:** The goals of this project are to address the challenge of transforming phospholipid bilayer vesicles into durable and functional self-assembled materials. The methods involve combined experiments and computer modeling involving fundamental studies of the structure and dynamics of nanoparticle-stabilized phospholipid vesicles, and integrated imaging, spectroscopic study, and force measurement. The integrated experimental and computational capabilities that we aim to develop are unique in design and generic in scope.

**Recent Progress:** The interaction of nanoparticles with phospholipid bilayers carries major interest. From the standpoint of biomolecular materials development, it affords the potential to produce liposomes that are stable against fusion even at the highest volume fractions of concentration. From the standpoint of biomolecular function, it affords the potential to develop

“soft” colloidal particles with proteins and other materials with biomolecular function embedded either within the membrane or contained inside. From the standpoint of national security and safety, it also affords venues through which to address how toxic agents function. The findings summarized below revolve around understanding the materials function of how charged nanoparticles interact with phospholipid membranes. A schematic diagram of a nanoparticle in close proximity to a phospholipid membrane is shown in Fig. 1.

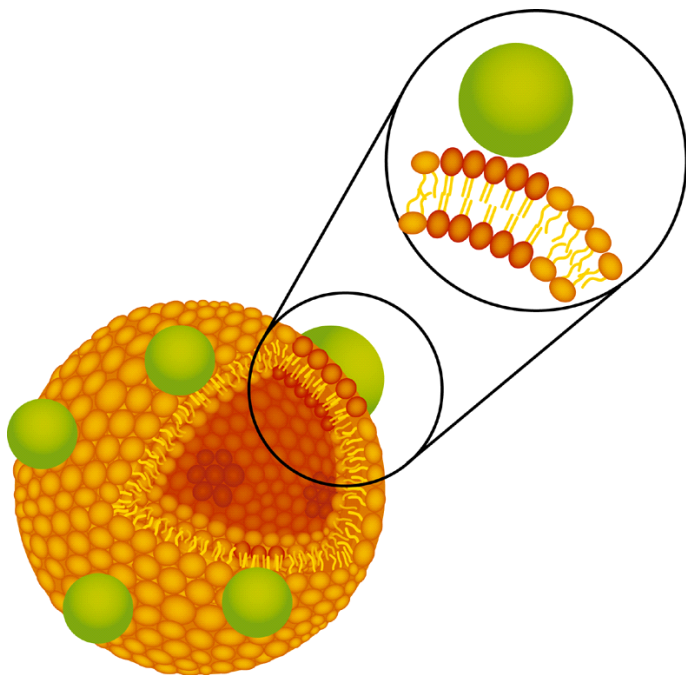


**Fig. 1.** Schematic diagram of a nanoparticle, exposed to a phospholipid vesicle whose bilayer spacing is comparable to the nanoparticle diameter. Research questions predicated on this scenario include:

*stability of the resulting suprastructure; its functions; mechanisms of surface reconstruction, within the phospholipid bilayer, that result upon exposure to the nanoparticle and the reasons why.*

Much has developed recently within this broad context. It emerges that upon adsorption to a phospholipid bilayer, charged nanoparticles (of either electrostatic potential, positively charged or negatively charged) induce major reorganization of the lipids underneath, even to the point of changing the phase of these lipids. Specifically, nanoparticles whose high surface charge density is negative induce reorientation of the phospholipid end-group that induces local reorganization into a denser local phase, located directly beneath the adsorbed nanoparticle. This general conclusion regarding alteration of the phase transition temperature has been confirmed by numerous ancillary studies.

Building on this breakthrough, we have met major progress in developing these new resulting materials to parallel the conventional “hard” colloidal-sized particles that have been studied so extensively. What is common, and what is distinct, as concerns soft colloids? What new materials functions may result? On the fundamental side, how does the underlying physics compare to what is known from so many studies of “hard” colloids?

Even more important is to understand how the local phase of phospholipids located directly underneath the nanoparticle adjusts to this proximity. The experiments conducted to date indicate the likelihood of a *local* phase transition – in other words, the phase state of the phospholipid bilayer depends not only on temperature and pressure in the fashion described so copiously in textbooks, but also on what’s adsorbed. Much recent data, obtained during this grant’s most recent award period, points in this exciting new direction.

Other recent activities include:

- *Highly concentrated liposome suspensions.* We compared the efficacy of cationic and anionic nanoparticles for the stabilization of DLPC, 1,2-dilauroyl-sn-glycero-3-phosphocholine. This is rationalized by considering that because the phospholipid zwitterionic headgroup terminates with positive charge, lipids beneath an adsorbed nanoparticle bind more weakly when the nanoparticle charge is cationic. Going beyond the earlier qualitative study, here single-particle tracking using epifluorescence imaging is used to quantify the mobility of individual liposomes. The distribution of diffusion coefficients between different liposomes in the sample was quantified. In contrast to the colloid behavior of traditional monodisperse hard-sphere colloids, these soft, flexible colloidal-sized objects remain fluid at 50% volume fraction.
- *Biomolecular functionality.* To address the significant problem of biomolecular functionality in the nanoparticle-stabilized liposomes developed by this project, we explored the access of receptor (streptavidin) to liposome-immobilized ligand (biotin) in cases where the liposomes are stabilized against fusion by allowing nanoparticles to adsorb. It is found that receptor binding persists over a range of nanoparticle surface coverage where liposome fusion and large-scale aggregation are prevented. This indicates that liposome outer surfaces, in the presence of stabilizers, remain biofunctionalizable, and may have bearing on explaining the long circulation time of stabilized liposomes as

drug delivery vehicles.

- *Supported lipid bilayers.* The translational diffusion coefficient ( $D$ ) of lipids located in the outer and inner leaflets of planar-supported fluid DLPC bilayers was discriminated, when polymer adsorbed at low surface coverage to the outer leaflet, using fluorescence correlation spectroscopy (FCS) and iodide quenching of fluorescent dyes located within the outer leaflet. We show that  $D$  slows relative to uncoated lipid and that within experimental uncertainty, its magnitude in both leaflets is the same. Implications of this inter-leaflet diffusion coupling was discussed speculatively.
- *Single particle tracking.* Phase-contrast microscopy and particle tracking algorithms are used to study the near-surface diffusion of poly(*N*-isopropylacrylamide) (PNIPAAm) brush functionalized micron-sized silica microspheres after sedimentation from aqueous suspension onto planar substrates coated with a similar polymer brush above and below the lower critical solution temperature (LCST) of PNIPAAm, 32°C. A small negative charge on the wall and the particles (zeta potential = -6 mV) prevents adhesion above and below the LCST. The near-surface translational diffusion coefficient ( $D_{\text{surface}}$ ) is compared to the bulk-phase translational diffusion coefficient ( $D_{\text{bulk}}$ ), which was measured by dynamic light scattering. We find that  $D_{\text{surface}}/D_{\text{bulk}} \approx 0.6$  at temperatures  $T < 32^\circ\text{C}$  but rises abruptly to  $\approx 0.8-0.9$  at  $T > 32^\circ\text{C}$ . Near-surface diffusion is expected to be slower than bulk diffusion owing to hydrodynamic coupling to the wall implying reduced hydrodynamic coupling at the higher temperatures, perhaps mediated by enhanced electrostatic repulsion above the LCST transition.
- *Spatially and time-resolved measurements.* An invited review article in a prestigious journal synthesized measurements from diverse fields of study to draw attention to the significance of spatially-resolving systems whose ensemble-average differs fundamentally from the spatially-resolved individual elements. Examples were taken from the field of fluid phospholipid bilayers to which macromolecules adsorb; from the field of polymer physics when flexible chains adsorb to the solid-liquid interface; and from the field of lubrication when two solids are squeezed close together with confined fluid retained between them.

**Future Plans:** These exciting new developments will be pursued. In the area of biosensors and nanoparticle stabilization, one problem of intense interest will be to explore the physical mechanism of interaction between phospholipid bilayers and nanoparticles that stabilize them. The methods of investigation will be fluorescence anisotropy, calorimetry, NMR, and advanced computer simulation. In the area of glassy dynamics of nanoparticle-stabilized liposomes, single-particle tracking will be combined with computer simulation to separate system-specific from generic aspects of the surprising phenomenological behavior revealed in our preliminary analysis. In the area of studies of enzymes within the confined space afforded by nanoparticle-stabilized vesicles, experiments and simulation analysis will be initiated at the single-molecule level.

**Publications 2005-2007:**

*“Molecular Motion at Soft and Hard Interfaces: from Phospholipid Bilayers to Polymers and Lubricants,”* S. Granick and S. C. Bae, *Annu. Rev. Phys. Chem.* **58**, 353 (2007).

*“Ligand-Receptor Binding on Nanoparticle-Stabilized Liposome Surfaces,”* L. Zhang, K. Dammann, S. C. Bae, and S. Granick, *Soft Matter* **3**, 551 (2007).

*“Cationic Nanoparticles Stabilize Zwitterionic Liposomes Better than Anionic Ones,”* Y. Yu, S. M. Anthony, L. Zhang, S. C. Bae, and Steve Granick, *J. Phys. Chem. C* **111**, 2833 (2007).

*“Inter-Leaflet Diffusion Coupling when Polymer Adsorbs onto One Sole Leaflet of a Supported Phospholipid Bilayer,”* L. Zhang and S. Granick, *Macromolecules* **40**, 1366 (2007).

*“Brush-Sheathed Particles Diffusing at Brush-Coated Surfaces in the Thermally-Responsive PNIPAAm System,”* H. Tu, L. Hong, S. Anthony, P. V. Braun, S. Granick, *Langmuir* **23**, 2322 (2007).

*Molecular Dynamics Simulations of the Transport Properties of a Single Polymer Chain in Two Dimensions,* T. P. Desai, P. Keblinski, S. K. Kumar, and S. Granick, *J. Chem. Phys* **124**, 084904 (2006).

*Dynamical Heterogeneity in Planar Supported Phospholipid Bilayers,* L. Zhang and S. Granick, *MRS Bulletin*, **31**, 527 (2006)..

*How to Stabilize Phospholipid Liposomes (using Nanoparticles),* L. Zhang and S. Granick, *Nano Letters* **6**, 694 (2006); Highlighted: *Science* **311**, 1347 (2006); *Nature Materials* **5**, 249 (2006).

*Methods to Track Single Molecule Trajectories,* S. Anthony, L. Hong, and S. Granick, *Langmuir* **22**, 5266 (2006).

*Nanoparticle-Assisted Surface Immobilization of Phospholipid Vesicles,* L. Zhang, L. Hong, S. Anthony, Y. Yu, S. C. Bae, and S. Granick, *J. Am. Chem. Soc.* **128**, 9026 (2006).

*Charged Polypeptide Diffusion at Very High Ionic Strength,* L. Hong and S. Granick, *J. Polym. Sci. Polym. Phys. Ed.* **43**, 3497 (2005).

*Slaved Diffusion in Phospholipid Bilayers,* L. Zhang and S. Granick, *Proc. Nat. Acad. Sci. USA* **102**, 9118 (2005).

*Lipid Diffusion Compared in Outer and Inner Leaflets of Planar Supported Bilayers,* L. Zhang and S. Granick, *J. Chem. Phys.* **123**, 211104 (2005).

*Electrostatic Stitching in Gel-Phase Supported Phospholipid Bilayers,”* L. Zhang, T. Spurlin, A. A. Gewirth, and S. Granick, *J. Phys. Chem. B* **110**, 33 (2006); Highlighted: *Science* **310**, 1871 (2005).

# Programming Function via Soft Materials

Jeff Moore (PI)

Subtask co-PIs: Erik Luijten, Steve Granick

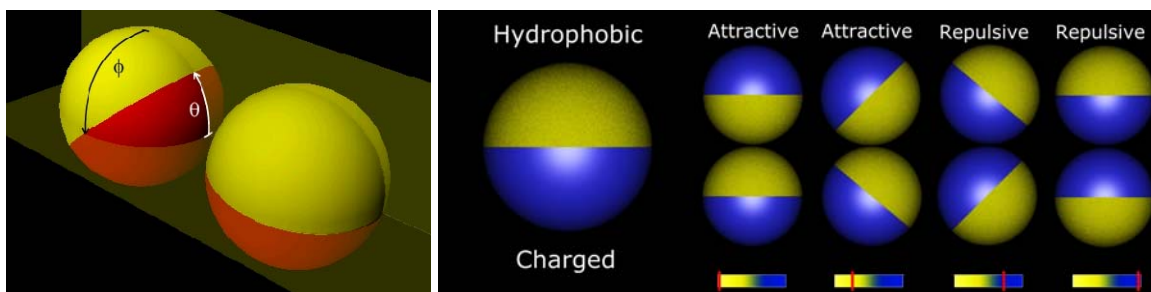
University of Illinois at Urbana-Champaign  
Frederick Seitz Materials Research Laboratory  
Department of Materials Science and Engineering  
1304 West Green Street  
Urbana, IL 61801

[luijten@uiuc.edu](mailto:luijten@uiuc.edu); [sgranick@uiuc.edu](mailto:sgranick@uiuc.edu)

**Program Scope:** This program focuses on the organization of nano-, micro-, and mesoscale objects of dissimilar classes of materials into well-defined macroscale structures with new, complex, and tunable functional behavior. It involves PIs with expertise in materials synthesis, assembly, physical measurement, computer simulation and theory, and is aimed at understanding the assembly of complex building blocks into functional materials.

This abstract describes recent progress and future plans for a specific subtask within this program, namely the study of particles with heterogeneous surface chemistry, so-called “patchy” particles.

**Recent Progress:** Orientation-dependent interactions can drive unusual self-assembly of colloidal particles. We have synthesized colloidal spheres that have different surface chemistries on both hemispheres, and observed their self-assembly behavior in water. In addition, we have performed corresponding Monte Carlo simulations that reproduce the observed structures and provide information on the orientation of the anisotropic colloids within each structure.



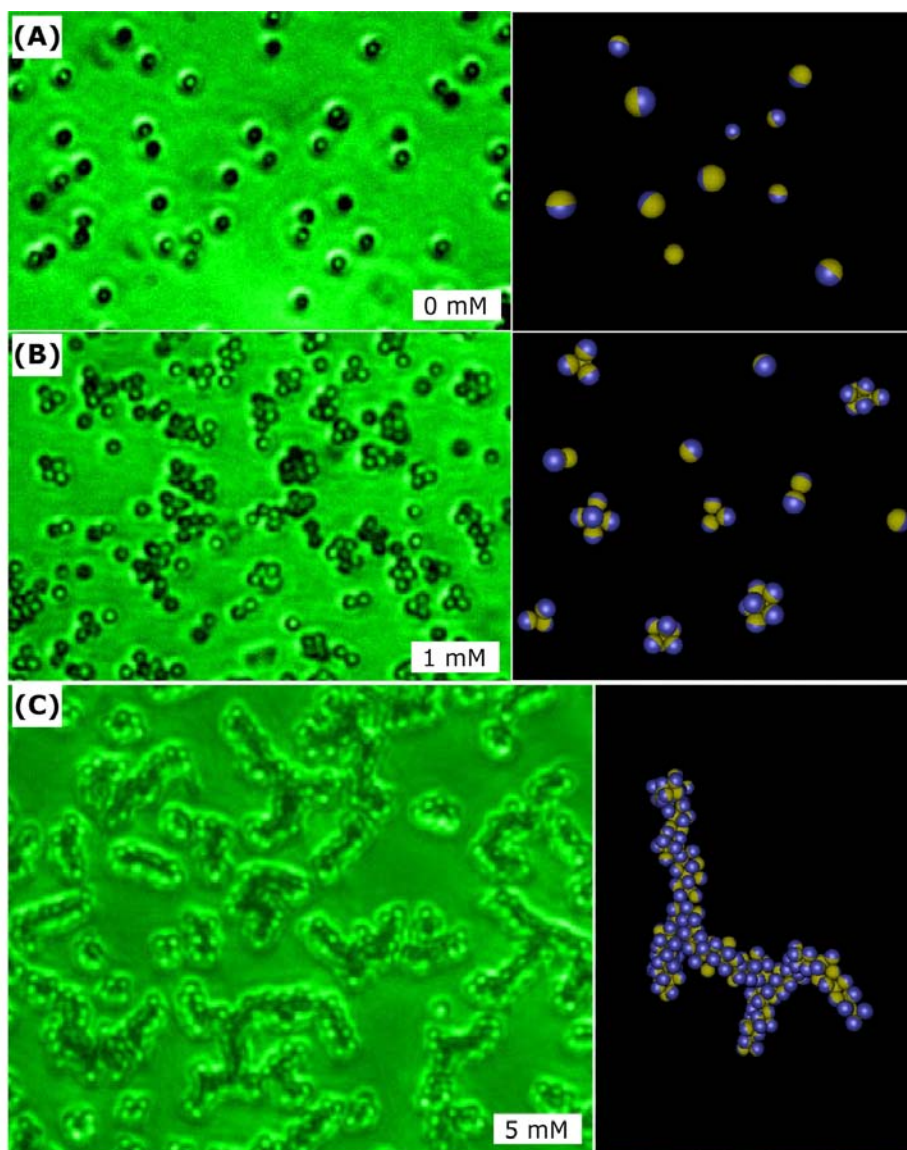
*Different types of “Janus” particles have been synthesized, such as dipolar particles (left), or amphiphilic particles (right). Through a combination of experiments and computer simulations we have been able to demonstrate that these particles aggregate into specific structures that can be controlled by means of parameters such as surface charge density and salt concentration.*

Specifically, we have shown that amphiphilic colloidal spheres, hydrophobic on one hemisphere and charged on the other, assemble in water into extended structures not formed by spheres of uniform surface chemical makeup. Small, compact clusters each comprised of less than ten of these Janus spheres link up, as increasing salt concentration enhances electrostatic screening, into wormlike strings (see figure next page). This study, based on combined epifluorescence microscopy and Monte Carlo simulations, generalizes to colloidal particles the concept of molecular amphiphilicity that is so pervasive and useful in nature and technology.

**Future Plans:** The structures that we have observed are analogous to the micellar shapes adopted by standard molecular amphiphiles, although an agenda for future study will be to understand the delicate question of how their shapes evolve from the dilute concentrations considered here to concentrated suspensions. Our findings can be generalized in several ways. We have recently developed scale-up methods that make it possible to functionalize a wide range of particle sizes, as small as 200 nm, to be chemically asymmetric, giving this concept potential application in industrial practice to replace molecular surfactants in certain functions. Furthermore, other self-assembled structures can be expected when the balance is varied between the respective areas of the hydrophobic and hydrophilic patches, and also when solid surfactants of different sizes are mixed. On the applications side, it is expected that solid surfactants of the kind described here will segregate strongly to liquid interfaces, thus stabilizing emulsions and foams. We conjecture that the wormlike strings (see figure) may also modify suspension rheology as well as serve as vehicles within which to encapsulate cargo for subsequent release.

An extension that can be easily implemented is the use of more complex shapes than spheres. In the same spirit, whereas we have first focused on amphiphilicity because it is one of the most pervasive forms of chemical asymmetry, the exploration of more subtle interactions, such as hydrogen bonding, molecular recognition, and the attachment of macromolecules, offers other potential extensions.





Variation of salt concentration causes amphiphilic particles (diameter  $1\ \mu\text{m}$ ) in aqueous solution to assemble into clusters of various sizes and shapes. The images with green background represent epifluorescence experiments. In the Monte Carlo computer simulations, blue and yellow colors represent charged and hydrophobic hemispheres, respectively. **Panel A** shows discrete particles for the case of particles in deionized water. **Panel B** ( $1\ \text{mM}\ \text{KNO}_3$ ) shows small clusters (up to nonahedra) in equilibrium with one another. **Panel C** ( $5\ \text{mM}\ \text{KNO}_3$ ) shows long, branched wormlike strings. The simulations (right) confirm that the assembly of small clusters into strings occurs as the range of the electrostatic repulsion, relative to hydrophobic attraction, decreases with increasing salt.

## **Publications 2005–2007:**

“Generalized geometric cluster algorithm for fluid simulation,” J. Liu and E. Luijten, Phys. Rev. E **71**, 066701 (2005).

“Interparticle interactions and direct imaging of colloidal phases assembled from microsphere–nanoparticle mixtures,” C.J. Martinez, J. Liu, S.K. Rhodes, E. Luijten, E.R. Weeks and J.A. Lewis, Langmuir **21**, 9978–9989 (2005).

“Structure and stability of self-assembled actin–lysozyme complexes in salty water,” L.K. Sanders, C. Guáqueta, T.E. Angelini, J.-W. Lee, S.C. Slimmer, E. Luijten and G.C.L. Wong, Phys. Rev. Lett. **95**, 108302 (2005).

“Colloidal stabilization via nanoparticle halo formation,” J. Liu and E. Luijten, Phys. Rev. E **72**, 061401 (2005).

“Fluid Simulation with the Geometric Cluster Algorithm,” E. Luijten, Computing in Science and Engineering **8**(2), 20–29 (2006).

“Self-avoiding flexible polymers under spherical confinement,” A. Cacciuto and E. Luijten, Nano Letters **6**, 901–905 (2006).

“Confinement-driven translocation of a flexible polymer,” A. Cacciuto and E. Luijten, Phys. Rev. Lett. **96**, 238104 (2006).

“Effective interactions in mixtures of silica microspheres and polystyrene nanoparticles,” S.A. Barr and E. Luijten, Langmuir **22**, 7152–7155 (2006).

“Salt-induced collapse and reexpansion of highly charged flexible polyelectrolytes,” P.-Y. Hsiao and E. Luijten, Phys. Rev. Lett. **97**, 148301 (2006).

“Translocation of polymers out of confined geometries,” E. Luijten and A. Cacciuto Comp. Phys. Comm. **177**, 150–153 (2007).

## **Program Title: Designing Two-Level Biomimetic Fibrillar Interfaces**

*Anand Jagota*, Department of Chemical Engineering, Lehigh University, Iacocca Hall, Bethlehem PA 18017. 610 867 2820; [anj6@lehigh.edu](mailto:anj6@lehigh.edu)

*Chung-Yuen Hui*, Department of Theoretical and Applied Mechanics, Cornell University, Ithaca, NY 14853. 607 255 3718; [ch45@cornell.edu](mailto:ch45@cornell.edu)

### ***Program Scope:***

The program objective is to study, to design, and to optimize the adhesive strength, toughness, and frictional properties of bio-inspired fibrillar structures. The proposed work combines fabrication and modeling of, and experiments on model fibrillar materials. These include a novel film-terminated fibrillar structure that has demonstrated significantly enhanced adhesion compared to an unstructured, flat control sample. Our approach is to

- a) Fabricate and characterize model two-level structures with superior contact, adhesive, and frictional properties.
- b) Establish theory behind and design principles for these structures.

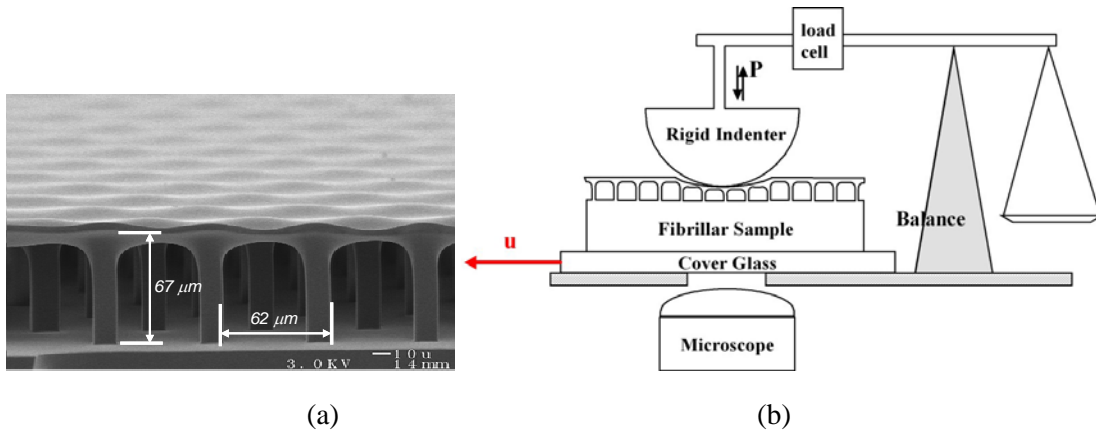
### ***Recent Progress***

We have recently begun an investigation of the frictional properties of our film-terminated fibrillar samples. Figure 1(a) shows a typical scanning electron micrograph of the fibrillar sample, which consists of a thick backing topped by a set of fibrils that themselves are terminated by a film. All components are fabricated using poly(dimethylsiloxane) (PDMS) by molding it into microfabricated silicon wafers [1,2]. The fibrils have square cross-sections with 10 microns sides. They have variable length and inter-fibrillar spacing.

While we and others have recently studied how such fibrillar structures can enhance adhesion as measured by normal separation of the interface, little work has been conducted on the behavior of these novel materials under shear [1-4]. In contrast, most adhesion enhancement in natural systems has been found under shear loading [5,6]. The connection between adhesion and friction is an important fundamental problem [7,8] and our fibrillar architecture can provide a model material for its study.

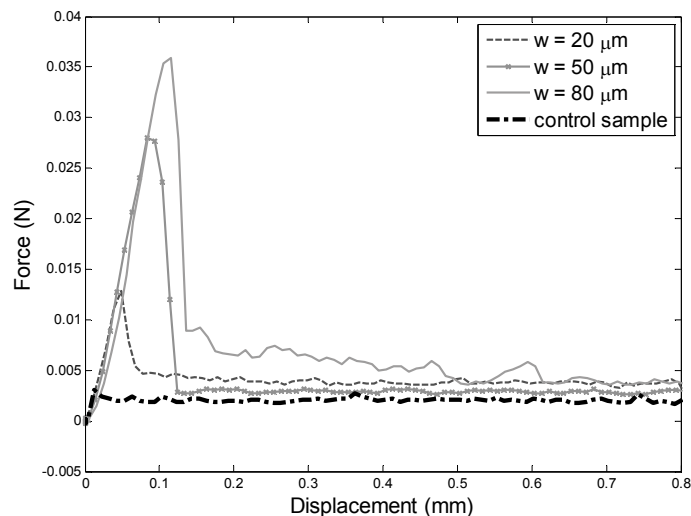
Our experimental set-up is shown schematically in Figure 1(b). A fixed vertical load is applied to the specimen through a spherical glass indenter; its magnitude is controlled by a mechanical balance. The assembly is mounted on an inverted optical microscope and the sample is pulled horizontally at a fixed rate by a DC motor. Simultaneously, we record the force that resists this motion as well as images of the contact region.

Figure 2 shows typical measured shear force-displacement traces for three fibrillar samples with fibrillar length of 30 microns and three different values of inter-fibrillar spacing,  $w$ . Also shown is the force-displacement trace for an unstructured flat control sample. A striking feature is the presence of a “static friction” peak that signifies initiation of steady sliding. The peak shear force is many times greater in magnitude than both the shear force required to sustain steady sliding (the “dynamic friction” force) and the shear force required to initiate sliding in the control. For the fibrillar samples the static friction peak increases with inter-fibrillar spacing. The effective work of adhesion, which we have measured in an independent experiment, also increases with inter-fibrillar spacing in a similar fashion, suggesting a connection between adhesion and friction. Another interesting feature of these data is the fact that the dynamic friction force is nearly the same for all inter-fibril spacings. In addition, it is very similar in magnitude to that of the flat control.



**Figure 1.** (a) Scanning electron micrograph of a synthetic fibrillar array with a terminal thin film. (b) Schematic drawing of the experimental set-up for friction measurements.

Figure 3 shows a sequence of optical micrographs of the contact region at different shear displacements applied at a constant rate. Darker areas indicate better contact between the film and the indenter. The top and the bottom of the fibril image separately and differently, which allows us to measure the deformation of each fibril. Contours of relative shear displacement of the top and bottom of the fibrils are shown below each micrograph. Figure 3(a) represents the initial contact under normal compression with no applied shear, as is apparent also from the contour plot. With the application of shear displacement buckling is observed at the leading edge of the contact and the region of intimate contact decreases in size. At a critical load, represented by Fig 3(c), there is a sudden reduction of the size of the region with intimate contact and this is accompanied by the large load drops seen in Figure 2 and in the contour plots, after which steady sliding commences. Note that the contact region during sliding shows a different contrast than that seen before the peak load. We interpret this to be due to partial contact between the film and the indenter due to the detachment of the film from the indenter between fibrils.



**Figure 2** Shear force as a function of shear displacement for fibrillar samples with inter-fibril spacing of 20, 50 and 80 microns and for a flat control sample.

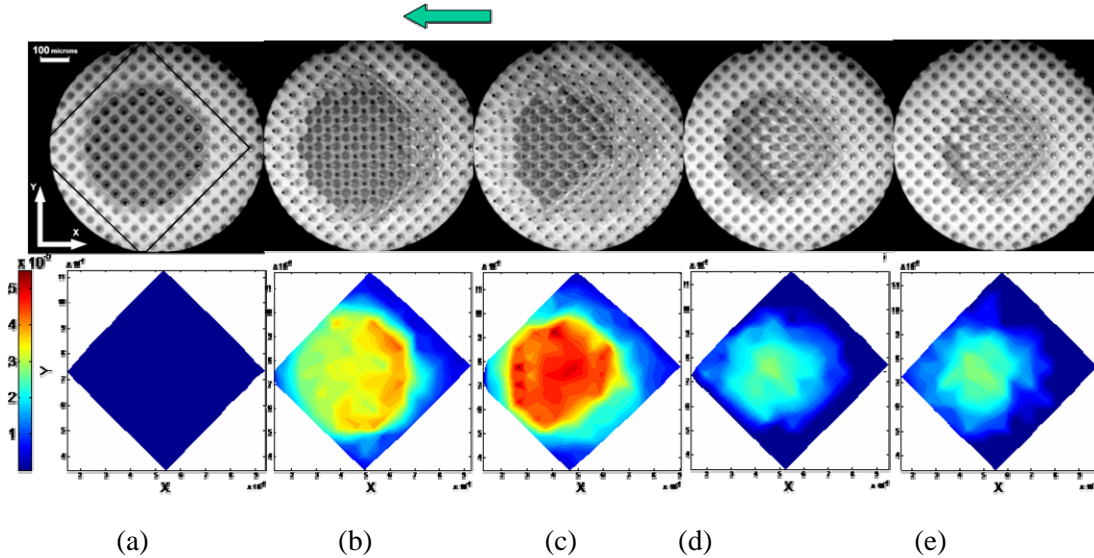


**Figure 3** Sequence of images and corresponding contours of relative shear displacement between the top and bottom of the fibrils. The green arrow represents the direction of motion of the sample relative to the (fixed) indenter. (a) Initial contact; zero shear displacement, (b) Static contact under shear, (c) Static contact under shear at peak load, (d) Contact just beyond peak load, (e) Contact under steady sliding.

Our experiments show that the fibrillar structure has very useful and unique properties under shear. For example, the static coefficient of friction of our material can be an order of magnitude greater than that of the control, without significantly altering its dynamic friction. Experiments have revealed several novel and interesting phenomena that require further study. For example, there is strong experimental support for the hypothesis that sliding is accommodated by the propagation of a Schallamach-like wave [9]. This proposed mechanism explains why the dynamic friction is unaffected by fibrillar architecture and is the same as for the flat control.

### ***Future Plans***

- 1) *Experimental:* Three of the most important and scientifically interesting characteristics of fibrillar structures are their behavior under shear loading, the relationship between adhesion and friction, and their performance against rough surfaces. Our plans are to explore all three experimentally using our film-terminated fibrillar design. We will systematically study the effect of normal load and loading rate on static and dynamic friction. We will correlate these measurements with normal indentation and other adhesion measurement techniques. It is known that small amounts of roughness can actually enhance adhesion and that natural fibrillar interfaces maintain their adhesion against rough surfaces. To determine if one can design materials with better performance against rough surfaces using a fibrillar architecture, we plan to perform adhesion experiments, for example, indentation with a roughened sphere.
- 2) *Theoretical:* We propose that the static friction peak is governed by a mechanical instability and that the dynamic friction force is controlled by Schallamach-like waves. We will develop theoretical models for the deformation of the fibrillar material under combined normal and shear loading. While this model will share some characteristics

with conventional contact mechanics, there are several features of this material that require considerable new development. For example, fibrils under the contact (see Fig 3(c)) are subjected to relative shear displacement in excess of their length. This circumstance leads to nonlinear coupling between normal and shear deformations. The coupling results, for example, in the initial increase of contact area with shear loading, in contrast to that predicted by current theories [7,8].

- 3) *New Designs.* We are currently pursuing two new designs. The first is an attempt to optimize the properties of the 2-level film-terminated structure. Two features require improvement. The first is due to the fact that our best performance is limited by the strength of the fibrils. We are developing new fabrication techniques with non-uniform fibril cross-sections and materials to optimize adhesion and friction properties. The second attempt is to develop a new approach that provides the characteristics we consider to be important: a fibrillar stalk, a compliant plate-like terminal element, and a design with directional properties. Our approach is to use a core-shell structure where the plate-like element is formed at the tip of a core-shell fiber by selective removal of the core. In model preliminary experiments with inclined fibrils we have demonstrated significantly enhanced friction by this technique. Our goal is to implement this design on an array.

### **References**

1. Nicholas J. Glassmaker, Anand Jagota, Chung-Yuen Hui, William L. Noderer, Manoj K. Chaudhury, *Proceedings of the National Academy of Sciences (USA)* **104** [26] 10786-10791 (2007).
2. W.L. Noderer, L. Shen, S. Vajpayee, N.J. Glassmaker, A. Jagota, C-Y. Hui, *Proceedings of the Royal Society A* **463** 2631-2654 (2007).
3. Gorb S., Varenberg M., Peressadko A., and Tuma J., *J.R.Soc.Interface*:2006 1-6.
4. S. Kim, M. Sitti, *Applied Physics Letters* 89 (26): 261911 2006.
5. Autumn, K., Liang, Y.A., Hsieh, T.S., Zesch, W., Chan, W.P., Kenny, T.W., Fearing, R. & Full, R.J. 2000 *Nature* **405**, 681-685.
6. Irschick, D. J., Austin, C. C., Petren, K., Fisher, R., Losos, J. B., & Ellers, O. (1996) *Biol. J. Linn. Soc.* **59**, 21-35.
7. K.L. Johnson, *Proc. R. Soc. Lond. A.* (1997) **453** 163-179.
8. A.R. Savkoor, G.A.D. Briggs, *Proc. R. Soc. Lond. A* (1977) **356** 1684 (103-114).
9. A. Schallamach, *Wear* (1971) 301.

## VIRUS ASSEMBLIES AS TEMPLATES FOR NANOCIRCUITS

Michael T. Harris<sup>1</sup> and James N Culver<sup>2</sup>

mtharris@ecn.purdue.edu, jculver@umd.edu

<sup>1</sup>School of Chemical Engineering, Purdue University, West Lafayette, IN 47907-1283

<sup>2</sup>Center for Biosystems Research, University of Maryland Biotechnology Institute,  
College Park, MD 20742-4450

### Program Scope

Bio-nanoscale technologies hold the potential to revolutionize a broad range of energy, manufacturing, environmental, and medical processes. Already, the microfabrication of devices that contain biologically active components such as enzymes, antibodies, and nucleic acids have transformed biosensing, genome/proteome analysis and drug discovery. Increasingly, bio-inspired processes are also being looked to as potentially cost effective methods to produce microelectronic devices. Accomplishing this goal will require an integrated approach utilizing expertise in a broad range of scientific and engineering fields. This proposal brings together expertise in materials chemistry/colloids and interfacial engineering (Dr. Harris) and protein engineering/biology (Dr. Culver) to address the application of biologically derived molecules for the production and patterning of nanoparticles. Specific efforts in this project focus on the use of a well-defined plant virus, *Tobacco mosaic virus* (TMV) to develop strategies for the assembly, patterning and functionalization of nanoscale surface features and devices. In the long term, the parameters and processes developed in this study should have broad application for the engineering of a diverse array of biologically derived templates.

### Recent Progress

Self-assembly of virus-structured high surface area nano-materials and their application as battery electrodes. One of the main goals in this project has been to develop strategies for the uniform coating of TMV, a 300nm x 18nm nanotube template, with various reactive metals. Previous efforts to coat biological molecules including TMV have generally resulted in irregular depositions of metal clusters onto the outer surface of the bio-template. These irregular coatings generally lack the density and uniformity needed to function effectively as conductive wires or electrodes, representing a significant obstacle to the integration of these templates into useful devices. To overcome this obstacle we used a novel combination of genetically engineered viruses and electroless plating techniques to obtain near uniform coatings of patterned virus templates (Fig. 1A). Genetic alterations introduced novel cysteine residues that conferred orientational control in the attachment of TMV to gold surfaces. Room temperature electroless plating methods were then used to coat surface attached TMV templates with nickel and cobalt. These processes yield evenly coated virus templates containing confluent metal clusters of ~60nm in diameter. The result is a procedure for significantly increasing the reactive surface area of an electrode or other device. We estimate that the presence of the virus increases the surface area ~500 fold, providing an area of ~583m<sup>2</sup> per 100ng of virus.

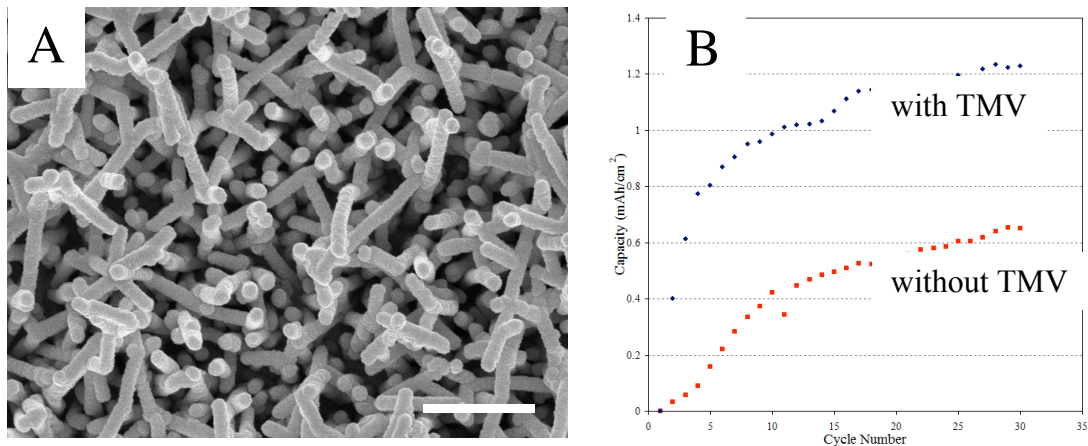


Fig. 1. TMV assembled high surface area battery electrode. A, Surface assembled TMV nanotemplates coated with nickel. Bar = 300nm. B, Enhanced battery electrode capacity using surface assembled TMV templates.

Within a nickel-zinc battery system, the incorporation of virus assembled electrode surfaces more than doubled the total electrode capacity (Fig.1B). This self-assembly process works at room temperature and under mild buffer conditions and produces nanostructured materials that are uniformly oriented and coated. The density of surface assembled virus and thus available surface area was easily tuned by varying the virus concentration of the assembly reaction. A simple electroless deposition method allowed the efficient and uniform metal coating of the assembled virus. Once coated, surface attached viruses were highly stable under a variety of conditions including repeated washings with acetone and vacuum drying. This stability was apparent in electrode performance, with FESEM analysis showing no noticeable loss in the structure of the coated viruses after 30 charge-discharge cycles. In summary, we have developed a robust method for the oriented self-assembly of metal functionalized virus nano templates onto gold surfaces.

Patterning self-assembled viral nanotemplates. Additional studies have focused on patterning TMV based templates via nucleic acid methodologies. Previously, we demonstrated that partial exposure of the viral 5' nucleic acid sequence could be used to attach virus templates onto silica chips containing patterned probe DNA. This patterning technique represents a significant advancement toward developing TMV as a bio-template for use in creating nano-circuits. More recently we have sought to expand the usefulness of this system to permit the patterning of differentially labeled viral templates (Fig. 2). Under the current scheme hybridization is limited to only sequences within the TMV 5' end, making it impossible to selectively address multiple viral templates at same time. To address this problem we developed a simple linker DNA approach as a means to add novel sequence specificities to the viral templates, making it possible to address differentially labeled viral templates to different locations on the same substrate. This process greatly aids in creating surface arrayed templates each with a different functionality such as sensor recognition or catalyst activity.



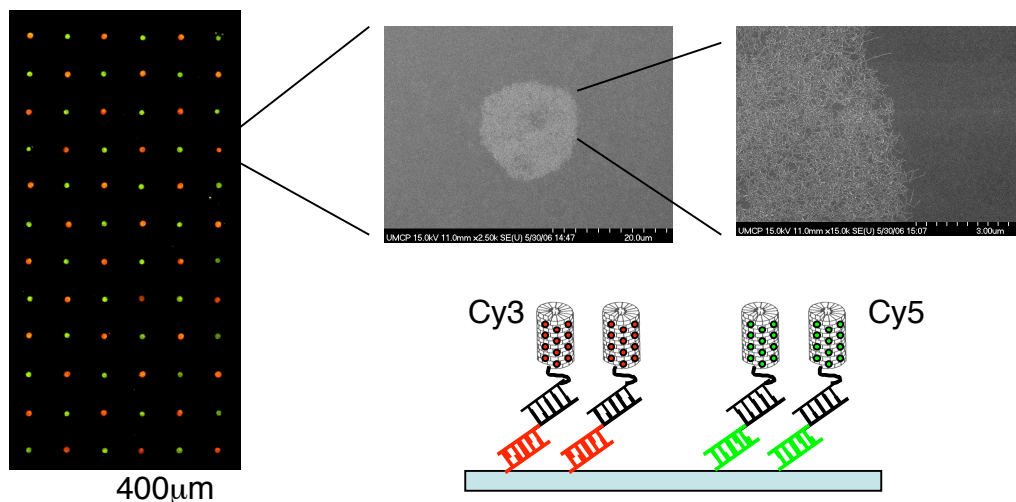


Fig. 2. Simultaneous patterning of differentially labeled TMV nanotemplates (Cy3 vs Cy5) via DNA probe specific addresses.

Multilayer coatings of viral assembled nanotemplates. Mixed or multilayered inorganic coatings can be used to introduce novel characteristics and functionalities into a device. We have recently developed strategies for the layered deposition of inorganic compounds onto the surface of TMV. Silica-coated TMV is successfully used as a template for platinum and palladium metal nanoparticle deposition. The coatings were comparable to previous improvements made over the wild-type virus using genetically modified TMV for the case of platinum, and were improved in the case of palladium over similar procedures on the unmodified wild-type TMV template. These results show the first layering of inorganic materials obtained using a virus template. This is advantageous as silica coating enables the use of organic solvents that would normally degrade the biological templates, opening the potential for a wide array of new coating techniques. Future potential for this technique also lies in the ability to alternate between silica and metallic nanoparticle shells with the intent to create nanomaterials with novel conducting or surface-reactive properties.

### Future Plans

We continue efforts to refine and expand the potential use of our continuously coated virus arrays as battery electrodes and capacitors. Specifically, we are investigating other electrode metals and chemistries with the aim of developing more robust energy generating and storage devices. We also continue efforts to optimize coating strategies for additional metals and inorganics, such as palladium, platinum, zinc and silver. Our goal is to assemble both cathode and anode electrodes using differentially coated virus templates. In addition, efforts are planned to expand upon our abilities to assemble and pattern virus templates onto different surfaces. At present we have utilized hybridized DNA probes on glass and chitosan surfaces or direct gold-thiol bonds to attach and pattern virus nanotemplates. We are currently modifying these existing methods and investigating additional strategies to pattern virus templates onto a variety of different substrates, including silica, conductive glass and polymers. Results from this study should lead to new applications for coated viruses, such as patterned conductive

surfaces on flexible polymer sheets. We continue efforts to genetically modify the virus template to display new amino acid residues and peptides that can be screened for novel inorganic binding properties. Finally, we are collaborating with a metrologist, Professor Eric Stach, (Purdue University) to develop techniques to measure the electrical properties of a single coated TMV nanorod and to use high resolution TEM to monitor in-situ the behavior of palladium coated TMV in the presence of gases such as hydrogen. Our long-term goal is to demonstrate the application of this easily renewable biotemplates for the assembly and enhancement of nano-devices.

### **DOE Sponsored Publications in 2005-2007**

- Yi H, Rubloff, GW, Culver, JN. 2007. TMV Microarrays: Hybridization-based assembly of DNA-programmed viral nanotemplates. *Langmuir*, 23:2663-2667.
- Widjaja E, Liu NC, Li M, Harris MT. 2007. Dynamics of Sessile Droplet Evaporation: A Comparison of the Spine and the Elliptic Mesh Generation Methods. *Computers in Chemical Engineering*, 31:219-232.
- Lee SY, Harris MT. 2006. Surface Modification of Maghemite Nanoparticles Capped by Oleic Acids: Characterization and Colloidal Stability in Polar Solvents. *J. Colloid Interface Sci.*, 293: 401-408.
- Royston E, Lee SY, Culver JN, Harris MT. 2006. Characterization of silica-coated Tobacco mosaic virus. *J Colloid Interface Sci.* 298:706-712.
- Lee SY, Choi J, Royston EJ, Culver JN, Harris MT. 2006. Deposition of Platinum Clusters on the Surface Modified Tobacco Mosaic Virus. *J. Nanoscience and Nanotechnology.* 6:974-981.
- Lee SY, Culver JN, Harris MT. 2006. Effect of CuCl<sub>2</sub> concentration on the aggregation and mineralization of Tobacco mosaic virus biotemplate. *J Colloid Interface Sci.* 15:706-712.
- Yi H, Wu LQ, Bentley WE, Ghodssi R, Rubloff GW, Culver JN, Payne GF. 2005. Biofabrication with chitosan. *Biomacromolecules.* 6(6):2881-94.
- Yi H, Nisar S, Lee SY, Powers MA, Bentley WE, Payne GF, Ghodssi R, Rubloff GW, Harris MT, Culver JN. 2005. Patterned assembly of genetically modified viral nanotemplates via nucleic acid hybridization. *Nano Lett.* 5(10):1931-6.
- Srinivasan K, Cular S, Bhethanabotla VR, Lee SY, Harris MT, Culver JN. Nanomaterials Sensing Layer Based Surface Acoustic Wave Hydrogen Sensors. 2005. IEEE Ultrasonics Symposium. Vols. 1-4:645-648.
- Lee SY, Royston E, Culver JN, Harris MT. 2005. Improved Metal Cluster Deposition on Genetically Engineered Tobacco Mosaic Virus Template, *Nanotechnology*, 16:S435-S441.

# Self-Assembling Biological Springs: Force Transducers on the Micron and Nanoscales.

B. Khaykovich<sup>1</sup>, N. Kozlova<sup>2</sup>, C. Hossain<sup>3</sup>, A. Lomakin<sup>2</sup>, D. E. Moncton<sup>1</sup>, and G. B. Benedek<sup>2,3,4</sup>

## *Program Scope and Definition*

Self-assembly of helical ribbons in complex fluids is an interesting phenomenon, which poses fundamental questions about the molecular structure, elastic properties and kinetic evolution of these objects. In particular, quaternary solutions such as human gallbladder bile, which contain cholesterol, non-ionic surfactants and lipids, spontaneously form helical ribbons with characteristic pitch angles of 11 and 54°. These helical ribbons form in a variety of axial lengths, widths and radii. Remarkably, however, they all have pitch angles of either 11 or 54° [1].

The first objective of our research program is to determine the molecular structure of the helical ribbons. We have suggested previously that the remarkable stability of each of the two pitch angles results from an underlying crystalline structure of the sterol ribbon strips. We believe that the two different pitch angles correspond to either two different crystal structures or growth directions of the ribbons. In order to probe the molecular structure of the ribbons, we used x-ray diffraction from individual helical ribbons. Using a synchrotron x-ray source we have indeed observed Bragg reflections from individual ribbons having 11° pitch angle and deduced the parameters of the unit cell [2].

Next, we have been able to tether fine glass capillaries to these ribbons and subject them to well defined axial forces [3]. We intend to use the helical ribbons as mesoscopic springs to measure quantitatively the forces acting in nano-scale biological systems. As a first step, we are studying the dependence of elastic moduli of the helices as a function of thickness.

## *Recent progress*

We report the results of x-ray scattering studies of individual helical ribbons formed in multicomponent solutions of cholesterol solubilized by various surfactants [2]. The solutions were: chemically defined lipid concentrate (CDLC) and model bile. The helical ribbons are long rectangular strips, which curl along a cylindrical surface. These objects form spontaneously upon supersaturation of the solution with respect to cholesterol by dilution. The most important observations on cholesterol helical ribbons are as follows [1,2]. (i) These helical ribbons form in a variety of axial lengths, widths and radii. Remarkably, however, almost all have pitch angles of either 11 or 54°. Helical ribbons of the same pitch angles have been observed in over 20

---

<sup>1</sup> Nuclear Reactor Laboratory, Massachusetts Institute of Technology, 138 Albany St., Cambridge, MA. 02139.

<sup>2</sup> Materials Processing Center, Massachusetts Institute of Technology, 77 Massachusetts Ave., Cambridge, MA 02139.

<sup>3</sup> Department of Physics, Massachusetts Institute of Technology, 77 Massachusetts Ave., Cambridge, MA 02139.

<sup>4</sup> Room 13-2005, Massachusetts Institute of Technology, 77 Massachusetts Avenue, Cambridge, MA 02139-4307. e-mail: [benedek@mit.edu](mailto:benedek@mit.edu),

solutions with variable sterols and surfactants. (ii) Sterols dominate the chemical composition of our strips. (iii) Our ribbons are much thicker than even multilamellar phospholipid membranes. We expect that the thickness ranges from tens of nanometers to several microns. (iv) Helical ribbons are metastable intermediates on the pathway of cholesterol crystallization in supersaturated solutions.

We summarize here briefly the results of x-ray diffraction measurements which we reported recently in Ref. [2]. We have demonstrated that the helical ribbons having pitch angle of  $11^\circ$  in CDLC and model bile are constituted of coiled single crystal strips. These strips have a crystal structure very similar to that of cholesterol monohydrate. The essential difference between these two structures is in the tripling of the size of the unit cell along the  $c$  axis for our helices. The plane of the strip lies in the  $ab$ -plane, while the direction of preferred growth, i.e. the long edge of the strip lies along the  $b$ -axis. Since the angle between  $a$  and  $b$ -axes is  $101^\circ$ , the angle between the perpendicular to the edge of the ribbon and the  $a$ -axis is  $11^\circ$ , which coincides with the observed pitch angle. Thus, it appears that the preferential bending direction in low pitch helices is along the  $a$  crystallographic axis.

It appears that the range of spring constants of our helices is such that they are suitable for measuring forces acting between nano-scale biological objects, such as antigen-antibody and enzyme-substrate interactions, actin polymerization, etc. Therefore, the second major goal of our research program is to apply the helical ribbons for biological force spectroscopy. In order to measure the forces, we need to know the spring constant of individual ribbons. We believe that the spring constants can be determined entirely by the external dimensions of the helices. The geometry of the helical ribbons is characterized by the radius ( $R$ ), width ( $w$ ), thickness ( $t$ ), contour length ( $s$ ), and pitch angle ( $\psi$ ). The axial length of a ribbon is  $l = s \sin(\psi)$ . We have previously studied the elastic properties, including tension-induced phase transition, of these helical ribbons [3]. These results were analyzed and explained using a crystal model for the structure of the elastic free energy. According to the model, the radius of the ribbons is determined by a balance between strip elasticity and a spontaneous bending force. This force arises from different interfacial energies of the two opposite faces of a strip constituted of asymmetrical cholesterol molecules. The radius of the ribbon is given by  $R = (2/K_s)K_\alpha \cos^4(\psi)$ . Here  $\psi$  is the pitch angle and  $K_\alpha$  is a combination of the coefficients of the elastic modulus tensor associated with the bending of lines parallel to the contour length.  $K_s$  is a spontaneous curvature constant. The spring constant  $K_{spring} = (8w/R^2s)K_\alpha$ . We will measure both  $R$  and  $K_{spring}$  as function of the thickness and therefore determine the thickness dependence of the elastic moduli:  $K_\alpha$  and  $K_s$ . According to the crystal model,  $K_\alpha$  may scale as the cube of the ribbon thickness and  $K_s$  may depend linearly on the thickness [3]. However the actual dependence of the radius on thickness has never been measured. We also wish to determine if the experimentally observed distribution of radii of helices is a result of a distribution of strip thicknesses. From the dependence of  $K_\alpha$  and  $K_s$  on thickness we shall be able to determine the spring constant of any chosen ribbon solely on the basis of optically measurable external dimensions. We have already begun the measurements of the thickness of the ribbons.

The thickness of the ribbons is less than  $1 \mu\text{m}$ . This is below the resolution of most optical microscopes. Therefore, we established collaboration with colleagues at MIT Spectroscopy Laboratory. We are using a unique interference microscope recently developed in that Laboratory, a tomographic phase microscope [4]. This microscope is capable of determining the thickness of any selected ribbon curved in the solution. We are currently working on optimizing the optical setup for reliable measurements of the ribbons of different sizes. Figure 1 shows the result of a preliminary experiment. Figure 1b shows a two-dimensional map of the phase of the wavefront reaching the detector. Only the part of the ribbon which rests on the cover slip is in focus. The difference in phase is due to the difference of

refractive index between the ribbon and the media. The thickness  $t$  is deduced from the phase by  $t = \Delta\varphi / 2\pi(\lambda/\Delta n)$ , where  $\Delta\varphi$  is the phase difference between the ribbon and the background,  $\lambda = 633\text{ nm}$  is the wavelength of light and  $\Delta n$  is the difference in refractive index between the ribbon and the medium. For the ribbon on Figure 2, the thickness is approximately 200 nm while the diameter of the ribbon is about 30  $\mu\text{m}$  (as determined by regular phase-contrast microscope).

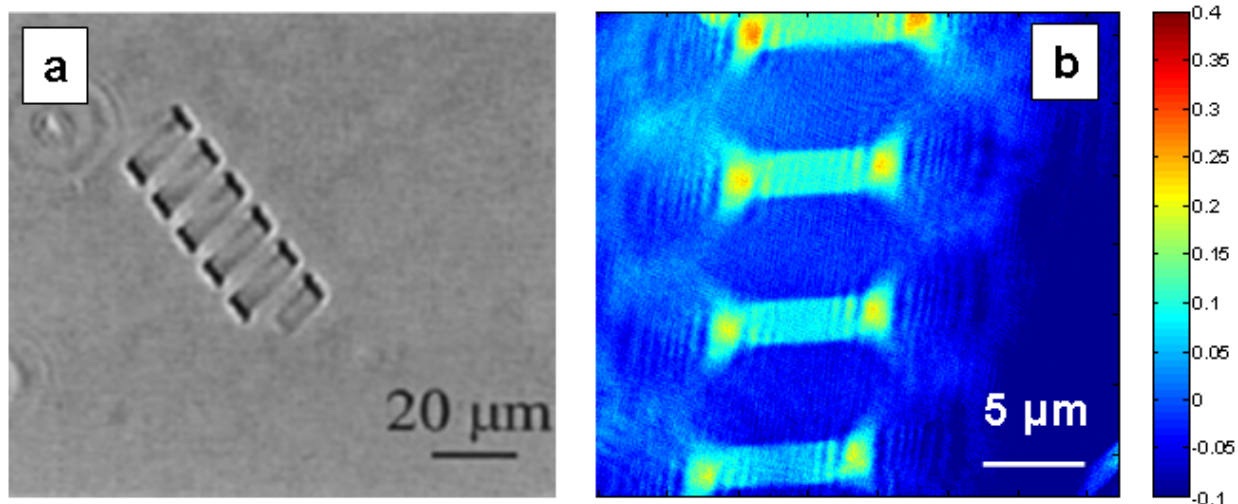


**Figure 1** Images of different helical ribbons taken by (a) standard phase-contrast and (b) interference microscopes. In figure (b) the colors correspond to the relative phase of the light wave reaching the detector. The phase difference is proportional to the thickness.

## ***Future Plans***

Once the connection between the thickness and radius is established, the next crucial step is to determine the spring constant of individual ribbons as a function of the thickness. This information will allow us to determine the elastic constant of any ribbon just by measuring its radius, length and width. Since the ribbons come in a wide range of radii, we would then be able to choose a spring of desired elastic constant. The measurements of the spring constants will be done by measuring elongation under applied force. This will be possible once we refine the methods of tethering to individual ribbons.

In addition, we are currently working on developing reproducible and reliable methods of tethering to individual helical ribbons. We are pursuing two different, but related strategies. One direction is to modify existing helical ribbons in CDLC in order to functionalize their surface. Another direction is to specifically engineer new or modified classes of materials which would self-assemble into robust helical ribbons with high yield and have easily functionalizable surfaces.

## **References**

- [1] YV Zastavker, N Asherie, A Lomakin, J Pande, JM Donovan, JM Schnur, et al. Self-assembly of helical ribbons, Proc. Natl. Acad. Sci. USA. 96 (1999) 7883-7887.
- [2] B Khaykovich, C Hossain, JJ McManus, A Lomakin, DE Moncton, GB Benedek. Structure of cholesterol helical ribbons and self-assembling biological springs, Proc.Natl.Acad.Sci.U.S.A. 104 (2007) 9656-9660.
- [3] B Smith, YV Zastavker, GB Benedek. Tension-induced straightening transition of self-assembled helical ribbons, Phys. Rev. Lett. 87 (2001) 278101.
- [4] W Choi, C Fang-Yen, K Badizadegan, S Oh, N Lue, RR Dasari, et al. Tomographic phase microscopy, Nature Methods. 4 (2007) 717-719.

## **DOE Sponsored Publications in 2005-2007**

B Khaykovich, C Hossain, JJ McManus, A Lomakin, DE Moncton, GB Benedek. Structure of cholesterol helical ribbons and self-assembling biological springs, Proc.Natl.Acad.Sci.U.S.A. 104 (2007) 9656-9660.

## Protein Architectures for Photo-Catalytic Hydrogen Production

Trevor Douglas (PI), John Peters, and Mark Young

Department of Chemistry & Biochemistry  
Center for Bio-Inspired Nanomaterials  
Gaines Hall  
Montana State University  
Bozeman, MT 59717

Email: [tdouglas@chemistry.montana.edu](mailto:tdouglas@chemistry.montana.edu)

### Program Scope:

Materials scientists increasingly draw inspiration from the study of how biological systems fabricate materials under mild synthetic conditions using self-assembled macromolecular templates. This, together with the biological propensity for assembly into higher order structures with composite functionality are the inspiration for this investigation into the development of active catalyst systems for hydrogen production. Two approaches are being explored. In the first, container-like protein architectures such as viral capsids and ferritin are used as synthetic templates for controlled inorganic mineralization. These protein cages have three distinct interfaces that can be synthetically exploited for functional materials: the interior, the exterior and the interface between subunits (**Figure 1**). Subunits comprising the building blocks of these structures can be modified both chemically and genetically in order to impart designed functionality to different surfaces of the cage. Therefore, the cages possess a great deal of synthetic flexibility that allows for the introduction of multi-functionality in a single cage. In a second approach we are exploiting a unique class of molecular catalysts in the form of the hydrogenase enzymes (**Figure 2**), which are produced by a variety of microorganisms where they function in either hydrogen oxidation or proton reduction. Hydrogen oxidation is coupled to the generation of reducing equivalents to drive energy yielding or biosynthetic processes. During anaerobic fermentation, some microorganisms are capable of coupling the oxidization of sugars to the regeneration of electron carriers, which are used for

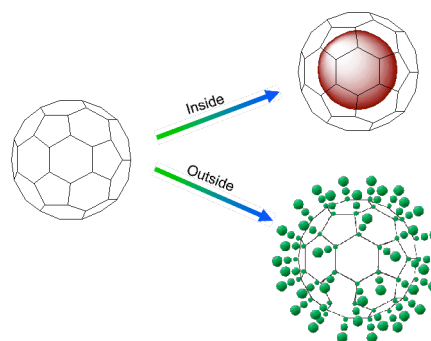


**Figure 1.** Schematic illustration of the different interfaces on the protein cages that can be modified either genetically or chemically for generation of functional materials.

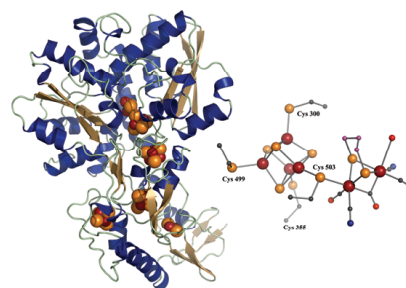


**Figure 2.** Left: Refined X-ray crystal structure (1.5 Å) of [FeFe]-hydrogenase (Cp1) from *C. pasteurianum*. Right: Atomic structure of the active site termed the H-cluster in the [FeFe]-hydrogenase (Cp1) from *C. pasteurianum*.

proton reduction and the production of hydrogen gas. Hydrogenases, incorporate unusual metal ion clusters at their active sites, which incorporate both  $\text{CN}^-$  and  $\text{CO}$ . These systems are useful both as an inspiration for biomimetic materials synthesis but also as starting material which can be incorporated into a functional composite material.

**Progress:**

*Protein Cages:* The internal interface of the protein-cage architecture can be utilized for directing encapsulation and synthesis of both organic and inorganic materials. Many viruses package their genomic nucleic acid within the viral capsid through condensation via fairly non-specific electrostatic interactions. The native positive charge density on the interior interface of empty (nucleic acid-free) Cowpea chlorotic mottle virus (CCMV) capsid has been utilized for initiating inorganic mineralization reactions to form spatially constrained nanoparticles of polyoxometalate salts (tungstates, molybdates, and vanadates) (**Figure 3**). These materials can be transformed into their corresponding sulfide mineral, which show significantly different spectroscopic and catalytic behavior from the oxides. In particular, the formation of molybdenum sulfides ( $\text{MoS}_x$ ) has been a focus because of their potential use as catalysts for  $\text{H}^+$  reduction and  $\text{H}_2$  formation.

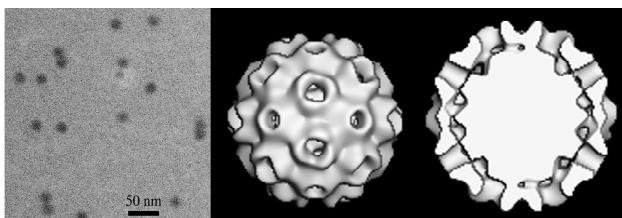


**Figure 3.** Left. TEM of polyoxomolybdate cages in CCMV. Cryo-TEM image reconstruction of mineralized CCMV showing the cage (center) and interior core (right).

The protein cages in our library are all assembled from multiple copies of identical subunits, which can be reversibly disassembled and reassembled. We have demonstrated that reassembly of cages from a population of differentially modified subunits results in chimeric structures, the composition of which parallels the input stoichiometry (**Figure 4**). This allows us to direct cage structures that incorporate multiple functionality (light harvesting and proton reduction for instance) through a self-assembly process.

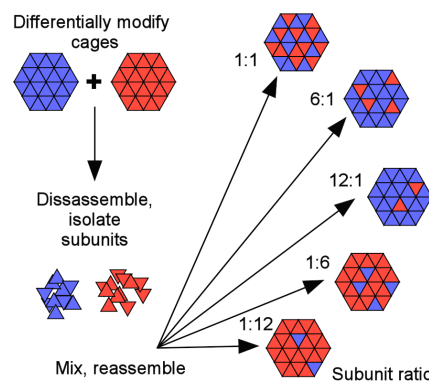


**Figure 4.** Chimeric proteins can be prepared using developed methods for disassembling differentially modified protein cages and reassembling them with various ratios of modified subunits.

We have demonstrated that light harvesting catalysts such as  $\text{Ru(II)(bpy)}_3^{2+}$ ,  $\text{Ru(II)(bpy)}_2\text{phen}^{2+}$ ,  $\text{Ir(ppy)}_2(\text{phen})^+$  can be covalently attached to both the cage-based catalysts and the hydrogenase enzyme systems. For both catalyst systems, light harvesting can be coupled to proton reduction and hydrogen formation by means of a chemical mediator such as methyl viologen. Future work will be directed towards engineering mediator-less proton reduction in these systems.



*Hydrogenase:* Structural studies on the [FeFe] hydrogenase from *Clostridium pasteurianum* are at an advanced stage and we have a high resolution structure at better than 1.4 Å. These studies allow for the design of informed substitutions that will allow us to maximize the coupling of photocatalysts and light harvesting antennae to the hydrogenase active site for maximal hydrogen production. While the [FeFe] hydrogenases are the most efficient known catalysts for hydrogen production the heterologous expression of active hydrogenases is limited by metal cluster assembly. We have developed an in-vitro activation of the [FeFe] hydrogenases in which the inactive HydA gene product can be activated by incubation with extracts of coexpressed accessory enzyme HydE, HydF, and HydG. The results of this work provide the first clues into the process of [FeFe] hydrogenases and indicate that the scaffold for H cluster biosynthesis is one of the accessory proteins and not the hydrogenase itself. These results not only lay the groundwork for defining the stepwise pathway for H cluster biosynthesis but provide a source of active hydrogenase protein for incorporation into materials for hydrogen production.

#### **Future Plans:**

Our future direction will be to focus on the MoS<sub>x</sub>-CCMV and TiO<sub>2</sub>-CCMV composite materials for photocatalytic and electrocatalytic H<sub>2</sub> formation. We have established the synthetic procedures and performed initial characterization of these materials. We will extend the characterization to include identification of the mineral polymorph, oxidation states of the metal ions using a combination of high resolution TEM, XPS, and XAS. In parallel with these studies, we will utilize enzymatic catalysts (hydrogenase) for H<sub>2</sub> formation and integrate the bio- and the biomimetic catalyst systems with light harvesting systems. We will expand and develop conjugation chemistry to selectively attach a range of light harvesting molecules directly to the interior or exterior of the protein cage or to the hydrogenase enzymes through engineered attachment sites for high-density presentation of these antennae. We will establish the necessary proximity between light harvesting molecules and catalytic mineral nanoparticles through a series of site-specific attachments, which can be achieved through genetic introduction of reactive sites on the protein catalyst systems. Electron transfer to the catalytic centers will be established through immobilization of protein-cage catalyst systems on electrode surfaces and characterization of their electrochemical behavior. The goal of this work will be directed towards engineering mediator-less proton reduction in these systems. In general, we are taking a bioengineering approach to both incorporate enzyme systems into functional materials and develop biomimetic approaches to generating functional mimics of the active sites of hydrogenase.

## **Biomolecular Sacs, Strings, and Membranes: From Nanometers to Centimeters with Self-Assembly**

Principle Investigator: Samuel I. Stupp

Address: Department of Materials Science and Engineering, Department of Chemistry,  
Department of Medicine, Northwestern University  
E-mail: s-stupp@northwestern.edu

Co-authors: Helena Azevedo, Ramille Capito, Megan A. Greenfield, Liang-shi Li, Alvaro Mata, Liam C. Palmer, Yuri S. Velichko, and Shuming Zhang

### **PROGRAM SCOPE**

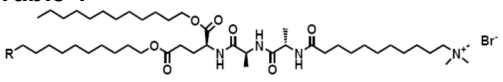
Our program explores self-assembly at all length scales as a strategy to create functional structures or patterns with significant order parameter out of disordered components. Our laboratory has pursued this objective over the past decade, seeking to develop self-assembly codes reaching the macromolecular scale.<sup>[1, 2]</sup> In analogy to polymers, we define the scale as that of assemblies in which the collective molar mass exceeds  $10^4$  daltons. The term “code” implies that a specific type of structure defined by its nanoscale architecture can be formed by design with diverse sets of molecules. Our work focuses specifically on systematic and iterative studies on designed molecules with supramolecular targets that mimic features of systems biological self-assembly. We are also interested in using the self-assembled soft matter structures to create hybrid materials with nanoscale inorganic compartments. The functional targets include materials with catalytic properties, energy transfer and transduction, as well as materials that can signal cells and control their behavior. Our efforts have been recently directed to crossing scales with self-assembly to reach into the macroscopic regime in three dimensions. This is precisely what is needed to integrate self-assembly into the manufacturing of functional materials and devices.

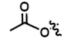
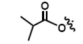
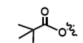
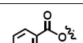
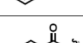
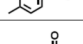
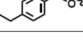
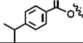
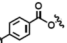
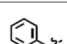
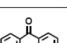
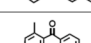
### **RECENT PROGRESS**

#### ***1. A Torsional Strain Mechanism to Tune Pitch in Supramolecular Helices***

It is known that torque applied to DNA double helices results in supercoiling into a structure of defined pitch. We have been interested in applying this phenomenon to synthetic helices. Peptide lipids (e.g., **1**) are a class of molecules composed of a regular surfactant molecule with a short,  $\beta$ -sheet-forming tripeptide in the middle. Previous studies have shown that these molecules form solid nanofibers in nonpolar solvents.<sup>[3]</sup> During our recent work on functionalization of such cylindrical nanofibers, we found simple modification of the compounds led to nanostructures with helical morphologies. Further study revealed a torsional strain mechanism to tune pitch of micron-long helical assemblies in the range of tens to hundreds of nanometers.<sup>[4]</sup>

Compounds **1** and **2** were synthesized with an acetate and a dimethylacetate endgroup, respectively. Both compounds dissolve in hot chlorocyclohexane and form translucent self-supporting gels upon cooling to room temperature. In this nonpolar solvent, these amphiphilic molecules assemble as a result of solvophobic interactions as well as intermolecular  $\beta$ -sheet formation among the peptide segments. The charged quaternary ammonium head groups are buried inside the nanofibers away from the organic solvent, and the less polar tails are presented on the surfaces of the nanofibers. Atomic force microscopy (AFM) studies revealed straight cylindrical fibers for compound **1**. In contrast, AFM images of the aggregates formed from compound **2** show helices with regular pitch. The significant morphology change for the assembly suggested that a bulkier substituent at the terminus of the alkyl segment forces

**Table 1**


Compound <sup>a</sup>	R	Pitch (nm)	Van der Waals volume (Å <sup>3</sup> )
1		∞	58.1
2		22 ±2	92.7
3		22 ±2	110.0
4		∞	113.4
5		160 ±30	130.7
6		40 ±3	148.0
7		22 ±2	165.3
8		22 ±2	182.6
9		∞	104.4
10		90 ±10	218.2
11		60 ±10	235.5
12		74 ±6	292.3

<sup>a</sup> All compounds were synthesized using L-amino acids.

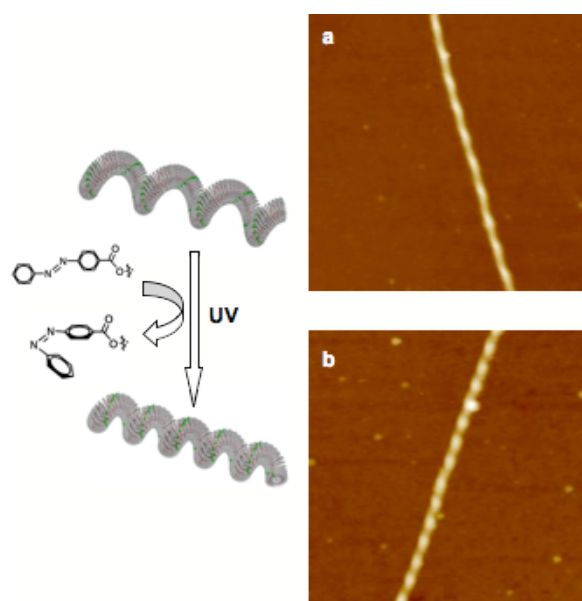


**Fig. 1.** AFM images (a) before and (b) after irradiation.

than the *trans*-isomer, the isomerization should result in an increase of sterically induced torque thus leading to a reduction in superhelical pitch.

twisting of initially cylindrical assemblies. The  $\beta$ -sheets in these aggregates define the primary helices, and the presence of the bulky endgroups could be generating torsional strains driving superhelix formation. Torsional strain caused by steric repulsion among the bulky substituents may overwind the  $\beta$ -sheets. To accommodate the bulky groups on the periphery of the  $\beta$ -sheets without disrupting the hydrogen-bonded network, the axis of the  $\beta$ -sheets forms a superhelix.

In order to support the torsional strain mechanism in the formation of the superhelices, we synthesized three series of additional compounds **1–3**, **4–8**, and **9–11** that covered a wide range of endgroups bulkiness. Within each of the series, the pitch of the helices decreases as the van der Waals volume of the endgroups increases (Table 1). (Straight cylindrical fibers are described as assemblies having infinite pitch.) Interestingly, in the first two series there appears to be the same lower limit on the pitch values (~22 nm), in spite of the structural differences between their endgroups. This common limiting value may result from the preference to maintain the hydrogen bonds in the  $\beta$ -sheets. We cannot yet quantitatively predict the pitch of the helical molecular assemblies, since the collective forces involved are complex and difficult to model with atomistic detail. However, our work clearly shows that steric forces on twisted  $\beta$ -sheets play an important role in the tunability of pitch in supramolecular assemblies.

Potential applications for nanostructures with tunable pitch include systems to control stereoselective chemistry and nonlinear optics. If the endgroups can be modified *in situ* to impart greater steric demands, then these systems could be used for sensing or actuation. As a proof of principle, we irradiated a suspension of nanofibers made of azobenzene derivative **12** in 360 nm and used AFM to study the actuation of the helices as a result of the *trans*-to-*cis* isomerization of the azobenzene moiety (Fig. 1). We observed that light-induced molecular isomerization leads to a reduction in the pitch of the supramolecular helices. Because the *cis*-isomer is less planar

## 2. Catalysis by Supramolecular Nanostructures

The efficiency and selectivity of enzymes have been a great source of inspiration to the development of robust synthetic catalysts. Supramolecular systems derived from polymers, nanostructures, and artificial proteins have been used to mimic enzymes by presenting reactive sites. Most of the synthetic particles investigated have spherical symmetry and lack the internal order characteristic of natural enzymes. The use of imidazolyl groups in artificial catalysts has been popular given the presence of histidine residues at the catalytic site of several hydrolytic enzymes including acetylcholine esterase, chymotrypsin, and trypsin. A considerable increase of reaction rates has been observed upon aggregation of active sites, presumably due to the higher concentration of reaction loci and cooperativity among functional groups.

We recently demonstrated hydrolysis of a model ester on the surface of peptide amphiphile (PA) nanofibers.<sup>[5]</sup> We explored the ability of these cylindrical supramolecular nanostructures to hydrolyze of 2,4-dinitrophenyl acetate (DNPA), a compound frequently used to study catalytic activity of enzymes and synthetic analogs. Histidine residues were incorporated into the peptide portion of PA molecules to mimic the natural hydrolytic enzymes discussed above. PA **13** contains the peptide sequence KLLLAALK followed by a palmitoyl tail on the  $\epsilon$ -amine of the C-terminal lysine residue.<sup>[6]</sup> Histidine residues were coupled to the N-terminal lysine residue to

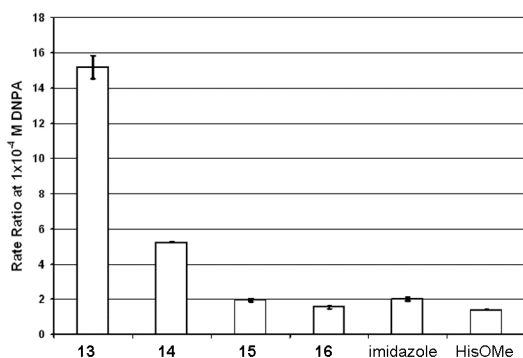
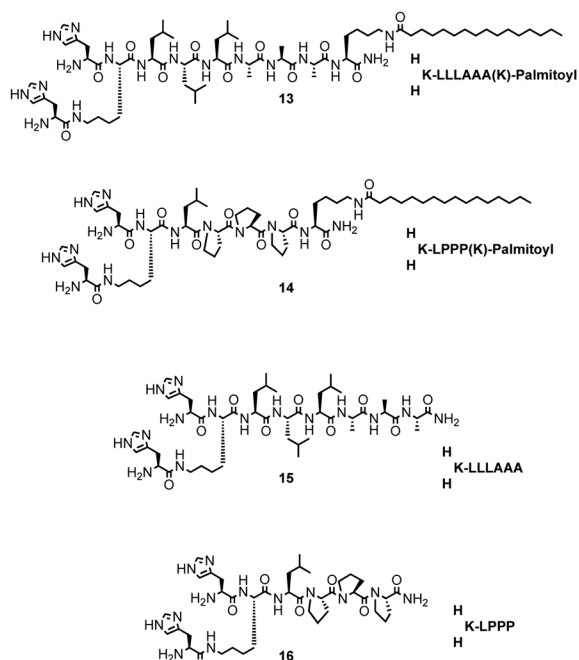


**Fig. 2.** Observed rate increase in DNPA hydrolysis as the level of molecular organization in the catalytic particles is varied.

incorporate catalytically active imidazolyl groups. PA **14** contains the same peptide sequence as in PA **13** without the palmitoyl group, preventing formation of well-defined cylindrical aggregates. PA molecules **15** and **16** contain proline residues to prevent  $\beta$ -sheet formation and promote assembly into spherical aggregates.<sup>[7]</sup> The predicted morphologies were confirmed by TEM microscopy.

Hydrolysis of DNPA of these imidazolyl-functionalized molecules (at 25 °C and pH 7.4 in HEPES buffer) was monitored by UV-vis spectroscopy to follow the formation of 2,4-dinitrophenol. The DNPA hydrolysis rates were calculated using various substrate conditions with a constant catalyst concentration (Fig. 2). Using the Michaelis–Menten model to calculate the hydrolysis rate constant with PA **13** under self-assembling conditions gave a value of  $1.67 \pm 0.13 \times 10^{-2} \text{ s}^{-1}$ . In contrast, the reaction rate increase was linear with increasing substrate concentration in the presence of histidine, imidazole, or the spherical aggregates of PAs **14–16**. We believe that the hydrolysis rate enhancement by the nanofibers is due to the high density of reactive sites presented on the nanofiber surface. The catalyst–substrate binding on the cylindrical nanofibers can be favored relative to spherical aggregates, which are expected to have much less internal order; greater order in the catalytic particle should reduce the entropic penalty of binding events. The observations suggest that nanofibers of high aspect ratio and internal order are potentially

interesting catalysts. The catalytic function of these nanostructures may be further expanded by co-assembling two or more different PAs, so that various molecular recognition and chemical events can be integrated into a single catalytic system.

### 3. Macroscopic Self-Assembly Between Large and Small Molecules

The organization of molecules at interfaces has been a phenomenon of great interest over several decades given its importance in the preparation of chemically defined surfaces and ordered materials. The classical systems include Langmuir–Blodgett (LB) films prepared by ordering molecules by compression at an air–water interface and subsequently depositing them as multilayers by repeated immersion of a solid substrate in the liquid. Another widely studied system is the self-assembling monolayer (SAM) formed at a solid–liquid interface by the reaction of dissolved molecules with a solid surface. We have recently discovered systems in which self-assembly goes well beyond the monolayer scale at the interface between two aqueous solutions: one containing high-molecular-weight charged macromolecules and the second one containing small self-assembling molecules of opposite charge. At specific pH conditions, a solid material with structural order forms instantly upon contact between the two

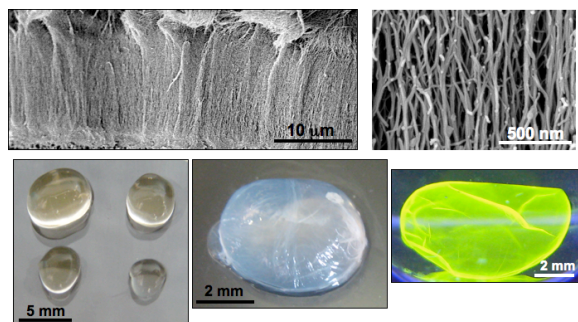


**Fig. 3.** TOP: SEM images of the membrane interface; BOTTOM: Fluid-filled sacs.

liquids (Fig. 3). The self-assembled structures observed grow to macroscopic dimensions with a high degree of hierarchical order across the scales. The instant initiation of the ordered structures also allows the formation of self-sealing sacs membranes with tailorable size and shape, and continuous strings. Furthermore, a large defect in the sac or membrane structures can be repaired by sequential exposure to the solutions of both components within the defect. These systems could find many applications in the control of cell behavior when their structure is biomolecular in nature.

### FUTURE PLANS

We plan to extend our work on supramolecular catalysis to other chemistries. The instantaneous self-assembly at aqueous interfaces will be adapted to the interface of miscible organic solvents to access broader functionality, such as the directed control of charge or energy transfer.

### REFERENCES

- [1] E. R. Zubarev, E. D. Sone, S. I. Stupp, *Chem.—Eur. J.* **2006**, *12*, 7313.
- [2] L. C. Palmer, Y. S. Velichko, M. O. de la Cruz, S. I. Stupp, *Phil. Trans. R. Soc. Ser. A* **2007**, *365*, 1417.
- [3] L.-s. Li, S. I. Stupp, *Angew. Chem. Int. Ed. Engl.* **2005**, *44*, 1833.
- [4] L.-s. Li, H. Jiang, B. W. Messmore, S. R. Bull, S. I. Stupp, *Angew. Chem. Int. Ed. Engl.* **2007**, *46*, 5873.
- [5] M. O. Guler, S. I. Stupp, *J. Am. Chem. Soc.* **2007**, In Press. (DOI 10.1021/ja075044n)
- [6] M. O. Guler, S. Soukasene, J. F. Hulvat, S. I. Stupp, *Nano Letters* **2005**, *5*, 249.
- [7] M. O. Guler, R. C. Claussen, S. I. Stupp, *J. Mater. Chem.* **2005**, *15*, 4507.

## In situ studies of nucleation and assembly at soft-hard interfaces

Pulak Dutta

Dept. of Physics & Astronomy, Northwestern University  
2145 Sheridan Road, Evanston, IL 60208  
pdutta@northwestern.edu

### Program scope

Many soft materials (whether thin films or living organisms) use hard materials for support and for added functionality, and many physical, chemical and biological processes take place at the soft-hard interface. Although traditional surface science has largely focused on hard surfaces and interfaces, the same techniques (in particular, synchrotron X-ray scattering) can be very useful for studies of soft surfaces and soft-hard interfaces.

The objective of this project is the in situ study of mineral nucleation and growth at organic surfaces. We want to learn when oriented growth occurs, and to observe the surface and bulk structures and dynamics during growth. While some of these studies may turn out to have relevance to biology, this proposal is primarily materials-oriented---we seek new ways to make thin films and to control their structure, growth and morphology.

### Recent progress

When the subphase of a Langmuir monolayer is a supersaturated solution, crystals will nucleate preferentially under the organic monolayer, and will have specific structures (in materials where more than one crystal structure is possible) and crystal orientations that depend on the monolayer material and on parameters such as temperature, pressure and pH. The organic-matrix-mediated-growth of a large variety of crystals (not just biomaterials) has been studied by a large variety of ex-situ methods, but these studies contain no direct information about the structural relationships that drive the nucleation process. We have used X-ray scattering, which averages over a large footprint and thus gives statistically significant information. When there is oriented growth, we have sought to determine what happens at the interface that favors oriented nucleation.

*Lead carbonate:* When a monolayer of heneicosanoic acid is spread on a supersaturated solution of lead carbonate, surface-sensitive grazing incidence X-ray scattering reveals diffraction peaks corresponding to oriented growth of the mineral hydrocerrusite,  $2\text{PbCO}_3 \cdot \text{Pb}(\text{OH})_2$ . In other words, the ordered monolayer not only orients the crystal but selects the material grown (limited, of course, by the ingredients available). In addition to the monolayer peaks and the bulk mineral peaks, we also see diffraction peaks corresponding to a  $\sqrt{7} \times \sqrt{7}$  supercell of the hydrocerrusite (001) surface lattice. This supercell has an area of 7.0 times the mineral lattice unit cell area (obviously), but it also has 9.0 times the unit cell area of the organic monolayer.

The appearance of a superlattice is surprising because while  $\sqrt{7} \times \sqrt{7}$  reconstruction is rather common, surface reconstruction has previously been seen only in ultraclean environments, such as UHV chambers or electrode surfaces with high potential gradients. The Langmuir monolayer system is relatively dirty, but it appears that the reconstructed layer is energetically favored

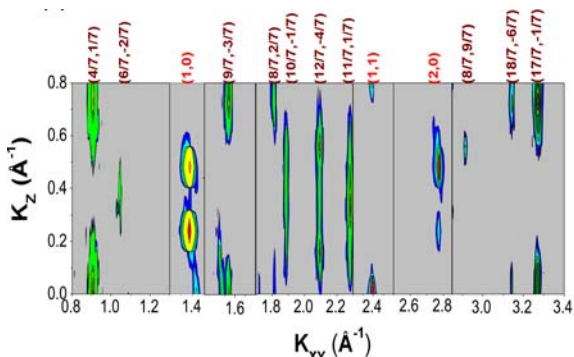


Fig. 1. Intensity contours (reconstructed from diffraction data) during nucleation from a supersaturated solution of lead carbonate. The six peaks labeled with integer indexes correspond to bulk hydrocerrusite. The fractional order peaks (all of which are very broad in the z-direction) are from a  $\sqrt{7} \times \sqrt{7}$  interfacial superlattice  $\sim 40\text{\AA}$  thick.

polysaccharides. Therefore, ordered organic monolayers (Langmuir films) floating on supersaturated calcium carbonate aqueous solutions have been used to simulate the biological process of oriented calcite nucleation,<sup>1</sup> and indications of templated growth have been reported in calcite crystals that are harvested after being grown under carboxylate monolayers. Unexpectedly, however, recent *in situ* structural studies<sup>2</sup> clearly show that there is growth but no average preferential alignment under carboxylate monolayers; the nucleate is a powder.

Calcite will also nucleate under Langmuir monolayers of alkyl sulfates.<sup>3</sup> Based on the symmetry of harvested crystals it has been postulated that calcite nucleates with its (0 0 1) plane parallel to the sulfate monolayer surface. The (0 0 1) orientation is often observed in biological minerals, even though it is not stable *in vacuo*. We have used *in-situ* grazing incidence diffraction (GID) to

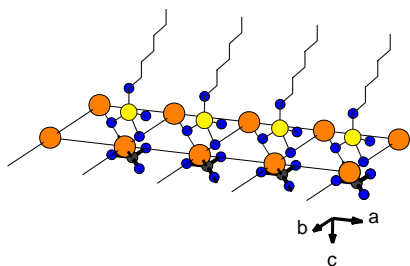


Fig. 2. Diagram of the sulfate-calcite interface based on our data. This structure was originally proposed in ref. 4; we now have evidence for it. (●:Ca; ●:O; ●:S; ●:C)

study the nucleation of calcite under floating arachydl sulfate monolayers. GID scans show clearly that in this case there is oriented growth in the (0 0 1) direction  $\pm 5^\circ$ . Thus sulfate monolayers, unlike acid monolayers, can nucleate oriented calcite. Arachydl sulfate forms a stable monolayer structure and there is a single in-plane diffraction peak at  $K_{XY} \sim 1.455 \text{\AA}^{-1}$  within our scan range. Based on the absence of other monolayer peaks in the vicinity, we conclude that the lattice is hexagonal. The hexagonal calcite (0 0 1) plane has exactly the same Ca-Ca distance as the intermolecular distance in the hexagonal sulfate monolayer ( $4.99 \text{\AA}$ ), i.e. there is a 1:1 commensurate relationship.<sup>4</sup>

because it ‘mediates’ between the bulk crystal lattice and the monolayer lattice by being commensurate with both of them.

*Calcium carbonate:* Calcite is one of the most common inorganic components in biomaterials. Highly oriented calcite crystals are found in shells where they provide mechanical strength, in trilobite eyes where they are used as optical elements, etc.. In exoskeletal materials, calcite nucleation and growth are presumably governed in some way by the organic matrices that are found within the biomineral. These consist of macromolecules rich in acidic peptides such as aspartic acid, and sulfated

<sup>1</sup> e.g. S. Mann, *Biomineralization: Principles and Concepts in Bioinorganic Materials Chemistry*, Oxford University Press, Oxford, 2001.

<sup>2</sup> E. Dimasi, M. J. Olszta, V. M. Patel and L. B. Gower, *CrystEngComm*, **5**, 346 (2003); J. Kmetko, C.-J. Yu, G. Evmenenko, S. Kewalramani and P. Dutta, *Phys. Rev. B* **68**, 085415 (2003)

<sup>3</sup> e.g. S. Mann, *Biomineralization: Principles and Concepts in Bioinorganic Materials Chemistry*, Oxford University Press, Oxford, 2001.

<sup>4</sup> B. R. Heywood and S. Mann, *Chem. Mater.* **6**, 311 (1994)

These results have specific implications for mineral nucleation in biological systems. It is quite possible for the sulfated polysaccharide molecules found within biominerals to adopt a conformation such that the sulfates match the calcium ion positions and stabilize the (0 0 1) crystal face. Thus, sulfate groups in biological systems may not only drive the calcium ions to the nucleation sites, but also determine the orientation of the nucleating crystal.

*Cadmium and manganese carbonate:* Grazing incidence X-ray scattering during the growth of  $\text{CdCO}_3$  and  $\text{MnCO}_3$  crystals from supersaturated aqueous solutions, under fatty acid and alcohol monolayer templates, shows that the nucleates are highly misoriented below a threshold supersaturation. However, at higher supersaturations, the crystals are preferentially oriented with the {0 1 2} direction vertical. Scanning electron microscope images of transferred samples show isolated crystals at low concentrations, while at higher concentrations the crystals have self-assembled to form linear chains and sheets. This is a different pathway to oriented film growth from aqueous subphases: orientation develops after nucleation.

Real-space pictures always carry the risk of showing nonrepresentative cases. However, our X-ray data confirm that the average orientation of the crystals increases when the amount of scattering material increases.

*Barium chloride and fluoride:* Our earlier studies<sup>5</sup> had established that barium and strontium fluoride grow oriented crystals under heneicosanoic acid Langmuir monolayers, and that this happens because there is epitaxy. Those studies were performed at high pH (>8). Considering the case of  $\text{BaF}_2$ , supersaturated solutions are prepared by mixing  $\text{BaCl}_2$  and HF. The compound  $\text{BaFCl}$  also has low solubility, but it doesn't grow. Just as with hydrocerussite (above), the interface selects not just a specific orientation but also a specific mineral. In the present case the bulk  $\text{BaClF}$  (001) square unit face has exactly half the area of the  $\text{BaF}_2$  (100) square unit face. Thus geometric match alone cannot explain the preferential nucleation of  $\text{BaF}_2$ . And in fact, when the pH is lowered to ~5.8, we see that *both* materials grow oriented crystals at the interface. A recent study<sup>6</sup> (combining simulation and experiment) has shown that chloride ions are more likely to be located at a pure water surface than fluoride ions. On the other hand, in the presence of a charged monolayer, fluoride ions are favored. We speculate that this is the reason for the observed trends as the subphase pH is changed.

## Future plans

*Template-directed nucleation:* The structure of a Langmuir monolayer is easily changed. It is reasonable to expect that different phases may nucleate different compounds (subject to the available ingredients) or polymorphs, or at least different crystal faces. We propose to explore this possibility in detail.

*From superlattice to crystal:* When fatty acid monolayers are spread on dilute solutions of various salts, a large number of in-plane diffraction peaks appears, and these can be indexed as a two-dimensional supercells of the Langmuir monolayer structure. This is a mystery: the ions are not large enough to justify such a large unit cell, and no such structures have been seen in bulk

---

<sup>5</sup> J. Kmetko, C. Yu, G. Evmenenko, S. Kewalramani and P. Dutta, *Phys. Rev. Lett.* **89**, 186102 (2002); J. Kmetko, C.-J. Yu, G. Evmenenko, S. Kewalramani and P. Dutta, *Phys. Rev. B* **68**, 085415 (2003)

<sup>6</sup> P. Jungwirth and D. J. Tobias, *Chem. Rev.* **106**, 1259 (2006)



crystals of these materials. But potentially the strain induced in a counterion monolayer by the organic lattice results in a modulation similar to the surface reconstruction we recently observed. We plan to follow the evolution of the metal-ion structure from a monolayer to the bulk crystal, by varying subphase concentration.

*Calcium carbonate:* Templating of calcite at Langmuir monolayers does not prove that there is templating in nature, but the laboratory process is interesting in itself and may provide insights for biology. We plan to study the sulfate monolayers to map out parts of the phase diagram and characterize the calcium carbonate nucleation process under different monolayer phases. We also plan study sulfonate and phosphonate monolayers, which have also been reported to nucleate calcite. We will study mixed monolayers containing carboxyl and sulfate groups, to see if there is phase separation and whether this leads to isolated and perhaps patterned nucleation sites.

*Organic deposition at inorganic surfaces:* We would like to look at sulfate monolayers transferred by the LB method to clean calcite surfaces, to see what order is induced in the organic film. We would also like to study organic deposition from aqueous solutions. Organic and inorganic components are interleaved within biominerals, so although this proposal is primarily focused on hard-material deposition at soft surfaces, the reverse process is also of interest. Such deposition may have environmental/geochemical relevance as well. We have previously studied the self-assembly of octadecyltrichlorosilane (OTS) on silicon using in situ X-ray scattering at the solid-liquid interface,<sup>7</sup> and these experiments would use the same methods.

### **Publications, 2005-present**

“Evidence of surface reconstruction during ‘bioinspired’ inorganic nucleation at an organic template”, S. Kewalramani, G. Evmenenko, C.-J. Yu, K. Kim, J. Kmetko, and Pulak Dutta, *Surface Science* **591**, 286 (2005)

“Aggregation-governed oriented growth of inorganic crystals at an organic template”, Sumit Kewalramani, Geoffrey Dommert, Kyungil Kim, Guennadi Evmenenko, Haiding Mo, Benjamin Stripe, and Pulak Dutta, *J. Chem. Phys.* **125**, 224713 (2006)

“Pathways for oriented assembly of inorganic crystals at organic surfaces”, Sumit Kewalramani, Jan Kmetko, Geoffrey Dommert, Kyungil Kim, Guennadi Evmenenko, Haiding Mo, and Pulak Dutta, *Thin Solid Films* **515**, 5627 (2007)

“Mechanisms for species-selective oriented crystal growth at organic templates”. Sumit Kewalramani, Kyungil Kim, Guennadi Evmenenko, Paul Zschack, Evguenia Karapetrova, Jianming Bai and Pulak Dutta, *J. Mat. Res.*, to be published 10/07

“Biomimetic growth of oriented calcite crystals at a sulfate template”, Sumit Kewalramani, Kyungil Kim, Benjamin Stripe, Guennadi Evmenenko, Geoffrey H. B. Dommert and Pulak Dutta, submitted

---

<sup>7</sup> A.G. Richter, C.J. Yu, A. Datta, J. Kmetko and P. Dutta, *Phys. Rev. E* **61**, 607 (2000); A.G. Richter, M.K. Durbin, C.J. Yu and P. Dutta, *Langmuir* **14**, 5980 (1998)

## **Water-Immersed Polymer Interfaces and the Roles of Their Materials Properties on Biolubrication**

Yingxi Elaine Zhu

Email: [yzhu3@nd.edu](mailto:yzhu3@nd.edu)

Department of Chemical and Biomolecular Engineering  
182 Fitzpatrick Hall, University of Notre Dame, Notre Dame, IN 46556

### **Program Scope**

This research aims to understand the roles of the structure and interfacial interactions of aqueous-immersed polymer thin films on biolubrication experimentally, and to go beyond this to molecular design tunable and functional polymeric thin films as artificial lubricious biofilm. Our goal is not only to characterize polymeric interfaces, but also to demonstrate a molecular design concept to construct tunable and functional biofilm by exploring stimuli-responsive colloid-polymer thin film as a rigorous model system. The specific goals of this research program include: 1) To probe the coupling of thin-film microstructures and interfacial forces at deformable polymeric interface and to elucidate how the lubrication behavior differs between soft and hard interfaces; 2) To construct a biocompatible hydrogel-polymer model system of tunable length and time scales to mimic biolubricants in the human body; 3) To address the roles of external stimuli such as temperature and mechanical perturbation on interfacial forces of biomimetic polymeric thin films.

### **Recent Progress**

In the first 3 months of the grant, we have made some notable progress in the areas of platform development and glassy dynamics of polymeric thin films. Specifically, we have completed the construction of micron-gap rheometer interfacing with confocal laser scanning microscopy to study the packing configuration and dynamics of confined colloidal thin films at a single particle resolution. The resulting combination of information obtained from microscopic visualization and ensemble-averaged force measurements allows us to revisit the problem of the origin of glassy transition of polymeric thin films. Successful experiments are performed with confined model hard-sphere suspensions and stimuli-responsive hydrogel thin films, all devoted to understanding microstructural dynamics that underlies friction. Our key accomplishments are highlighted below.

*1.* It is believed that the lubricity of interfacial biofilm is intimately related to the structure and dynamics of its polymeric aggregation under confinement<sup>1-2</sup>. However, such relevant microstructure and dynamics might be transient and do not leave permanent fingerprints. They are difficult to infer from bulk characterization or through coarse-grained continuum theory. Our custom-designed micron-gap rheometer combined with an inverted confocal microscope enables three-dimensional packing configuration and particle dynamics characterization of polymeric thin film impregnated with fluorescent dye with confocal over gap separation, shear frequency and amplitude. Hence, concurrent imaging and force-sensing experiments can be carried out to quantify the correlation between effective interactions and viscoelasticity of biomimetic thin films, which offers a direct and comprehensive study on how the polymeric microstructural dynamics endow specific biointerfacial interactions such as surface forces and lubrication.

2. With the new confocal micron-gap rheometer, we revisit the problem of glass transition as well as jamming phenomena of complex fluids by studying the slow dynamics of model hard-sphere poly (methyl methacrylate) (PMMA) suspension under confinement. We microscopically track multi-particle motions when PMMA suspension is confined between two flat surfaces of varied film thickness from as large as one desires down to 1-2 particle layers thick. The study of the confinement effect offers a new approach to understanding the physics of glass transition by limiting the range of accessible length scales, yet maintaining constant temperature and volume fraction, in dynamic structures that have been connected to the dramatic viscosity growth. We observe remarkable film-thickness dependence on glassy behaviors of confined PMMA suspension. The mobility and structural relaxation of very “fluid” PMMA suspensions become significantly impeded when colloidal film thickness is reduced to several particle layers, suggesting that glass transition can be induced “sooner” by spatial confinement. We expect these findings can be directly compared to the tribological study of molecular fluids by MD simulation. To determine experimentally the length scales of “cooperatively rearranging regions” (CRR) as well as to probe dynamic heterogeneity and hopping events in glassy colloidal thin films<sup>3</sup>, we recently start probing the single-particle dynamics of fluorescent tracers in super-cooled PMMA thin film by measuring the mean free paths of tracer nanoparticles of varied diameters. *A manuscript was recently submitted to Phys. Rev. E.*

3. Recent studies have shown that macromolecular structure and mechanical responses elicited by multi-macromolecular interactions in external force fields can produce a rich spectrum of macromolecular assemblies with tunable length and time scales, which are responsible for complex viscoelastic and lubrication behaviors of biological fluids. For example, it has been long believed that synovial fluids (SF) gets its superb lubrication properties from its constitute macromolecule, hyaluronic acid (HA)<sup>4</sup>. But new clinical as well as HA rheology studies demonstrated that a globular protein, lubricin, interacts with HA<sup>1,5</sup> to form linear, viscoelastic aggregates, resulting in shock-absorbing, wear-prevention structures inside SF. However, the details of intermolecular forces that decipher microscopic aggregation remain unclear. To understand the interfacial static and dynamic behaviors of thin biofilms under external forcing fields, which can be considerably different from the bulk, we study poly(N-isopropylacrylamide) (PNIPAM) hydrogel in aqueous medium as a model biomimetic lubricious system, considering that its high water content and viscoelastic nature, like other hydrogels, is similar to natural SF and tissues in addition to its biocompatibility. By using a confocal micron-gap rheometer, we observe 3D space-spanning gel structures with high compressibility and enhanced viscoelasticity in PNIPAM thin films in sharp contrast to chain-like weak aggregate clusters in the bulk suspension. We find its colloidal assembled structure can be tuned to achieve desired mechanical strength via strong or weak attraction of H-bonding and depletion by confinement, temperature and polymer additives. The study of its rheological properties with the addition of HA in comparison to the model SF consisting of HA and lubricin is currently ongoing. *A manuscript on the correlation of microstructure and viscoelasticity of confined PNIPAM thin films is in preparation.*

## **Future Plans**

The above-described research areas are currently being continued and extended into several directions. Our overarching goal is an improved understanding, at a microscopic level, of the interplay of microstructure and interfacial forces in polymeric thin films that underlies

soft lubrication in biological fluids, with an extension in developing “artificial lubricious biofilms” by molecular design of stimuli-responsive hydrogel-polymer assemblies of controllable length and time scales. Specifically, the following projects will be focused on in the second year of the grant:

1. *Study the coupling of normal and frictional forces at hard and soft interfaces.* Recent lubrication theory<sup>6</sup> for fluid-immersed soft interfaces predicted that elastic deformation of a compressible thin layer against a solid in relative motion results in a lifting force and thereby enlarges the gap distance by a mechanism that would not hold if the surfaces were hard for elastohydrodynamic lubrication. We will explore how sliding friction conversely modifies surface forces and surface-surface separation of hydrogel thin film of varied viscoelasticity in comparison to elastic self-assembled monolayers.

2. *Construct a biocompatible hydrogel-polymer system as artificial lubricious biofilms to mimic biolubricants in the human body.* To develop “artificial lubricious films” to achieve ultra-low friction coefficient comparable to natural SF, we pursue this idea with stimuli-responsive PNIPAM aqueous suspension added with polymer HA whose interparticle interaction and thus aggregation structure can be tuned by colloid-polymer interaction as well as environmental parameters such as temperature and pH.

3. *Active control of lubrication properties in biomimetic thin films.* Underlying the biofilm lubrication are the microscopic momentum/energy transfer mechanisms associated with different characteristic times,  $\tau_i$  of thin films as well as system operational time scales,  $\tau_o$ . We will explore how to modulate film interfacial forces by varying the Deborah number<sup>7</sup>,  $De \sim \tau_i/\tau_o$  where  $\tau_o$  can be varied over 3 orders of magnitudes independently by our shear or pumping devices, and the resulting microstructures will be concurrently examined microscopically. The new concept is the combination of external force fields in orthogonal directions to manipulate microstructure and viscoelasticity of biomimetic thin films.

## References

1. G. D. Jay, J. R. Torres, M. L. Warman, M. C. Laderer and K. S. Breuer, *Proc. Natl. Acad. Sci. USA* 104, 6194 (2007).
2. Y. Zhu and S. Granick, *Macromolecules* 36, 973 (2003).
3. *Jamming and Rheology*, Ed. by A.J. Liu and S. R. Nagel (Taylor & Francis, New York, 2001).
4. C. W. McCutchen, “*The Joints and Synovial Fluids*,” Ed. by L. Sokoloff (Academic Press, 1978), Chap.10, pp 437-483.
5. W. E. Krause, E. G. Bellomo, and R. H. Colby, *Biomacromolecules* 2, 65 (2001).
6. J. M. Skotheim and L. Mahadevan, *Phys. Rev. Lett.* 92, 245509 (2004) and *Phys. Fluid* 17, 092101 (2005).
7. J. Gao, W. D. Luedtke and U. Landman, *J. Phys. Chem. B.* 102, 5033 (1998).

## **Room-Temperature Synthesis of Semiconductor Nanowires by Templating Collagen Triple Helices and Their Precise Assembly into Electrical Circuits by Biomolecular Recognition**

*PI: Hiroshi Matsui*

*695 Park Ave., Dept. of Chemistry, City University of New York, Hunter College, New York, NY 10065, hmatsui@hunter.cuny.edu*

### *I. Program Scope*

Introduction of self-assembly in nanoscale building blocks is expected to accomplish robust bottom-up fabrications of electronics in a more reproducible, efficient, and economic manner; however it is necessary to selectively place multiple types of building blocks at specific locations on surfaces in high precision and reproducibility. From our previous DOE support (DE-FG-02-01ER4), we developed the bionanotechnology approach for affordable and efficient fabrications of nanoscale electronics using multifunctional “bionanotubes”, self-assembled from amphiphilic peptide monomers with glycine residues. While these peptide-assembled bionanotubes appeared to be promising building blocks for nanodevices, it is essential for these bionanotubes to have size-monodispersity, strength, and mass producibility in order to impact real-world applications. Unfortunately, most of biomolecular templates self-assembled from peptidic monomers tend to yield polydisperse materials with heterogeneous diameters and uncontrolled lengths. Here we design new collagen triple helix peptide as a template nanowire which appears to overcome the shortcomings of the bionanotubes and other biomolecular templates. The collagen triple helix is made of three polypeptide chains tightly twisted and bundled together to form a rigid, rod-shaped molecule. Collagen triple helices are monodisperse in length and diameter, which can be designed and amplified by using the recombinant technology, and these triple helices can be mineralized with metals and semiconductors and can, thus, be applied as rigid biomolecular templates for electronic nanowire fabrications. The production of the triple helix can be cost-effective when the *E. coli* expression system is optimized for the amplification.

Due to these advantageous features, biomimetic device fabrication processes developed by our previous DOE funding is further extended to fabricate collagen triple helix-based logic circuits. The overall hypothesis is that collagen triple helices can be converted to multifunctional nanowires incorporating both antibodies and “mineralizing peptides”. Specificity of the biomolecular recognition of antibody enables us to immobilize multiple types of triple helices at desired positions respectively, based on logic circuit designs. In that, circuit fabrications can be accomplished by labeling electrodes with complementary proteins and anchoring the antibody-functionalized triple helices at these locations. By using enzymatic functions of the peptides, semiconductor nanoparticles are grown on triple helices at room temperature. The specificity of peptide sequence and conformation will enable us to mineralize these nanoparticles on the triple helices in the controlled size, shape, and inter-particle distance, which ultimately tunes the conductivity of resulting triple helices. The triple helix assembly will be robust and easily scaled up, which meets the realistic expectation on the bottom-up nanofabrication. Our approach could resolve the current limitation of biomolecular nanowires in device applications because the collagen triple helices are completely monodisperse and more versatile templates.

The outcome of proposed researches will have broad impacts in basic sciences and applied engineering because this peptide-templated material synthesis method has potential to create new nanomaterials possessing novel physical, structural, and catalytic properties with no synthetic counterparts. Development of methodology to produce materials at room temperature, which currently require high temperature to synthesize, will become a significant intellectual merit for manufacturing industries since it will reduce the production cost, the facility size (such as cooling systems), and the manpower in the facility.

## II. Recent Progress

From our previous DOE support (DE-FG-02-01ER4) and the supplemental DOE support,

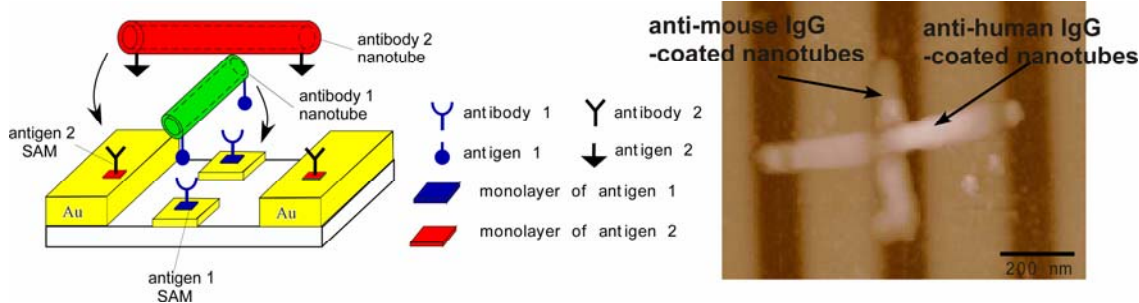


**Figure 1.** (left) Scheme to assemble two different antibody nanotubes, anti-mouse IgG-coated nanotube and anti-human IgG-coated nanotube, into the cross-bar geometry by biomolecular recognition. (right) AFM image of the two antibody nanotubes assembled in the cross-bar geometry. [X. Gao, H. Matsui, *Adv. Mater.*, **17**, 2037 (2005)]

we developed the bionanotechnology approach for affordable and efficient fabrications of nanoscale electronics using “bionanotubes”, self-assembled from amphiphilic peptide monomers with glycine residues, as building blocks. Through this approach, we demonstrated that simple circuit geometries could be created by anchoring these bionanotubes, whose ends were functionalized by “linking antibodies”, onto well-defined positions on the complementary protein-patterned substrates (Figure 1). By functionalizing circuit elements and connecting nanotubes with complementary biomolecular recognition units, we could mimic biological systems in which organic/inorganic nanoscale building blocks are routinely and precisely turned into complex structures by the biological functions with almost perfect reproducibility and high yields. By this biomimetic approach, we showed that the simultaneous immobilization of multiple bionanotubes functionalized by different linking antibodies could be “programmed” (i.e. each ligand on the bionanotube recognizes its binding site and attaches respectively) in aqueous solution without any complicated multi-step fabrication procedures to construct complex device geometries (Figure 1). Due to their robust and specific biomolecular recognition functions, the assembly of these bionanotubes could be scaled up to fabricate the bionanotube arrays.

While the biomolecular recognition makes biomolecular nanowires very attractive to apply for device fabrications, most of those nanowires made from DNAs or peptides do not possess suitable electronic properties for those applications. We recently developed a new metal/semiconductor coating method on bionanotubes by incorporating “mineralizing peptides” on the sidewalls of bionanotubes that could grow metal and semiconductor nanoparticles directly on the bionanotubes (Figure 2). An advantage of our method is that controls of the conformation and the sequence of mineralizing peptides allow us to tune sizes, inter-particle distances, and

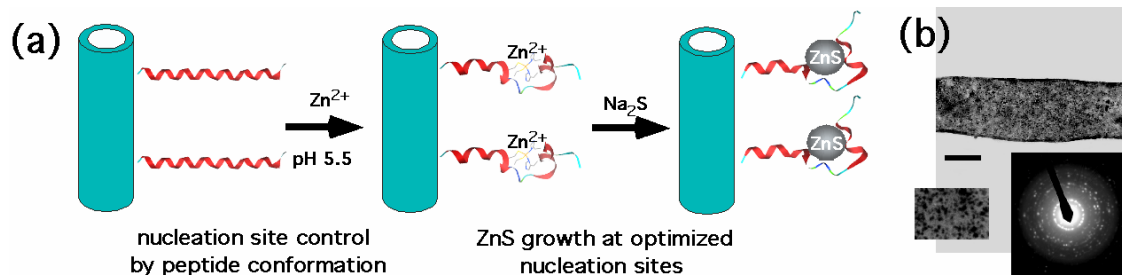


**Figure 2.** (a) Illustration of ZnS nanocrystal growth on the unfolding M1 peptides on the template bolaamphiphile nanotubes as a function of pH. (b) Transmission electron micrograph (TEM) of wurtzite ZnS nanocrystals grown on the M1 peptide coated nanotubes at pH 5.5. Inset (left): Magnified ZnS nanocrystal TEM image. Inset (right): Electron diffraction (ED) pattern of ZnS nanocrystals indicating the wurtzite structure. scale bar = 70 nm. [I.A. Banerjee, L. Yu, H. Matsui, *J. Am. Chem. Soc.*, **127**, 16002 (2005)]

shapes of nanoparticles grown on the bionanotubes, which ultimately determined the conductivity of resulting bionanotubes.

In the course of these developments, we also discovered that peptide assemblies in optimized conformations possess the unusual catalytic activity to grow nanocrystals of ZnS, BaTiO<sub>3</sub>, ZnO, and Ga<sub>2</sub>O<sub>3</sub>, which cannot be produced by any other synthetic methods at room temperature. This biomimetic room-temperature material synthesis technique is expected to have a significantly impact on manufacturing.

### III. Future Plan

The proposed biomimetic fabrication of electronics will consist of 3 steps:

Step 1: The “linking antibodies” are immobilized at the ends of collagen triple helices.

Step 2: The “mineralizing peptides” are coated on the sidewalls of collagen triple helices. Then nanoparticles (Au, ZnO, CdSe, PbSe) with certain sizes and inter-particle distances are grown on these functionalized triple helices at room temperature.

Step 3: These triple helices coated by those antibodies and nanoparticles are immobilized onto the complementary antigen-patterned Au substrates and their electronic properties in various circuit geometries are studied.

In the Step 1, we will first apply collagen triple helices designed as shown in Figure 3 in the dimension of 4 nm x 40 nm for the proposed circuit fabrication since this F877 triple helix was already demonstrated to be very rigid and stable by our group. The recombinant technology will also be applied to change their length between 40 and 300 nm by increasing the repeating units of collagen peptide sequences in the triple helix. The stabilizing sequence of the triple helix such as (GPP)<sub>x</sub> will be optimized in order to maintain their rigid structure to resist harsh semiconductor coating environments. N-terminus and C-terminus of collagen triple helix will be used to conjugate antibodies covalently at the ends of nanowires.

Proceeding to the Step 2, we will perform optical studies of metal- or semiconductor-coated triple helices to probe how their electronic structures are changed as functions of the size and the inter-particle distance of the coated nanoparticles. Then in the Step 3, semiconductor nanowires whose electric properties are optimized for logic gate designs in the Step 2 will be assembled into the electric circuit configurations via biomolecular recognition, and the performance of triple helix-based electric circuits will be evaluated.

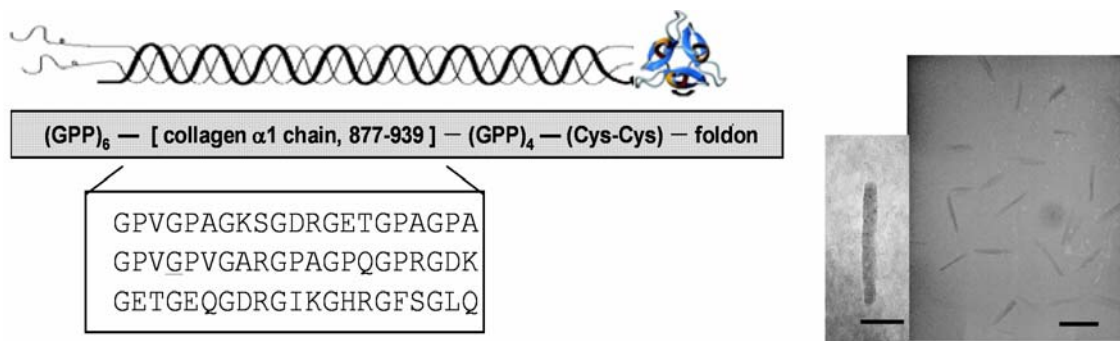


**Figure 3.** (left) Illustration of the collagen triple helix designed in a rigid structure via recombinant technology. (right) TEM image of resulting F877 collagen triple helix amplified by the *E. coli* expression system. [H. Bai, K. Xu, Y. Xu, and H. Matsui, *Angew. Chem. Intl. Ed.*, **46**, 3319 (2007)]

### IV. DOE-sponsored publications in 2005-2007

1. "Fabrication of Au nanowire of uniform length and diameter using a new monodisperse and rigid biomolecular template, collagen-like triple helix", H. Bai, K. Xu, Y. Xu, and H. Matsui, *Angew. Chem. Intl. Ed.*, **46**, 3319 (selected as a hot paper) (2007).
2. "Biomimetic and Aggregation-Driven Crystallization Route for Room-Temperature Material Synthesis: Growth of  $\beta$ -Ga<sub>2</sub>O<sub>3</sub> Nanoparticles Using Peptide Assemblies as Nanoreactors", S.Y. Lee, X. Gao, H. Matsui, *J. Am. Chem. Soc.*, **129**, 2954 (2007).
3. "Single crystalline nanoneedles with fast conductance switching properties from an interfacial polymerization-crystallization of 3, 4-ethylenedioxythiophene", K. Su, N. Nuraje, L. Zhang, I.W. Chu, R.M. Peetz, H. Matsui, and N-L. Yang, *Adv. Mater.*, **19**, 669 (2007).
4. "Mineralization of semiconductor nanocrystals on peptide-coated bionanotubes and their pH-dependent morphology changes", I.A. Banerjee, G. Muniz, S-Y. Lee, and H. Matsui, *J. Nanosci. Nanotechnol.*, **7**, 2287 (2007).
5. "Fabrication of Magnetic Nanowires by Self-Assembling FePt Nanoparticles on Peptide Nanotubes", L. Yu, P. Porrata, H. Matsui, *ACS series, Self-Organized Photonic Materials*, in print (2007).
6. "Highly Accurate Immobilization of Antibody Nanotubes on Protein-Patterned Arrays with Their Biological Recognition by Tuning Their Ligand-Receptor Interactions", Z. Zhao, H. Matsui, *Small*, 1390 (2007).
7. "Room Temperature-Synthesis of Ferroelectric Barium Titanate Nanoparticles Using Peptide Nano-Rings as Templates", N. Nuraje, K. Su, A. Haboosheh, J. Samson, E.P. Manning, N-L. Yang, and H. Matsui, *Adv. Mater.*, **18**, 807 (2006).
8. "Self-Assembly of Au Nanoparticle-Containing Peptide Nano-Rings on Surfaces", N. Nuraje, K. Su, J. Samson, A. Haboosheh, R.I. MacCuspie and H. Matsui, *Supramol. Chem.*, **18**, 429 (2006). (the top 10 most accessed article in 2006 in *Supramol. Chem.*)
9. "Room-Temperature Wurtzite ZnS Nanocrystal Growth on Zn Finger-Like Peptide Nanotubes by Controlling Their Unfolding Peptide Structures", I.A. Banerjee, L. Yu, and H. Matsui, *J. Am. Chem. Soc.*, **127**, 16002 (2005).
10. "Fabrication and Application of Enzyme-Incorporated Peptide Nanotubes", L. Yu, I.A. Banerjee, X. Gao, N. Nuraje, H. Matsui, *Bioconjugate Chem.*, **16**, 1484 (2005).
11. "Peptide-Based Nanotubes and Their Applications in Bionanotechnology", X. Gao, H. Matsui, *Adv. Mater.*, **17**, 2037 (2005).
12. "Simultaneous Targeted Immobilization of Anti Human-IgG-Coated Nanotubes and Anti Mouse-IgG-Coated Nanotubes on the Complementary Antigen-Patterned Surfaces via Biological Molecular Recognition", Z. Zhao, I.A. Banerjee, H. Matsui, *J. Am. Chem. Soc.*, **127**, 8930 (2005).
13. "Simple Separation of Peptide Nanotubes by Using Size-Exclusion Columns and Fabrication of 1D Single-Chains of Au Nanoparticles on the Thin Peptide Nanotubes", X. Gao, R. Djalali, A. Haboosheh, J. Samson, N. Nuraje, H. Matsui, *Adv. Mater.*, **17**, 1753 (2005).
14. "Magnetic Nanotube Fabrication by Using Bacterial Magnetic Nanocrystals", I.A. Banerjee, L. Yu, M. Shima, T. Yoshino, H. Takeyama, T. Matsunaga, H. Matsui, *Adv. Mater.*, **17**, 1128 (2005).
15. "Controlled Growth of Se Nanoparticles on Ag Nanoparticles in Different Ratios", X. Gao, L. Yu, R.I. MacCuspie, H. Matsui, *Adv. Mater.*, **17**, 426 (2005).
16. "Applications of biological nanotubes to device fabrications and material syntheses", OyoButsuri, *Appl. Phys. Japan*, **74**, 1576-1582 (2005).
17. "Bionanotechnology: Device fabrication using natural and synthetic peptides", H. Matsui, in *Bio-Industry*, CMC Publisher, Tokyo, **22**, 27-32 (2005)



Material lessons of biology: Structure-function studies of protein sequences Involved in inorganic - organic composite material formation.

John Spencer Evans

Laboratory for Chemical Physics, New York University, 345 E. 24th Street, New York, NY 10010. tel: 212/998-9605 email: jse1@nyu.edu

### **Program (BES) Scope**

Nature has developed unique strategies for designing and constructing composite materials that combine the functional aspects of organic polymers and inorganic solids. This is best seen in biomineralizing organisms, where a wide range of crystalline and amorphous inorganic - base materials are synthesized under ambient and extreme conditions under the direction of proteins. These materials not only provide mechanistic advantages, but in some instances are capable of participating in energy-related tasks such as light amplification/transmission, generation of electric and magnetic fields, and detection. These materials have evolved over millions of years, and now provide the materials and nanotechnology fields with useful models.

The mollusk shell is a laminate material comprised of nanostructured, opposing layers of calcium carbonates (calcite, aragonite polymorphs) that exist in close proximity. The nacre layer of the shell are nearly 3,000 x more fracture-resistant than pure calcium carbonates, and thus the mollusk shell has important implications for the fabrication of artificial organic/inorganic laminates, ceramics, and other hybrid materials for energy applications.

The nacreous or aragonite layer is the primary focus of our DOE - sponsored research since this layer possesses two very important processes: **polymorph selection/stabilization and fracture resistance**. If we can understand the molecular principles that are at work in the nacre layer, then we can exploit some of the strategies involved in these processes for materials design and synthesis.

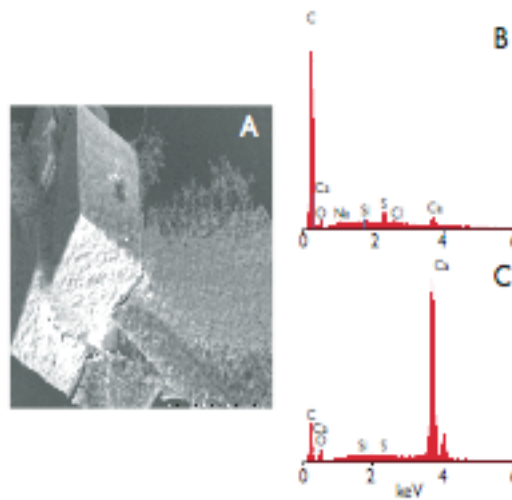
### **Recent Progress**

**Polypeptide sequence modification and its impact on crystal growth and nucleation.** We have altered the sequences of various nacre-specific polypeptides (n16N, AP7N) to determine which amino acids are important for

crystal growth and nucleation. We have determined that negatively charged amino acids such as Asp or Glu play an important role in two respects: first, to allow interaction with positively charged metal ions at the crystal interface, and, to fine tune the structure of the polypeptide for mineral interaction.

Future goals: We plan to investigate the role of other amino acids in these sequences.

**Figure 1:** (A) Backscatter SEM image of calcium carbonate crystal/thin film grown in the presence of 100 mM n16NN; (B) EDX spectrum taken of typical n16NN generated thin film; (C) EDX spectrum taken of the surface of a typical calcium carbonate crystal grown in the presence of n16NN.



**Identification of protein regions which promote assembly.** One of the strategies that Nature employs is to team up biomineralization proteins together as functional complexes or “molecular factories”. This ensures that efficiency and energetics are conserved as the growth of crystals proceeds in organisms. To assemble these “factories”, certain biomineralization proteins possess regions which allow them to dock or interact with other proteins and bring the complex together. In the nacre-associated protein, AP7, we have identified a protein docking domain that shares similarities with a family of sequences known as C-RING. This domain binds Zn (II) and is configured as a helical region that is punctuated by turn and coil regions. Since AP7 is known to associate with another nacre protein, AP24, we believe that this C-RING-like region on AP7 is responsible for allowing AP7 - AP24 complexes to form in the nacre layer and inhibit the growth of the calcite polymorph in favor of the aragonite polymorph. Future goals: We intend to identify which region(s) of AP24 that can dock with this C-RING domain of AP7.

**Structural features of proteins that are involved in crystal nucleation and growth.**

In concert with our studies of protein docking domains, we have also identified the full three dimensional structure of the AP7 protein itself. The protein possesses two important regions, the C-terminal domain, which is believed to be a protein docking domain, and, the N-terminal domain, which is the mineral interaction/modulation region of AP7. The two domains are structurally oriented 90 degrees apart, thus maintaining spacing and orientation that would allow a second protein to bind to the C-terminal region of AP7 without physically obscuring or compromising the N-terminal region’s ability to interact with ion clusters and inorganic interfaces. Future goals: Our next step is to



determine the structure of other nacre-associated proteins that participate in aragonite formation, and, expand these studies to other proteins involved in the formation of other minerals.

**Figure 2:** NMR-determined solution structure of 66 AA AP7, shown from side and top perspectives. “DD” refers to Asp-Asp mineral interaction sites within the N-terminal region of AP7. The C-terminal end is the location of the C-RING domain.

**Interaction of polypeptides at the mineral interface.** The actual events that occur when a polypeptide binds at mineral surfaces is still elusive, and yet, this process is a highly desirable goal that needs to be achieved in order to successfully translate Nature’s strategies to the laboratory setting. To address this issue, we have employed X-ray microscope XANES spectroscopy to analyze the bonding states that exist at the calcium carbonate - polypeptide mineral interface. We used N-terminal sequence fragments from the following nacre-associated proteins: AP7, AP24, and n16. Our data shows that the sidechains of these sequences undergo reorganization upon adsorption, indicating that there is conformational

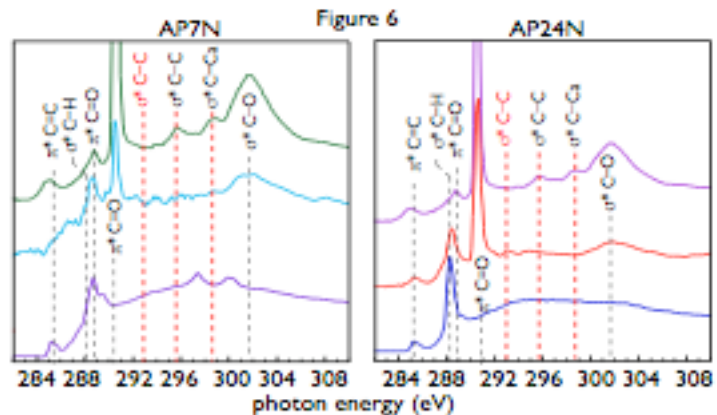


**Figure 3:** XANES spectra of AP7 - and AP24-N-terminal fragments adsorbed onto calcite crystals. For comparison, the XANES spectra of plain calcite crystals and the pure polypeptides are shown for comparison.

adaptation when these sequences bind at the calcite crystal. Moreover, the XANES data indicates that the lattice structure of calcite also undergoes some degree of reordering or distortion when these polypeptides interact. Future goals: This surprising result will be followed up via additional studies of other proteins and minerals to determine how widespread this phenomena may be.

## Recent DOE-Funded Publications

Delak, K, Collino, S, Evans, JS (2007) Expected and unexpected effects of amino acid substitutions on polypeptide-directed crystal growth. *Langmuir*, submitted.

Metzler, RA, Kim, IW, Evans, JS, Zhou, D, Beniash, E, Wilt, F, Abrecht, M, Susan N. Coppersmith, SN, Gilbert, PUPA (2007) Probing the organic-mineral interface (OMI) at the molecular level in model biominerals. *Langmuir*, submitted.

Collino, S, Evans, JS, (2007) Structural features that distinguish kinetically distinct biomineralization polypeptides. *Biomacromolecules* 8: 1686-1694.

Kulp, JL III, Minamisawa, T, Shiba, K, Evans, JS (2007) Conformational properties of an artificial protein that regulates the nucleation of inorganic and organic crystals. *Langmuir* 23: 3857-3863.

Kim, IW, Darragh, MR, Orme, C, Evans, JS (2006) Molecular "tuning" of crystal growth by nacre-associated polypeptides. *Crystal Growth and Design*, **5**: 5-10.

Collino, S, Kim, IW, Evans, JS, (2006) Identification of an "acidic" C-terminal mineral modification sequence from the mollusk shell protein, Asprich. *Crystal Growth and Design*, **6**: 839-842.

Kim, IW, Collino, S, Morse, DE, Evans, JS (2006) A crystal modulating protein from molluscan nacre that limits the growth of calcite *in vitro*. *Crystal Growth and Design*, **6**: 1078-1082.

## WET INTERFACES: DEVELOPING A MOLECULAR FRAMEWORK FOR UNDERSTANDING THE BEHAVIOR OF MATERIALS IN AQUEOUS SOLUTIONS

Geraldine L. Richmond  
Department of Chemistry  
1253 University of Oregon  
Eugene, Oregon 97403-1253  
richmond@uoregon.edu

### *Program Scope and Motivation*

There is no denying that this nation and the world are facing serious challenges in having sustainable energy resources for future generations. Materials chemistry has a leading role to play in these areas as well as in addressing many other important societal issues that rely on advanced technologies. Over the past decade we have witnessed many exciting advances in the laboratory towards the development of new materials, particularly in the area of molecular architecture and nanoscience. Many of these new materials are being made in more complex and reactive environments than in the past where vacuum or clean-room conditions were often employed. The assembly of thin films at liquid/solid and liquid/liquid interfaces fall into this category as well the multitude of unique nanostructured materials that assemble at liquid surfaces. This increased complexity of the materials growth environment is usually accompanied by less predictability, often because of our limited knowledge of the fundamental molecular interactions that lead to the assembly and stability of these interfaces. The focus of the science in the DOE sponsored research in this laboratory is on making key contributions to our understanding of interfacial interactions that play a key role in the creation, assembly and stability of thin films, polymers and nanoparticles at complex interfaces. In these current and future planned studies we are examining (1) the molecular and ionic factors that control the assembly of molecular monolayers at charged mineral surfaces in aqueous media,<sup>1,2,6,7</sup> (2) the dynamics of molecular and nanoparticle assembly at solid/liquid interfaces<sup>11</sup> and liquid/liquid interfaces respectively, and (3) the molecular behavior of water, solutes and surfactants at the surface of hydrophobic films and polymers.<sup>3,4,5,8,9,10</sup> The fundamental studies pursued have direct relevance to many important areas of interest to the Department of Energy including surface wetting, flotation, dissolution, lubrication, nanoparticle structure, molecular assembly, carbon sequestration and biocompatibility. Our approach is one that closely couples experiment with computation. Surface vibrational sum frequency spectroscopy (VSFS) is used to probe the molecular properties in-situ in addition to using other traditional surface characterization methods. These studies are intimately coupled to our increasing expertise in molecular dynamics simulations. This combination of experiment and simulation provides us with powerful capabilities for understanding the molecular complexity of these important interfacial systems. Provided below is a brief description of some of our most recent studies on the dynamics of monolayer adsorption and assembly at mineral/water interfaces.

### *Recent Progress on Project (2): Surfactant Adsorption Dynamics at the Solid–Liquid Interface*

Self assembly of surface active agents at solid–liquid interfaces is critical for many processes in nature and technology, including the stability of suspension, detergency, wetting and mineral separation.<sup>1</sup> Historically, a detailed understanding of nanometer–scale layers has emerged. However, surprisingly little is known about their *dynamics* — the key to non–equilibrium phenomena. Even in equilibrium, there is a constant exchange of monomers between bulk and monolayer. Determination of the associated rate constants has been previously undertaken by evaluating adsorption and desorption kinetics. These methods are not practical near equilibrium adsorption as they rely upon a changing surface concentration. Hence, little can be learned about the true equilibrium state of a monolayer. The importance of dynamical properties at solution interfaces has long been realized and relaxation techniques, utilizing the system's response to perturbation from equilibrium have developed into powerful tools. Unfortunately, these methods do not adapt easily to the rather slow kinetics typically found at the solid–liquid interface.

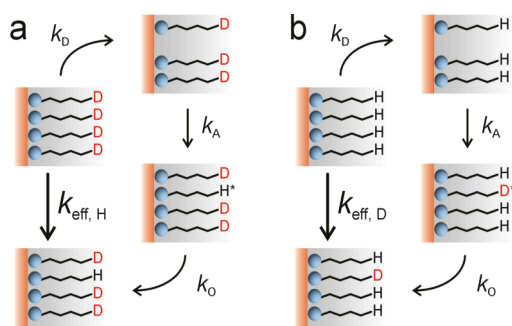


**Figure 1.** Idealized monomer exchange mechanism. Isotope labeling of C12Na is indicated by H (CH<sub>3</sub> terminus) or D (CD<sub>3</sub> terminus). Exchange reaction starting from a fully deuterated (a) or hydrogenated (b) monolayer.

phenomena occurs from the bulk into a randomly oriented state ( $k_A$ ) on the surface. Finally an ordered monolayer is reformed ( $k_O$ ). During the experiment, exchange kinetics, characterized by  $k_{\text{eff, H}}$  or  $k_{\text{eff, D}}$ , were followed by measuring the resonance response of the nonlinear susceptibility  $\chi^{(2)}$  at frequencies characteristic of the carboxylate headgroup ( $\nu\text{CO}$ , 1453  $\text{cm}^{-1}$ ) as well as the symmetric stretch of its terminal CH<sub>3</sub> group ( $\nu\text{CH}_3$ , 2873  $\text{cm}^{-1}$ ). Unlike linear spectroscopies, VSFS utilizes a coherent process within the temporal and spatial overlap of a visible (VIS, 532 nm) and IR beam (tunable).<sup>1,6,7</sup> In our experiment, the intensity of the sum-frequency (SF) signal is directly proportional to the square of the interface susceptibility,  $\chi_{\text{yz}}^{(2)}$ , which is a measure for the number of oriented molecules at the interface. Note that this intrinsic sensitivity for molecular orientation has important consequences for the effective (observable) exchange rates (Fig. 1):  $k_{\text{eff, H}}$  encompasses all three steps with only the final species SF active, whereas  $k_{\text{eff, D}}$  is determined by the desorption process ( $k_D$ ), as this key step reduces the number of SF oscillators.

Typical experimental data is presented in Fig. 2. The total adsorption density, as measured by the  $\nu\text{CO}$  susceptibility, remains constant as expected from the similarity of C12-H and C12-D. This demonstrates equilibrium adsorption. In looking at the  $\nu\text{CH}_3$  response, the rapid onset of the exchange reaction suggests a fast transport of surfactant monomers from the bulk into the interfacial region. Surfactant molecules close to the interface but not incorporated into the monolayer are replaced on a timescale much faster than the observed kinetics, in agreement with other studies of loosely bound surfactant aggregates.

A series of exchange experiments were performed varying the age of the surface (1 to 20 h), and at two bulk surfactant concentrations, 10 and 30  $\mu\text{M}$ . These concentrations are both above the hemi-micellar critical limit ( $\sim 1 \mu\text{M}$ ), but well below the critical micellar concentration. Kinetic analysis revealed no significant effect of monolayer aging or bulk concentration on the exchange rate constants  $k_{\text{eff, D}}$  and  $k_{\text{eff, H}}$ , which relate to the exchange reaction between a monolayer, initially composed of neat C12-H or C12-D, and a liquid phase containing C12-D or C12-H, respectively. Both constants were found to be equal at an average value of  $(8.1 \pm 2.0) \times 10^{-4} \text{ s}^{-1}$ . The desorption reaction ( $k_D$ , Fig. 1) is then rate-determining and the ordering step ( $k_O$ ) is very fast. The fraction of disordered (i.e., non SF-active) molecules in the

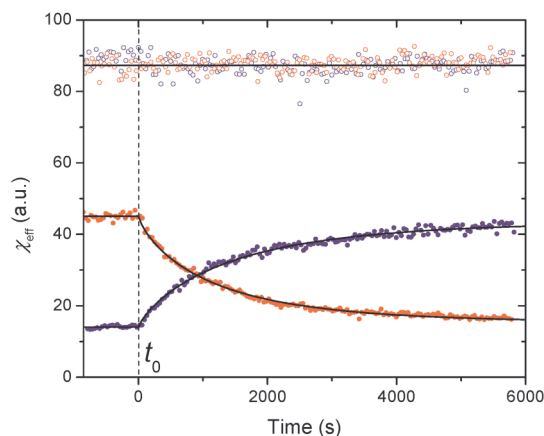


**Figure 2.** Monomer exchange kinetics of a C12-D (blue) and C12-H (red) monolayer. At time  $t_0$ , the liquid phase was replaced by a solution of identical concentration (10  $\mu\text{M}$ ), but opposite isotope labeling.

equilibrium monolayer must thus be small. For comparison, *non-equilibrium* desorption experiments (similar to those reported by others and used to characterize exchange dynamics) were performed (Fig. 3). From the temporal profile of the surface density of SF active species (vCO) desorption into neat water is obviously much slower initially and characterized by a substantial induction period. A detailed analysis of these studies has been submitted for publication.

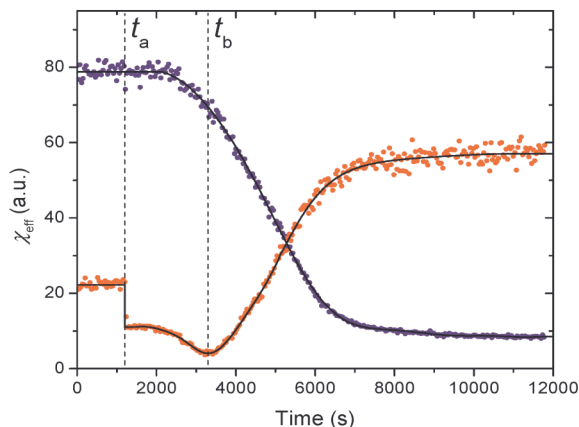


**Figure 3.** Desorption kinetics of a C12-H monolayer. At time  $t_a$ , the surfactant solution was replaced by neat water. Charge neutrality of the interfacial water layer is reached at  $t_b$ .

their hydrogen atoms pointing toward the liquid phase, whereas water molecules above an intact monolayer are oppositely oriented. During this same time the defect concentration of the monolayer reaches a critical level and desorption then proceeds at a much higher rate.

The direct measurement of monomer exchange rates of interfaces at *equilibrium* adsorption density has important implications for our understanding of self-assembled monolayers. A simplified, three step, monomer exchange process is described in Fig. 1. The surfactant is first released from the monolayer (rate constant  $k_D$ ). The novel, non-linear spectroscopic approach presented here reveals the dynamism of such interfaces. These VSFS results also demonstrate the importance of understanding the structure of liquid adjacent to the monolayer as this structure strongly affects system dynamics. From this realization we may also infer a reason for the wide variation in reported rates of equilibrium and non-equilibrium kinetic parameters.<sup>11</sup> The structure of the liquid phase adjacent to the monolayer governs the energetic barriers and thus the kinetics of monomer exchange. This structure is demonstrably highly fragile. Only very few molecules can be withdrawn from the monolayer at a given time and if they are not replenished instantly, further desorption incurs high energetic cost because it disturbs the highly-coordinated hydrogen bond structure of water molecules within the interfacial region.

### *Ongoing and Near-Future Plans*

Our planned studies of monolayer structure and assembly at the solid/liquid interface include:

- measuring the molecular structure and bonding of charged surfactants as they assemble at the surface of charged mineral surfaces in solution and exploring how the interfacial water plays a role in the assembly of surfactants at the aqueous/mineral interface.
- determining how surface-adsorbate interactions and the assembly process vary with the composition of the aqueous phase (i.e. inorganic salt, pH, ionic strength etc.).
- conducting time-resolved spectroscopic measurements of the assembly process to determine the rates of adsorption and desorption of monomers during the assembly process, the dynamic behavior of interfacial water, and the effect of ions, solutes and surface composition and charge on these rates.

As part of the desorption experiments we concurrently monitored the number of oriented water molecules in the interfacial region (done via measuring their SF intensity at  $3150\text{ cm}^{-1}$ ). When neat water is introduced, this intensity immediately drops by 50% (Fig. 3). This indicates a severe disruption of interfacial water structure induced by minute changes in the surface layer. Slowly, monomer desorption ensues. The monolayer is negatively charged at full coverage, a phenomenon commonly referred to as overcharging,<sup>1</sup> and retains this charge during this initial period. Gradually, the point of charge neutrality is reached at  $t_b$ . At this time a degree of structure returns to water in the region, but a detailed analysis of the phase of the VSFS response demonstrates that the interfacial water molecules have flipped to an orientation with

In another area (not described above that involve publications 3, 4, 5, 8, 9, 10) we seek to expand our knowledge of the molecular properties of water, solutes and surfactants at the surface of hydrophobic films and polymers in aqueous solutions by:

- measuring the structure and bonding of water and solutes at fluorinated polymers, and fluorocarbon (FC) monolayer assemblies, and comparing them with their hydrocarbon (HC) counterparts.
- using signature vibrational modes of water that are indicative of weak bonding interactions to measure the behavior of weakly interacting water molecules found at these interfaces and to examine the factors that lead to (where possible) penetration into hydrophobic films.
- examining what effect pH, adsorbed solutes and different charged ions have on molecular structure and bonding at the FC-monolayer/water, HC-monolayer/water and polymer/water interfaces.
- conducting computational studies that calculate the VSF spectrum using MD simulations, determining from these calculations the best model(s) to use to accurately describe the system by comparison with experiment, and extracting additional molecular information from the results to complement and augment the understanding derived from the experimental studies.

### **Publications**

1. "Surfactant Adsorption at the Salt/Water Interface: Comparing the Conformation and Interfacial Water Structure for Selected Surfactants", K. A. Becraft and G.L. Richmond, *J. Phys. Chem. B*, 109 (5108 – 5117) 2005.
2. "Investigations of the Solid-Aqueous Interfaces with Vibrational Sum Frequency Spectroscopy," A. J. Hopkins, C. L. McFearin and G.L. Richmond, *Curr. Opin. in Solid State and Mater. Science*, 9 (19-27) 2005.
3. "Recent Experimental Advances in Studies of Liquid/Liquid Interfaces", M.A. Leich and G.L. Richmond, *Faraday Discuss.* 129 (1-21), 2005. (includes monolayer studies)
4. "Vibrational Sum Frequency Spectroscopic Investigations of Molecular Interactions at Liquid/Liquid Interfaces", M. R. Watry and G.L. Richmond, in *Interfacial Nanochemistry*, ed. H. Watarai, Kluwer Academic/Plenum Publishers, pgs 25-56, 2005.
5. "Understanding the Population, Coordination, and Orientation of Water Species Contributing to the Nonlinear Optical Spectroscopy of the Vapor-Water Interface through Molecular Dynamics Simulations", D.S. Walker, D.K. Hore and G.L. Richmond, *J. Phys. Chem. B* 110 (20451 – 20459) 2006.
6. "In-situ Investigation of Carboxylate Adsorption at the Fluorite/Water Interface by Sum Frequency Spectroscopy", S. Schrödle, F.G. Moore and G.L. Richmond, *J. Phys. Chem. C*, 111, (8050-8059) 2007.
7. "Surface Speciation at Solid/Liquid Interfaces: A Vibrational Sum-Frequency Study of Acetate at the Fluorite/Water Interface", S. Schrödle, F.G. Moore and G.L. Richmond, *J. Phys. Chem. C*, 111 (10088-10094) 2007.
8. "Layered Organic Structure at the Carbon Tetrachloride–Water Interface" D. Hore, D. Walker and G. Richmond, *J. Amer. Chem. Soc.*, 129 (752-753) 2007.
9. "Molecular Structure of the Chloroform-Water and Dichloromethane-Water Interfaces", D. K. Hore, D. S. Walker, L. MacKinnon and G. Richmond, *J. Phys. Chem. C*, 111 (8832-8842) 2007.
10. "Depth Profiling of Water Molecules at the Liquid-Liquid Interface using a Combined Surface Vibrational Spectroscopy and Molecular Dynamics Approach", D. S. Walker and G.L. Richmond, *J. Amer. Chem. Soc.*, 129 (9446-9451) 2007.
11. "Monomer Exchange Dynamics of Self-Assembled Surfactant Monolayers at the Solid-Liquid Interface", S. Schrödle and G.L. Richmond, *Chem. Phys. Chem.*, in press.



Program Title: Design, Synthesis & Characterization of Novel Electronic & Photonic BioMolecular Materials

Principal Investigators: J.K. Blasie, W.F. DeGrado, J.G. Saven & M.J. Therien

Mailing Address: Department of Chemistry, University of Pennsylvania, 231 South 34<sup>th</sup> Street, Philadelphia, PA 19104-6323

Email: [jkblasie@sas.upenn.edu](mailto:jkblasie@sas.upenn.edu)

Program Scope:

Linearly extended conjugated chromophores can now be designed to possess an electron donor-bridge-acceptor motif, and thereby exhibit efficient light-induced electric charge separation over large nano-scale distances. Closely related chromophores can be designed to also minimize their HOMO-LUMO bandgap and thereby optimize their molecular non-linear optical polarizability. These exceptional microscopic properties can be exploited to result in novel macroscopic electro-optical materials if the following can be controlled and thereby optimized: a) the positional & orientational ordering of the chromophores in a 2-D or 3-D ensemble, b) the conformation & symmetry of the chromophore within the ensemble, and c) the interaction among the chromophores in the ensemble. Exceptionally stable, artificial  $\alpha$ -helical peptides based on n-helix bundle structural motifs (e.g., n=2-6) can now be computationally designed to achieve these three key goals. The interior of the bundle can be designed to control the local environment, conformation and vectorial orientation of the chromophore within the bundle. The exterior can be designed to control the vectorial orientation and ordering of the peptide-chromophore complexes within both 2-D and 3-D ensembles. Importantly, incorporation of the chromophore into the core of the bundle with its exterior controlling the nature of the ordering of the complex in the ensemble provides for the additional control over chromophore-chromophore interactions within the ensemble. For example, in non-linear optics, the lack of control of interactions between chromophores is thought to be responsible for the inability of chromophore ensembles to achieve their predicted material properties. In the case of light-induced electric charge separation, the inability to achieve purely uni-directional charge separation over large nano-scale distances is thought to contribute substantially to their relatively low efficiencies. The n-helix bundle structural motifs are chosen for the artificial peptides because of their significantly higher stability compared to natural proteins. However, the interior of the bundle scaffold may not be so stable to the supramolecular assembly process required to form a sufficiently ordered material. Thus, it is important to monitor structurally the various stages of the self-assembly process starting from the designed peptide, e.g. a particular n-helix bundle, to the incorporation of the extended conjugated chromophore, through to the supramolecular assembly of the peptide-chromophore complexes into an ensemble material ordered on a macroscopic scale. Since the desired material properties need not require long-range periodic order, as opposed to orientational order, in two or three dimensions, structural determination in the absence of such "crystallinity" is essential. As a result, the research program necessarily involves a strong coupling of chromophore design and peptide design, with essential structural and functional characterization at the microscopic level of the isolated chromophore-peptide complex, as well as at both the microscopic and macroscopic levels within the 2-D & 3-D ensembles. These essential structural and functional characterizations can then provide important feedback to the chromophore and peptide design process to result in the desired optimization of the macroscopic material properties of the ensemble. Thus, the research program described can only be accomplished via a highly collaborative multi-investigator approach.

## Recent Progress:

A recent example is used to demonstrate our approach. Extended conjugated chromophores, based on linear arrays of metallo-porphyrins and/or metal-polypyridyl complexes, exhibit exceptional non-linear optical (NLO) properties. As mentioned above, these microscopic properties can be exploited to result in a macroscopic electro-optical material if the following can be controlled and thereby optimized: a) the positional & orientational ordering of the chromophores in a 2-D to 3-D ensemble, b) the conformation & symmetry of the chromophore within the ensemble, and c) the interaction among the chromophores in the ensemble. With regard to chromophore conformation, it has been recognized that  $D_2$  &  $D_{2d}$  symmetries, for example, could be exploited for the design of single-oscillator octupolar NLO chromophores. Such conformations have been recently detected only as thermally accessible, minor sub-populations of the otherwise symmetric chromophores, e.g., ethyne- & butadiyne-bridged Zn-porphyrin dimers, present in solution, via their second order NLO response measured by hyper-Rayleigh light scattering (publication 2).

A *de novo* designed amphiphilic 4-helix bundle peptide, designated AP0, has been utilized to incorporate extended conjugated NLO chromophores. Previous experimental studies demonstrated that altering the position of the chromophore's binding site in the primary sequence of the helices, e.g. through a histidyl residue binding a metallo-porphyrin in the chromophore via axial ligation of the metal atom, appears to effectively control the chromophore's spatial position and vectorial orientation within the peptide scaffold (publication 8). The bundle's designed amphiphilicity provided for the orientational ordering of peptide-chromophore complexes within 2-D ensembles at the liquid-gas and solid-gas interfaces with high in-plane chromophore density (publication 9). Second Harmonic Generation (SHG) has recently been demonstrated for one such complex at the latter interface, importantly demonstrating the preservation of the chromophore's molecular hyperpolarizability in the macroscopic response of the ensemble.

Nevertheless, the atomic-level 3-D structure and dynamics of the complex must be investigated. The peptide is expected to modulate the conformation & symmetry of the chromophore, which is key to optimizing the chromophore's hyperpolarizability and resulting nonlinear optical response of the material. Unfortunately, the structural methods utilized to demonstrate the orientational & positional ordering of the peptide-chromophore complexes at these interfaces are capable of providing neither atomic-resolution detail concerning the chromophore's conformation and local environment nor its dynamics within the peptide-chromophore complexes, especially in the absence of long-range, 2-dimensionally crystalline order in the ensemble. Classical Molecular Dynamics (MD) simulations are capable of providing such information, and importantly, the predictions from such simulations can be rigorously tested experimentally (publication 10). We have found that the designed coiled-coil structure of the particular 4-helix bundle peptide and the local environment of the chromophore in the bundle are dominant in determining the conformation and dynamics of the chromophore (publication 11). The designed coiled-coil structure induces an inter-planar twist of 20-25° between the two Zn-porphyrin least-squares planes about the axis of the butadiyne bridge of the chromophore, dependent neither upon the choice of initial configuration nor the chromophore's inter-planar torsional potential employed in the MD simulations. Importantly, the fluctuations about the mean twist-angle are limited to less than  $\pm 5^\circ$ . Thus, it would appear that gaining control over coiled-coil structure of the 4-helix bundle peptide should provide an elegant tool to optimize the chromophore's NLO response (see below).

## Future Plans:

*Non-Linear Optics:* With regard to the example described in the Progress section above, a computational design approach based in statistical thermodynamics (publication 3) will be used to design 4-helix bundle peptides to incorporate such extended conjugated chromophores, based on linear arrays of metallo-porphyrins and/or metal-polypyridyl complexes, with selected coiled-coil structures, described by inter-helical crossing-angles ranging from  $\sim 30^\circ$  (i.e., highly coiled helices) down to  $\sim 0^\circ$  (i.e., uncoiled straight helices). Recent progress has already demonstrated such control by design over the coiled-coil structure of an amphiphilic 4-helix bundle peptide in the absence of an incorporated extended chromophore. The structures and dynamics of these so-designed 4-helix bundle peptide/extended chromophore complexes in 2-D monolayer ensembles will be investigated by MD simulations and compared with experimental results from x-ray & neutron reflectivity and grazing-incidence x-ray diffraction, with regard to bundle structure and inter-bundle ordering, and from circular dichroism and hyper-Rayleigh light scattering, with regard to chromophore conformation. In addition, this computational design approach will be utilized to a) gain control over the orientational and positional ordering of the peptide-chromophore complexes in 2-D monolayer ensembles to approach 2-D crystalline order and to b) utilize folded single-chain peptide designs instead of associated quaternary structures to better control the vectorial association of the complexes with inorganic surfaces, key to both single particle and ensemble based device applications for such peptide-chromophore complexes. 3-D crystalline ordering of a water-soluble 3-helix bundle peptide in the absence of an incorporated chromophore has already been achieved by design and demonstrated experimentally. Folded single-chain designs incorporating a non-biological chromophore have also been recently achieved and demonstrated experimentally (publication 4).

*Light-Induced Electric Charge Separation:* In addition to the above, we plan to extend our approach to the closely related, linearly extended conjugated chromophores possessing a donor-bridge-acceptor motif to exhibit efficient light-induced electric charge separation over large nano-scale distances. The computational design approach will again be key to gaining control over chromophore conformation within the n-helix bundle/chromophore complex critically important to maximizing charge separation and minimizing charge recombination. Similarly, the structures and dynamics of these so-designed n-helix bundle peptide/extended chromophore complexes in 2-D monolayer ensembles will be investigated by MD simulations and compared with experimental results from x-ray & neutron reflectivity and grazing-incidence x-ray diffraction, with regard to bundle structure and inter-bundle ordering, and from polarized transient absorption/emission spectroscopy, with regard to chromophore conformation. Electric charge separation & charge recombination rates will be determined at the microscopic level in the monolayer ensembles via transient IR spectroscopy, while charge separation efficiency will be measured with traditional approaches for ultrathin film devices at the macroscopic level. In addition, this computational design approach will similarly be utilized to a) gain control over the orientational and positional ordering of the peptide-chromophore complexes in 2-D monolayer ensembles to approach 2-D crystalline order and to b) utilize folded single-chain peptide designs instead of associated quaternary structures to better control the vectorial association of the complexes with inorganic surfaces, key to both single particle and ensemble based device applications for such peptide-chromophore complexes.

*Extension from 2-D to 3-D:* The plans described above concern primarily 2-D monolayer assemblies of the peptide-chromophore complexes with regard to both potential device applications. Future work will also include new peptide design approaches for the step-wise directed assembly of linear arrays of the peptide-chromophore complexes. This development, based on orthogonal protection/deprotection chemistry employing non-biological amino-acids, is important for both single particle nano-gap and multilayer ensemble based device applications for such peptide-chromophore complexes. The first phase of such an approach has also been recently achieved (publication 5).

Publications (Principal Investigators in **boldface**):

- 1) Molecular Engineering of Intensely Near-Infrared Absorbing Excited-States in Highly Conjugated Oligo(Porphinato)Zinc-(Polypyridyl)Metal(II) Supermolecules, T. V. Duncan, T. Ishizuka, and M. J. **Therien**, (2007) *J. Am. Chem. Soc.* 129: 9691-9703.
- 2) Strongly Coupled Oscillators having  $D_2$  Symmetry: an Alternative Structural Motif for Potent Octopolar Nonlinear Optical Chromophores, T. V. Duncan, K. Song, I. Miloradovic, A. Persoons, T. Verbiest, M. J. **Therien**, and K. Clays, *Angew. Chemie, Int. Ed. Engl.* Submitted.
- 3) Computational Protein Design: Structure, Function and Combinatorial Diversity, Kang, S-G. and **Saven**, J.G. (2007) *Current Opinion in Chemical Biology* 11: 329-334.
- 4) De Novo Design of a Single Chain Diphenylporphyrin Metalloprotein, G. M. Bender, A. Lehmann, H. Zou, H. Cheng, H. C. Fry, D. Engel, M. J. **Therien**, J.K. **Blasie**, H. Roder, J. G. **Saven**, and W. F. **DeGrado**, (2007) *J. Am. Chem. Soc.* 129: 10732-10740.
- 5) Using  $\alpha$ -Helical Coiled-Coils to Design Nanostructured Porphyrin Arrays, K. A. McAllister, H. Zou, F. V. Cochran, G. M. Bender, A. Senes, H. C. Fry, V. Nanda, P. A. Keenan, J. D. Lear, M. J. **Therien**, J. K. **Blasie**, and W. F. **DeGrado**, *J. Am. Chem. Soc.* Submitted.
- 6) Amphiphilic 4-Helix Bundles Designed for Light-Induced Electron Transfer Across Soft Interfaces, Ye, S., Discher, B.M., Strzalka, J.W., Xu, T., Wu, S.P., Noy, D., Kuzmenko, I., Gog, T., **Therien**, M.J., Dutton, P.L. and **Blasie**, J.K. (2005) *Nano Lett.* 5(9):1658-1667.
- 7) *In situ* Determination of Orientational Distributions in Langmuir Monolayers by Total Internal Reflection Fluorescence, Tronin, A., Xu, T. and **Blasie**, J.K. (2005) *Langmuir* 21: 7760-7767.
- 8) Incorporation of Designed Extended Chromophores into Amphiphilic 4-helix Bundle Peptides for Nonlinear Optical Biomolecular Materials, Xu, T., Wu, S.P., Miloradovic, I., **Therien**, M.J., and **Blasie**, J.K. (2006) *Nano Lett.* 6(11): 2387-2394.
- 9) Structural Studies of Amphiphilic 4-helix Bundle Peptides Incorporating Designed Extended Chromophores for Nonlinear Optical Biomolecular Materials, Strzalka, J., Xu, T., Tronin, A., Wu, S.P., Miloradovic, I., Kuzmenko, I. Gog, T., **Therien**, M.J., and **Blasie**, J.K. (2006) *Nano Lett.* 6(11): 2395-2405
- 10) 3-D Structure and Dynamics via Molecular Dynamics Simulation of a *de novo* Designed, Amphiphilic Heme Protein Maquette at Soft Interfaces, Zou, H., Strzalka, J. Xu, T., Tronin, A. and **Blasie**, J.K. (2007) *J. Phys. Chem. B* 111: 1823-1833.
- 11) Structure & Dynamics of an Extended Conjugated NLO Chromophore within an Amphiphilic 4-Helix Bundle Peptide by Molecular Dynamics Simulation, Zou, H., **Therien**, M.J. and **Blasie**, J.K. *J. Phys. Chem. B.* Submitted.

**P. Leslie Dutton.**

**The Johnson Research Foundation, Department of Biochemistry and Biophysics,  
 University of Pennsylvania, Philadelphia, PA 19104. dutton@mail.med.upenn.edu**

The long-term goal of this grant is to equip synthetic protein designs with light activated electron tunneling-mediated charge-separation and then couple electron transfer to bond-breaking/forming catalysis of water-splitting to form oxygen and hydrogen. This goal relies on learning how to abstract and translate sophisticated photocatalysis from natural to synthetic molecular system (maquettes). Although many bio-inspired structures have been constructed, structure without function is insufficient. The first section describes engineering guidelines we are uncovering to couple electron tunneling to redox catalysis. The second is corresponding assembly instructions for building function into maquette structures, while the third describes scanning probe microscopy of amphiphilic versions of the redox maquette helical bundles. The final section describes construction and incorporation of various redox centers, including Fe and Mn clusters for hydrogen and oxygen evolving catalytic sites.

**Engineering guidelines derived from natural oxidoreductases:** We are extending our empirically-derived principles of molecular engineering of electron tunneling in natural oxidoreductase proteins to include the coupling of electron transfer cofactor chains to substrate sites where adiabatic high-barrier, bond breaking and forming chemical catalysis takes place. Column 1 of Figure 1 describes a conventional biochemical catalytic reaction with no electron transfer in which it is difficult to predict reaction rates. Column 4 describes long distance electron transfer without catalysis, in which our understanding in redox cofactor chains is now good, quite predictive and sufficient to have been reproduced in synthetic constructs including our designed model maquette proteins. In between these two

extremes, electron transfer is coupled to catalysis over short, bond-scale distances (Column 2) or longer than bond distances (Column 3). Column 2 includes dehydrogenases with an increasingly understood mechanism of paired electron transfer occurring as hydride closely associated with bonds often linking flavin or nicotinamide and substrate. Column 3 involves single electron transfer over several Å coupled to wide-ranging chemistry, but has not been fully recognized and is far from understood.

Conventional catalysis	Borderline catalysis	Interfacial catalysis	Chain electron tunneling
$\text{H}_2\text{O} + \text{A-B}$ no e <sup>-</sup> transfer $\text{AH} + \text{HOB}$	$\text{A}^{\text{e-}}\text{-H} + \text{B}$ $\rightarrow \parallel \leftarrow$ interface small $\text{A}^{\text{e-}}\text{-H-B}$	$\text{A}^{\text{e-}} + \text{X-B}$ $\longleftrightarrow$ interface substantial $\text{A} + \text{Y}^{\text{e-}} + \text{B}$	$\text{A}^{\text{e-}} + \text{B}$ long distance e <sup>-</sup> tunneling $\text{A} + \text{B}^{\text{e-}}$
Example Hydrolysis Bond break? Yes Equation Eyring Potential surfaces	Hydride transfer Yes Eyring	Oxygen reduction Yes Eyring/Marcus	Charge transfer No Marcus

We contend that some of the basic electron tunneling engineering principles uncovered for natural electron transfer chains also operate when electron tunneling is coupled to catalysis. Moreover, it appears that Nature has exploited the ability to use short distances to speed inherent electron tunneling rates as a means to overcome significant energetic barriers associated with the catalysis. Thus, we recognize that in such a role, the single electron tunneling interface between redox cofactor chain and bond making and breaking chemistry is positioned to exert major influence over the rates and perhaps direction of the catalysis itself. These developing principles abstracted from nature are beginning to inform synthetic maquette protein constructions designed to perform significant light and oxidant or reductant driven catalysis. This long-term piece of work done by Christopher C. Moser, Christopher C. Page, Sarah E. Chobot and P. Leslie Dutton is approaching completion, to be submitted to Proc. Natl. Acad. Sci. USA.

**Uncovering the assembly instructions of function in proteins using hydrophilic maquettes:** We have adopted a different approach to address how many engineering elements are required to achieve a particular biological function. Our questions ask what are the individual biochemical and structural

tolerances of these elements and how much of a protein infrastructure is consumed in accommodating the function? We have shown that through the stepwise incorporation of engineering elements, it is possible to start from a functionally featureless peptide comprising just three different amino acids with a length and sequence selected to ensure association as a water-soluble, molten globular four- $\alpha$ -helical bundle, and produce a heme-containing protein maquette with native-like tertiary structure that performs the myoglobin or neuroglobin-like function of dioxygen binding to the ferrous heme. We find as schematically presented in Figure 2, that inclusion of two such elements to create a strained bis-histidine-heme ligation is only sufficient to support oxygen binding at low temperature (H10A24-HP6); inclusion of a third element (HP7) to restrict inter-helix motion renders the oxyferrous-heme state stable at 16°C. Restriction of this motion is crucial as water penetration is minimized for stable oxyferrous-heme formation. The demonstration of an uncovering of the ‘assembly instructions’ for maquettes promoting stable generation of the primary step in respiration and a wide variety of oxidative chemistry represents a major step forward for the development of catalytic maquettes. This sequential, biochemically-informed maquette approach appears viable for the design of synthetic proteins performing catalysis generally. This work was done by Ron L. Koder, J. L. Ross Anderson, K.S. Reddy, Lee A Solomon, Christopher C. Moser and P. Leslie Dutton, is complete and will be submitted to Nature.

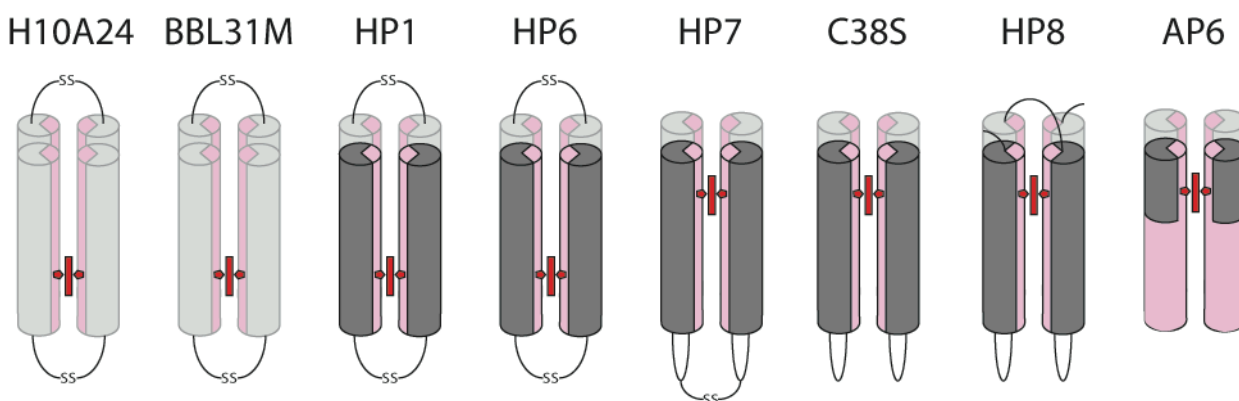


Fig 2. Stable room temperature oxyferrous-heme A or B is formed in maquettes with strained heme Fe histidine ligation *and* constrained helix motion; this is achieved in hydrophilic (HP) maquettes, HP7 and variants. The first four are defined maquette designs altered progressively until HP7. HP8 is a single sequence peptide of the next generation. Early work with amphiphilic (AP) maquette, AP6, also revealed formation of the oxyferrous state and opens the door to functionalizing membrane associated maquettes. Dark grey represents tertiary structures of the helices induced by heme ligation; a second heme added to HP1 structures all four helices (not shown).

**Amphiphilic Maquettes:** We have synthesized a new set of amphiphilic maquettes (AP6 series) schematically shown in Figure 3. The tetrameric AP-6 maquettes assemble with up to six ferric hemes B per tetramer. The AP maquettes co-solubilize with diblock copolymers or lipids and on an air-water interface, they compress to specific surface pressure, and can be transferred by Langmuir - Blodgett technique on HOPG (highly ordered pyrolytic graphite) surface. The films containing diblock copolymers reveal a surface roughness of about 5 nm, which is unacceptable for electrical measurements because of a crosstalk between topographical signal and electrical conductivity measured. The films with saturated lipids demonstrate that the roughness of supported lipid films with embedded AP-6 maquette decreased to about 0.5 nm. Using the lipid-maquette mixtures, we have tested several scanning probe microscopy techniques that would allow us to measure the electrical properties of the films. We have determined that the mode that leads to most reproducible measurements of the current is conductive AFM with torsional resonance feedback. In this mode, the amplitude of torsional oscillations of the tip is kept constant allowing the surface distance and the conductivity between the tip and the surface to be measured simultaneously. We are currently improving the resolution and current stability by switching from measurements of DC conductivity to AC conductivity in a wide range of frequency from 20 kHz to 1 MHz, thereby improving the signal-to-noise ratio of the electrical signal. The second scanning microscopy technique that will provide useful means of characterization is scanning impedance microscopy, scanning probe technique based on the detection of the phase change of cantilever oscillations induced by a lateral bias applied to the sample. This technique can be used to determine 2D impedance at the nanoscale level (Fig. 3). This work is being done in collaboration with Prof. Dawn Bonnel at the department of Materials Science and Engineering at the University of Pennsylvania and it

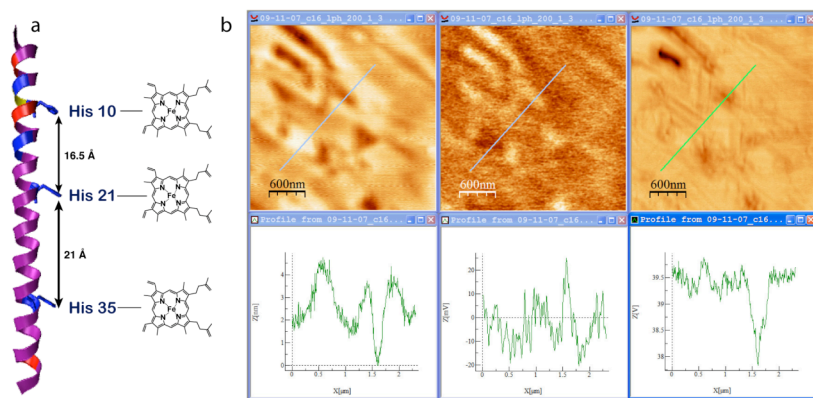


Fig.3: (a) Schematic drawing of an AP-6 maquette with 3 heme *b* binding sites. (b) Topographic, impedance, and noise images for patch of the film containing heme/AP6/DPPC = 3:1:200 on HOPG surface. Line profile for topography and impedance images revealed 2 layers formation within the film. The impedance scales linearly with the number of layers.

will be submitted to Nano Letters: M.P. Nikiforov, D.A. Bonnell, P.L. Dutton, B.M. Discher. Assembly and electrochemical characterization of biomolecular electronic interfaces from redox-active protein maquettes incorporated into lipid monolayers.

### Redox centers

**a) Naphthoquinone amino acid for one- and two-electron chemistry at potentials reducing enough for H<sub>2</sub> production.** In membrane proteins, with few exceptions, quinones are bound weakly and have neither clear binding site sequence nor structural

consensus. We have dodged these problems to include a quinone in our maquette designs by synthesizing a novel, Fmoc-protected naphthoquinone amino acid (**Naq**) functionally similar to the natural menaquinone or vitamin K family. Naq was chosen in part because in the quinone form usefully is physically similar to tryptophan to aid modeling. Naq has been proved to successfully incorporate in peptides along with other natural amino acids using a synthesizer, and without damage from the de-blocking measures required to expose the quinone carbonyls. Naq oxidation-reduction contained in a heptamer (Figure 4, heptaNaq) in aqueous media follows a typical two-electron ( $n=2.0$ ) oxidation-reduction coupled to two-proton exchange ( $E_{m7} - 0.05V$ ), while in aprotic solvent Naq potentials for the Qox/SQ and SQ/Qred at  $-0.60V$  and  $-1.33V$  (vs NHE) are well below the potentials of  $2H^+/H_2$  under most conditions. This work is done by Lichtenstein, B.R. Cerda, J.F., Koder, R.L. and Dutton, P.L. and will be submitted as “Reversible Proton Coupled Electron Transfer in a Peptide-incorporated Naphthoquinone Amino Acid.” to Chemical Communications.

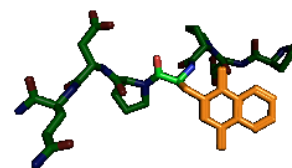


Fig. 4) synthetic redox amino acid Naq in a peptide

**b) Flavins modified for protein association for one and two electron chemistry:** The more water-soluble redox analogue of quinones are the flavins. Flavins are ubiquitous in water-soluble oxidoreductase proteins where they can perform one electron chemistry, clear two-step electron/proton oxidation-reductions as well as be a partner for hydride transfer with strict two electron transfers substrates such as the nicotinamides and carbon-carbon bond redox chemistry common in intermediary metabolism (Figure 1, Column 2). They also are well known to support photo-activated electron transfer. Thus, the flavin is an important multipurpose cofactor for consideration in our functional designs. However, the high complexity and reactivity of the flavin has represented a challenge to characterization and does not have the broad range of variants offered by the quinones. We have approached the examination of the flavin moiety as a viable catalytic component by initially synthesizing simplified flavin variants that are highly soluble in organic solvents such as benzene that interact minimally with the several polar groups of flavin and discourage aggregation. Hence molecules such as TPARF and DBF (Fig. 5 left) open the door to analysis by a full range of spectroscopies especially NMR and IR and electrochemistry (see refs 3 and 4) and shown specifically interacting with Rotello H-bonding partners (Fig. 5 right).

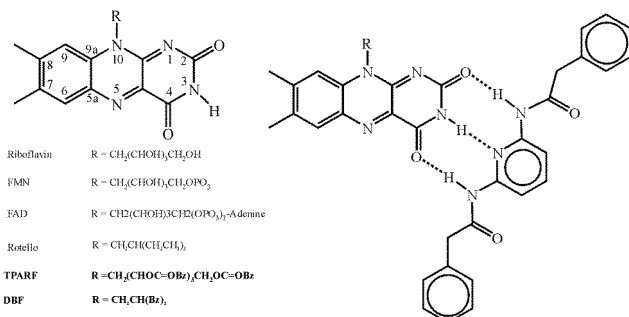


Fig. 5) Controlling H-bonding in flavins

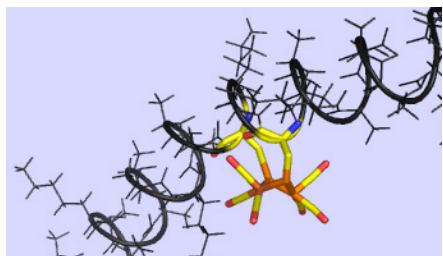
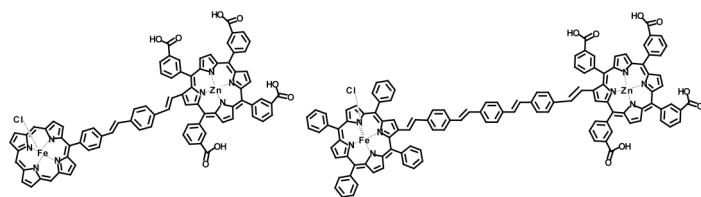


Fig 6) Di-iron hexacarbonyl center akin to H<sub>2</sub>ase in a alpha helical synthetic protein.

production catalysts for use in environmentally friendly energy production strategies (Ref. 5).

**d) Incorporating Mn clusters.** A novel terpyridine amino acid, designed to ligate a Mn<sub>2</sub>O<sub>2</sub> cluster in the form that Gary Brudvig shows catalytically splits water in solution, is well on its way to successful synthesis. This material is ready to be Fmoc protected and incorporated into a small Trp-zipper peptide using standard solid phase synthesis to confirm that this peptide geometry is indeed appropriate for Mn<sub>2</sub>O<sub>2</sub> ligation (ongoing work by R.L. Koder, B.R. Lichtenstein, and P.L. Dutton).



**e) Multimeric Zn- porphyrins.** We are testing a family of photoactive porphyrin dimers that have the potential to be made into dendrimers thereby becoming light harvesting. This is work with David Officer (Wollangong) and Keith Gordon (Dunedin NZ) Binding was achieved to HP-7.

1. Noy, D., Discher, B. M., Rubtsov, I. V., Hochstrasser, R. A., and Dutton, P. L. (2005) Design of amphiphilic protein maquettes: Enhancing maquette functionality through binding of extremely hydrophobic cofactors to lipophilic domains. *Biochemistry* 44, 12344-12354.
2. Koder, R.L., Valentine, K.G., Cerda, J.F., Noy, D., Wand, A.J., and Dutton, P.L. Native-like Structural Structure in Designed Four  $\alpha$ -helix Bundles Driven by Buried Polar Interactions. *J. Am. Chem. Soc.*, 128: 14450-14451, 2006.
3. Koder, R.L., Potyim, M., Walsh, J., Dutton, P.L., Wittebort, R.A., and Miller, A-F. N Solid-state NMR Provides a Sensitive Probe of Flavin Reactive Sites. *J. Am. Chem. Soc.*, Vol 128, 45: 15200-15208, 2006.
4. Koder, R.L., Lichtenstein, B.R., Cerda, J.F., Miller, A-F., and Dutton, P.L. A Flavin Analogue with Improved Solubility in Organic Solvents, *Tetrahedron Letters*, 48, 5517-5520, 2007.
5. Jones, A.K., Lichtenstein, B.R., and Dutton, P.L. Synthetic Hydrogenases: Incorporation of an Iron Carbonyl Thiolate into a Designed Peptide. *J. Am. Chem. Soc.* (Communication). Provis. accepted subject to amendments 09.07.
6. Nikiforov, M.P., Bonnell, D.A., Dutton, P.L., and Discher, B.B. Assembly and Optoelectrical Properties of Amphiphilic Peptides with Chain of Cofactors for Electron Transfer between Interfaces. Biophysical Society Meeting, March 3-7, 2007, Baltimore, MD, USA.
7. Farid T.A., Lichtenstein B.R., Koder R.L., Moser C.C., and Dutton P.L. Design and Synthesis of Light-harvesting Maquettes. Biophysical Society Meeting, March 3-7, 2007, Baltimore, MD, USA.
8. Lichtenstein, B.R. Cerda, J.F., Koder, R.L. and Dutton, P.L. Incorporation of a Naphthoquinone Amino Acid into de novo Peptides. Biophysical Society Meeting, March 3-7, 2007, Baltimore, MD, USA.
9. Cerda, J.F., Koder, R.L., Lichtenstein, B.R., Moser, C.C. Miller, A-F, and Dutton, P.L. Hydrogen Bond-free Flavin Redox Properties: Managing Flavins in Extreme Aprotic Solvents., *Organic and Biomolecular Chemistry*, Submitted 06/2007.



### *Program Title*

## **A Hybrid Biological-Organic Photochemical Half-Cell for Generating Dihydrogen**

John H. Golbeck (PI), Donald A. Bryant (Co-PI)

Department of Biochemistry and Molecular Biology, 310 South Frear Building, The Pennsylvania State University, University Park, PA 16802

e-mail: [jhg5@psu.edu](mailto:jhg5@psu.edu), [dab14@psu.edu](mailto:dab14@psu.edu)

### *Program Scope or Definition*

The goal of this work is to design, fabricate, characterize, and optimize a biological/organic hybrid electrochemical half-cell that couples Photosystem I (PS I), which efficiently captures and stores energy derived from sunlight, with either a Fe-Fe H<sub>2</sub>ase or a Ni-Fe H<sub>2</sub>ase, which is capable of a high rate of H<sub>2</sub> evolution. The core idea is to deliver the electron from PS I to the H<sub>2</sub>ase rapidly and efficiently using a covalently bonded molecular wire that will connect the active sites of the two enzymes. The PS I-molecular wire-H<sub>2</sub>ase complex will be tethered to a gold electrode through a baseplate of cytochrome *c*<sub>6</sub>, which will additionally serve as a conduit of electrons from the gold to PS I. Cytochrome *c*<sub>6</sub> will be covalently bonded to the electrode through a self-assembling monolayer of functionalized alkanethiols. The device should be capable of transferring at least 1000 e<sup>-</sup> per second from PS I to the H<sub>2</sub>ase to carry out the reaction:  $2\text{H}^+ + 2\text{e}^- + 2\text{h}\nu \rightarrow \text{H}_2$ .

### *Recent Progress*

#### *1) Minimizing the mismatch between electron transfer rates of PS I and H<sub>2</sub>ase*

Under full sunlight, PS I is capable of processing ~500 electrons per PS I per second. The electron transfer rate is limited by the solar flux, not by an inherent rate limitation in the electron transfer properties of PS I. The Fe-Fe H<sub>2</sub>ase is capable of evolving >1000 H<sub>2</sub> per second and the Fe-Ni H<sub>2</sub>ase is capable of evolving >3000 H<sub>2</sub> per second. One approach to ameliorate the mismatch in electron transfer rates is to incorporate a larger antenna system in PS I. Under iron stress, the *isiA* gene is induced in *Synechocystis* sp. PCC 6803, which leads to the synthesis of the Chl-containing IsiA protein. Eighteen of these proteins form a ring containing ca. 225 Chl around the PS I trimer, thereby increasing the antenna size by a factor of ~2. The main problem is that the iron-limited cells grow slowly and are sensitive to light-induced chlorosis. We made the recent discovery (Balasubramanian et al. 2006) that *Synechocystis* cells grow well under iron limitation and do not become chlorotic when the *iscA* gene is interrupted. This gene, we believe, functions in a signal transduction cascade, leading to changes that guarantee iron is available only for metabolically required activities. The formation of the PS I/IsiA supercomplexes were verified in the *iscA* mutant strain using low temperature fluorescence, EPR, time-resolved optical and cryo-EM spectroscopies. Steady state kinetic experiments revealed that NADP<sup>+</sup> reduction rates mediated by flavodoxin for WT PS I and PS I/IsiA supercomplexes were 113 and 201 μmol/mg chl/hr, respectively, thereby showing that PS I/IsiA supercomplexes promote electrons at a rate faster than WT PS I. These PS I-IsiA supercomplexes will be used in the future for tethering the H<sub>2</sub>ase enzyme.

#### *2) Engineering PsaC with a Gly ligand at Cys13 and attachment to PS I.*

PsaC binds two low-potential [4Fe-4S]<sup>1+,2+</sup> clusters termed F<sub>A</sub> and F<sub>B</sub>. In the C13G/C33S variant of PsaC, Gly has replaced Cys at position 13 creating a protein that is missing one of ligating amino acids to Fe/S cluster to F<sub>B</sub>. The present work tests the idea that a rescue ligand consisting of an external thiolate is retained when inorganic Fe/S clusters are inserted *in vitro* into a variant of *Escherichia coli*-expressed PsaC. Using a variety of analytical techniques, including non-heme iron and acid-labile sulfur assays, and EPR, resonance Raman, and Mössbauer spectroscopies, we showed that the C13G/C33S variant of PsaC binds two [4Fe-

$4S]^{1+,2+}$  clusters despite the absence of one of the biological ligands.  $^{19}F$  NMR spectroscopy showed that an external thiolate indeed replaces Cys 13 as a substitute ligand to the  $F_B$  cluster. The finding that site-modified  $[4Fe-4S]^{1+,2+}$  clusters can be chemically rescued with external thiolates shows that it is possible to attach an additional electron transfer cofactor to the protein via a bound, external ligand. Following this logic, the methyl viologen derivative, 1-(3-thiopropyl)-1'-(3-(acetylthio)propyl)-4,4'-bipyridinium, was synthesized and used to chemically rescue the  $F_B$  cluster of the C13G/C33S variant of PsaC. The chemical coupling was accomplished by loading a Sephadex PD-10 column with the viologen derivative and flowing the variant PsaC, at a ratio of 1:1, through the column. The tethered PsaC product was washed by ultrafiltration over a 3 kDa cutoff membrane, allowing any unbound viologen to pass through. UV/Visible absorption and EPR spectroscopies were performed on the chemically-reduced, tethered PsaC product, which confirmed the presence of two reduced  $[4Fe-4S]^{1+}$  clusters and a viologen radical. The tethered PsaC was rebound to  $F_X$  cores in the presence of PsaD, thereby resulting in a reconstituted PS I-tether complex. To verify the ability of the tethered viologen to accept an electron from P700 at high quantum yields, steady state kinetics at 600 nm and flat cell, room temperature EPR techniques are currently being employed. Reference: (Antonkine et al. 2007)

### 3) Photosystem I/metal nanoparticle bioconjugates for the photocatalytic production of $H_2$

The following-proof of concept experiment showed that electrons can be removed from PS I via the molecular wire and transferred to a Pt catalyst, thereby leading to small amounts of  $H_2$ . This work was guided by the knowledge that catalytic production of  $H_2$  has previously been accomplished with the aid of metal nanoparticles (NPs). Photocatalytic production of  $H_2$  has been achieved by means of ethanol reforming on the surface of Au and Pt NPs supported on semiconductor materials such as titania ( $TiO_2$ ). These semiconductor materials supply an input of energy in the form of reducing electrons. A major drawback to this type of photocatalysis of  $H_2$  is that the light must have energy greater than the bandgap of titania in order to produce a charge separated state that is capable of sustaining the reaction of  $2H^+ + 2e^- \rightarrow H_2$ . The bandgap is 3.2 eV and corresponds to light with wavelengths shorter than  $\sim 350$  nm. This means that only a very small fraction of incident solar radiation has sufficient energy to produce this state. Covalent attachment of PS I to Au and Pt NPs provides an attractive alternative to these titania-supported particles for the photocatalytic production of  $H_2$ . PS I has highly favorable properties that lend to its use in such an application. The pigments that comprise the antenna complex of PS I absorb all wavelengths of light shorter than 700 nm, which represents 43 to 46% of the total solar emission that reaches the surface of the Earth. Nearly all of the photons that are absorbed are converted into the charge separated state  $P_{700}^+ F_B^-$ , which means that PS I has a quantum yield that  $\sim 1.0$ . The charge separated state is stable for  $\sim 100$  ms, and the low potential electrons are poised at a redox potential favorable for  $H_2$  evolution. The challenge is to transfer the electron from PS I to the nanoparticle surface within this 100 ms timeframe. The C13G/C33S variant of PsaC can be chemically rescued by thiolate ligands and is redox active when bound to P700- $F_X$  cores. As indicated above, this construct has the ability to transfer electrons from the  $F_B$  cluster to a covalently bound external acceptor. Facile surface modification of Au and Pt NPs coupled with a capacity to catalyze the reduction of protons to  $H_2$  make these particles attractive candidates for this approach. The functionalization of Au and Pt NPs by thiolated molecules is an extensively explored and well-documented field of study. PS I can be covalently attached to the surface of these NPs via a dithiol linker molecule. One functional group of the molecule acts to modify the surface of the particle while the other functional group serves as the ligand to the  $F_B$  cluster. 1,6-hexanedithiol was chosen for these studies due to its relatively short length ( $\sim 1.2$  nm), which will allow for electron transfer from PS I to the NP

before the charge recombination between  $P_{700}^+$  and  $F_B^-$  can occur according to Marcus theory. GC analysis shows that only PS I/Au and Pt NP bioconjugates under illumination were able to generate  $H_2$ . PS I/Au NP bioconjugates produced  $3.4 \mu\text{mol } H_2 \text{ h}^{-1} \text{ mg Chl}^{-1}$  while PS I/Pt NP bioconjugates were able to produce  $9.6 \mu\text{mol } H_2 \text{ h}^{-1} \text{ mg Chl}^{-1}$ . No  $H_2$  was evolved by any of control that lacked one or more of the components. These results prove that the electron is being transferred to the NPs only when the rebuilt PS I is covalently attached to the particle surface by the dithiol linker, and that light produces the charge separated state in PS I necessary for  $H_2$  evolution. This proof-of-concept experiment shows that an approach that links PS I to a site-engineered Fe-Fe or Fe-Ni  $H_2$ ase for the efficient photoproduction of  $H_2$  constitutes a realistic strategy.

#### 4) Re-engineering the small subunit of the Ni-Fe hydrogenase to accept a rescue ligand.

The next step in constructing a viable device is to replace the NP with a site-engineered  $H_2$ ase. We have been working with a heterodimeric membrane-bound Ni-Fe  $H_2$ ase (MBH) of *Ralstonia eutropha* H16. The MBH is composed of a large 67.1 kDa subunit, which harbors the Ni-Fe active site, and a small 34.6 kDa subunit, which binds three Fe/S clusters. The advantage of this system is that because the two subunits can be expressed separately in *E. coli*, it should be possible to tether the small subunit to PS I and determine the quantum yield of electron transfer through the three Fe/S clusters independent of  $H_2$  generation. The external ligand is attached by engineering an open coordination site in the distal [4Fe-4S] cluster of the small subunit. A 43 amino acid deletion at the N-terminus of the small subunit, which is the site responsible for affixing the protein to the membrane, has been made to allow for increased solubility. The distal [4Fe-4S] cluster has a unique His ligation (His187) that has been varied to a Gly to create an open coordination site. The small subunit lacking the N-terminal domain with and without the H187G variation has been expressed in an *E. coli* Rosetta derivative with a C-terminal Strep-Tag for ease of purification. The *E. coli* cells are grown in excess imidazole so that the distal Fe/S cluster can be chemically-rescued *in vivo*. It will eventually be displaced by the tethered viologen *in vitro*. The presence and type of Fe/S clusters is currently under study by electrochemistry, and by optical and EPR spectroscopy.

#### 5) Re-engineering the Fe-Fe hydrogenase to accept a rescue ligand.

We are also attempting to couple PSI to a fully functional, expressed Fe-Fe  $H_2$ ase. We have selected the  $H_2$ ase, HydA, of *C. acetobutylicum* ATCC 824 as the optimal enzyme for these studies based on its ease of genetic manipulation (King et al. 2006; Ghirardi et al. 2007), hydrogen evolution capacity ( $2.4 \text{ L } H_2 \text{ L}^{-1} \text{ culture h}^{-1}$ ) (Soni 1987), and its relative stability in the presence of  $O_2$ . HydA is highly similar in sequence to the *C. pasteurianum* hydrogenase, CpI, the structure of which has been solved by X-ray crystallography (Peters et al. 1998). Based upon the homology between HydA and CpI, a distal [4Fe4S] cluster, is more exposed than the other Fe/S clusters to the surface of HydA. We showed earlier that a missing cysteinyl ligand to a [4Fe-4S] cluster can be successful rescued using an external alkyl thiolate (Antonkine et al. 2007). Thus, these observations led us to consider replacing a similarly-located Cys ligand in HydA with a non Cys amino acid. If it is possible to rescue the Fe/S cluster with an external ligand in HydA, a mechanism will exist to attach the tether to insure a rapid transfer electrons from PS I to the active site of a  $H_2$ ase. Point mutations in the second Cys ligand to the [4Fe-4S] cluster have been constructed (G, D, S, A and R). As shown in the Table, whole *E. coli* cells harboring the WT *hydA* gene as well as the site-specific mutants have been tested for  $H_2$  evolution using a tested protocol (King et al. 2006). Current studies are focused on obtaining larger amounts of relatively pure HydA to enable us to do optical and EPR spectroscopic analyses, electrochemistry, reconstitution experiments of apo-HydA, and rescue of the missing cysteinyl ligand in the mutants. Studies are also being

conducted to optimize the rate of H<sub>2</sub> evolution from the PS I/NP bioconjugate system. Current efforts are aimed at optimizing the rate of electron donation to PS I, thereby increasing the number of electrons that are available for H<sub>2</sub> reduction at the NP surface.

<b>H<sub>2</sub> evolution activities of [Fe-Fe]-H<sub>2</sub>ases anaerobically co-expressed with the <i>C. acetobutylicum</i> maturation proteins (HydE, HydF, and HydG) in <i>E. coli</i> cells DE-3 (BL21)</b>		
Organism	[FeFe]-H <sub>2</sub> ase	Whole cells extracts (nmolH <sub>2</sub> .ml <sup>-1</sup> .min <sup>-1</sup> )
<i>E.coli</i>		21
<i>C. acetobutylicum</i>	HydA	286
<i>C. acetobutylicum</i>	HydA cys97gly	154
<i>C. acetobutylicum</i>	HydA cys97ser	219
<i>C. acetobutylicum</i>	HydA cys97arg	140 <sup>+</sup>
<i>C. acetobutylicum</i>	HydA cys97ala	156 <sup>+</sup>
<i>C. acetobutylicum</i>	HydAcys97asp	145 <sup>+</sup>
<i>C. acetobutylicum</i>	HydA*	30 <sup>+</sup>

The entry denoted HydA\* represents a doubly tagged HydA protein, which carries a hexa-histidine tag at its N-terminus and a StrepTagII at its C-terminus. The entries marked with a “<sup>+</sup>” represent provisional values that will be remeasured to ensure reproducibility.

### Future Plans

In addition to the work described above, additional work is currently underway to construct G82C/D87C variants of cytochrome c<sub>6</sub> from *Synechocystis* sp. PCC 6803. These changes lie on an  $\alpha$ -helical portion of the protein that opposes the heme. These introduced changes are designed to orient the cyt c<sub>6</sub> on the gold electrode for optimal electron transfer to PS I. Replacement of DCPIP/ascorbate with cyt c<sub>6</sub> is believed to increase the rate of reduction of P<sub>700</sub><sup>+</sup>. Additionally, crosslinking of cyt c<sub>6</sub> to PS I via a zero-length cross linker like EDC will provide an additional increase in electron transfer.

### References

- Antonkine M L, Maes E M, Czernuszewicz R S, Breitenstein C, Bill E, Falzone C J, Balasubramanian R, Lubner C, Bryant D A, Golbeck J H (2007a) Chemical rescue of a site-modified ligand to a [4Fe-4S] cluster in PsaC, a bacterial-like dicluster ferredoxin bound to Photosystem I. *Biochim Biophys Acta* 1267:712-724
- Balasubramanian R, Shen G, Bryant D A, Golbeck J H (2006) Regulatory roles for IscA and SufA in iron homeostasis and redox stress responses in the cyanobacterium *Synechococcus* sp. strain PCC 7002. *J Bacteriol* 188:3182-3191
- Ghirardi M L, Posewitz M C, Maness P C, Dubini A, Yu J, Seibert M (2007) Hydrogenases and hydrogen photoproduction in oxygenic photosynthetic organisms. *Annu Rev Plant Biol* 58:71-91
- King P W, Posewitz M C, Ghirardi M L, Seibert M (2006) Functional studies of Fe-Fe hydrogenase maturation in an *Escherichia coli* biosynthetic system. *J. Bacteriol.* 188:2163-2172
- Peters J W, Lanzilotta W N, Lemon B J, Seefeldt L C (1998) X-ray crystal structure of the Fe-only hydrogenase (CpI) from *Clostridium pasteurianum* to 1.8 Ångstrom resolution. *Science* 282:1853-1858
- Soni B K, Soucaille, P, Goma, G (1987) Continuous acetone butanol fermentation: influence of vitamins on the metabolic activity of *Clostridium acetobutylicum*. *Appl Microbiol Biotechnol* 27:1-18

Anna C. Balazs  
Chemical Engineering Department  
1233 Benedum Hall  
University of Pittsburgh,  
Pittsburgh, PA 15261  
[balazs1@engr.pitt.edu](mailto:balazs1@engr.pitt.edu)

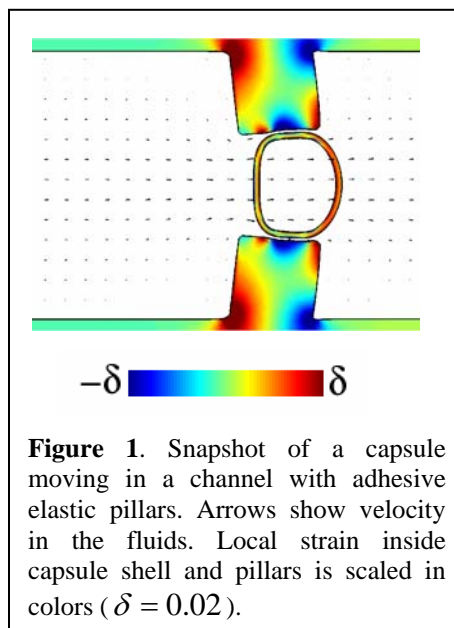
### Scope of the Research

The aim of our research is design effective methods for manipulating polymeric microcapsules and biological cells in microfluidic devices. Our system consists of the following components: soft particles (the microcapsules and cells) that are composed of a deformable shell and encapsulated fluid, an underlying compliant surface and a host solution. Using theory and simulation, we determine how the characteristics of the substrate, the polymeric shell, encapsulated fluid and the surrounding solution affect the motion of the particles in the system [1-13]. Our goal is to establish how synergistic interactions among the components can be harnessed to yield the desired behavior, including the movement of the particles to specified locations along the surface, the rupture of shell and the controlled release of the payload. Some of our recent findings are described below.

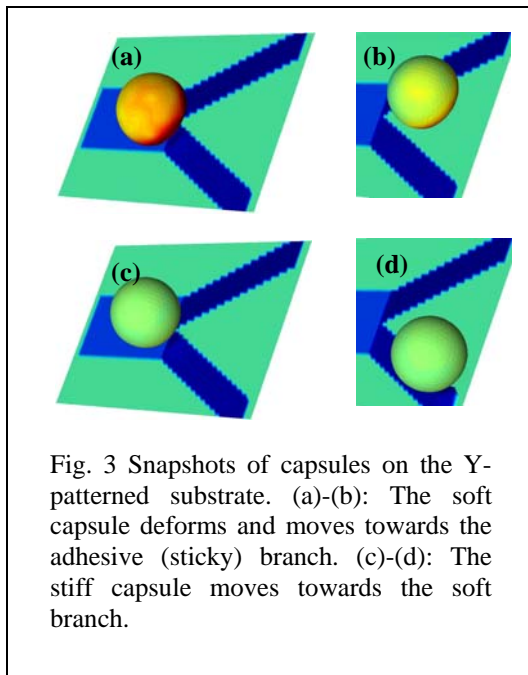
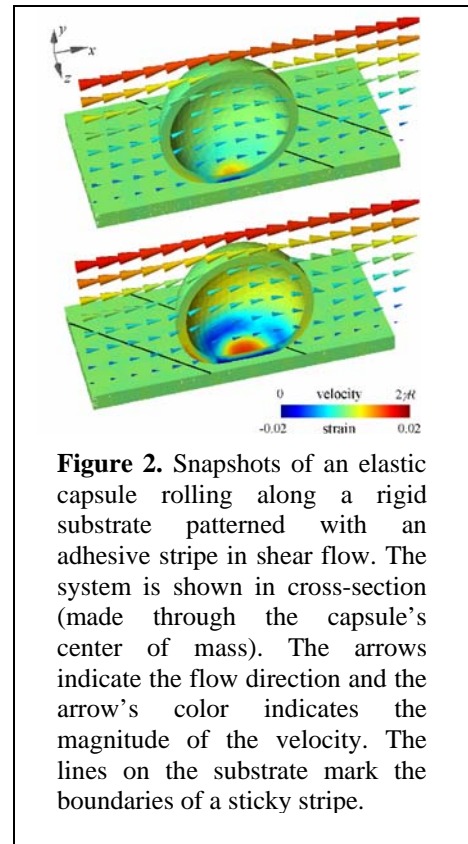
### Recent Progress

We investigated [1,2] the fluid-driven motion of compliant particles through constrictions, which are formed by pillars that extend from the top and bottom walls of a microchannel (see Fig.1). The entrapment of micron-sized particles in microscopic pores is beneficial for the efficient functioning of filtration systems and microfluidic devices for analyzing individual biological cells. To optimize the performance of these systems, it is important to isolate factors that regulate the passage of particles through micron-sized constrictions. In our simulations, the separation between the pillars that make up these constrictions is approximately 10 percent larger than the diameter of the undeformed capsules. We introduced an attractive interaction between the capsules and the tops of the pillars and varied the elasticity of both the capsules and pillars. Surprisingly, we found that this simple system shows a selectivity towards capsules of intermediate stiffness. Softer capsules are readily deformed by the viscous forces and do not experience the attractive interaction with the pillars, while stiffer capsules cannot deform to maximize the favorable contact with the “sticky” tops. By varying the elasticity of the pillars, we can tailor the range of capsules that become stuck between the pillars.

The findings provide guidelines for designing filtration systems and yield insight into the factors that drive particles to block microscopic channels. The results also yield design criteria for designing effective bioassays for sorting cells by their mechanical properties—a vital function, as described below.



For both biological cells and synthetic microcapsules, mechanical stiffness is a key parameter since it can reveal the presence of disease in the former case and the quality of the fabricated product in the latter case. To date, however, assessing the mechanical properties of such micron scale particles in an efficient, cost-effective means remains a critical challenge. By developing a three-dimensional computational model of fluid-filled, elastic spheres rolling on substrates patterned with diagonal stripes, we demonstrated a useful method for separating cells or microcapsules by their compliance [3]. In particular, we examined the fluid-driven motion of these capsules over a hard adhesive surface that contains soft stripes or a weakly adhesive surface that contains “sticky” stripes (see Fig. 2). As a result of their inherently different interactions with the heterogeneous substrate, particles with dissimilar stiffness are dispersed to distinct lateral locations on the surface. Since mechanically and chemically patterned surfaces can be readily fabricated through soft lithography and can easily be incorporated into microfluidic devices, our results point to a facile method for carrying out continuous “on the fly” separation processes.



Building on the above studies, we simulated the motion of fluid-filled, compliant microcapsules on a surface that is decorated with a Y-shaped pattern (see Fig. 3); as compared to the stem of the Y, one branch is relatively soft and the other branch is relatively sticky [4]. The capsules are driven to move over this substrate by an imposed fluid flow. Upon reaching the junction point, we found that deformable capsules preferentially move onto the sticky branch, while stiffer capsules move onto the soft branch. Thus, through their inherent interactions with the patterned domains, the microcapsules are driven to “make decisions” about their path along surface. Such surface patterning provides a facile means of routing particular capsules to specified locations in microfluidic devices and can form a fundamental component in creating fluidic circuits where microcapsules carry out simple logic operations.

We note that since the explosion of interest in microfluidics, considerable effort has focused on employing fluid droplets to carry out a host of functions. There have, however, been

far fewer studies on harnessing the dynamic behavior of polymeric microcapsules in microchannels for technological applications. Microcapsules present a variety of advantageous features: for example, the capsule's surface can be chemically altered, permitting significant control of the capsule-substrate interactions. Additionally, the mechanical properties of the outer shell can be varied, so that the capsules can display a broad range of compliances. Using computational modeling, we showed how interactions between flowing capsules and surfaces can be exploited to selectively divert the soft capsules, drive these capsules to burst (see Fig. 4) and thereby deliver their payload to specified locations in microfluidic devices [5,6]. The findings not only reveal that microcapsules can serve as effective micro-flasks, but also provide guidelines for creating small-scale filtration devices that isolate and destroy specific microbes.

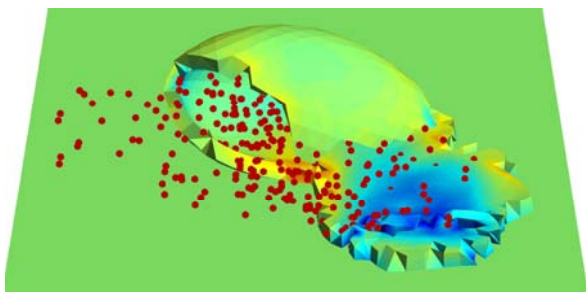


**Figure 4.** Graphical output from 3D simulation of a capsule bursting on a substrate. The fluid-driven capsule rolls along an adhesive surface and when the strain in the shell becomes sufficiently large, a crack is initiated on the capsule's surface. Cracks propagate and ultimately, the capsule is ruptured. The red dots are tracer particles that follow the streamlines of the external, flowing fluid.

We also modeled the rolling motion of a fluid-driven, particle-filled microcapsule along a heterogeneous, adhesive substrate to determine how the release of the encapsulated nanoparticles can be harnessed to repair damage on the underlying surface [7]. We integrated the lattice Boltzmann model for hydrodynamics and the lattice spring model for the micromechanics of elastic solids to capture the interactions between the elastic shell of the microcapsule and the surrounding fluids. A Brownian dynamics model was used to simulate the release of nanoparticles from the capsule and their diffusion into the surrounding solution. We focused on a substrate that contains a damaged region (e.g., a crack or eroded surface coating), which prevents the otherwise mobile capsule from rolling along the surface. We isolated conditions where nanoparticles released from the arrested capsule can repair the damage and thereby enable the capsules to again move along the substrate. Through these studies, we established guidelines for designing particle-filled microcapsules that perform a “repair and go” function and thus, can be utilized to repair damage in microchannels and microfluidic devices.

### Future Plans

These results imply that the intrinsic compliance and adhesiveness of the capsules and cells constitute a code, and this code can be deciphered through the use of chemically and mechanically patterned substrates. The coupling between the encoded particles and the decoding surfaces opens up new methods for performing simple logic operations. In future studies, we will harness this design principle to construct logic gates and more complex circuits, where cells or microcapsules carry out the logic operations, by analogy with the functions carried out by droplets and bubbles in microfluidic devices [14,15].

## References

1. Zhu, G. Alexeev, A. and Balazs, A. C. “Designing Constricted Microchannels to Selectively Entrap Soft Particles”, *Macromolecules*, 40 (2007) 5176.
2. Zhu, G. Alexeev, A. Kumacheva, E. and Balazs, A. C. “Modeling the Interactions Between Compliant Microcapsules and Pillars in Microchannels”, *J. Chem. Phys.*, 127 (2007) 034703
3. Alexeev, A. Verberg, R. and Balazs, A. C. “Patterned Surfaces Segregate Compliant Microcapsules”, *Langmuir*, 23 (2007) 983.
4. Usta, O. B., Alexeev, A. and Balazs, A.C., “Fork in the Road: Patterned Surfaces Direct Microcapsules to Make a Decision”, *Langmuir*, in press.
5. Alexeev, A. and Balazs, A. C. “Designing smart surfaces to selectively trap and burst microcapsules”, submitted, *Soft Matter*.
6. Balazs, A. C. “New approaches for designing ‘programmable’ microfluidic devices”, *Polymer*, in press.
7. Verberg, R., Dale, A. T., Kumar, P., Alexeev, A. and Balazs, A. C., “Healing Substrates with Mobile, Particle-Filled Microcapsules: Designing a “Repair and Go” System”, *Journal of the Royal Society Interface*, 4 (2007) 349—web published Oct. 3, 2006.
8. Alexeev, A. Verberg, R. and Balazs, A. C. “Modeling the Motion of Capsules on Compliant Polymeric Surfaces”, *Macromolecules*, 28 (2005) 10244.
9. Alexeev, A. Verberg, R. and Balazs, A. C. “Modeling the interactions between deformable capsules rolling on a compliant surface”, *Soft Matter*, 2 (2006) 499.
10. Alexeev, A. Verberg, R. and Balazs, A. C. “Designing Compliant Substrates to Regulate the Motion of Vesicles”, *Phys. Rev. Letts.*, 96 (2006) 148103.
11. Alexeev, A. Verberg, R. and Balazs, A. C. “Motion of Compliant Capsules on Corrugated Surfaces: A Means of Sorting by Mechanical Properties”, *J. Polymer Science. Part B: Polymer Physics*, 44 (2006) 2667.
12. Smith, K.A., Alexeev, A. Verberg, R. and Balazs, A. C., “Designing a Simple Ratcheting System to Sort Microcapsules by Mechanical Properties”, *Langmuir*, 22 (2006) 6739.
13. Verberg, R., Alexeev, A. and Balazs, A. C., “Modeling the Release of Nanoparticles from Mobile Microcapsules”, *J. Chem. Phys.*, 126 (2006) 224712.
14. Fuerstman, M. J.; Garstecki, P.; Whitesides, G. M. *Science* 2007, *315*, 828.
15. Prakash, M.; Gershenfeld, N. *Science* 2007, *315*, 832.



## Theoretical Research Program on Bio-inspired Inorganic Hydrogen Generating Catalysts and Electrodes.

Annabella Selloni (PI); Roberto Car

Department of Chemistry, Princeton University, Princeton, NJ 08544

[aselloni@princeton.edu](mailto:aselloni@princeton.edu), Tel: 609- 258- 3837; [rcar@princeton.edu](mailto:rcar@princeton.edu), Tel 609-258-2534

**Program Scope:** Our overall goal is to establish through simulation the theoretical feasibility of efficient electrocatalytic H<sub>2</sub> production from water by abiotic catalysts derived from the di-iron subsite [2Fe]<sub>H</sub> of the active site of Fe-only hydrogenases and which are attached to the surface of an Fe-S electrode.

In a first step, we have determined for the first time the reaction pathways and the associated barriers for H<sub>2</sub> production in vacuo for several related model molecules in different configurations, one example of which is shown in Fig. 1. Our results support the possibility of efficient H<sub>2</sub> production by a [2Fe]<sub>H</sub>-based molecule outside the enzyme pocket. Subsequent studies will concern compositional stabilization of the optimal configuration we have found as well as the influences of an aqueous environment and of electrode attachment on the reaction pathway and the associated kinetics.

**Recent Progress:** We have shown that the configuration of the [2Fe]<sub>H</sub> cluster energetically stablest at each stage of the H<sub>2</sub> production cycle, one with a terminal CO on the Fe<sup>d</sup> instead of the bridging CO of Fig. 1, has too large a barrier for H<sub>2</sub> production, 0.54 eV. The configuration of Fig.1, equivalent to that of the [2Fe]<sub>H</sub> cluster in the enzyme, while metastable relative to the terminal CO configuration at each stage, has a much lower barrier, but is endothermic by 0.28 eV. However, with the terminal CN<sup>-</sup> on Fe<sup>d</sup> in the *up* position instead of the *trans-down* position of Fig.1, the CO bridging configuration is only 0.1 eV less stable than the terminal CO configuration, almost within computational uncertainty. Moreover the reaction becomes exothermic by 0.18 eV, and the barrier decreases to only 0.09 eV. The enzyme environment of the [2Fe]<sub>H</sub> subsite within the enzyme must thus stabilize it in the CO-bridging and CN<sup>-</sup> *down-trans* configuration of Fig. 1 and mitigate the exothermicity. Nevertheless, our results for the CO bridging and CN<sup>-</sup> *up* configuration strongly support the possibility that the enzymatic environment is not essential for efficient H<sub>2</sub> production.

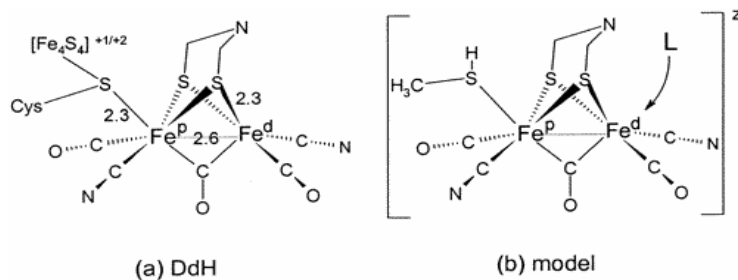
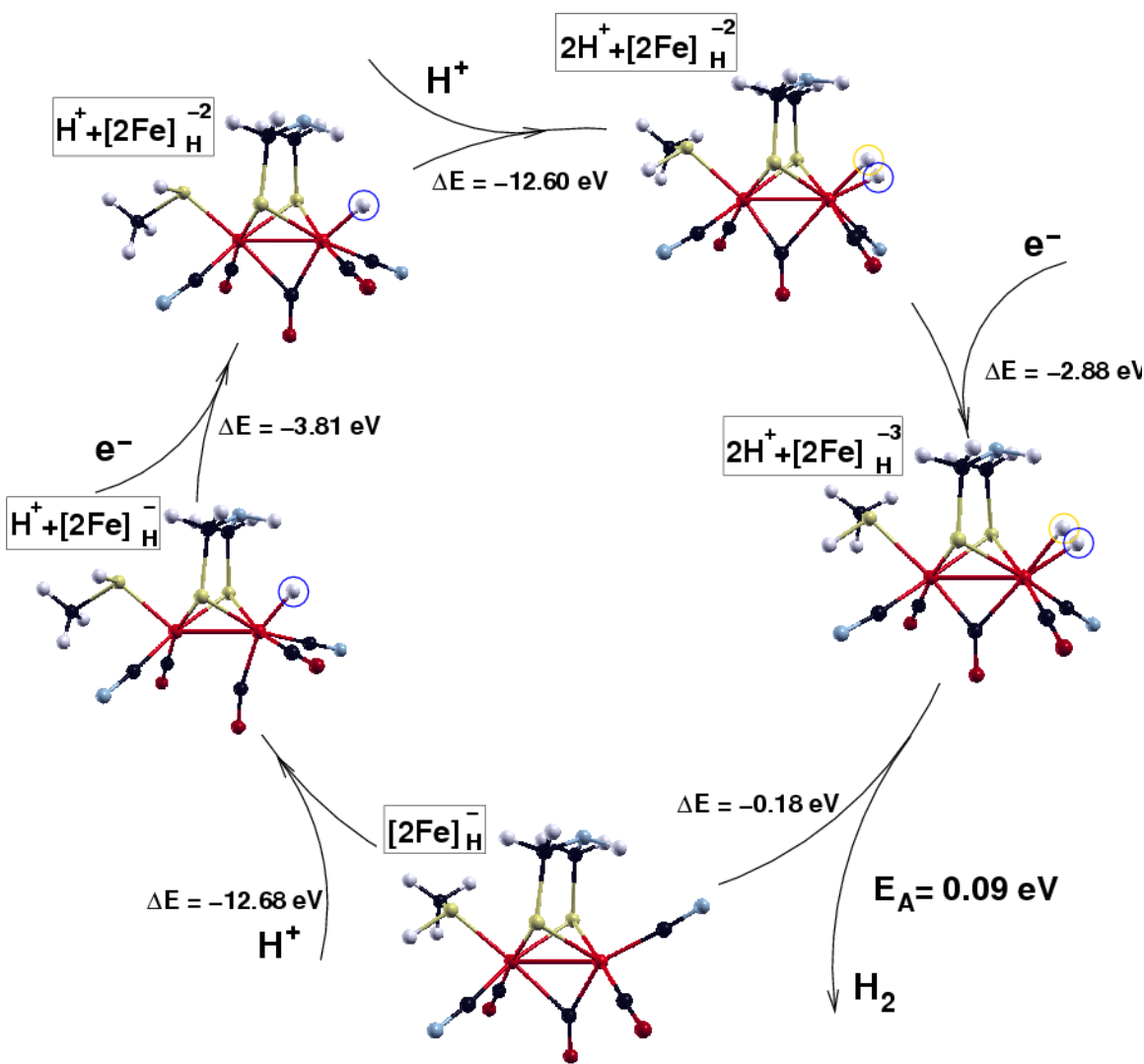


Figure 1: (a) Active site of the Fe-only hydrogenase, as determined experimentally for *D. desulfuricans*, (b) A model of the [2Fe]<sub>H</sub> subcluster used in our calculations. A DTN bridging group is assumed.

This most favorable cycle consists of 6 steps: **1.**  $[2\text{Fe}]_{\text{H}}^{-1}$  is in the initial partially-reduced active-ready state; **2.** the first proton is adsorbed at  $\text{Fe}^{\text{d}}$  ( $\text{H}^+ + [2\text{Fe}]_{\text{H}}^{-1}$ ); **3.** the first one-electron reduction occurs ( $\text{H}^+ + [2\text{Fe}]_{\text{H}}^{-2}$ ); **4.** the second proton is adsorbed at  $\text{Fe}^{\text{d}}$  or DTN ( $2\text{H}^+ + [2\text{Fe}]_{\text{H}}^{-2}$ ); **5.** the second one-electron reduction with both protons at  $\text{Fe}^{\text{d}}$  ( $2\text{H}^+ + [2\text{Fe}]_{\text{H}}^{-3}$ ); **6.** desorption of  $\text{H}_2$  occurs leaving the  $[2\text{Fe}]_{\text{H}}^{-1}$  in the active-ready state ( $\text{H}_2 + [2\text{Fe}]_{\text{H}}^{-1}$ ). This cycle and the relative energies of the steps are shown in Fig. 2.



**Figure 10** Energetics of the catalytic cycle for  $\text{H}_2$  production along the optimal  $\text{Fe}_d^{\text{up}}$ -pathway.  $\Delta E$  indicates the energy change (in eV) and  $E_{\text{A}}$  the energy barrier associated with desorption of an  $\text{H}_2$  molecule. The different structures assumed by the  $[2\text{Fe}]_{\text{H}}$  subcluster along the cycle are portrayed in ball and stick representation: Fe atoms are in light red, S atoms in yellow, C atoms in black, N atoms, in light blue, O atoms in red, and H atoms in white. The blue and yellow circles indicate, respectively, the first and the second protons captured by the  $[2\text{Fe}]_{\text{H}}$  subcluster.

We have investigated the effect of changing the di-thiol bridge from DTN to PDT and of changing the thiol termination on Fe<sup>P</sup> in Fig. 1 to CH<sub>3</sub>S<sup>-</sup> and found no significant changes.

**Future Plans:** Our computations thus strongly suggest that the model [2Fe]<sub>H</sub> cluster we have studied is a good candidate catalyst for meeting our long term goals. We propose to continue our simulations by linking it via the thiol connection to Fe<sup>P</sup> to the surface of an Fe-S electrode. We shall search for a ligand to complete the thiol connection to the Fe<sup>P</sup> which we can use to tune the stability of the CO bridging configuration. Maintaining the CO bridging configuration is essential for obtaining favorable kinetics because it blocks the too-tightly-binding H-bridging site which is accessible in the CO terminal configuration. Moreover, the CO bridging configuration must remain delicately balanced with respect to the terminal configuration as, during the course of the reaction, the configuration shifts subtly between more or less asymmetrical bridging of the 2 Fe's. This search is a worthwhile challenge which can be guided by our recently developed chemical reactivity theory. In addition, we shall simulate the water environment of the [2Fe]<sub>H</sub> activated Fe-S surface, studying the influence of the electrode and the water on configuration stability and reaction pathway.

**Publications:** On the basis of the results outlined above, we are preparing a manuscript in which we provide a detailed comparison between different pathways for the production of H<sub>2</sub>.

**Collaborators:** Dr Carlo Sbraccia (Post-Doctoral Fellow), Department of Chemistry, Princeton University; Dr Morrel H. Cohen (Senior Research Staff), Dept. of Chemistry, Princeton University, and Department of Physics and Astronomy, Rutgers University, Piscataway, New Jersey

**(1) Title:** Biopolymers Containing Unnatural Amino Acids

**(2) Principal Investigator:** Peter G. Schultz, Ph.D.

**(3) Address:**

The Scripps Research Institute  
10550 N. Torrey Pines Rd., SR202  
La Jolla, CA 92037  
schultz@scripps.edu

**(4) Overview**

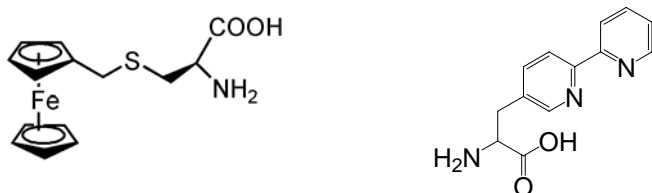
The genetic codes of all known organisms encode the same 20 amino acid building blocks with the rare exceptions of selenocysteine and pyrrolysine. Although conventional site-directed mutagenesis allows substitutions among these common 20 amino acids, our ability to modulate protein structure and function remains quite limited in comparison to chemists' ability to manipulate small molecules. The ability to genetically encode additional amino acids (beyond the common twenty), including those containing spectroscopic probes, post-translational modifications, metal chelators, photoaffinity labels, and unique functional groups, will provide new tools for exploring protein structure and function, and generating proteins, or possibly entire organisms, with new or enhanced properties. To this end, we recently developed a general method that makes it possible to genetically encode unnatural amino acids (UAAs) with diverse physical, chemical or biological properties in *Escherichia coli*, yeast, and mammalian cells. Over 40 UAAs have been cotranslationally incorporated into proteins with high fidelity and efficiency by means of a unique codon and corresponding tRNA–synthetase pair. A key feature of this methodology is the orthogonality between the new translational components and their endogenous host counterparts. Specifically, the codon for the UAA does not encode a common amino acid; neither the new tRNA nor cognate aminoacyl tRNA synthetase cross-react with any endogenous tRNA–synthetase pairs; and the new synthetase recognizes only the UAA and not any of the 20 common amino acids.

**(5) Recent Accomplishments**

Our recent efforts have focused on: (1) increasing the repertoire of unnatural amino acids that can be genetically encoded in both prokaryotic and eukaryotic organisms; (2) improving the overall efficiency of the methodology; and (3) characterizing the properties of the evolved orthogonal aminoacyl-tRNA synthetases.

A. We have recently genetically encoded photocaged amino acids in both bacteria and yeast. These include 2-nitrobenzyl tyrosine derivatives and 4,5-dimethoxy-2-nitrobenzyl serine derivatives which can be photocleaved with >365 nm light to release tyrosine and serine, respectively. These amino acids have been used to photocage the activity of enzymes and to photocage signaling pathways, the latter directly in yeast. In addition, a photoisomerizable amino acid, phenylalanine-4-azobenzene, was used to reversibly photocontrol the binding affinity of catabolite activator protein to its promoter. The ability to selectively incorporate these photoreactive amino acids into proteins at defined sites should make it possible to regulate a variety of biological processes with light, including enzyme, receptor and ion channel activity.

B. Two metal binding amino acids, bipyridylalanine and a ferrocene derivative of cysteine, have been genetically encoded in bacteria in response to the amber nonsense codon TAG in high yield and with good fidelity. We are currently using these amino acids to control protein redox activity; engineer catalytic sites (hydrolytic/redox) into antibodies; and generate oligomeric proteins/peptides (Fabs, peptides, etc.).



C. A number of chemically reactive amino acids have been genetically encoded in yeast and bacteria including: (1) phenylselenocysteine, which can be oxidatively transformed into dehydroalanine, and subsequently derivatized with thio-sugars, thio-lipids and other thiol containing moieties; and (2) p-azidophenylalanine which can be selectively derivatized in high yield in a selective Staudinger modification reaction. These methods allow the selective modification of proteins with a wide array of biophysical probes, tags, catalytic groups, etc.

D. A number of spectroscopic probes have been site-specifically introduced into proteins in bacteria including: (1) p-nitrophenylalanine which acts as a distance probe by quenching the intrinsic fluorescence of Trp; (2) L-(7-hydroxycoumarin-4-yl) ethylglycine which is an environmentally and pH sensitive fluorophore; and (3) p-cyanophenylalanine which is a sensitive vibrational probe of environment and dielectric. These methods provide useful probes of protein structure, conformation and biomolecular interactions both *in vitro* and *in vivo*.

E. We have determined the crystal structures of two substrate-bound *Methanococcus jannaschii* tyrosyl aminoacyl-tRNA synthetases that charge the unnatural amino acids *p*-bromophenylalanine and 3-(2-naphthyl)alanine (NpAla). A comparison of these structures with the substrate bound WT synthetase, as well as a mutant synthetase that charges *p*-acetylphenylalanine, shows that altered specificity is due to both side-chain and backbone rearrangements within the active site that modify hydrogen bonds and packing interactions with substrate, as well as disrupt the  $\alpha_8$ -helix, which spans the WT active site. The high degree of structural plasticity that is observed in these aminoacyl-tRNA synthetases is rarely found in other mutant enzymes with altered specificities and provides an explanation for the surprising adaptability of the genetic code to novel amino acids.

F. We have optimized the systems for incorporating unnatural amino acids in yeast and bacteria by improving the expression of the tRNA and aminoacyl-tRNA synthetase (aaRS), improving the processing of the tRNA, and enhancing the activity of the aaRS. We have also simplified the evolution of novel aaRSs and the introduction of UAAs into proteins of interest.

## (6) Future Experiments

We will focus on the following:

- (1) increase the number of UAAs that can be incorporated into proteins by decreasing codon redundancy in *E. coli*
- (2) photocage specific biological processes including ion channel activity, cell division and cell signaling
- (3) introduce metal ion proteolytic sites into antibodies
- (4) selectively couple proteins to two dimensional surfaces and electrodes
- (5) expand the number of metal ion binding and fluorescent amino acids that can be genetically encoded
- (6) attempt to enhance the catalytic activity or thermal stability of a protein by the introduction of UAAs

Xie, J., Schultz, P.G. "An Expanding Genetic Code." *Methods*, 36(3):227-38, **2005**.

Turner, J.M., Graziano, J., Spraggon, G., Schultz, P.G. "Structural Characterization of a p-Acetylphenylalanyl Aminoacyl-tRNA Synthetase." *J. Am. Chem. Soc.*, 127(43): 14976-14977, **2005**.

Xie, J., Schultz, P.G. "Adding Amino Acids to the Genetic Repertoire." *Curr. Opin Chem Biol.*, 9:548-554, **2005**.

Tsao, M., Tian, F., Schultz, P.G. "Selective Staudinger Modification of Proteins Containing p-Azidophenylalanine." *ChemBioChem*. 6(12): 2147-2149, **2005**.

Bose, M., Groff, D., Xie, J., Brustad, E., Schultz, P.G. "The Incorporation of a Photoisomerizable Amino Acid into Proteins in *E. coli*." *J. Am. Chem. Soc.*, 128(2):388-9, **2005**.

Ryu, Y., Schultz, P.G. "Efficient incorporation of unnatural amino acids into proteins in *Escherichia coli*." *Nature Methods*, 3(4):263-5, **2006**.

Deiters, A., Groff, D., Ryu, Y., Xie, J., Schultz, P.G. "A Genetically Encoded Photocaged Tyrosine." *Angew. Chemie*, 45(17):2728-2731, **2006**.

Turner, J.M., Graziano, J., Spraggon, G., Schultz, P.G. "Structural plasticity of an aminoacyl-tRNA synthetase active site." *Proc. Natl. Acad. Sci.*, 103(17):6483-8, **2006**.

Berezhna, S.Y., Supekova, L., Supek, F., Schultz, P.G., Deniz, A.A. "siRNA in human cells selectively localizes to target RNA sites." *Proc. Natl. Acad. Sci.*, 103(20):7682-7687, **2006**.

Tsao, M.L., Summerer, D., Ryu, Y., Schultz, P.G. "The genetic incorporation of a distance probe into proteins in *Escherichia coli*." *J. Am. Chem. Soc.*, 128(14):4572-3, **2006**.

Wang, L., Xie, J., Schultz, P.G. "Expanding the Genetic Code." *Ann. Rev. Biophys. Biomol. Struct.*, 9(35):225-249, **2006**.

Wang, J., Xie, J., Schultz, P.G. "A Genetically Encoded Fluorescent Amino Acid." *J. Am. Chem. Soc.*, 128(27):8738-9, **2006**.

Zeng, H., Xie, J., Schultz, P.G. "Genetic introduction of a diketone-containing amino acid into proteins." *Bioorg Med Chem Lett.*, 16: 5356–5359, **2006**.

Xie, J., Schultz, P.G. "A chemical toolkit for proteins – an expanded genetic code." *Nat. Rev. Mol. Cell Biol.*, 7(10):775-82, **2006**.

Schultz, K.C., Supekova, L., Ryu, Y., Xie, J., Perera, R., Schultz, P.G. "A Genetically Encoded Infrared Probe." *J. Am. Chem. Soc.*, 128(43):13984-5, **2006**.

Tippmann, E., Schultz, P.G. "A Genetically Encoded Metallocene Containing Amino Acid." *Tetrahedron*, 63: 6182–6184, **2007**.

Chen, S., Schultz, P.G., Brock, A. "An improved system for the generation and analysis of mutant proteins containing unnatural amino acids in *Saccharomyces cerevisiae*." *J. Mol. Biol.*, 371: 112–122, **2007**.

Wang, J., Schiller, S., Schultz, P.G. "A Biosynthetic Route to Dehydroalanine Containing Proteins." *Angew. Chem., epub*, **2007**.

Lemke, E.A., Summerer, D., Geierstanger, B.H., Brittain, S.M., Schultz, P.G. "Activation of a kinase pathway using a genetically encoded, photocaged amino acid and visible light." *Nature Chem. Biol.*, *in press*, **2007**.

Xie, J., Liu, W., Schultz, P.G. "A Genetically Encoded Bidentate, Metal-binding Amino Acid." *Angew. Chem., submitted*, **2007**.

# ***INVITED TALKS***



## **Biomolecular Stability and Life in Extreme Conditions**

Frank Robb

*Center of Marine Biotechnology, University of Maryland Biotechnology Institute*  
Baltimore, MD 21202

Abstract: We will address questions such as, how do hyperthermophilic organisms protect labile metabolites, nucleic acids and proteins from the negative effects of temperatures up to the current upper limit of life, 122C? The molecular mechanisms of stabilization and assembly of macromolecular complexes under extreme conditions, including pH=1.0 or 10.0, and the effects of ion composition on the stability of protein/protein complexes will be reviewed. Current research on the enzymology of protein folding under extreme conditions will be described in some detail.

**DNA: Not Merely the Secret of Life**, Nadrian C. Seeman, Department of Chemistry, New York University, New York, NY 10003, USA, ned.seeman@nyu.edu

DNA is well-known as the genetic material of living organisms. Its most prominent feature is that it contains information that enables it to replicate itself. This information is contained in the well-known Watson-Crick base pairing interactions, adenine with thymine and guanine with cytosine, leading to the well-known double helical structure. However relevant the double helix is to genetics, it is a limiting feature when the goal is to prepare more complex chemical species, because the helix axis is linear, in the sense that it is unbranched. Consequently, the only structures that can be obtained by combining molecules with linear helix axes are longer linear molecules or perhaps cyclic species, including knots and catenanes. This problem can be solved by using the notion of reciprocal exchange, which leads to branched species. The topologies of these species are readily programmed through sequence selection; in many cases, it is also possible to program their structures. Branched species can be connected to one another using the same interactions that genetic engineers use to produce their constructs, cohesion by molecules tailed in complementary single-stranded overhangs, known as 'sticky ends.' Such sticky-ended cohesion is used to produce N-connected objects and lattices.

Structural DNA nanotechnology is based on using stable branched DNA motifs, like the 4-arm Holliday junction, or related structures, such as double crossover (DX), triple crossover (TX), and paranemic crossover (PX) motifs. We have been working since the early 1980's to combine these DNA motifs to produce target species. From branched junctions, we have used ligation to construct DNA stick-polyhedra and topological targets, such as Borromean rings. Branched junctions with up to 12 arms have been produced. We have also built DNA nanotubes with lateral interactions.

Nanorobotics is a key area of application. PX DNA has been used to produce a robust 2-state sequence-dependent device that changes states by varied hybridization topology. We have used this device to make a translational device that prototypes the simplest features of the ribosome. A protein-activated device that can be used to measure the ability of the protein to do work, and a bipedal walker have both been built. We have also built a robust 3-state device.

A central goal of DNA nanotechnology is the self-assembly of periodic matter. We have constructed 2-dimensional DNA arrays from many different motifs. We can produce specific designed patterns visible in the AFM. We can change the patterns by changing the components, and by modification after assembly. Recently, we have used DNA scaffolding to organize active DNA components, as well as other materials. Active DNA components include DNAzymes and DNA nanomechanical devices; both are active when incorporated in 2D DNA lattices. Multi-tile DNA arrays have also been used to organize gold nanoparticles in specific arrangements.

The key structural challenge in the area is the extension of the 2D results obtained so far to 3D systems with a high degree of ordering. Several motifs have been produced that can produce 2D arrays in each of the three directions containing a pair of the vectors that span the 3D space. Crystals with dimensions as large as a millimeter, ordered to 10 Å resolution (as determined by X-ray diffraction) have been produced. Ultimately, we expect to produce high resolution crystals of DNA host lattices with heterologous guests, leading to bio-macromolecular systems amenable to diffraction analysis.

This research has been supported by the National Institute of General Medical Sciences, the National Science Foundation, the Army Research Office, NYNBIT and the W.M. Keck Foundation.

## What can we learn from nature about the principles of hierarchical materials?

Huajian Gao  
Division of Engineering  
Brown University

The importance of mechanics and mechanical properties in biological functions has been widely recognized. The present study has been motivated by the observation that multi-level structural hierarchy is a rule of nature. Hierarchical structures/materials can be observed in all biosystems from chromosome, protein, cell, tissue, organism, to ecosystems. Mechanics of hierarchical materials inspired by nature may provide useful hints for materials engineering. Some questions of interest include: what are the roles and principles of structural hierarchy? What determines the size scales in a hierarchical material system? Is it possible to design hierarchical materials with designated mechanical and other properties/behaviors? Specifically, natural materials such as bone, shell, tendon and the attachment system of gecko exhibit multi-scale hierarchical structures which seem to primarily serve their mechanical functions. This talk will be focused on the basic mechanical principles behind these hierarchical materials. We perform detailed analyses on two idealized, self-similar models of hierarchical materials, one mimicking the mineral-protein composite structure of bone and bone-like materials, and the other mimicking gecko's attachment system, to demonstrate that structural hierarchy leads to simultaneous enhancement of multiple mechanical properties/functions such as stiffness, toughness, flaw tolerance and work of adhesion. In conventional homogeneous materials, the fracture energy is a material constant. In contrast, hierarchical materials do not have a unique fracture resistance, rather their fracture toughness depends on length scale: the bigger the scale, the larger the fracture resistance. This has been demonstrated by determining the traction-separation laws (cohesive laws) at different length scales in a hierarchical material.

### Selected references:

- H. Gao, B. Ji, I.L. Jaeger, E. Arzt and P. Fratzl, *PNAS*, **100**, 5597–5600 (2003).
- H. Gao, and H. Yao, *PNAS*, **101**, 7851-7856 (2004).
- M.J. Buehler, H. Yao, H. Gao and B. Ji, *MSMSE*, **14**, 799-816 (2006).
- H. Yao and H. Gao, *JMPS*, 2006, **54**, 1120-1146 (2006).

***AUTHOR INDEX***  
***AND***  
***PARTICIPANT LIST***

## Author Index

Adiga, S. ....	17	Garcia, R. ....	80	Parikh, A. ....	56, 92
Akinc, M. ....	1, 9	Geissler, P. ....	42, 46	Pesavento, J. ....	54
Alam, T. ....	76	Gilmer, G. ....	50	Peters, J. ....	138
Alivisatos, P. ....	29, 46	Golbeck, J. ....	172	Prozorov, R. ....	5
Alper, M. ....	46	Goldstein, R. ....	13	Prozorov, T. ....	5
Archer, L. ....	110	Gourley, P. ....	72	Reiss, B. ....	17
Aronson, I. ....	13	Granick, S. ....	118, 122	Richmond, G. ....	160
Auciello, O. ....	17	Greenfield, M. ....	141	Robb, F. ....	187
Azevedo, H. ....	141	Groves, J. ....	46	Rocha, R. ....	56
Bachand, G. ....	64, 84	Gugliotti, L. ....	104	Rotello, V. ....	114
Balazs, A. ....	176	Hanson, D. ....	17	Rouge, J. ....	104
Bazylinksi, D. ....	5	Harris, M. ....	130	Safinya, C. ....	100
Belfort, G. ....	108	Hossain, C. ....	134	Samuels, W. ....	60
Benedek, G. ....	134	Huber, D. ....	76	Sasaki, D. ....	56, 72, 76, 80
Bertozzi, C. ....	31, 46	Hui, C.-Y. ....	126	Saven, J. ....	164
Blasie, J. ....	164	Isermann, H. ....	108	Schmalian, J. ....	5
Boal, A. ....	84	Iyer, S. ....	56	Schmidt-Rohr, K. ....	1, 9
Bouchard, A. ....	84	Jagota, A. ....	126	Schultz, P. ....	183
Brinker, C. ....	68	Khaykovich, B. ....	134	Seeman, N. ....	188
Browning, N. ....	54	Kozlova, N. ....	134	Selloni, A. ....	180
Brozik, J. ....	56	Kuhl, T. ....	88	Shelnutt, J. ....	80
Bryant, D. ....	172	Kumar, S. ....	108	Shin, Y. ....	60
Bunker, B. ....	64, 76, 84	Laible, P. ....	17	Shreve, A. ....	56
Bunz, U. ....	114	Lamm, M. ....	5	Sinclair, M. ....	72
Canfield, P. ....	5	Lee, J. ....	54	Singh, S. ....	68
Capito, R. ....	141	Li, L.-S. ....	141	Sinha, S. ....	92
Car, R. ....	180	Li, Y. ....	100	Sknepnek, R. ....	5
Carnes, E. ....	68	Lomakin, A. ....	134	Song, Y. ....	80
Challa, S. ....	80	Lopez, D. ....	68	Spoerke, E. ....	64, 84
Checco, A. ....	25	Luijten, E. ....	118, 122	Srinivasarao, M. ....	114
Culver, J. ....	130	Mallapragada, S. ....	1, 5, 9	Stevens, M. ....	76
De Yoreo, J. ....	50, 54	Manion, J. ....	104	Stupp, S. ....	141
DeGrado, W. ....	164	Martinez, J. ....	56	Therien, M. ....	164
Dolska, M. ....	104	Mata, A. ....	141	Trauner, D. ....	46
Dorin, R. ....	80	Matsui, H. ....	152	Travasset, A. ....	1, 5
Douglas, T. ....	138	Maye, M. ....	21	Van der Lelie, D. ....	21
Dutta, P. ....	145	Moncton, D. ....	134	van Swol, F. ....	80
Dutton, P. ....	168	Moore, J. ....	122	Velichko, Y. ....	141
Eaton, B. ....	104	Morse, D. ....	96	Wang, H.-L. ....	56
Evans, J. ....	156	Narasimhan, B. ....	5	Wang, L. ....	5, 60
Ewert, K. ....	100	Nilsen-Hamilton, M. ....	5	Wheeler, D. ....	76
Exarhos, G. ....	60	Noy, A. ....	50	Yang, L. ....	25
Feldheim, D. ....	104	Nykypanchuk, D. ....	21	Young, M. ....	138
Firestone, M. ....	17	Ocko, B. ....	25	Zapol, P. ....	17
Francis, M. ....	35, 46	Ocola, L. ....	17	Zhang, S. ....	141
Fréchet, J. ....	39, 46	Orendorff, C. ....	76	Zhang, Y.-B. ....	21
Fukuto, M. ....	25	Osbourn, G. ....	84	Zhu, Y. ....	149
Gang, O. ....	21	Palmer, L. ....	141		
Gao, H. ....	189	Palo, P. ....	5		

## Biomolecular Materials Contractors' Meeting - 2007

### Participants

Lastname	Firstname	Organization	Phone	Email
Alivisatos	Paul	Lawrence Berkeley National Laboratory	510-486-4999	paul.alivisatos@gmail.com
Alper	Mark	Lawrence Berkeley National Laboratory	510-486-6581	MDAAlper@lbl.gov
Archer	Lynden	Cornell University	607-254-8825	laa25@cornell.edu
Aronson	Igor	Argonne National Laboratory	630-252-9725	aronson@msd.anl.gov
Ashton	Christie	U.S. Department of Energy, BES	301-903-0511	christie.ashton@science.doe.gov
Bachand	George	Sandia National Laboratories	505-844-5164	gdbacha@sandia.gov
Balazs	Anna	University of Pittsburgh	412-648-9250	balazs1@engr.pitt.edu
Belfort	Georges	Rensselaer Polytechnic Institute	518-276-6376	sorels@rpi.edu
Bertozzi	Carolyn	Lawrence Berkeley National Laboratory	510-486-4829	<a href="mailto:CRBertozzi@lbl.gov">CRBertozzi@lbl.gov</a>
Blasie	Kent	University of Pennsylvania	215-898-6208	jkblasie@sas.upenn.edu
Brinker	Jeff	Sandia National Laboratories	505-272-7627	cjbrink@sandia.gov
Bunz	Uwe	Georgia Institute of Technology	404-385-1795	uwe.bunz@chemistry.gatech.edu
Burns	Christopher	Argonne National Laboratory	630-252-3468	burns@anl.gov
Checco	Antonio	Brookhaven National Laboratory	631-344-3319	checco@bnl.gov
Chiechi	Ryan	Harvard University	617-495-9436	rchiechi@gmwgroup.harvard.edu
Culver	James	University of Maryland, Biotechnology Institute	301-405-2912	jculver@umd.edu
Dattelbaum	Andrew	Los Alamos National Laboratory	505-665-0142	amdattel@lanl.gov
De Yoreo	Jim	Lawrence Livermore National Laboratory	925-423-4240	deyoreo1@llnl.gov
Douglas	Trevor	Montana State University	406-994-6566	tdouglas@montana.edu
Dutta	Pulak	Northwestern University	847-491-5465	pducta@northwestern.edu
Dutton	P. Leslie	University of Pennsylvania	215-898-0991	dutton@mail.med.upenn.edu, silvanb@mail.med.upenn.edu
Eaton	Bruce	University of Colorado at Boulder	303-735-1002	bruce.eaton@colorado.edu
Evans	John	New York University	212-998-9605	jse1@nyu.edu
Exarhos	Gregory	Pacific Northwest National Laboratory	509-376-4125	greg.exarhos@pnl.gov
Firestone	Millicent	Argonne National Laboratory	630-252-8298	firestone@anl.gov
Francis	Matthew	Lawrence Berkeley National Laboratory	510-643-9915	MBFrancis@lbl.gov

Fréchet	Jean	Lawrence Berkeley National Laboratory	510-643-3077	<a href="mailto:J_Frechet@lbl.gov">J_Frechet@lbl.gov</a>
Gang	Oleg	Brookhaven National Laboratory	631-344-3645	<a href="mailto:ogang@bnl.gov">ogang@bnl.gov</a>
Gao	Huajian	Brown University	401-863-2626	<a href="mailto:huajian_gao@brown.edu">huajian_gao@brown.edu</a>
Geissler	Phillip	Lawrence Berkeley National Laboratory	510-642-8716	<a href="mailto:geissler@cchem.berkeley.edu">geissler@cchem.berkeley.edu</a>
Gersten	Bonnie	U.S. Department of Energy, BES	301-903-0002	<a href="mailto:Bonnie.Gersten@science.doe.gov">Bonnie.Gersten@science.doe.gov</a>
Golbeck	John	The Pennsylvania State University	814-865-1163	<a href="mailto:jhg5@psu.edu">jhg5@psu.edu</a>
Goldstein	Raymond	University of Cambridge	+44 (0)1223 337908	<a href="mailto:R.E.Goldstein@damtp.cam.ac.uk">R.E.Goldstein@damtp.cam.ac.uk</a>
Gourley	Paul	Sandia National Laboratories	505-844-5806	<a href="mailto:plgourl@sandia.gov">plgourl@sandia.gov</a>
Granick	Steve	University of Illinois at Urbana-Champaign	217-333-5720	<a href="mailto:sgranick@uiuc.edu">sgranick@uiuc.edu</a>
Groves	John T.	Lawrence Berkeley National Laboratory	510-643-0186	<a href="mailto:JTGroves@lbl.gov">JTGroves@lbl.gov</a>
Harris	Michael	Purdue University	765-494-4966	<a href="mailto:mtharris@purdue.edu">mtharris@purdue.edu</a>
Heilshorn	Sarah	Stanford University	650-723-3763	<a href="mailto:heilshorn@stanford.edu">heilshorn@stanford.edu</a>
Hui	Chung-Yuen	Cornell University	607-255-3718	<a href="mailto:ch45@cornell.edu">ch45@cornell.edu</a>
Izumi	Michi	University of California, Santa Barbara	805-893-3416	<a href="mailto:izumi@lifesci.ucsb.edu">izumi@lifesci.ucsb.edu</a>
Jagota	Anand	Lehigh University	610-758-4396	<a href="mailto:anj6@lehigh.edu">anj6@lehigh.edu</a>
Kelley	Richard	U. S. Department of Energy, BES	301-903-6051	<a href="mailto:richard.kelley@science.doe.gov">richard.kelley@science.doe.gov</a>
Khaykovich	Boris	Massachusetts Institute of Technology	617-263-2861	<a href="mailto:bkh@mit.edu">bkh@mit.edu</a>
King	Wayne	Lawrence Livermore National Laboratory	925-423-6547	<a href="mailto:king17@llnl.gov">king17@llnl.gov</a>
Kini	Aravinda	U.S. Department of Energy, BES	301-903-3565	<a href="mailto:a.kini@science.doe.gov">a.kini@science.doe.gov</a>
Kuhl	Tonya	University of California, Davis	530-754-5911	<a href="mailto:tkuhl@ucdavis.edu">tkuhl@ucdavis.edu</a>
Kumar	Sanat	Columbia University	212-854-2193	<a href="mailto:sk2794@columbia.edu">sk2794@columbia.edu</a>
Kung	Harriet	U.S. Department of Energy, BES	301-903-0497	<a href="mailto:harriet.kung@science.doe.gov">harriet.kung@science.doe.gov</a>
Lewis	Jennifer	University of Illinois at Urbana-Champaign	217-244-4973	<a href="mailto:jalewis@uiuc.edu">jalewis@uiuc.edu</a>
Liu	Jun	Pacific Northwest National Laboratory	509-375-4443	<a href="mailto:jun.liu@pnl.gov">jun.liu@pnl.gov</a>
Luijten	Erik	University of Illinois at Urbana-Champaign	217-244-5622	<a href="mailto:luijten@uiuc.edu">luijten@uiuc.edu</a>
Martinez	Jennifer	Los Alamos National Laboratory	505-665-0045	<a href="mailto:jenm@lanl.gov">jenm@lanl.gov</a>
Masafumi	Fukuto	Brookhaven National Laboratory	631-344-5256	<a href="mailto:fukuto@bnl.gov">fukuto@bnl.gov</a>
Matsui	Hiroshi	City University of New York, Hunter College	212-650-3918	<a href="mailto:hmatsui@hunter.cuny.edu">hmatsui@hunter.cuny.edu</a>
Morse	Daniel	University of California, Santa Barbara	805-893-7442	<a href="mailto:d_morse@lifesci.ucsb.edu">d_morse@lifesci.ucsb.edu</a>

Mukhopadhyay	Mrinmay	Argonne National Laboratory	630-252-0285	mrinmay@aps.anl.gov
Narasimhan	Balaji	Ames Laboratory	515-294-8019	nbalaji@iastate.edu
Nilsen-Hamilton	Marit	Ames Laboratory	515-294-9996	marit@iastate.edu
Noy	Aleksandr	Lawrence Livermore National Laboratory	925-424-6203	noy1@llnl.gov
Ocko	Benjamin	Brookhaven National Laboratory	631-344-4299	ocko@bnl.gov
Palmer	Liam	Northwestern University	847-492-4049	liam-palmer@northwestern.edu
Perera	Roshan	The Scripps Research Institute	858-784-9335	perera@scripps.edu
Perez-Salas	Ursula	Argonne National Laboratory	630-252-8621	<a href="mailto:perez-salas@anl.gov">perez-salas@anl.gov</a>
Phillips	Ronnie	Georgia Institute of Technology	404-295-0429	gtg239g@mail.gatech.edu
Prissel	Matt	Montana State University	406-944-6855	mprissel@chemistry.montana.edu
Prozorov	Tatiana	Ames Laboratory	515-294-3376	tprozoro@ameslab.gov
Richmond	Geraldine	University of Oregon	541-346-4635	richmond@uoregon.edu
Robb	Frank	University of Maryland, Center for Marine Biotechnology	410-234-8872	<a href="mailto:robb@umbi.umd.edu">robb@umbi.umd.edu</a>
Rouge	Jessica	University of Colorado at Boulder	303-735-1617	jessica.rouge@colorado.edu
Royston	Elizabeth	University of Maryland, Biotechnology Institute	301-405-2852	esadar@gmail.com
Safinya	Cyrus	University of California, Santa Barbara	805-893-8635	safinya@mrl.ucsb.edu
Sanii	Babak	University of California, Davis	530-400-1495	bsanii@ucdavis.edu
Sasaki	Darryl	Sandia National Laboratories	925-294-2922	dysasak@sandia.gov
Saven	Jeffery	University of Pennsylvania	215-573-6062	saven@sas.upenn.edu
Schmidt-Rohr	Klaus	Ames Laboratory	515-294-6105	srohr@iastate.edu
Seaman	Nadrian	New York University	212-998-8395	<a href="mailto:ned.seeman@nyu.edu">ned.seeman@nyu.edu</a>
Selloni	Annabella	Princeton University	609-258-3837	aselloni@princeton.edu
Sharma	Sumit	Columbia University	518-301-5052	ss3116@columbia.edu
Shelnutt	John	Sandia National Laboratories	505-272-7160	jsheln@unm.edu
Shen	lulin	Cornell University	607-351-5379	ls276@cornell.edu
Shreve	Andrew	Los Alamos National Laboratory	505-667-6933	shreve@lanl.gov
Simmons	Blake	Sandia National Laboratories	925-294-2288	<a href="mailto:basimmo@sandia.gov">basimmo@sandia.gov</a>
Sinha	Sunil	University of California, San Diego	858-822-5537	ssinha@physics.ucsd.edu
Spoerke	Erik	Sandia National Laboratories	505-284-1932	edspoer@sandia.gov



Stupp	Samuel	Northwestern University	847-491-3002	c-gilchrist@northwestern.edu
Tao	Andrea	University of California, Santa Barbara	805-893-3416	tao@lifesci.ucsb.edu
Therien	Michael	University of Pennsylvania	215-898-0087	therien@sas.upenn.edu
Thiyagarajan	P.	Argonne National Laboratory	630-252-3593	<a href="mailto:Thiyaga@anl.gov">Thiyaga@anl.gov</a>
Thomas	Samuel	Harvard University	617-495-9433	stthomas@gmwgroup.harvard.edu
Tortorelli	Peter	Oak Ridge National Laboratory	865-574-5119	tortorellipf@ornl.gov
Träskelin	Petra	University of California, Davis	530-754-5627	pttraskelin@ucdavis.edu
Trauner	Dirk	Lawrence Berkeley National Laboratory	510-643-5507	DTrauner@lbl.gov
Travesset	Alex	Ames Laboratory	515-294-7191	trvsst@ameslab.gov
Vajpayee	Shilpi	Lehigh University	484-951-2334	shv205@lehigh.edu
Voigt	James	Sandia National Laboratories	505-845-9044	javoigt@sandia.gov
Wang	Hsing-Lin	Los Alamos National Laboratory	505-667-9944	hwang@lanl.gov
Yang	Lin	Brookhaven National Laboratory	631-344-5833	lyang@bnl.gov
Zhu	Yingxi Elaine	University of Notre Dame	574-631-2667	yzhu3@nd.edu